The effects of metformin on the gastrointestinal tract

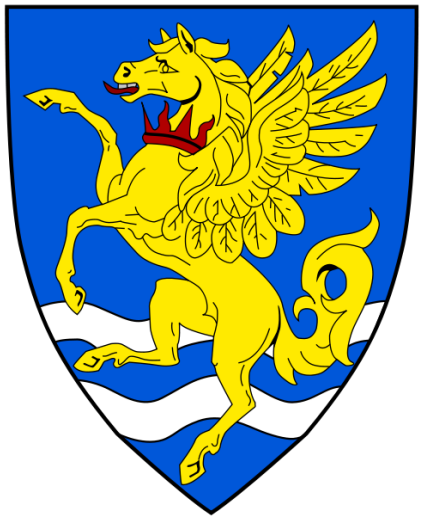

Ming Yang

Robinson College, University of Cambridge

This dissertation is submitted for the degree of Doctor of Philosophy

September 2019

Abstract

Metformin is the world's most prescribed drug and is recommended first-line therapy for the treatment of Type 2 Diabetes Mellitus (T2DM). Numerous clinical studies have demonstrated that metformin is an effective oral agent in normalising blood glucose levels. Metformin is also one of the very few antidiabetic agents that causes modest weight loss in overweight and obese subjects. Despite its introduction into the clinic over 60 years ago, the mechanisms of metformin action are still elusive.

Many of the previous studies into metformin action have focussed on its role in inhibiting endogenous glucose production in the liver, due the central role of the liver in insulin resistance and glycaemic control. However, metformin also accumulates at the highest concentrations in the small intestine, and clinical studies demonstrate that metformin formulations with low bioavailability achieve similarly effective glycaemic control compared to standard metformin formulations. These studies suggest that the gastrointestinal tract may also be an important site of metformin action.

In this thesis, 2D monolayer cultures generated from intestinal organoids were used to investigate the mechanisms of metformin action in intestinal cells. Bulk RNA-sequencing and pathway analysis identified changes in glucose and amino acid metabolism pathways, as well as the upregulation of novel signalling pathways associated with the metformin response in intestinal cells. The results from RNA-seq experiments were used as the basis for functional studies into metformin action in intestinal cells.

GDF-15 is a stress activated hormone that acts on its cognate receptor GFRAL expressed almost exclusively in the brainstem to elicit an inhibition of food intake. GDF-15 was one of the serum biomarkers identified in T2DM patients associated with metformin use. In a multidisciplinary collaboration, we demonstrated that *Gdf15* upregulation in the distal small intestine and colon were associated with the weight loss effects of metformin. The results from transcriptomic analysis in this study identified *Gdf15* as one of the most significantly upregulated genes in metformin treated intestinal cultures. Transcriptomic analysis of selected genes involved in mitochondrial function, and secretion studies reported that metformin stimulated GDF-15 secretion through mitochondrial stress and activating the integrated stress response.

Previous observations from Position Emission Tomography-Computed Tomography (PET-CT) imaging in mice and T2DM patients demonstrated that oral metformin administration caused non-metabolisable fluoro-deoxyglucose (F-2DG) tracer to accumulate predominantly in the gut. This suggests that metformin increased intestinal glucose utilisation as one mechanism associated with its glucose lowering effects. In intestinal cells, metformin increased the expression of *Slc2a1* (encoding

GLUT1), whilst decreasing the expression of *Slc2a2* (GLUT2) and *Slc5a1* (SGLT1). This was replicated in the distal small intestine of HFD-fed mice treated with metformin. Metformin also increased GLUT-transporter mediated glucose uptake in cultures. These mechanisms may potentially be mediated by AMPK and HIF1A signalling pathways. By inhibiting mitochondrial respiration, metformin also limited the metabolic plasticity of intestinal cells to utilise other metabolic fuels, which instead relied almost exclusively on glycolysis.

In summary, this study suggests that increased glucose uptake mediated by GLUT transporters and increased glycolysis mediates intestinal glucose utilisation as a mechanism by which metformin causes its glucose lowering effects. Metformin may also stimulate GDF-15 secretion from the GI tract as an atypical “gut hormone”, which acts on the brainstem to reduce food intake and enhance weight loss. Together, the results from this study argue that the GI tract is an important site where metformin mediates glycaemic control and weight loss.

Declaration

This dissertation is submitted for the degree of Doctor of Philosophy.

I hereby declare that this dissertation is the result of my own work and includes nothing which is the outcome of work done in collaboration with others except as specified in the main text.

Marcella Ma and Brian Lam performed cDNA library preparation, read alignment and generating quantitative raw counts for bulk RNA-sequencing data as discussed in chapter 3. Pierre Larraufie performed preliminary experiments on RNA sequencing analysis. High fat diet mouse models, in vivo metformin administration, and tissue collection were performed by Tony Coll, Debra Rimmington and Irene Cimino for chapters 4 and 5.

The thesis is not substantially the same as any that I have submitted, or, is being concurrently submitted for a degree or diploma or other qualification at the University of Cambridge or any other University or similar institution. I further state that no substantial part of my dissertation has already been submitted, or, is being concurrently submitted for any such degree, diploma, or other qualification at the University of Cambridge or any other University or similar institution.

This dissertation does not exceed 60,000 words, excluding figures, tables, appendices and bibliography.

Ming Yang, September 2019.

Contents

Abstract ..... **i**
Declaration ..... **iii**
Abbreviations **1**
Acknowledgements **5**
Chapter 1: Introduction **6**
1.1. Type 2 Diabetes Mellitus and Obesity 6
1.3. Treatments for obesity and T2DM 6
1.3.1. Glucose lowering agents 6
1.3.2. Appetite regulating drugs for Obesity 8
1.3.3. Bariatric surgery 9
1.4. Metformin in the clinic 10
1.4.1. Brief history of metformin 10
1.4.2. Metformin as a glucose-lowering agent to treat T2DM 11
1.4.3. Metformin and the prevention of T2DM 12
1.4.4. Effect of metformin on body weight 13
1.4.5. Other clinical effects and applications of metformin 14
1.4.6. Side effects of metformin use 15
1.4.7. Genetic variants and patient responses to metformin 15
1.5. Background of the digestive system and the gastrointestinal tract 17
1.5.1. The small intestinal epithelial architecture 18
1.5.2. Enterocytes and nutrient absorption 20
1.5.3. Intestinal nutrient metabolism 20
1.5.4. The GI tract as an endocrine organ 21
1.5.5. Intestinal organoids 21
1.6. Mechanisms of metformin action in the liver and GI tract 22
1.6.1 Cellular mechanisms of action 22
1.6.2 Liver metabolism 22
1.6.3 Intestinal glucose handling and lactate production 24
1.6.4 The microbiome 25
1.6.5. Bile acid homeostasis 25
1.6.6. GLP-1 and incretin hormones 26
1.6.7. New metabolic hormones- GDF-15 and FGF21 26
1.6.8. The gut-brain axis 27
1.7. Metformin pharmacokinetics, bioavailability and biodistribution 27

1.6.1 Metformin tissue biodistribution 28
1.6.2 Intestinal metformin transporters 28
1.8. The importance of the GI tract in metformin action 29
1.7.1 Routes of metformin administration 29
1.7.1 Delayed release metformin formulations 29
1.9. Aims of the Thesis 31
Chapter 2: Materials and Methods 32
2.1 Materials and Reagents 32
2.2 Media and Buffer components 34
2.3 Intestinal organoid lines 34
2.4 High fat diet mouse experiments 35
2.4.1 Acute metformin gavage in HFD-fed wild type mice 35
2.4.2 Long-term metformin dosing in HFD-fed wild type mice 35
2.4.3 Tissue processing 35
2.5 Small intestinal organoid culture 37
2.5.1 Crypt isolation from mouse intestine 37
2.5.2 Maintenance 37
2.5.3 Cryopreservation and thawing 37
2.5.4 2D monolayer culture and drug treatments 38
2.5.5 Plasmid amplification and Transfection 38
2.6 Imaging experiments 39
2.6.1 Live cell imaging preparations 39
2.6.2 Perceval imaging of intracellular ATP 40
2.6.3 Peredox imaging of cytosolic NADH/NAD+ ratio 41
2.6.4 Autofluorescence imaging of NAD(P)H and FAD 42
2.6.5 FRET imaging 42
2.6.5.1 FLII12Pglu-700µδ6 Glucose sensor 42
2.6.5.2 FLIPQ-TV3.0_2 m Glutamine sensor 44
2.6.5.3 Pyronic sensor 44
2.7 Seahorse Measurements 44
2.8. Secretion and Enzyme Activity Assays 47
2.8.1 Lactate Secretion Assay 47
2.8.2 GDF-15 Secretion Assay 47
2.8.3 LDH (Lactate dehydrogenase), AST (Aspartate transaminase) and ALT (Alanine transaminase) Assay 48
2.9 Techniques to analyse Gene Expression 49

2.9.1 Real-time quantitative PCR (RT-qPCR) 49
2.9.2 RNA-Sequencing 50
2.10 Statistical Analysis 51
Chapter 3: Transcriptomic characterisation of metformin responsive genes in intestinal cells 52
3.1 Summary 52
3.2 Background 52
3.2.1 AMPK-dependent mechanisms of Metformin 52
3.2.2 Metformin and other signalling pathways 53
3.2.3 Metformin and cellular processes 54
3.2.4 Metformin and intestinal functions 54
3.2.5 Transcriptomic and genomic studies into metformin action 55
3.3 Aims 55
3.4 Results 55
3.4.1 DE-Seq analysis of differentially expressed genes altered by metformin treatment 55
3.4.2 The effects of metformin on metabolic and signalling pathways in intestinal cells 58
3.5 Discussion 81
3.5.1 Metformin and glucose/sugar metabolism 81
3.5.2 Transcriptomic changes of amino acid sensing, transport and metabolism pathways by metformin 83
3.5.3 Metformin and intestinal lipid metabolism 85
3.5.4 Transcriptomic effects of metformin to signalling pathways and cellular processes 86
3.5.5 Conclusions 88
Chapter 4: Mechanisms of GDF-15 induction by metformin in intestinal cells 89
4.1 Summary 89
4.2 Introduction 89
4.2.1 GDF-15 as a metabolic hormone 89
4.2.2 Mechanisms of GDF-15 induction 90
4.2.3 Metformin and GDF-15 91
4.3 Aims 92
4.4 Results 92
4.4.1. Mitochondrial stress and GDF-15 induction in intestinal cells 92
4.4.2. The effect of metformin on the expression of mitochondria-associated genes 98
4.4.3. Metformin activates ISR and the HIF-1A signalling pathway to stimulate GDF-15 induction 102
4.5 Discussion 106
4.5.1 Mechanisms of metformin-stimulated GDF-15 secretion in intestinal cells 106

4.5.2 The gastrointestinal tract in metformin-stimulated GDF-15 secretion 110
4.5.3 Comparing the effects of metformin on GDF-15 and other stress hormones/metabolic growth factors 111
4.5.4 Conclusions 112
Chapter 5: Mechanisms of metformin action on glucose uptake in intestinal cells 113
5.1 Summary 113
5.2 Introduction 113
5.2.1 Glucose transport in intestinal enterocytes 113
5.2.2 Metformin and intestinal glucose absorption 114
5.2.3 The “glucose sink” model of metformin action in the intestines 115
5.3 Aims 116
5.4 Results 116
5.4.1 The effect of metformin on the mRNA expression of glucose transporters in intestinal cultures 116
5.4.2 Metformin increases glucose uptake in intestinal cells mediated by a GLUT transporter 119
5.4.3 Signalling pathways involved in the regulation of glucose uptake and expression of glucose transporters by metformin 123
5.4.4 The effects of metformin on the mRNA expression of glucose transporters in intestinal tissues of HFD-fed mice 126
5.5 Discussion 129
5.5.1 Does metformin increase basal glucose uptake by upregulating GLUT1 transporters? ... 129
5.5.2 The effect of metformin on the expression of other glucose transporters 130
5.5.3 The contributions of the AMPK and HIF-1A signalling pathways to glucose transport changes mediated by metformin 132
5.5.4 Conclusions 134
Chapter 6: Metformin and nutrient metabolism in intestinal cells 135
6.1 Summary 135
6.2 Background 135
6.2.1 Nutrient metabolism in intestinal cells 135
6.2.2 Cellular mechanisms of metformin on nutrient metabolism 136
6.2.3 Metformin and intestinal nutrient metabolism 137
6.3 Aims 137
6.4 Results 138
6.4.1 Metformin decreases glucose oxidation but maximises glycolysis in intestinal cells 138
6.4.2 Metformin increases glycolytic metabolism of pyruvate towards lactate and alanine 142
6.4.3 The effect of metformin on pyruvate and glutamine metabolism 148

6.4.4 The effect of metformin on ATP generation from glycogen and lipid sources in intestinal cells 153
6.5 Discussion 157
6.5.1 Metformin and mitochondrial oxidation in intestinal cells 157
6.5.2 Metformin and intestinal glucose metabolism 158
6.5.3 Metformin and intestinal energy stores 160
6.6 Conclusions 161
Chapter 7: General Discussion 163
7.1. Summary of findings 163
7.1.1. Metformin alters the transcriptome of intestinal cells 163
7.1.2. Metformin stimulates GDF-15 secretion through mitochondrial stress 164
7.1.3. Metformin increases GLUT transporter mediated glucose uptake 166
7.1.4. Metformin limits the metabolic plasticity of intestinal cells 168
7.2 Limitations of this study 170
7.3. Other considerations into metformin action in the GI tract 171
7.3.1. The physiological effects of metformin: the liver or the gut? 171
7.3.2. Metformin stimulated GDF-15 secretion and glucose utilisation- all of the cells? 171
7.3.3 Are the mechanisms of metformin action in the gut the same as those following bariatric surgery? 172
7.4. Concluding remarks 172
References 174
Appendix 235

Abbreviations

2-DG	2-Deoxyglucose
5-HT	5-hydroxytryptamine
ADA	American Diabetes Association
ADF media	Advanced DMEM/F-12 media
ADOPT	A Diabetes Outcome Progression Trial
ADP	Adenosine diphosphate
AICAR	5-Aminoimidazole-4-carboxamide ribonucleotide
ALT	Alanine transaminase
AMP	Adenosine monophosphate
AMPK	5' AMP-activated protein kinase
ANOVA	Analysis of variance
AOA	Aminooxyacetic acid
AP	Area Postrema
AST	Aspartate transaminase
ATF4	Activating Transcription Factor 4
ATM	Ataxia Telangiectasia Mutated
ATP	Adenosine triphosphate
B0AT1	Sodium-dependent neutral amino acid transporter 1
BCA	Bicinchoninic acid assay
BCAA	Branched chain amino acid
BIGPRO	Biguanides and Prevention of Risks in Obesity study
BiP	2,2'-bipyridine
BME	Basement membrane extract
BMI	Body Mass Index
BMP	Bone morphogenetic proteins
CBP	CREB-binding protein
CCK	Cholecystokinin
CDK	Cyclin-dependent kinases
CFP	Cyan fluorescent protein
CHOP	C/EBP homologous protein
CHT	Choline transporter
CIC	Citrate transporter
CO_2	Carbon dioxide
cAMP	Cyclic adenosine monophosphate
CREB	cAMP response element-binding protein
CRP	C-reactive protein
CRTC2	CREB Regulated Transcription Coactivator 2
CVD	Cardiovascular Disease
dCMP	Deoxycytidine monophosphate
DE gene	Differentially expressed gene
DMEM	Dulbecco's Modified Eagle Medium
DNA	Deoxyribonucleic acid
DPP	Diabetes Prevention Programme
DPPOS	Diabetes Prevention Programme Outcomes Study
EASD	European Association for the Study of Diabetes
ECAR	Extracellular acidification rate
EDTA	Ethylenediaminetetraacetic acid
EGF	Epithelial Growth Factor

eIF2α	Eukaryotic Initiation Factor 2 alpha
ENR media	EGF, Noggin, R-Spondin media
ER	Endoplasmic reticulum
ERK	Extracellular signal–regulated kinases
F-2DG	Fluoro-2-deoxy-2-D-glucose
FAD	Flavin adenine dinucleotide
FAO	Fatty Acid Oxidation
FBP	Fructose-1,6-bisphosphatase
FBS	Fetal bovine serum
FCCP	Carbonyl cyanide-*4*-(trifluoromethoxy)phenylhydrazone
FDA	Food Drug Administration
FFA	Free fatty acid
FGF15	Fibroblast growth factor 15
FGF21	Fibroblast growth factor 21
FRET	fluorescent-resonance energy transfer
FXR	Farnesoid receptor
GCN2	General control nonderepressible 2
GDF-15	Growth Differentiation Factor 15
GDM	Gestational Diabetes Mellitus
GDS	German Diabetes Study
GFP	Green fluorescent protein
GFRAL	GDNF family receptor alpha like
GI	Gastrointestinal
GIP	Glucose-dependent insulinotropic ptpide
GLP-1	Glucagon-like Peptide 1
GLUT	Facilitated glucose transporters
GO	Gene Ontology
GPS	Glycerolphosphate shuttle
GTCA	Genome-wide complex trait analysis
GUDCA	Glycoursodeoxycholic Acid
GWAS	Genome-wide Association Study
HbA1c	Glycated Haemoglobin levels
HEPES	4-(2-hydroxyethyl)-1-piperazineethanesulfonic acid
HFD	High fat diet
HIF-1α	Hypoxia induced factor-1 alpha
HRI	Heme regulated inhibitor
IFN-γ	Interferon-gamma
IL-1β	Interleukin-1 beta
ISR	Integrated stress response
ISRIB	Integrated Stress Response Inhibitor
KEGG	Kyoto Encyclopedia of Genes and Genomes database
LABS	Longitudinal Assessment for Bariatric Surgery study
LB broth	Lysogeny broth
LCFA	Long chain fatty acid
LDH	Lactate dehydrogenase
LDL	Low density lipoprotein
LKB-1	Liver kinase B1
MAPK	Mitogen-activated protein kinase
MAS	Malate aspartate shuttle
MCM	Minichromosome maintenance
MCT	Monocarboxylic acid transporters

MCU	Mitochondrial calcium uniporter
MEF	Mouse embryonic fibroblasts
metformin-DR	Metformin delayed release
metformin-IR	Metformin immediate release
metformin-XR	Metformin extended release
mRNA	Messenger ribonucleic acid
mtDNA	Mitochondrial deoxyribonucleic acid
mTOR	mammalian Target of rapamycin
mtUPR	Mitochondrial unfolded protein response
NADH	Nicotinamide adenine dinucleotide
NADPH	Nicotinamide adenine dinucleotide phosphate
NDMA	N-Nitrosodimethylamine
NF-kB	Nuclear factor kappa-light-chain-enhancer of activated B cells
NMN	Nicotinamide mononucleotide
NMNAT	Nicotinamide mononucleotide adenylyltransferase
NQO-1	NAD(P)H Quinone Dehydrogenase 1
NTS	Nucleus tractus solitarii
OCR	Oxygen consumption rate
OCT	Organic cation transporter
ORC	Origin recognition complex
OXPHOS	Oxidative phosphorylation
PBS	Phosphate buffered saline
PCOS	Polycystic Ovarian Syndrome
PEPCK	Phosphenolpyruvate carboxykinase
PERK	Protein kinase R (PKR)-like endoplasmic reticulum kinase
PET-CT	Position Emission Tomography-Computed Tomography
PGC-1α	PPAR-γ coactivator 1 alpha
PhS	Phenylsuccinic Acid
PI3K	Phosphoinositide 3-kinase
PKA	Protein kinase A
PKR	Protein kinase R
PMAT	Plasma membrane monoamine transporter
POMC	Pro-opiomelanocortin
PPAR-γ	Peroxisome proliferator activated receptor gamma
PPP	Pentose phosphate pathway
PYY	Peptide YY
RIG1	retinoic acid-inducible gene I
RIN	RNA integrity number
ROCK	Rho-associated, coiled-coil containing protein kinase
ROS	Reactive oxygen species
RT-qPCR	Real-time quantitative polymerase chain reaction
RYGB	Roux-en-Y gastric bypass
SCFA	Short chain fatty acid
SERT	Serotonin transporter
SGLT	Sodium-dependent glucose cotransporters
SHP	Src homology region 2 domain-containing phosphatase-1
SNAT2	Sodium-coupled neutral amino acid transporter 2
SREBP	Sterol regulatory element-binding proteins
SST	Somatostatin
STZ	Streptozotocin
T2DM	Type 2 Diabetes Mellitus

TAZ	transcriptional coactivator with PDZ-binding motif
TCA cycle	Tricarboxylic acid cycle
TGF-β	Transforming growth factor β
TNF	Tumor necrosis factor
UKPDS	UK Prospective Diabetes Study
UPR	Unfolded protein response
VDAC	Voltage dependent anion channel
VHL	Von Hippel–Lindau tumor suppressor
VSG	Vertical sleeve gastrectomy
VST	Variance Stabilising Transformation
WT	Wild-type
YAP1	Yes-associated protein 1
YFP	Yellow fluorescent protein
YFP	Yellow fluorescent protein
β-CLA	β-chloro-L-alanine

Acknowledgements

I would like to thank my supervisors Fiona Gribble and Frank Reimann at the University of Cambridge for providing me the guidance and support throughout my PhD. I would also like to thank Deborah Goldspink, who has been my postdoctoral supervisor throughout much of my PhD and supported me in my day-to-day experiments.

I have been fortunate enough to be involved in translational research across the Institute of Metabolic Sciences and I would like to thank each person in the department who have provided me with advice throughout my PhD. Particularly, I would like to thank the people, both past and the present, in the Gribble/Reimann group who have helped me in my day-to-day experiments during the course of my PhD.

My mother, Haizhu, who has been the driving force during my PhD, has provided me the encouragement that I needed most in my PhD through a combination of maternal compassion and responsible realism. My stepfather, Chris, has provided me the motivation to persevere in this rollercoaster ride.

Chapter 1: Introduction

1.1. Type 2 Diabetes Mellitus and Obesity

Type 2 diabetes (T2DM) and obesity are major global health concerns in the 21st century. As many as 1.9 billion people worldwide were either overweight or obese in 2016, and 422 million people were living with diagnosed T2DM in 2014 according to the World Health Organisation (WHO) *(1, 2)*. T2DM and obesity are strongly associated, with obesity being a prevalent risk factor for the development of T2DM (being overweight accounts for a 61% increased risk in developing T2DM) *(3, 4)*. Patients with obesity and/or T2DM can develop cardiovascular complications *(5–7)*. A total of £8.8 billion has been invested for the treatment of T2DM in 2012 and £7.4 billion has been invested for treating obesity by the NHS from 1998-2010, respectively *(8, 9)*. Therefore, effective long-term management of T2DM and obesity is a strategic priority to delay disease complications and improve quality of life.

The two core defects in T2DM are beta-cell dysfunction and insulin resistance *(10)*. Insulin resistance (the inability of tissues such as the liver, skeletal muscle and adipose tissue to respond to insulin) frequently precedes the development of T2DM and causes stress on the beta-cells, contributing to beta-cell failure and impaired insulin secretion *(10)*. This leads to incremental elevations in blood glucose levels, and T2DM is clinically diagnosed if fasting blood glucose levels are >7 mmol/L *(10, 11)*. Obesity is the result of increased fat deposition as a result of imbalance between energy expenditure and food intake *(12)*. Metabolic changes in adipose tissues and neuroendocrine changes in appetite also accompany obesity *(12)*. Although obesity is associated with insulin resistance, T2DM does not usually occur unless there is also beta-cell dysfunction *(13)*. A complex association of genetic and environmental factors contributes to the development of obesity and T2DM *(10, 12)*. Both obesity and T2DM have also been reported to be associated with systematic inflammation which contributes to insulin resistance *(10, 12)*.

1.3. Treatments for obesity and T2DM

Although lifestyle interventions (diet and physical exercise) remain the basic component for mild T2DM or prediabetes and obesity, pharmacological and surgical approaches have been developed for patients who struggle to maintain glycaemic control and/or weight loss *(12, 14)*.

1.3.1. Glucose lowering agents

1.3.1.1. Sulphonylureas

Sulphonylureas (such as glibenclamide) and glinides (such as nateglinide) inhibit the K_{ATP} channels expressed in beta-cells to stimulate endogenous insulin secretion, which causes hyperinsulinaemia to

overcome insulin resistance *(14)*. Although sulphonylureas are effective insulin secretagogues that causes an initial decline in fasting blood glucose levels, they do not provide long term protection of beta-cell function and may even accelerate beta-cell failure *(15–17)*. Sulphonylurea use is commonly associated with weight gain and recurrent hypoglycaemia (when blood glucose levels reach dangerously low levels) *(14)*.

1.3.1.2. Thiazolidinediones

Thiazolidinediones (TZDs such as rosiglitazone, pioglitazone and troglitazone) are insulin sensitising agents which enhance insulin sensitivity in the skeletal muscle, liver and adipose tissue, as well as augmenting and preserving beta-cell function *(14)*. TZDs exert multiple insulin-sensitising effects, such as increasing peripheral glucose uptake, reducing systemic inflammation and stimulating lipogenesis in adipose tissues through the PPAR-γ and PGC-1α signalling pathways *(14)*. TZDs are clinically effective in lowering stabilising glycated haemoglobin (HbA1c) levels in the long term *(14)*. Amongst the side effects of TZDs are reduced bone density, weight gain and fluid retention *(14)*. TZDs are either withdrawn or are currently not frequently used in the clinic due to potential adverse effects such as hepatotoxicity and risk of bladder cancer *(14)*.

1.3.1.3. Insulin

Insulin is used for the treatment of T1DM, although under severe cases of T2DM insulin would be considered as the last-resort treatment option when all other pharmacological interventions fail in normalising blood glucose levels *(18)*. Blood glucose levels needs to be closely monitored in patients given insulin injections to prevent hypoglycaemia *(18)*. Like sulphonylureas, insulin therapy also causes weight gain *(18)*. Recent developments in insulin analogues and the closed-loop insulin pump (artificial pancreas) aim to improve glucose monitoring and reduce hypoglycaemia risk *(19, 20)*.

1.3.1.4. GLP-1 Modulators

Recently developed antidiabetic agents target the incretin hormone Glucagon-like peptide 1 (GLP-1) *(14)*. The incretin effect, which is associated with higher insulin secretion in response to oral compared with intravenous administration of glucose due to the augmentation of insulin release by gut hormones such as GLP-1, is impaired during T2DM *(14, 21, 22)*. Dipeptidyl peptidase 4 (DPP4) inhibitors (such as sitagliptin) inhibit circulating GLP-1 degradation and prolong the half-life of endogenous active GLP-1 *(14)*. DPP4 inhibitors increase insulin secretion but have modest effects in lowering HbA1c *(14)*. GLP-1 receptor agonists (such as liraglutide and exenatide) pharmacologically mimic the actions of GLP-1, stimulating insulin secretion and normalising glycaemic control *(14)*. GLP-1 receptor agonists also inhibit glucagon secretion, promote weight loss, delay gastric emptying and improve plasma lipid profiles *(14)*. GLP-1 modulators are generally safe and well tolerated, although

there is mixed evidence on their association with pancreatitis and GLP-1 receptor agonists have been reported to cause nausea *(14)*.

1.3.1.4. SGLT2 Inhibitors

Sodium/glucose co-transporter 2 (SGLT2) inhibitors (such as dapagliflozin and canagliflozin) block glucose reabsorption in the kidneys, leading to excretion of glucose in urine to reduce plasma glucose *(14)*. SGLT2 inhibitors have been reported to be effective glucose-lowering agents that also improve insulin sensitivity *(14)*. However, their efficacy is mitigated to some extent by the compensatory expression of SGLT1 to increase glucose reabsorption in the kidneys, as well as reported side effects associated with reduced blood pressure and urinary tract infections *(14)*.

1.3.2. Appetite regulating drugs for Obesity

Pharmacological approaches for obesity are only reserved for cases of moderate to severe obesity, and there is not an ideal medication so far *(12)*. The most widely used treatment is lifestyle intervention, and many appetite regulating drugs only augment better adherence to lifestyle interventions *(12)*.

1.3.2.1. Pancreatic lipase inhibitors

Pancreatic lipase inhibitors (such as orlistat and cetilistat) reduce dietary lipid absorption in the intestines, which reduces circulating free-fatty acids, modulates adipokine release and causes modest weight loss *(23)*. Orlistat is most effective when used in combination with a low-calorie diet and exercise to promote the weight loss benefits of T2DM *(23)*.

1.3.2.2. Lorcaserin

Lorcaserin is a selective small-molecule agonist of the 5-HT or serotonin receptor (5HT2C), which suppresses appetite by targeting serotonergic neurotransmission in the hypothalamus *(23)*. Lorcaserin preferentially inhibits 5HT2C over its isoform 5HT2B, which has led to the withdrawal of other serotonergic inhibitors from clinical use due to its association with cardiovascular disease *(23)*. Lorcaserin has been demonstrated to cause effective weight loss by 4.5-10% in two clinical trials and was approved for the treatment of obesity by the FDA in 2012 *(23–25)*. Side effects such as headache and nausea have been reported *(23)*.

1.3.2.3. Naltrexone and Bupropion combination treatment

Naltrexone is an opioid receptor antagonist, whilst bupropion is a dopamine and noradrenaline reuptake inhibitor, both of which have been reported to suppress appetite by targeting pro-opiomelanocortin (POMC) neurons in the hypothalamus *(23)*. Combination treatments of Naltrexone

and Bupropion were shown to be more effective in achieving effective weight loss and appetite suppression compared to modest effects achieved by monotherapy regimens or placebo *(23)*. Side effects include nausea, vomiting and constipation *(23)*.

1.3.3. Bariatric surgery

Bariatric surgery is a clinically available option for the treatment of severe obesity (clinical criteria vary, but often it is only considered if BMI is >40kg/m^2 or >35kg/m^2 plus comorbidities) *(26)*. There are three commonly used surgical procedures in bariatric surgery *(26)*. Laparoscopic gastric banding involves placing an inflatable gastric band below the gastro-oesophageal junction, creating a small gastric pouch with a narrow stoma *(26)*. Vertical sleeve gastrectomy (VSG) places a staple line across the greater curvature of the stomach, reducing the stomach to ~15% of its original size *(26)*. Roux-en-Y gastric bypass (RYGB) is a more surgically complex approach that involves transection of the upper stomach and dividing the small intestine at the jejunum *(26)*. The first anastomosis is then made between the stomach pouch and the distal jejunum (forming the Roux limb), bypassing the stomach and duodenum *(26)*. A second anastomosis is made between the remaining stomach, duodenum and upper jejunum, and the roux limb (forming the Biliopancreatic limb) *(26)*.

The Swedish Obese Subjects study was the first prospective clinical study to investigate the long-term effects of bariatric surgery (RYGB and gastric banding) in over 2,000 individuals with obesity and T2DM *(27–30)*. The study reported significant weight loss by 25% and 14% for RYGB and gastric banding after 10 years, respectively *(27)*. The study also reported drastically improved glycaemic control (and resolution of T2DM), decreased hyperlipidaemia and reduced overall mortality rates *(27, 30)*. The Longitudinal Assessment for Bariatric Surgery (LABS) study conducted in the US demonstrated significant weight loss associated with RYGB (31.5%) and gastric banding (15.9%) after 3 years in addition to similar improvements in risk factors for comorbidities *(31)*.

The exact mechanisms underlying the effects of bariatric surgery in weight loss and glycaemic control are still debateable *(32)*. Weight loss effects in bariatric surgery have been attributed in some studies to caloric malabsorption and altered levels of bile acids in the gut and circulation *(32)*. Bariatric surgery also affects central control of food intake, since patients often report a loss of appetite following bariatric surgery *(32, 33)*. More exaggerated release of the gut hormone Peptide YY (PYY) has been reported post-surgery, which acts as an anorexigenic hormone via signalling to the appetite regulating centres in the hypothalamus and brainstem *(32)*. Studies in PYY receptor knockout mice showed reduced effects of RYGB on weight loss, demonstrating the potential importance of this peptide in controlling food intake *(34)*.

Although there is some evidence that the weight-dependent effects underlie improved glycaemic control after bariatric surgery, changes in glucose metabolism have been observed immediately after surgery in T2DM, suggesting weight-loss independent mechanisms *(35)*. The foregut hypothesis suggests that exclusion of the proximal small intestine is associated with reduced circulating levels of an "anti-incretin" signal which counters incretin-stimulated insulin secretion *(35–37)*. In support of this idea, studies involving duodenal-jejunal bypass surgery in rodents demonstrated normalisation of glycaemic control with limited effects on body weight and food intake *(36, 37)*. The hindgut hypothesis suggests enhanced delivery of nutrients to the distal GI tract, which causes exaggerated GLP-1 release to stimulate insulin secretion, beta-cell function and mass *(35, 38, 39)*. Experiments involving the GLP-1 receptor antagonist Exendin 9-39 and antibodies against the receptor have demonstrated the roles of GLP-1 in glycaemic control after RYGB or VSG *(40, 41)*. Other studies have reported adaptations in the alimentary (roux) limb such as tissue hypertrophy, increased glucose utilisation and transcriptomic changes *(42, 43)*.

1.4. Metformin in the clinic

Currently, metformin is the world's most prescribed drug and is recommended first-line monotherapy for T2DM by most clinical guidelines, including the American Diabetes Association (ADA) and European Association for the Study of Diabetes (EASD) *(44, 45)*.

1.4.1. Brief history of metformin

The history of metformin could be linked to *Galega officinialis*, a medieval medical herb found in Europe which had been used to treat symptoms of diabetes from as early as 1772 *(46, 47)*. Chemical analysis of the herb from the mid-1800s found that it was rich in Guanidine, a chemical which was later demonstrated to lower blood glucose levels in animals in 1918 *(47, 48)*. The chemical development of biguanides was first reported in the 19th Century, which formed the basis of metformin (dimethylbiguanide) synthesis by Werner and Bell in 1922 *(49)*. Metformin was first reported to lower blood glucose levels in animals in 1929, although it was temporarily ignored along with other guanide drugs for over a decade due to the widespread availability of insulin and the reported toxicity associated with guanides *(47, 50, 51)*.

Interest into the glucose lowering effects of metformin was revived in the 1950s when Jean Sterne, a clinician from Aron Laboratories in Suresnes, France, further investigated the physiological effects of metformin and other biguanides (such as phenformin) in animal studies *(47)*. This led to the first breakthrough clinical study demonstrating that metformin reduced blood glucose levels and eliminated the need for insulin in patients with maturity onset diabetes in 1957 *(47, 52)*. At the same

time, similar clinical studies were also reported for phenformin, which showed greater glucose lowering efficacy than other biguanides, resulting in its approval for clinical use *(53–55)*. However, in the 1970s, the University Group Diabetes Programme trial in the USA and other clinics in the USA and Europe reported lactic acidosis associated with phenformin use, which led to its withdrawal in 1978 *(56–58)*. Interest into metformin resurfaced in the 1980s due to its better reported safety profile and its action as an insulin sensitizer during a time when the concept of insulin resistance was becoming central to the understanding of T2DM pathophysiology *(47, 59–64)*. Metformin was reconsidered for clinical use by the US food and drug administration (FDA) in 1986, which led to its approval in the US in 1994 for the treatment of T2DM (although metformin has been introduced to treat diabetes in the UK and Europe from as early as 1958) *(47)*.

1.4.2. Metformin as a glucose-lowering agent to treat T2DM

The therapeutic efficacy of metformin as a glucose-lowering agent for the treatment of T2DM was best demonstrated in a 1995 clinical trial from DeFronzo et al., involving 289 obese patients with uncontrolled T2DM *(65)*. Daily administration of metformin for 29 weeks was reported to lower the mean fasting plasma glucose by 2.9mmol/l compared to the placebo group, whilst HbA1c also decreased by 1.4% *(65)*. A subsequent clinical study involving 451 patients with T2DM demonstrated that the glucose-lowering efficacy of metformin was dose dependent, whereby 500mg metformin treatment for 14 weeks resulted in a reduction in HbA1c by 0.6%, whereas 2000mg treatment resulted in decrease in HbA1c by 2.0% *(66)*.

A landmark study investigating the long-term glucose-lowering efficacy of metformin is the UK Prospective Diabetes Study (UKPDS), a randomised trial which recruited 1,704 overweight patients with T2DM with two primary aims; (1) to investigate the effects of metformin on glucose control and (2) to compare the glycaemic efficacy of metformin with sulphonylureas chlorpropamide and glibenclamide, and insulin as separate monotherapies *(44)*. The study was conducted over a period of 10 years *(44)*. The UKPDS trial reported decreased median HbA1c levels (metformin lowered HbA1c levels to 7.4% whilst conventional treatment groups achieved 8.0%) as well as reduced risk of diabetic complications *(44)*. Compared to insulin and sulphonylureas, metformin was the most effective at decreasing other diabetes-related endpoints and incidences of death *(44)*.

Clinical observations from the A Diabetes Outcome Progression Trial (ADOPT) was reported in 2002, which compared the glycaemic efficacy of metformin with glibenclamide and the thiazolidinedione rosiglitazone as monotherapies in 4,360 recently diagnosed T2DM patients from 500 centres across Europe, Canada and North America *(16)*. After 5 years, 21% of patients in the metformin group experienced glycaemic failure (classified as the inability to maintain blood glucose levels below

10mmol/l) compared to 15% and 34% of patients in the rosiglitazone and glibenclamide groups, respectively *(16)*. Similarly, patients on metformin maintained intermediate optimal glycaemic control (as measured by HbA1c) with a mean duration of 45 months compared to 57 months for rosiglitazone and 33 months for glibenclamide, respectively *(16)*. Patients from the metformin group experienced intermediate improvement in insulin sensitivity compared to the other treatment groups, but also experienced a gradual decline in β-cell function *(16)*. The outcomes from the ADOPT trial demonstrated that despite achieving glucose-lowering efficacy compared to insulin secretagogues, metformin monotherapy was insufficient to prevent gradual β-cell failure and progression of T2DM *(16)*.

Clinical trials have also demonstrated improved efficacy of metformin in combination therapy with other antidiabetic agents for the management of T2DM (Reviewed in *(45)*). The original study by DeFronzo *et al.*, showed that metformin treatment in combination with glibenclamide for 29 weeks gave superior glycaemic outcomes (as measured by HbA1c reduction) compared to glibenclamide monotherapy and switching back to metformin monotherapy later in the trial did not produce further clinical benefit *(65)*. A 16-week trial involving 390 T2DM patients demonstrated that metformin and insulin combination therapy also improved glycaemic control and reduced dependence on insulin *(67)*. Another randomised controlled trial in 96 patients with poorly controlled T2DM demonstrated that metformin and insulin treatment caused the greatest reductions in HbA1c levels after 1 year compared to other combination therapies involving insulin and glibenclamide or insulin treatment alone *(68)*. A clinical study involving combination of insulin sensitizers metformin and troglitazone for T2DM treatment showed additive benefits in glycaemic control in a cohort of 29 T2DM patients, which was associated with differences in the drugs' mechanisms of action (metformin reduced hepatic glucose production, whilst troglitazone increased peripheral glucose handling) *(69)*. Recent studies have explored combination therapy involving metformin and novel antidiabetic agents such as DPP4 inhibitors, GLP-1 receptor agonists and SGLT2 inhibitors *(70–75)*.

1.4.3. Metformin and the prevention of T2DM

The role of metformin in the prevention of T2DM was explored in two studies: Diabetes Prevention Programme (DPP) and Diabetes Prevention Programme Outcome Study (DPPOS) *(76–80)*. The DPP was a double-blinded, randomised trial involving 3,234 participants at high risk of developing T2DM, who were given metformin or moderate-intensity lifestyle intervention from 1996 to 2001 *(78, 79)*. During the 3.2 year follow-up of the trial, daily metformin administration was associated with a 31% reduced risk in diabetes incidence and significantly lowered mean HbA1c compared to placebo *(79)*. Following the DPP trial, 88% participants were enrolled in the follow-up DPPOS post-randomisation programme involving continued metformin therapy and lifestyle-intervention *(76, 77, 80)*. From the DPPOS study,

metformin use was associated with an 18% reduced risk in developing T2DM although glycaemic, metabolic and cardiovascular complications were no different from placebo *(77)*. The results from the DPP/DPPOS studies show the additional benefit of metformin in reducing the risk of T2DM development, in addition to its role in treating patients living with diagnosed T2DM *(76, 77, 80)*.

1.4.4. Effect of metformin on body weight

About half of the clinical studies investigating metformin in T2DM reported weight loss after treatment whilst there are no studies to date reporting an indication of weight gain associated with metformin use (Reviewed in *(81)*). The ADOPT trial reported that patients from the metformin group lost weight over 4 years whereas the other antidiabetic agents (particularly participants on Rosaglitazone) were associated with weight gain *(82)*. Other clinical studies demonstrated that metformin combination therapy with insulin or sulphonylureas either resulted in significant weight loss, or reduced the weight gain effects caused by insulin or sulphonylurea monotherapies *(83–86)*. A trial involving magnetic resonance imaging in T2DM subjects showed that metformin use reduced visceral fat mass, as opposed to rosiglitazone *(87)*.

Multiple trials in obese but non-diabetic patients have also investigated the weight-loss effects of metformin *(81)*. The Biguanides and Prevention of Risks in Obesity (BIGPRO) study was the first to show a trend towards weight loss and metformin treatment in 324 abdominally obese patients *(88)*. A trial involving 150 obese women demonstrated that metformin treatment for 6 months displayed comparable efficacy in weight loss, BMI and waist circumference compared to other clinically approved weight loss drugs sibutramine and orlistat *(89)*. The DPP study involving participants with impaired glucose tolerance (but not diagnosed with T2DM) also reported significantly greater weight loss and reduced waist circumference in the metformin treated group (particularly those who were highly adherent to their medications) compared to placebo *(79)*. The follow up DPPOS study similarly reported slightly greater weight loss in the metformin group compared to placebo (~2% vs 0.2%) after 10 years associated with metformin adherence *(76)*.

Multiple meta-analyses of numerous clinical trials demonstrated significant weight reduction associated with metformin therapy compared to patients on sulphonylurea treatment (which increased body weight in every trial), but not in the placebo group *(63, 90, 91)*.

From the reported clinical studies to date, the weight loss effects of metformin have been modest and were not entirely consistent across all of the studies *(81)*. However, metformin is unlike most antidiabetic agents in that it does not cause weight gain and has been reported to limit the weight gain effects caused by insulin and sulphonylureas when given as combination therapy *(83–86)*.

1.4.5. Other clinical effects and applications of metformin

The effects of metformin in cardiovascular disease (CVD) were demonstrated in the UKPDS study, which reported that metformin use significantly reduced the incidence of cardiovascular events in 344 obese patients *(44)*. Similarly, the DPP study reported that metformin lowered CVD risk factors such as lipoprotein fractions, C-reactive protein and tissue plasminogen activator *(79, 80)*. Although long term monitoring in the DPPOS study did not reveal differences in CVD risk factors compared to placebo, metformin use reduced the presence of coronary artery calcium levels, suggesting reduced atherosclerotic plaque formation *(77)*. However, no substantial conclusions on the clinical benefits of metformin and cardiovascular disease were reached in a recent meta-analysis based on 4 clinical trials which collected data on CVD outcomes, due to the scarcity of data *(92)*.

Metformin is also clinically approved to treat women with polycystic ovarian syndrome (PCOS), based on studies in the 1990s reporting that metformin reduced testosterone levels in about 20-25% of women with PCOS and improved metabolic and reproductive abnormalities such as irregular menstruation and glucose intolerance *(93, 94)*. The clinical benefit of metformin has been associated with improved insulin sensitivity and correction of hyperinsulinaemia, although the exact mechanisms are still unclear *(93, 94)*.

Several clinical studies and meta-analyses have highlighted the benefits of metformin for the treatment of gestational diabetes mellitus (GDM) (Reviewed in *(95)*). The Metformin in Gestational Diabetes (MiG) trial, which investigated 751 women with GDM randomised for metformin or insulin treatment, showed reduced incidence of severe hypoglycaemia and no safety problems (such as short-term effects on fetal development) with metformin compared with insulin *(96)*. However, since metformin is able to cross the placenta, many of the current concerns are associated with potential long-term effects on the child, and long term studies are currently ongoing *(95)*.

Beyond cardiometabolic and endocrine disorders, the effects of metformin on cancer have also been explored *(97)*. Several meta-analyses of case-control and cohort studies have concluded that metformin use in diabetic patients was associated with as much as 10-40% reduction in incidence of, and mortality from, lung, breast, colon, liver, pancreas, prostate and endometrial cancers *(98–108)*. To date, there are 17 reported clinical trials investigating the effects of metformin on cancer-related biomarkers (Reviewed in *(97)*). Several clinical trials involving patients with breast, prostate and endometrial cancers reported that oral metformin administration prior to surgery resulted in reduced expression of Ki-67 proliferation markers in tumour biopsies *(109–114)*. Metformin treatment for 1 month has also been reported to decrease the numbers of aberrant crypts in multiple colorectal cancer prevention studies *(115)*. From this clinical and epidemiological evidence, several phase III

clinical trials are ongoing to provide more robust evidence in assessing the effects of metformin in cancer *(97)*.

1.4.6. Side effects of metformin use

As previously discussed in section 1.4.1, metformin generally has a better safety profile compared to other biguanides *(45)*. The most common side effects associated with oral metformin use are GI related, including abdominal discomfort, diarrhoea and nausea *(45)*. A small number of patients have severe GI intolerance to metformin, associated with gene variants in metformin transporters (See section 1.4.7 below) *(45, 116–118)*. By contrast to phenformin, the risk of metformin use and lactic acidosis is extremely rare, with 3-10 per 10,000 reported cases, which could have been attributed to reduced kidney clearance of lactate *(45)*. Therefore, severe kidney dysfunction (with a glomerular filtration rate of <60 ml min^{-1}) is a contraindication for metformin use, although metformin use is permitted in patients with mild or moderate impairment in kidney function *(45, 119)*. Some clinical studies (including DPPOS) also report Vitamin B12 malabsorption as a side effect of metformin use in 10% of patients and higher prevalence of peripheral neuropathy associated with chronic metformin use *(120, 121)*.

1.4.7. Genetic variants and patient responses to metformin

Genome-wide complex trait analysis (GCTA) showed that as much as 34% of the glycaemic response to metformin is determined by heritability, demonstrating a genetic contribution to the individual responsiveness to metformin *(122)*. Many studies have sought to identify the associated gene variants, which could identify potential mechanisms of metformin action as well as improving stratified medicine (Reviewed in *(123)*).

Initial genetic investigations into the metformin response were performed by investigating associations in candidate genes *(123)*. The DPP trial investigated 40 candidate genes (associated with monogenic obesity, diabetes, drug interactions and hormonal regulation) and their interaction with metformin response in overweight or obese subjects (see section 1.4.3) *(124)*. The study reported interactions in the genes encoding AMPK subunits *Prkaa1* and *Prkaa2*, AMPK regulatory kinase *Stk11*, and AMPK target genes *Pgc1a* and *Hnf4a* with the metformin response *(124)*. Moreover, associations were also reported in Sulphonylurea responsive genes, including *Abcc8* and *Kcnj11* with the metformin response *(124)*.

The first genome-wide association study (GWAS) investigating metformin pharmacogenetics was the GoDARTs study, which investigated 3,200 metformin-treated diabetic patients using electronic health data from hospitals in Scotland *(125)*. The study identified the variant rs11212617 located near the

locus encoding ataxia telangiectasia mutated gene (ATM) in chromosome 11, which was associated with 0.18% lower haemoglobin-A1c (HbA1c) levels in response to metformin treatment *(125)*. ATM encodes a serine/threonine kinase involved in cell cycle control and DNA repair, although the investigators showed that ATM regulates AMPK activation in hepatocytes (yet the specificity of the ATM inhibitor involved has been disputed) *(125, 126)*. Other studies replicated the association between ATM and the metformin response, although a separate cohort of 2,994 patients from the DPP study did not replicate any association, which could be due to differences in the ethnicity and genetic background of patients *(127, 128)*.

In a meta-analysis involving 10,557 participants of European descent, statistically significant associations were found in a variant rs8192675 identified within the *Slc2a2* locus and 0.17% greater reductions in HbA1c associated with metformin treatment *(129)*. Slc2a2 encodes the glucose transporter GLUT2, which is expressed in the liver and the gastrointestinal tract associated with hepatic glucose output and glucose absorption *(129)*. Expression studies also demonstrated that the same variant was associated with levels of GLUT2 expression in liver samples, suggesting the potential importance of GLUT2 in glycaemic control associated with metformin *(129)*. A recent study in a smaller cohort of 508 patients with recent onset T2DM in the German Diabetes Study (GDS) group also confirmed interactions with the GLUT2 variant and the metformin response *(130)*.

Perhaps the most studied genetic association of metformin treatment is *Slc22a1*, a highly polymorphic gene which encodes the metformin transporter OCT1 *(131–133)*. Initial candidate pharmacogenetic studies by Shu et al., demonstrated that healthy volunteers with reduced-function variants in *Slc22a1*, namely R61C, G465R, G401S and M420del displayed significantly higher blood glucose levels following an oral glucose tolerance test compared to individuals without these variants during metformin treatment *(131)*. These results were confirmed in a prospective South Danish Diabetes study showing that patients with more of these four variants achieved lower HbA1c reductions following metformin treatment, whereas radioisotope labelling in human liver samples showed that carriers of these variants had reduced tissue accumulation of metformin *(134, 135)*. The Rotterdam study identified rs622342 A>C polymorphism in *Slc22a1* associated with glycaemic response to metformin, although this finding was inconsistent with other studies in different cohorts *(136)*. However, the GoDARTs study failed to identify any associations between two of the reduced-function *Slc22a1* polymorphisms and glycaemic response to metformin in their cohort *(137)*. The GoDARTs study did identify associations with at least two reduced function variants of *Slc22a1* with gastrointestinal (GI) intolerance to metformin in 251 metformin-intolerant T2DM patients, suggesting the importance of OCT1 in metformin pharmacokinetics (see below section 1.6.2) *(117)*.

Multiple studies have identified genetic associations between the variant rs2289669 in the intron of *Slc47a1* (which encodes the metformin transporter MATE1) and improved efficacy of metformin in achieving HbA1c reduction *(124, 138–140)*. A recent IMI DIRECT trial involving 286 severely metformin-intolerant patients reported that, in addition to a variant found in OCT1, another variant rs3889348 in the *Slc29a4* was associated with reduced expression of the plasma membrane monoamine transporter (PMAT) in intestinal tissues and higher odds ratio of GI intolerance *(118)*. Another GWAS study from 10,251 T2DM patients with a history of cardiovascular disease in the ACCORD trial identified common variants in the *Cpa6* (encoding the carboxypeptidase A6) and *Prpf31* (encoding pre-mRNA processing factor 31) that were associated with better and worse glycaemic responses to metformin, respectively *(141)*.

The genetic studies highlight novel genes associated with metformin response and gastrointestinal intolerance and provide insights into the mechanisms of metformin action. However, the variants so far identified have a very minimal effect of the metformin response (most variants contribute to <1% of the difference of metformin treatment in the glycaemic response), suggesting that there are still yet to be identified variants that warrant investigation *(123)*.

1.5. Background of the digestive system and the gastrointestinal tract

The digestive system includes the GI tract and its accessory organs, the liver, gallbladder and the pancreas. The GI tract is the centre of nutrient absorption and an important site of exocrine and endocrine secretions. A physical barrier guarding against ingested toxic chemicals and microbial and viral insults, the GI tract also hosts a biodiverse microbiota which regulates local gut interactions and is implicated in inter-organ physiology and disease *(142)*. The GI tract is also richly innervated by the enteric nervous system and communicates with the central nervous system to regulate appetite *(143)*. Within the GI tract, the stomach is important in mechanical and chemical digestion of foodstuffs, whilst regulation of stomach emptying controls the rates of nutrient absorption in the small intestine. The three parts of the small intestine (the duodenum, jejunum and ileum) are the primary sites of nutrient absorption. The different parts of the small intestine differ considerably in cell composition, protein expression and gastrointestinal functions (including nutrient transport and hormone secretion) *(144)*. The colon is divided into the proximal colon, distal colon and the rectum. The colon is involved in the reabsorption of water and electrolytes and storing undigested material before excretion as faeces.

Within the accessory organs of the digestive system, the liver produces bile, which is then transported into the gallbladder for storage before release into the small intestinal lumen. The liver is also essential in regulating blood glucose levels by regulating glucose storage and endogenous glucose production. Bile acids are involved in the emulsification of fats and aids in absorption. The exocrine pancreas secretes digestive enzymes and bicarbonates to neutralise the acidity of the luminal contents, whilst the endocrine pancreas secretes insulin and glucagon necessary for systemic glycaemic control.

1.5.1. The small intestinal epithelial architecture

The intestinal epithelia are the second largest tissue in the body, consisting a complex monolayer of stem cells and different cell types involved in absorption of nutrients and secretion of mucus, hormones and immune mediators *(142)*. The epithelial layer is highly dynamic and undergoes a cycle of renewal every 3-5 days in the small intestine *(142)*. Small intestinal tissue homeostasis is highly organised into crypt-villus structures (see Figure 1.1) *(142)*. At the base of the crypts, invaginates in the intestinal lumen, reside adult stem cells - pluripotent cells which self-renew and are responsible for providing the sources of new intestinal epithelial cells *(142, 145–148)*. Also located in the stem cell niche are Paneth cells, which secrete antimicrobial chemicals such as defensins and lysozymes to protect the stem cell pool and provide nutrients and paracrine factors necessary for stem cell maintenance *(142, 149, 150)*.

Continuously dividing intestinal stem cells give rise to progenitors called transit amplifying cells, which rapidly proliferate but are committed to a particularly lineage *(146, 151, 152)*. Once the cells leave the transit amplifying zone and begin to mature by migrating towards the villus, the cells differentiate into one of six intestinal epithelial cell types with specialised functions *(142)*. The majority of cells are absorptive cells known as enterocytes, which maximise the surface area for transport and absorption of digested nutrients *(142, 153, 154)*. M cells resides in Peyer's patches which sense and transport antigens from the lumen to lymphoid cells *(155, 156)*. Less than 5% of differentiated cells are secretory cells. These include goblet cells, which secrete mucus coating the epithelial layer *(157)*, different subtypes of enteroendocrine cells *(158–160)*, tuft cells, involved in host immunity and helminth defences *(161, 162)*, and Paneth cells *(142, 149)*.

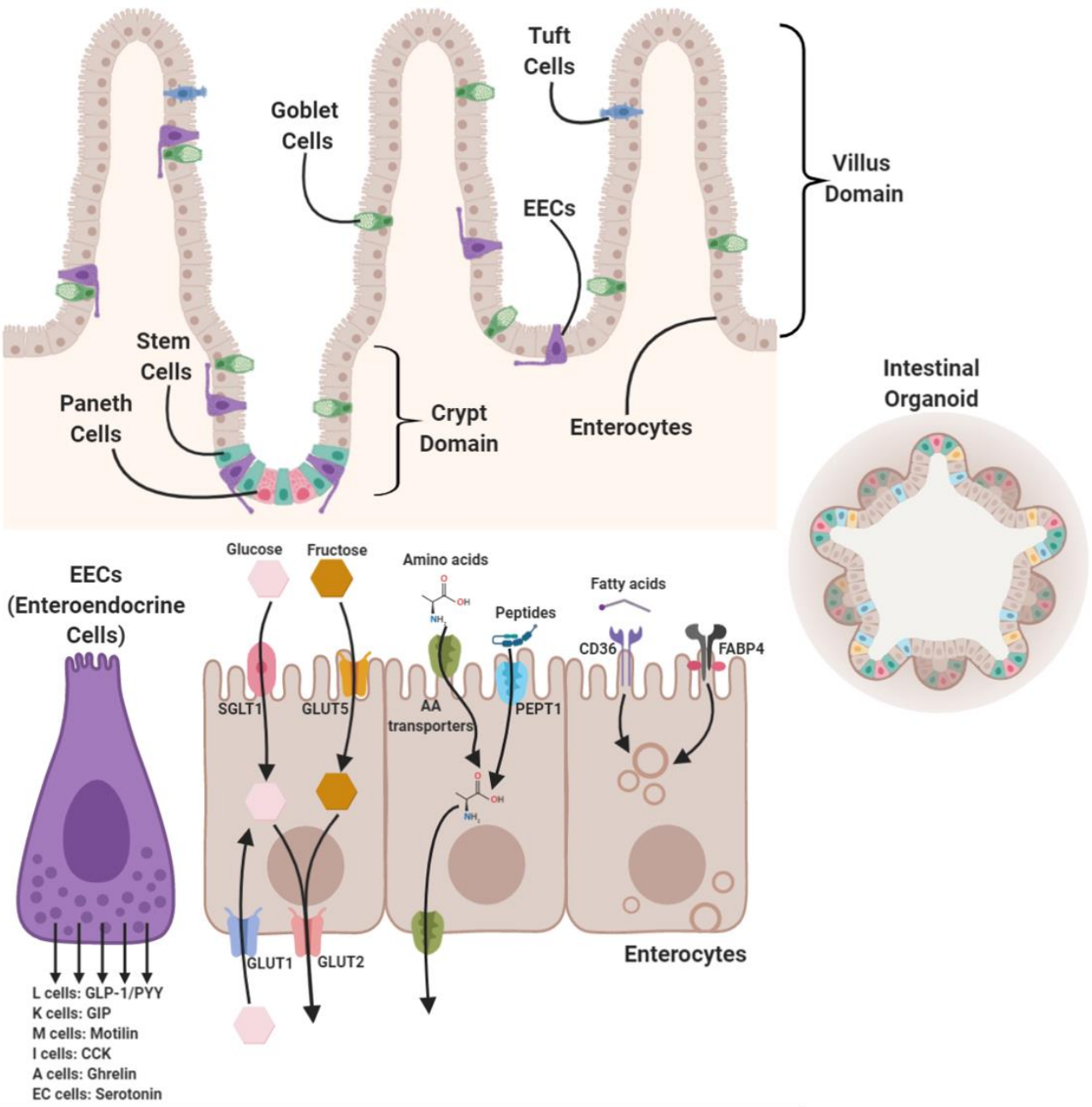

Figure 1.1. The architectural organisation of the gastrointestinal tract. Above: the cellular components of the intestinal epithelium, including the crypt and villus domains. The different cell types in the intestinal epithelium are labelled (M cells are not included in the diagram). Picture of an intestinal organoid is shown on the right. Below: the expression of different transporters involved in nutrient transport in enterocytes and functions of enteroendocrine cells.

Maintenance of the crypt-villus axis requires coordinated growth factor gradients, predominantly WNT and BMP *(142)*. WNT factors are secreted by Paneth cells and mesenchymal cells at the base of the crypt (telocytes) that maintain the intestinal stem cell pool, with less WNT signalling further from the base of the crypts *(149, 163–169)*. At the crypt-villus junction, BMP growth factors are abundant, which induce epithelial cell maturation, whilst BMP inhibitors are released by mesenchymal cells at the crypts, to establish a BMP gradient *(170–173)*. EGF and TGF-α ligands are secreted by Paneth cells to maintain an intestinal stem cell pool at the base of the crypts *(149)*. Notch signalling regulates the fate of neighbouring progenitor cells towards either absorptive or secretory lineages via lateral inhibition *(151, 157, 160)*.

1.5.2. Enterocytes and nutrient absorption

Intestinal enterocytes are absorptive cells which encompass >90% of epithelial cells in the GI tract. On the apical side, enterocytes contain microvilli facing the lumen of the intestine whilst the basolateral side faces the blood supply and neurons innervating the GI tract *(174)*. Enterocytes express different transporters according to their apical-basal polarity to enable sensing and transport directionality of digested nutrients from the lumen into the blood (see Figure 1.1) *(174)*. Enterocytes predominantly transport digested carbohydrates as free glucose and fructose *(174)*. The cells express the sodium-dependent glucose co-transporter SGLT1 on the apical side which actively imports glucose using the inward sodium gradient, and the facilitative glucose transporter GLUT2 on the basolateral side for passive transport of glucose out into the bloodstream *(174)*. Fructose transport is mediated by GLUT5 mediated uptake on the apical side, and exit via GLUT2 *(174)*. Proteins are either transported as di- or tri-peptides via the H^+ dependent peptide transporter PEPT1 which are then hydrolysed into amino acids in the cytosol, or as free amino acids via apical amino acid transporters, and subsequently extruded from the cells via basolateral amino acid transporters *(174)*. Free fatty acid uptake is mediated by passive diffusion as micelles or transported through cluster of differentiation 36 (CD36) or fatty acid transport protein 4 (FATP4) *(174)*. Short chain fatty acids are transported in colonocytes via monocarboxylate transporters such as SCMT1 or MCT1-4 *(174)*.

1.5.3. Intestinal nutrient metabolism

The small intestine is a highly metabolically active organ that sustains the energy demanding processes of nutrient digestion and absorption *(175, 176)*. Initial studies using intestinal perfusion models have identified glucose and glutamine as the main sources of fuel utilised by intestinal cells *(177–185)*. A recent study by Jang *et al.* measured arterial and venous differences in metabolite concentrations from 11 different organs in pigs to study organ-specific metabolite production and consumption, and reported that the intestines have the greatest absolute uptake flux of glucose and amino acids compared to other organs *(186)*. Other studies have demonstrated the heterogeneity of nutrient

metabolism amongst different cell types, reflecting intestinal stem cell renewal and cell differentiation along the crypt-villus axis *(150, 187–189)*.

1.5.4. The GI tract as an endocrine organ

The intestinal epithelium contains enteroendocrine cells (EECs), which are responsible for the release of gut hormones into the circulation such as GLP-1 and PYY (L-cells), GIP (K-cells), Cholecystokinin (I-cells), Motilin (M-cells), Secretin (S-cells), Ghrelin (A-cells) or Serotonin (enterochromaffin cells) (see Figure 1.1) *(190)*. The expression of the gut hormones overlaps between EECs and different EECs are localised with different frequencies along the GI tract *(190)*. Two clinically relevant gut hormones are GLP-1 and GIP, which are responsible for the incretin effect and potentiate postrandial insulin secretion *(190)*. Some gut hormones (such as PYY, Ghrelin and GLP-1) regulate food intake and appetite via receptor signalling in the hypothalamus and brainstem whilst others (such as CCK, Secretin and Motilin) play major roles in the regulation of GI secretion and motility *(190)*.

1.5.5. Intestinal organoids

Breakthrough studies by Sato *et al.,* Ootani *et al.,* and Spence *et al.,* demonstrated that intestinal stem cells are capable of growing into purely epithelial structures representing “mini-guts” in a three dimensional in vitro environment (see Figure 1.1) *(148, 165, 191)*. These intestinal organoids are capable of self-renewal and form a morphological hierarchy of differentiated cells with crypt and villus domains resembling the intestinal epithelium in vivo *(148, 165, 191)*. The intestinal organoid cultures could be grown from isolated primary intestinal crypts from the stomach, small intestine and colon, or even from a single intestinal stem cell expressing the biomarker Lgr5 *(148, 165, 191)*. Similar to a cell line, intestinal organoids could also be passaged and subjected to cryogenic freezing without any loss in viability *(148)*. Furthermore, gene modifications of intestinal organoids have previously been reported to generate transgenic organoids expressing fluorescent proteins *(192, 193)* , or editing of a mutant gene *(194)*. Other studies have reported that the transcriptomic signatures of single cells isolated from intestinal organoids faithfully reproduce intestinal cells in vivo *(144)*. Intestinal organoids have been used to study various physiological processes such as stem cell biology, enteroendocrine cell function and microbiome and immunity interactions, as well as disease modelling and drug screening approaches *(148, 149, 195–200)*. Thus, the development of intestinal organoids holds substantial promise as an in vitro system to study intestinal cellular mechanisms.

1.6. Mechanisms of metformin action in the liver and GI tract

1.6.1 Cellular mechanisms of action

Many of the cellular effects of metformin have focussed on mitochondria function, since metformin accumulates at high concentrations in the mitochondria compared to other cellular compartments *(201)*. Previous studies reported that high concentrations of metformin inhibit complex I (NADH dehydrogenase) of the mitochondrial electron transport chain and thereby impair mitochondrial respiration (see Figure 1.2) *(201–204)*. Consequent to inhibiting mitochondrial respiration, metformin has been reported to reduce flux of TCA cycle intermediates responsible for oxidative metabolism *(205, 206)*, increasing lactate production from glycolysis *(59, 64, 207, 208)* and indirectly activating AMPK through increased intracellular AMP levels (see Figure 1.2) *(209)*. Activation of AMPK has also been considered a central aspect of metformin action based on studies in primary hepatocytes *(210–214)*. AMPK regulates cellular processes through phosphorylation, but also regulates the transcriptome through the regulation of CREB co-transcriptional activators, CREB-binding protein (CBP), CRTC2 and SHP, which inhibit the ability of CREB to regulate gene expression *(210, 215–217)*. AMPK activation occurs downstream of the serine/threonine kinase LKB-1, which phosphorylates the α-subunit of AMPK *(218)*. However, metformin also mediates its effects through AMPK-independent mechanisms *(219)*. Experiments by Foretz et al., reported that mice with liver-specific knockout of AMPK showed normal glycaemic control compared to wild-type controls *(220)*. Other studies have highlighted the importance of inhibiting cAMP/PKA, mTORC1 and PPAR-α signalling pathways downstream of metformin action *(221–224)*.

1.6.2 Liver metabolism

Considering the important effects of the liver as an insulin-sensitive, metabolically important organ, and that metformin has been reported to be an insulin sensitizer, many of the early studies into the metabolic effects of metformin action were focused on liver function *(213)*. A key metabolic function of the liver is endogenous glucose production to regulate blood glucose levels (Figure 1.2). Numerous animal and human studies have since established that metformin inhibits endogenous glucose production to achieve its glucose lowering effects, although the exact mechanisms are unclear *(220, 225–227)*. However, some of the recent studies challenge this mechanism to show that metformin increases endogenous glucose production in HFD-fed mouse models and in patients with recent onset type-2 diabetes *(207, 228)*.

Metformin has also been associated with suppressing lipid biosynthesis and increasing fatty acid oxidation (FAO) in the liver through AMPK activation *(210, 211, 229, 230)*. This may aid in the

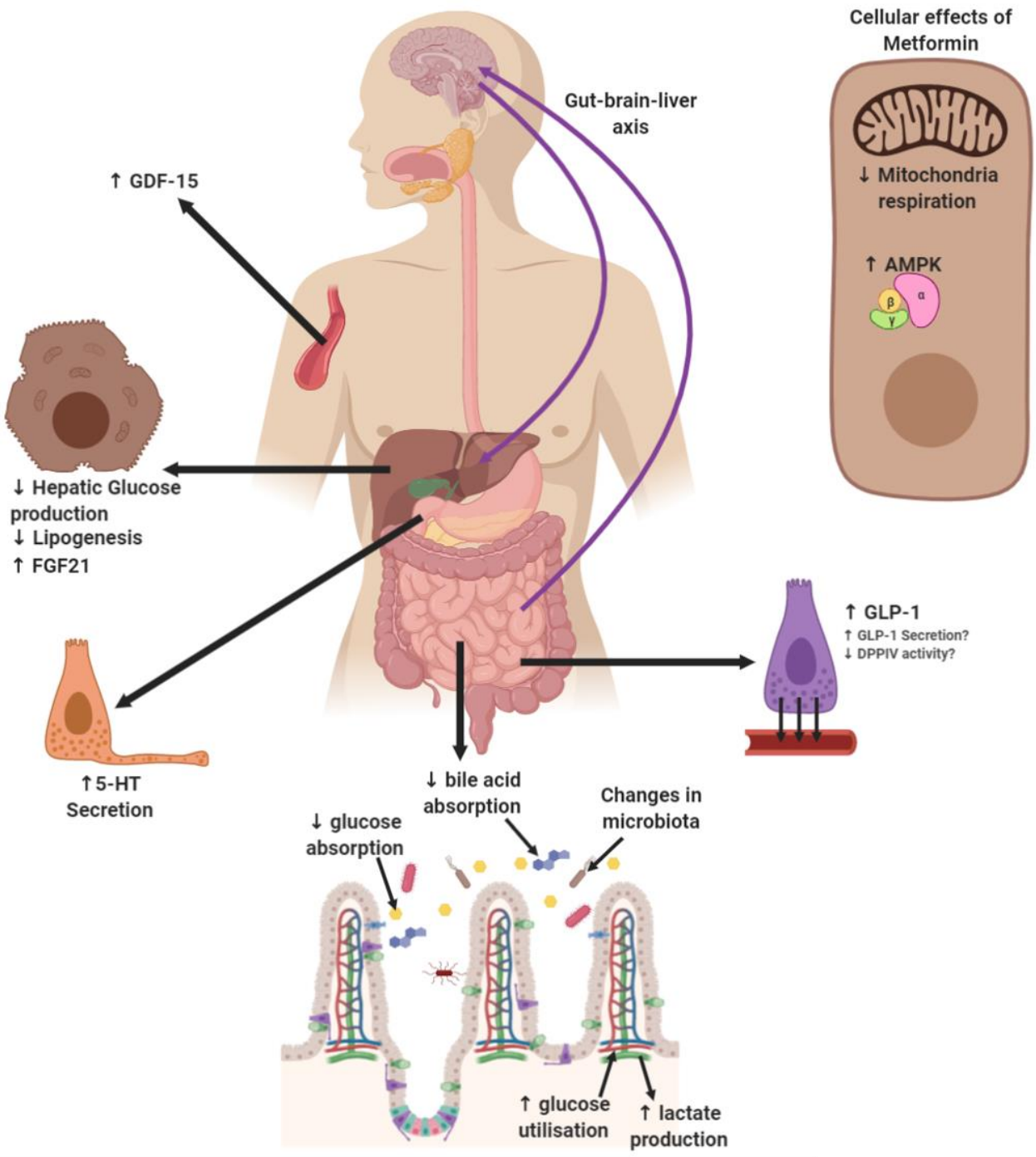

Figure 1.2. The effects of metformin on the various biological functions in the liver and GI tract.

protective mechanisms of metformin against Non-alcoholic fatty liver disease (NAFLD) and improving insulin sensitivity during diet-induced obesity *(231–233)*. These results were based on studies in liver-specific constitutive AMPK active mice *(231, 232)* and in mouse models with loss-of-function mutations in fatty acid metabolism genes Acetyl-CoA carboxylase genes Acc1 and Acc2 (downstream targets of AMPK activation) *(233)*.

1.6.3 Intestinal glucose handling and lactate production

There is also evidence that metformin directly regulates intestinal glucose handling (Figure 1.2). Several early studies demonstrated that administering biguanides or metformin in the intestinal lumen ex vivo or orally in vivo decreased intestinal absorption of glucose in isolated rat intestine models and the rate of glucose appearance in the blood, respectively *(234, 235)*. A recent study using position emission tomography-computed tomography (PET/CT) scan imaging following orally administered fluoro-2-deoxy-2-D-glucose F-2DG demonstrated that oral metformin administration delayed intestinal glucose transit in HFD-fed mice *(236)*. However, the underlying mechanisms and the glucose transporters involved, and whether metformin affects glucose absorption and intestinal glucose transit in humans have yet to be determined.

Conversely, effects of metformin on intestinal uptake of glucose from the blood have also been reported in mouse models and patients with T2DM *(237–239)*. Early experiments in rats demonstrated that intrajejunal administration of metformin increased accumulation of 2-deoxyglucose (2-DG) in intestinal tissues and increased the rate of plasma glucose disappearance when 2-DG introduced intravenously *(239)*. Studies from PET/CT scans showed that the intravenously injected non-metabolic glucose tracer 18Fluoro-2DG selectively accumulates in the gastrointestinal tract in metformin users *(237, 238)*. Increased uptake of the glucose tracer in the colon was associated with lower fasting plasma glucose levels in T2DM patients *(237)*.

Several studies performed in rodents and in human intestinal tissues demonstrated that metformin increased intestinal glucose metabolism into lactate, which was then released into the serosa fluid or splanchnic bed *(64, 116, 207, 239–242)*. Since oral metformin use has been associated with increased lactate levels in the intestinal wall and the plasma, the gastrointestinal tract could be a major site of lactate production in the plasma during metformin therapy *(64, 207, 240)*. Whether lactate production by the intestine is a cause for the side effects of lactic acidosis and gastrointestinal intolerance associated with metformin use remains to be determined.

1.6.4 The microbiome

The role of the microbiome is increasingly gaining attention, due to the important proposed roles of the microbiome in regulating intestinal function, metabolism and the gut-brain axis. Large-scale metagenome-wide studies have reported dysbiosis (dysregulation of the microbiome) in patients with obesity and T2DM *(243–245)*. Metformin altered the biodiversity of the microbiome in mouse models and human studies, partially reversing the dysbiosis in patients with T2DM and obesity (Figure 1.2) *(245–248)*. Analysis of 784 metagenomes from Swedish, Chinese and Danish cohorts demonstrated that metformin restored the abundance of *Escherichia* and butyrate producing bacterial strains and decreased the abundance of *Intestinibacter* strains in T2DM patients with dysbisosis *(247)*. Faecal microbiota transplant experiments from metformin treated donors into obese mice resulted in improved glucose tolerance *(246)*. Another metagenome-wide study in Columbian participants reported that metformin generally decreased the biodiversity of the microbiome and increased the composition of *Akkermansia Muciniphila*, a bacterial strain which increases mucus-secreting goblet cells *(248)*. Increasing *A.Muciniphila* populations in HFD-fed mice and obese human subjects was associated with improved glucose tolerance, weight loss and reduced inflammatory markers *(249, 250)*. Metformin also increased the intestinal abundance of *Lactobacillus* in HFD-fed mice, associated with restoration of glucose sensing in intestinal cells *(251)*.

1.6.5. Bile acid homeostasis

Bile acids are produced from cholesterol in the liver and released from the gallbladder into the intestinal lumen, to facilitate the absorption of lipids *(252)*. Bile acids are then reabsorbed into the circulation through enterocytes in the jejunum and ileum *(252)*. Metformin has been reported to stimulate bile acid pools in the small intestine through inhibiting active absorption of bile acids into the bloodstream (Figure 1.2) *(253–256)*. Mechanistically, metformin, through the activation of AMPK signalling, suppresses the activation of the farnesoid receptor FXR, a bile acid receptor involved in regulating bile acid production and reabsorption in the ileum *(257)*. Metformin treatment has also been associated with decreased serum FGF19 (human homologue of FGF15) levels in type 2 diabetes patients, a hormone expressed in the small intestine (particularly the ileum) which functions to inhibit bile acid production in the liver and promote gallbladder filling *(258–260)*. A recent study from Sun *et al.,* demonstrated that metformin use was associated with reduced abundance of the bacteria *Bacteroides Fragilis* in Chinese patients with early onset T2DM and poor glucose tolerance in mice *(260)*. Reduced *B. Fragilis* composition increased the secretion of the bile acid salt glycoursodeoxycholic acid (GUDCA), which inhibited FXR signalling and FGF19 secretion to regulate bile acid homeostasis *(260)*.

Increasing bile acids in the intestine could be a mechanism by which metformin reduces circulating cholesterol levels in the long term (as cholesterol is utilised for bile acid biosynthesis in the liver) *(254, 256)*. FXR activation by bile acids was associated with improved insulin sensitivity *(260)*. Furthermore, bile acids retained in the intestines could regulate osmotic fluid flow and may contribute to diarrhoea in patients with metformin intolerance *(256)*.

1.6.6. GLP-1 and incretin hormones

GLP-1, an incretin hormone produced from the preproglucagon gene by enteroendocrine L cells located predominantly in the ileum and colon, is associated with increased insulin secretion, decreased glucagon secretion and appetite suppression, resulting in lower plasma glucose levels *(261)*. Numerous clinical studies showed that oral metformin administration increased circulating GLP-1 levels in obese non-diabetic subjects *(262)* and in T2DM patients *(73, 263–267)*. A recent clinical trial demonstrated that co-application of a GLP-1 receptor antagonist Exendin 9-39 reduced the beneficial effects of metformin on glucose tolerance in patients with T2DM, demonstrating a contribution of GLP-1 in the glucose lowering effects of metformin *(263)*. Metformin modestly increased circulating PYY levels but did not increase circulating levels of GIP in one study *(264)*.

The mechanisms underlying metformin-elicited elevations in circulating GLP-1 levels are elusive. Numerous mouse and human studies have demonstrated that metformin reduces DPP4 activity, thereby increasing the half-life of active GLP-1 in the circulation by slowing its degradation *(262, 265, 266, 268–271)*. Other studies demonstrated that metformin directly stimulates GLP-1 secretion. Experiments in mice demonstrated that metformin increased the expression of proglucagon gene and GLP-1 protein levels in the intestines, as well as increasing GLP-1 secretion in intestinal cultures *(263, 272)*. However, there is no consensus regarding the precise secretion mechanisms targeted by metformin. Mechanisms such as insulin and WNT signalling *(273)*, muscarinic receptors *(274)* and AMPK signalling *(263)* have been identified. Metformin has also been demonstrated to indirectly increase GLP-1 secretion through increasing bile acids, which activate the receptor TGR5 to stimulate GLP-1 secretion *(267, 275)*.

1.6.7. New metabolic hormones- GDF-15 and FGF21

GDF-15 (Growth differentiation factor 15) has been identified as the top serum biomarker associated with metformin use in patients with Type 2 Diabetes (Figure 1.2) *(276, 277)*. GDF-15 is a stress response cytokine and a distant member of the transforming growth factor β (TGF-β) superfamily of growth factors *(278)*. Although almost every tissue type is capable of secreting GDF-15 in response to cellular stressors, under physiological conditions GDF-15 expression is only limited to the lung, liver, kidney, intestines, adipose tissues, and is produced in large amounts by placental trophoblasts *(279–*

287). Circulating serum GDF-15 concentrations are relatively high in healthy individuals *(288)* but are especially elevated with age, pregnancy, recent surgery, mitochondrial disease and metabolic diseases such as cachexia, obesity and T2DM *(reviewed in 12, 13)*. Various studies using transgenic knockout or overexpression studies in mice have demonstrated the importance of GDF-15 as an anorexigenic hormone *(291–294)*. Recent studies have identified the receptor for GDF-15 called GFRAL, expressed in the area postrema and Nucleus Tractus Solitarii (NTS) located in the brainstem, whose functions include the control of taste aversion *(295, 296)*.

Metformin has also been reported to elevate circulating levels of FGF21 in rodents and human subjects and elicit FGF21 expression in hepatocytes (Figure 1.2) *(297, 298)*. FGF21 is a hormone primarily released by the liver in response to low amino acid levels and high levels of carbohydrates *(299–301)*. Initially identified from a phenotypic screening of glucose uptake in adipocytes in an insulin-independent manner, FGF21 was later reported to greatly enhance insulin sensitivity in vivo via signalling in adipose tissues *(302, 303)*. Exogenous FGF21 administration has also been reported to suppress sweet taste preference and sugar intake, and decrease activation of central reward pathways *(301, 304, 305)*. Other studies reported that administration of FGF21 or its analogues reduced body weight and food intake in non-human primates and humans *(304, 306–308)*.

1.6.8. The gut-brain axis

A recent study demonstrates that oral metformin increases the activity of AMPK in the duodenum, which activates the gut-brain axis to limit hepatic glucose production *(212)*. In the proposed mechanism, metformin stimulates GLP-1 signalling in afferent nerve terminals, which relays the signal to NMDA receptors in the NTS (Figure 1.2). This in turn signals the liver to limit endogenous glucose production via hepatic vagus efferent nerves *(212)*. Interference in any part of the pathway, either via GLP-1 receptor antagonists, NDMA receptor inhibitors, or hepatic vagotomy, limited the effects of metformin on endogenous glucose production *(212)*. Metformin is reported to stimulate 5-HT secretion from enterochromaffin cells in human duodenal cultures *(309)*. It remains to be determined whether metformin elevates circulating 5-HT levels in vivo, which could otherwise influence nausea and vomiting centres through 5-HT_3 receptors *(310)*.

1.7. Metformin pharmacokinetics, bioavailability and biodistribution

Metformin is administered orally as a hydrochloride salt, which exists as a hydrophilic cation in solution at physiological pH, limiting its diffusional passage through lipid membranes *(311)*. Metformin is mostly absorbed in the small intestine (rarely in the stomach or the colon), with a bioavailability of

50-60%. In the circulation, metformin remains unbound to plasma proteins, and is not metabolised *(311)*. Most of the plasma metformin is cleared in the kidney and excreted in urine *(311)*.

1.6.1 Metformin tissue biodistribution

Studies by Wilcock and Bailey investigated the biodistribution of orally administered metformin in various tissues in wild-type and streptozotocin (STZ)-induced diabetic mice over a period of 24 hours *(312)*. Following a single dose, 14C-metformin accumulated at the highest concentrations in the proximal jejunum (147-2297µmol/kg), jejunal ileal junction (419-1173µmol/kg) and the distal ileum (276-3355 µmol/kg) of wild-type mice within the first four hours following administration *(312)*. After the small intestine, the kidneys also accumulated metformin at high concentrations (121-428 µmol/kg), whilst similar concentrations were reported in the colon (160-350 µmol/kg) *(312)*. The liver accumulated metformin at lower concentrations (37-182 µmol/kg) whilst metformin accumulation was modest in other tissues such as the white adipose tissue, skeletal muscle, heart and the brain *(312)*. Plasma levels of metformin did not reach beyond 50 µmol/kg when sampled from the hepatic portal vein or inferior vena cava *(312)*. Similar metformin biodistribution was also reported in STZ-induced diabetic mice *(312)*. Studies involving whole-body PET scan imaging of 11C-metformin biodistribution in human subjects reported similar findings, in which oral administered metformin accumulated predominantly in the small intestine, liver and kidneys *(313)*.

1.6.2 Intestinal metformin transporters

Since metformin is unable to freely diffuse through the plasma membrane, metformin transporters are required for intestinal metformin absorption *(116)*. Various metformin transporters have been identified, which include the organic cation transporter (OCT) family, plasma membrane monoamine transporter (PMAT), serotonin transporter (SERT), choline transporters (CHT) and multi-drug extrusion protein (MATE) *(314)*. Pharmacological and knock-down experiments in Caco-2 cells demonstrated that multiple metformin transporters, OCT1, PMAT, SERT and CHT are localised in the apical membrane responsible for metformin uptake, although CHT expression was not found in human intestinal tissues in other studies *(314)*. As discussed in section 1.4, pharmacogenetic studies have shown that gene variants in metformin transporters OCT1 and PMAT were associated with GI intolerance of metformin, supporting the important roles of these transporters in metformin transport in the gut *(117, 118)*. Studies of transport kinetics showed that whilst metformin was efficiently transported into cells from the apical side, this was more limited from the basolateral side of enterocytes, suggesting asymmetrical membrane localisation of metformin transporters *(315)*. This mechanism might explain the observations from biodistribution studies that metformin accumulates

at high concentrations in the small intestine relative to the circulation, as it is readily absorbed from the lumen but not readily released into the bloodstream *(312)*.

1.8. The importance of the GI tract in metformin action

In addition to the evidence for metformin accumulation in the intestines, other studies have altered the pharmacodynamics and pharmacokinetics of metformin to demonstrate that the GI tract is an important site of metformin action.

1.7.1 Routes of metformin administration

Pharmacokinetic studies attempted to investigate the primary site of metformin action in its glucose-lowering response *(311, 316)*. Stepensky *et al.,* assessed the effects of metformin administration in STZ-induced diabetic rats via different routes; intraduodenal bolus or infusions (administering metformin into the lumen of the GI tract), hepatic-portal infusion (administering metformin into the hepatic portal vein) and intravenous infusion *(316)*. Although metformin reached similar plasma concentrations with each route of administration, metformin administration via the intraduodenal route resulted in the most potent glucose-lowering effects, seconded by hepatic-portal infusion, whereas intravenous administration exhibited minimal effects *(316)*. Similarly, intravenous metformin injections in non-diabetic subjects did not significantly affect fasting plasma glucose, insulin, C-peptide or glucagon levels *(317)* and intravenous metformin injection in T2DM patients did not affect glucose disposal or endogenous glucose production *(318)*. These studies suggest that metformin administration from the lumen of the intestine is more efficacious compared to administration directly into the circulation.

1.7.1 Delayed release metformin formulations

A recent phase I clinical study compared the effects of immediate release metformin (metformin-IR) and an extended release formulation of metformin (metformin-XR, a variant formulation coated with a polymer matrix which slows the release of metformin in the gut to improve GI tolerance but having similar bioavailability and efficacy) to a delayed release metformin (metformin-DR) formulation in healthy subjects *(319)*. The metformin-DR formulation includes metformin encased in an enteric coat, which delays the dissolution of metformin until it reaches the ileum at a pH of 6.5, thus greatly delaying metformin absorption and decreasing plasma bioavailability by 50% compared to other metformin formulations *(319)*. In these cohorts, daily oral administration of metformin-DR for a period of 12 weeks enhanced glycaemic control (measured fasting plasma glucose levels and baseline HbA1c) with 40% improved potency compared to extended release metformin formulations *(319)*. The

metformin-DR formulation was also well tolerated, and plasma lactate measurements were similar compared to the placebo group *(319)*. Similar conclusions were also reached in two separate clinical trials comparing metformin-DR and metformin-IR in patients with T2DM, particularly in a larger cohort involving 571 subjects *(86, 320)*. Metformin-DR also elevated GLP-1 and PYY levels in the circulation *(86)*.

1.9. Aims of the Thesis

This thesis aims to establish the cellular effects of metformin action in intestinal cells. The results would provide further insight into the pharmacological effects of metformin on glycaemic control and weight loss.

The effects of metformin on the signalling and metabolic pathways in the liver have been well established. The gastrointestinal tract is an important site of metformin pharmacokinetics and accumulates at the highest concentrations, although the cellular mechanisms of how intestinal cells respond to metformin treatment are not well established. The first aim of this thesis is to explore changes in signalling and metabolic pathways and gene expression profiles using RNA-sequencing in 2D monolayer cultures from murine intestinal organoids in response to high dose metformin exposure (Chapter 3). The results from the RNA-sequencing data would inform on further investigations into responsive genes and pathways associated with metformin action.

Metformin is one of the very few antidiabetic agents that causes modest weight loss as monotherapy or reduce the effects of weight-gain of other antidiabetic agents when given in combination. The newly discovered anorexigenic hormone GDF-15 has been identified as a key biomarker associated with metformin use in T2DM patients. Experiments performed by Tony Coll and Stephen O'Rahilly have found that GDF-15 expression is upregulated in the small intestine in HFD fed mice, which may be responsible for the observed increased serum levels of GDF-15 in mice and humans *(321)*. Another aim of this study is to investigate the signalling pathways associated with metformin stimulated GDF-15 secretion in intestinal cells (Chapter 4).

The gastrointestinal tract is an important site of glucose absorption and consumption. Whilst evidence suggests that one of the glucose-lowering mechanisms of metformin is to reduce glucose absorption and increase glucose disposal in the gastrointestinal tract, the molecular mechanisms involved are not well understood. One of the aims of this thesis is to study the effect of metformin on the expression of glucose transporters in intestinal tissues from mice fed with HFD and short or long-term oral metformin gavage, and in 2D monolayer cultures from intestinal organoids, as well as the mechanisms regulating glucose flux in intestinal cells following metformin exposure (Chapter 5). Finally, the metabolic effects of metformin on nutrient metabolism are assessed via live-cell imaging of metabolites in intestinal epithelial cells and Seahorse bioassays (Chapter 6).

Chapter 2: Materials and Methods

2.1 Materials and Reagents

REAGENT/RESOURCE	SOURCE	IDENTIFIER
Cell culture reagents		
Advanced DMEM-F12 (ADF) medium	Life Technologies	12634010
R-Spondin	Trevigen	#3710-001-01
EGF	Life Technologies	PMG8041
Noggin	Peprotech EC Ltd	250-38-500
N2 Supplement	Life Technologies	17502048
B27 Supplement	Thermo Fisher	A1895601
Penecillin/Streptomycin	Sigma	P0781-100ml
L-Glutamine	Sigma	G7513-100ml
N-acetylcysteine	Sigma	A9165-5G
ROCK inhibitor Y27632	Tocris	1254/10
DMEM (no glucose, no pyruvate, no glutamine)	Life Technologies	A1443001
Basement matrix extract	R&D Technology	3533-010-02
Matrigel	Corning	354234
TrypLE express reagent	Life Technologies	12605010
FBS	Gibco	10270-106 500ml
PBS	Sigma	D8537
Lipofectamine 2000	Invitrogen	11668019
Optimem	Thermo Fisher	31985-062
EDTA	Sigma	03690-100ML
70µm cell strainer	Thermo Fischer	11597522
Drugs/Reagents		
Glucose	Sigma	G7528-250G
Fructose	Sigma	F0127
Sodium Pyruvate	Sigma	S8636-100ml
Metformin	Sigma	PHR1084-500MG
Rotenone	Sigma	R8875-1G
Antimycin A	Sigma	A8674-25mg
Oligomycin A	Sigma	R8875-1G
FCCP	Tocris	0453/1
UK-5099	Sigma	PZ0160-5MG
Az-991	Gift from AstraZeneca	
B-Nicotinamide Mononucleotide	Sigma	N3501-25MG
MitoTEMPO	Sigma	SML0737-5MG
MitoPQ	Gift from Mike Murphy	
MitoCDNB1	Gift from Mike Murphy	
Duroquinone	Sigma	D223204-1G
Doxycycline Hyclate	Sigma	D9891-5G
Actinonin	Sigma	A6671-10MG
MitoBloCK6	Merck	505759
ISRIB	Gift from David Savage (originally from Sigma)	
GSK 2606414	Gift from David Savage (originally from Sigma)	

A-92	Axon Medchem	2720
KC7F2	Sigma	SML-1043
NSC-134754	Sigma	400086
Phloretin	Sigma	P7912-25MG
Phloridzin	Sigma	274313-1G
Forskolin	Sigma	F6886-10MG
2-Deoxyglucose	Sigma	D8375-1G
Oxamate	Sigma	O2751-5G
AR-C155858	Tocris	4960/1
Syrosingopine	Sigma	SML1908-5MG
Aminooxyacetic Acid (AOA)	Sigma	C13408-1G
β-chloro-L-alanine (βCLA)	Sigma	C9033-250MG
Phenylsuccinic Acid (PhS)	Sigma	P35200-25G
iGP1	Merck	530655
GPi-688	Tocris	3967/10
Etomoxir	Sigma	E1905-5MG
Plasmids and extraction reagents		
FLII12Pglu-700μδ6 plasmid	Addgene	#28002
FLIPQ-TV3.0_2 m plasmid	Addgene	#63732
GW1-PercevalHR plasmid	Addgene	#49082
GW1-Peredox-mCitrine plasmid	Addgene	#32386
PcDNA3.1-Pyronic plasmid	Addgene	#51308
Midi Prep plasmid DNA purification kit	Qiagen	12643
Ampicillin	Sigma	A0166
RNA extraction and RT-qPCR		
RNeasy Micro Plus kit	Qiagen	74034
RNeasy MinElute Cleanup kit	Qiagen	74204
Bioanalyser RNA Nano kit	Agilent Technologies	5067
Qiazol lysis reagent	Qiagen	79306
Rnase OUT (inhibitor)	Thermo Fisher Scientific	10777019
dNTP (25mM)	Thermo Fisher Scientific	R1121
Random Primers	Promega	C1181
Superscript II enzyme	Life Technologies	18080093
TaqMan Universal master mix	Thermo Fisher Scientific	4352042
Taqman Assay Probes		
β-actin	Thermo Fisher Scientific	Mm02619580_g1
Slc2a1 (GLUT1)	Thermo Fisher Scientific	Mm00441480_m1
Slc2a2 (GLUT2)	Thermo Fisher Scientific	Mm00446229_m1
Slc2a5 (GLUT5)	Thermo Fisher Scientific	Mm00600311_m1
Slc5a1 (SGLT1)	Thermo Fisher Scientific	Mm00451203_m1
Ddit3 (CHOP)	Thermo Fisher Scientific	Mm01135937_g1
Seahorse and Secretion reagents		
Seahorse XF24 FluxPaks	Agilent Technologies	100850-001
Seahorse XF base medium without Phenol red	Agilent Technologies	103335-100
GDF-15 assay kit	R&D Systems	MGD-150
Lactate assay kit	Siemens Healthcare	DF-16

LDH assay kit	Siemens Healthcare	DF-54
Alanine transaminase assay kit	Siemens Healthcare	DF-143
Aspartate transaminase assay kit	Siemens Healthcare	DF-41A

2.2 Media and Buffer components

Saline buffer for imaging experiments: 138mM NaCl, 4.5mM KCl, 4.2mM $NaHCO_3$, 1.2mM NaH_2PO_4, 2.6mM $CaCl_2$, 1.2mM $MgCl_2$, 10mM HEPES. pH adjusted to 7.4 with 1M NaOH.

Saline buffer for imaging experiments using Oxamate:

(Buffer 1: no oxamate) 38mM NaCl, 100mM Mannitol, 4.5mM KCl, 4.2mM $NaHCO_3$, 1.2mM NaH_2PO_4, 2.6mM $CaCl_2$, 1.2mM $MgCl_2$, 10mM HEPES. pH adjusted to 7.4 with 1M NaOH.

(Buffer 2: with oxamate) 38mM NaCl, 50mM Na-Oxamate, 4.5mM KCl, 4.2mM $NaHCO_3$, 1.2mM NaH_2PO_4, 2.6mM $CaCl_2$, 1.2mM $MgCl_2$, 10mM HEPES. pH adjusted to 7.4 with 1M NaOH.

Lysis buffer: 0.25g deoxycholic acid, 0.5ml of Igepal CA-630, 2.5ml of 1M Tris-HCL, 1.5ml 5M NaCl, 1 tablet of complete EDTA-free protease inhibitor cocktail, made up to 50ml with water.

EGF, Noggin, R-Spondin (ENR) media: 50ng/ml murine EGF, 100ng/ml murine noggin, 1µg/ml human RSpondin-1, 1% penicillin/streptomycin, 2mM L-glutamine, N2 supplement (1X), B27 supplement (2X), 1µM N-acetyl-L-cysteine and 10µM Y-27632 ROCK inhibitor diluted in advanced DMEM/F-12 (ADF).

Neutralisation media: 10% FBS and 10µM Y27632 in ADF.

Cryopreservation media: 50% FBS, 10% DMSO and 10µM Y27632 in ADF.

2.3 Intestinal organoid lines

Most of experiments were performed using three organoid lines generated from:

1. Wild-type mouse (ROSA26-GCaMP3+/+)
2. GIP-cre/ROSA26-tdRFP+/+ mouse - transgenic mice expressing the reporter tdRFP in cre expressing cells, under the control of the GIP promoter, as described in *(322)*.

3. SST-cre/ROSA26-tdRFP+/+ mouse - transgenic mice expressing the reporter tdRFP in cre expressing cells, under the control of the SST promoter, as described previously *(323)*. Organoids were initially established by Lawrence Billing.

Note the presence of RFP fluorophore in GIP and SST positive cells does not affect imaging experiments as all of the sensors used were excited at <500nm and tdRFP would only be visualised upon excitation at ~535nm.

CHOP knockout mouse used to generate organoids were a gift from Dr. Jane Goodall (University of Cambridge), with the line from Jackson Laboratory, Maine, USA (B6.129S(Cg)- Ddit3tm2.1Dron/J, Stock No: 005530). B0AT1 knockout (Slc6a19-/-) mouse to generate organoids were a gift from Professor Stefan Broer (Australian National University) . SNAT2 knockout (Slc38a2-/-) mouse to generate organoids were a gift from Dr. Miguel Constancia (University of Cambridge).

2.4 High fat diet mouse experiments

The experimental procedures used in HFD mouse experiments were described in *(321)*. All mouse studies were performed in accordance with UK Home Office Legislation regulated under the Animals (Scientific Procedures) Act 1986 Amendment, Regulations 2012, following ethical review by the University of Cambridge Animal Welfare and Ethical Review Body (AWERB). The in vivo mouse studies involving metformin administration were performed by Anthony Coll, Irene Cimino and Debra Rimmington.

2.4.1 Acute metformin gavage in HFD-fed wild type mice

Male C57BL6/J mice were switched from standard chow to 45% HFD for 1 week and then fed with 60% HFD for 3 weeks. Metformin (Sigma Aldrich) was reconstituted in water and fed at a single dose of 600mg/kg (or matched volume of sham) for oral gavage. The mice returned to 60% HFD diet ad libitum. After 6 hours, the mice were sacrificed.

2.4.2 Long-term metformin dosing in HFD-fed wild type mice

Male C57BL6/J mice were switched from standard chow to 60% HFD 3 days before the single dose of metformin treatment. Mice received daily oral gavage of metformin at 300mg/kg for 11 days and remained on 60% HFD ab libitum. On day 11, mice were sacrificed by terminal anaesthesia 4 hours post gavage.

2.4.3 Tissue processing

The small intestine (from the stomach to the ileal-cecal junction) was isolated into three equal length segments and intestinal tissues were taken from the middle of each segment (Figure 2.4). These

segments were termed proximal, middle and distal small intestine, respectively. The colon was isolated from the ileal-cecal junction to the anus, and the colonic tissue was taken from the middle of the segment. The tissues were collected in Lysing Matrix D homogenisation tube (MP Biomedicals) on dry ice and stored at -80°C before RNA extraction.

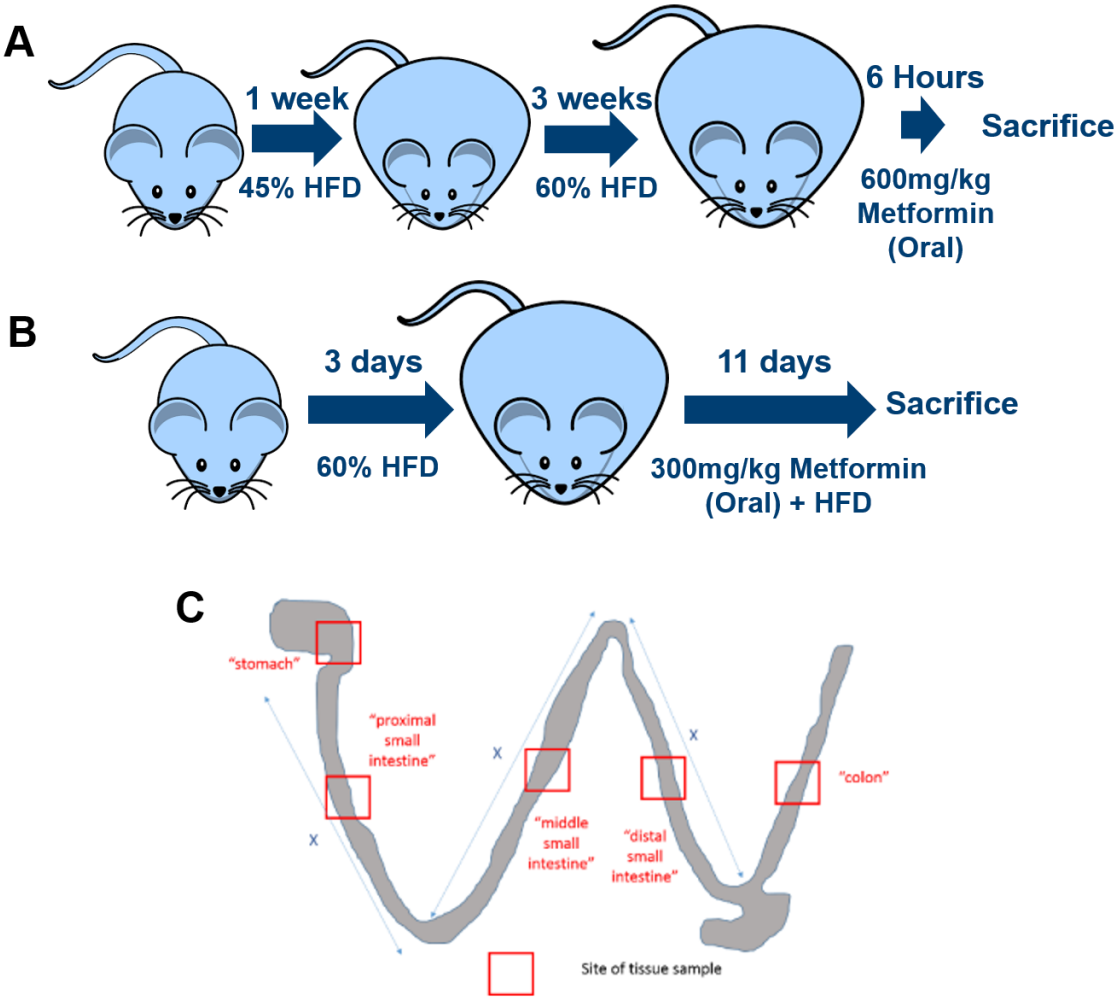

Figure 2.1. Experimental protocol involving HFD-fed mice. (A) acute single-dose metformin oral gavage and (B) 11 day metformin oral gavage. (C) Schematic showing the different samples taken from different sections of the proximal, middle and distal small intestine and the colon.

2.5 Small intestinal organoid culture

2.5.1 Crypt isolation from mouse intestine

Intestinal organoid generation protocols were adapted from *(148, 324)*. To establish duodenal intestinal organoids, the intestines were isolated from the proximal 3cm of the small intestine distal to the stomach. To establish ileal intestinal organoids, the intestines were isolated from the distal 10cm of the small intestine proximal to the ileal-cecal junction. The intestines were sectioned into small segments. Crypt isolation from the small intestine was performed as previously described *(324)*. Briefly, to facilitate crypt isolation, intestinal segments were treated with 30mM EDTA in ice cold PBS for 5 minutes followed by vigorous shaking in PBS. After 2-3 rounds of EDTA digestion, fractions containing the highest yield of dissociated crypts and lowest yield of villi were filtered through a 70µm cell strainer (Thermo Fisher) to remove villus contaminants. The purified fractions containing mostly crypts were centrifuged at 200 x g for 5 minutes at 23^{o}C and the crypt pellet was resuspended with 200µl of basement membrane extract (BME, R&D Technology) and pipetted dropwise to form a dome on the centre of each well in a 48 well plate. The plates were incubated at 37^{o}C for 30-60 minutes to allow Matrigel polymerisation. Intestinal organoids were then supplemented with 250µl per well of EGF-Noggin-R-spondin-1 (ENR) media (modified from *(148)*, see section 2.2 for materials) and placed in a 37^{o}C humidifying incubator with 5% CO_2.

2.5.2 Maintenance

After 5-8 days of culture, intestinal organoids were passaged by incubation with TryPLE express dissociation reagent (Life Technologies) at 37^{o}C for 2-5 minutes, followed by neutralisation using ADF media containing 10% FBS and 10µM Y27632. The suspension was centrifuged at 300g for 5mins, and the supernatant removed. The organoid pellets were thoroughly triturated by pipetting using a P200 pipette tip to facilitate mechanical breakup of organoids before resuspension in matrigel and plated dropwise in a 48 well plate in the same manner as seeding crypts (Nunc). Organoids were split between 1:2 to 1:8 ratio. Medium was changed twice a week.

2.5.3 Cryopreservation and thawing

After 4-7 days of culture, intestinal organoids were collected using ice cold TryPLE reagent immediately followed by addition of neutralisation media. The suspension was centrifuged at 300 g for 5 minutes at 23^{o}C. After removal of supernatant, the organoids were resuspended in Cryopreservation media. The suspended organoids were aliquoted into 1ml cryogenic vials, which were placed into a Mr. Frosty cryopreservation container at -80^{o}C overnight. The cryotubes were then transferred into liquid N_2 filled tanks.

To recover frozen organoids, the cryogenic vials were warmed in a 37°C water bath and the contents were transferred into a falcon tube containing 5ml neutralisation media. The organoids were pelleted at 150 x g for 5 minutes at 23°C and resuspended using BME as described for the crypt isolation procedure.

2.5.4 2D monolayer culture and drug treatments

The experimental time from the generation of 2D monolayer cultures to the day of experiments requires multiple days, a schematic is shown in Figure 2.5. On day 1, intestinal organoids were dissociated to generate 2D monolayer cultures. Procedures for establishing intestinal organoids into 2D monolayers were reproduced from *(324)*. Briefly, wells of 24 well plate, 48 well plate, or 35mm^2 glass bottomed dishes were pre-coated with ADF media containing 2% matrigel (Corning) for 1 hour at 37°C. Intestinal organoids cultured in matrigel were collected in ice cold ADF media (for experiments requiring >16 organoid wells), and the suspension was centrifuged at 300 g for 5 mins, followed by removal of the supernatant. The above step was omitted for experiments requiring <16 wells and organoids were directly collected with warm TryPLE reagent. Organoids were treated with TryPLE reagent for 2-4 minutes at 37°C, followed by mechanical trituration using a P1000 tip and neutralisation. The organoid fragments were pelleted at 300-600xg for 5 minutes. The pellet was further mechanically dissociated by repeated trituration by ~50 times to form organoid fragments. The pellet was resuspended in ENR media with 10µM Y-27632 before pipetting the suspension onto each well/dish for incubation overnight.

On day 2, after observing that the 2D monolayers were formed, the supernatant was removed from the wells/dishes and cultures were treated with ENR containing drug reagents. For metformin pre-treatments, metformin was formulated at 10mM stock by dissolving into ADF. Metformin was used at a working concentration of 1mM (1:10 dilution in ENR). The plates/dishes were incubated for 37°C in the humidifying chamber for 24 hours.

2.5.5 Plasmid amplification and Transfection

Bacteria containing plasmids purchased from Addgene were plated onto agar plates containing Ampicillin and incubated at 37°C overnight. Bacterial colonies were picked using a P200 pipette tip and propagated as starter cultures for 4-6 hours at 37°C. 1ml of starter cultures were transferred into a conical flask containing 250ml of LB broth and Ampicillin (100µg/ml) and incubated for 16-20 hours at 37°C. The propagated cultures were collected into 50ml falcon tubes and spun at 4000 g for 10 minutes at 4°C. Plasmids were extracted from the bacterial pellets using the Midi Prep plasmid DNA purification kit (Qiagen) according to manufacturer's instructions. Plasmid sequence were verified by restriction digest.

For imaging studies, on day 2 of experiments (as described for section 2.5.4) and before drug pre-treatment, the 2D monolayer cultures were transfected with the plasmid of interest. A transfection mix was prepared by mixing 2µg of plasmid DNA with 2µl of Lipofectamine 2000 reagent in 100µl of Lipofectamine per reaction and incubated for 10 minutes at 23°C. 100µl of transfection mix was added carefully onto the centre of the imaging dish and incubated at 37°C for 4-8 hours.

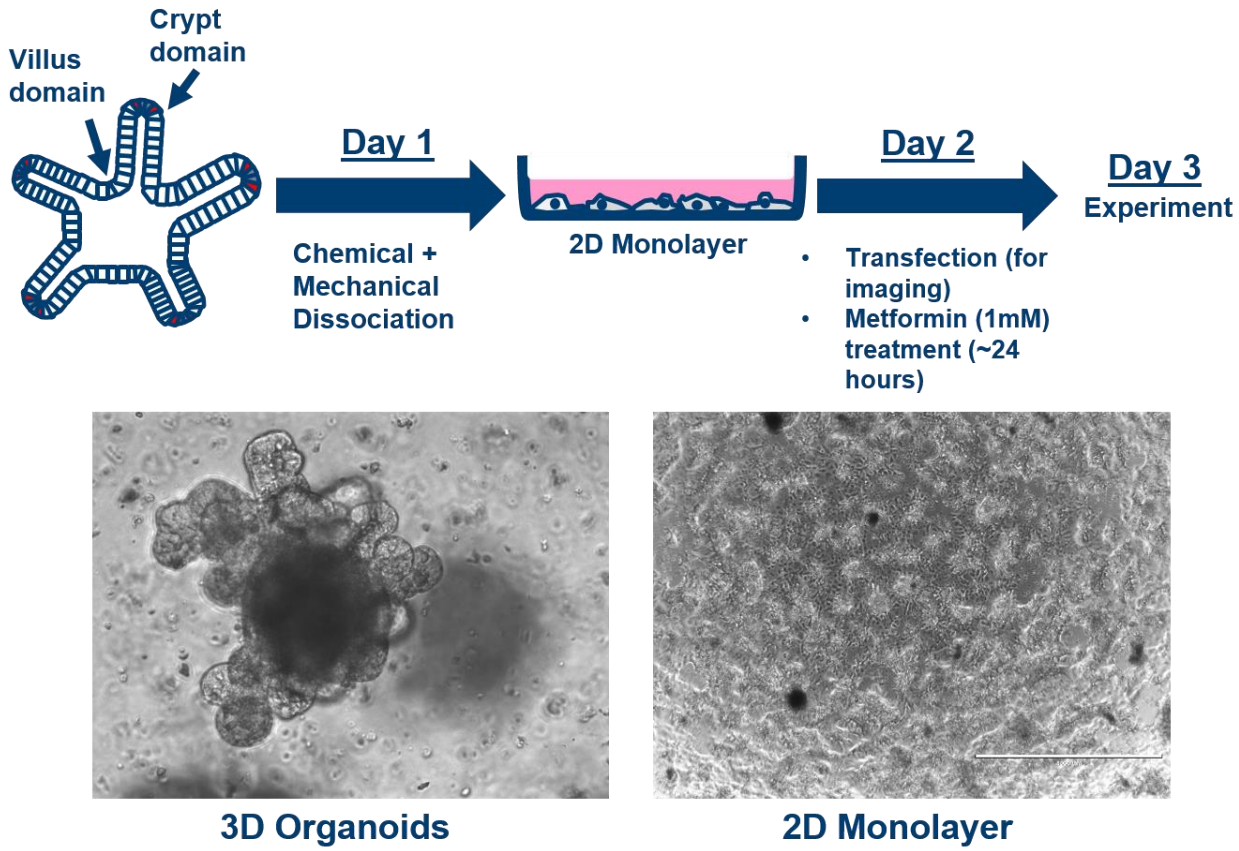

Figure 2.2. Experimental protocol involving seeding of 2D monolayers and treatment of cultures with metformin. Images of organoids in 3D form and in 2D monolayers are shown below.

2.6 Imaging experiments

2.6.1 Live cell imaging preparations

Before imaging, the 2D organoid cultures were washed thoroughly with 138 saline buffer (with no glucose, unless indicated). Cells were preincubated at 37°C for 5-15 minutes prior to measurements. All treatments were made up in 138 saline buffer. During imaging, treatments were perfused at a rate of ~2ml per minute.

2.6.2 Perceval imaging of intracellular ATP

Perceval HR is a genetically encoded fluorescent intracellular ATP and ADP sensor as described in *(325)*. The Perceval HR sensor contains an ATP/ADP binding bacterial histidine kinase (GlnK) tagged with a circularly permuted Venus fluorescent protein (Figure 2.6A) *(325)*. The Perceval HR sensor is an improved variant of the original Perceval sensor identified from mutagenesis of amino acid residues around the ATP-binding pocket, with an increased fluorescence response to a wide range of intracellular ATP and ADP concentrations. The sensor has two excitation peaks, at ~420nm and ~500nm to detect ATP and ADP binding to the sensor, as well as an isosbestic point at 455nm (Figure 2.6B). The sensor has an emission peak at ~520nm.

Perceval imaging was performed on 2D monolayer cultures 2 days after seeding in 35mm^2 glass bottomed dishes and a day following transfection of the plasmid encoding Perceval HR. Imaging was performed using an inverted fluorescence microscope (Olympus IX71, Olympus, Southend on Sea, UK) with a x40 oil-immersion objective lens. Perceval HR was excited at 490±2nm and 450nm sequentially using a 75W xenon arc lamp connected to a monochromator (Cairn Research, Faversham, UK), controlled by MetaFluor software (Molecular Devices, Wokingham, UK). Emissions were captured using an Orca ER camera (Hamamatsu, Welwyn Garden City, UK), and images were acquired every 10 seconds. Images were background subtracted using MetaFluor software, and the fluorescence intensities were transcribed to an excel spreadsheet. The Perceval fluorescence ratio (FI/F0) was calculated by dividing the fluorescence at 490nm by 450nm (Figure 2.6C). Fluorescence at 490nm was dictated by changes in intracellular ATP concentrations, whilst the isosbestic point remained constant (Figure 2.6C). Data points were smoothened with a sliding average over 60 seconds. Changes in Perceval fluorescence were calculated by subtracting the differences from the minimum fluorescence response during treatment to the minimum fluorescence 120 seconds prior to treatment (basal).

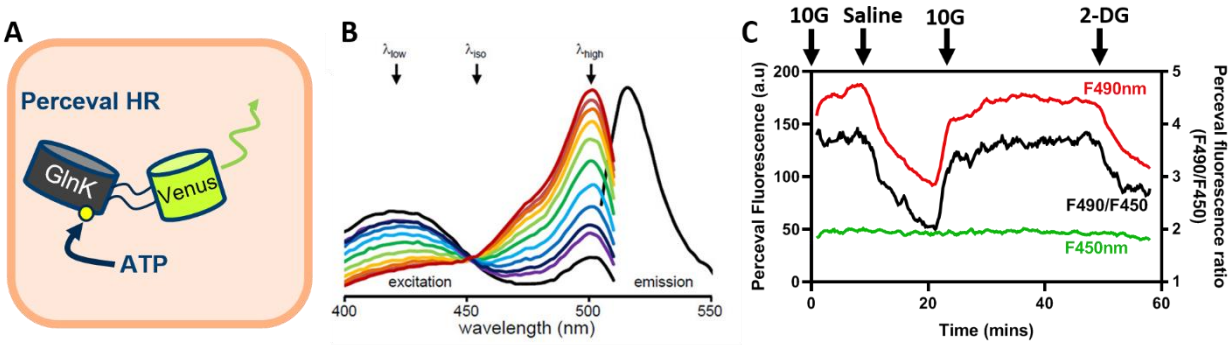

Figure 2.3. Measurement of intracellular ATP levels in live cells via Perceval-HR fluorescence. (A) Diagram of Perceval HR ATP sensing. (B) Excitation and emission spectra of Perceval HR. (C) Changes in Perceval HR fluorescence in response to Saline, 10mM glucose (10G) and glycolysis inhibitor 2-DG, as measured by monitoring 450nm and 490nm excitation wavelengths and calculation of the Perceval fluorescence ratio (F490nm/F450nm).

2.6.3 Peredox imaging of cytosolic NADH/NAD+ ratio

Peredox is a genetically encoded fluorescent sensor exclusively localised in the cytosol and not in the mitochondria, enabling compartmentalised imaging of cytosolic NADH concentrations (as a measurement of the cytosolic NADH/NAD+ redox ratio), as described in *(326)*. The Peredox sensor contains a bacterial NADH binding protein, T-Rex tagged with a circularly permuted GFP T-Sapphire with an excitation peak at ~400nm and emission at ~500nm and increases in fluorescence correlated with increased cytosolic NADH (Figure 2.7A-2.7B). The sensor also contains a sensor mCitrine attached in tandem to enable ratiometric measurements.

Peredox imaging was performed on 2D monolayer cultures 2 days after seeding in 35mm^2 glass bottomed dishes and a day following transfection of the plasmid encoding Peredox, using the same equipment and similar to the procedures described for Perceval imaging. The T-Sapphire and mCitrine fluorescence of Peredox was sequentially excited at 405±20nm and 480±10nm, respectively and images were acquired every 10 seconds. Background subtraction was performed on MetaFluor software and fluorescence measurements were transcribed in an excel spreadsheet. Peredox fluorescence ratio (FI/F0) was calculated by dividing the fluorescence at 405nm by 480nm (Figure 2.7C). T-Sapphire fluorescence was increased correlating with cytosolic NADH concentrations, whilst the mCitrine fluorescence remained constant throughout the experiment (Figure 2.7C). Data points were smoothened with a sliding average over 60 seconds. Changes in Perceval fluorescence were calculated by subtracting the differences from the maximal fluorescence response during treatment to the maximal fluorescence 120 seconds prior to treatment (basal).

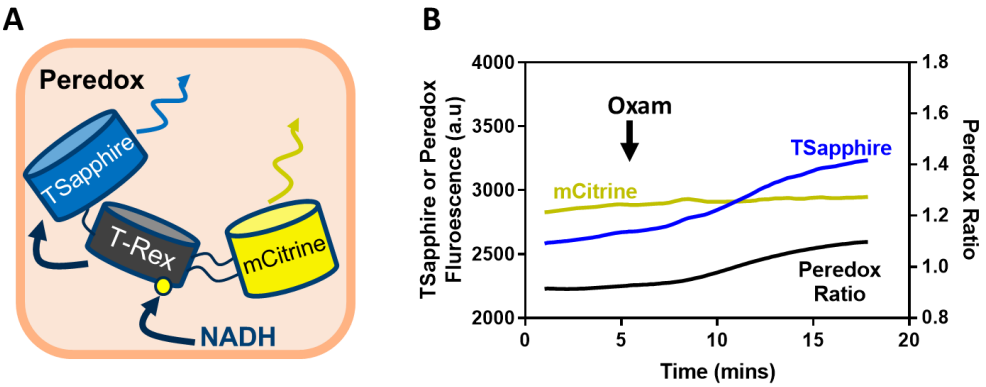

Figure 2.4. Measurement of cytosolic NADH levels in live cells via Peredox fluorescence. (A) Diagram of Peredox-mCitrine NADH sensing. (B) Changes in Peredox and mCitrine fluorescence in response to LDH inhibitor Oxamate, as measured by monitoring fluorescence of the fluorophore when excited at 405nm and 480nm, and calculation of the Peredox fluorescence ratio (F405nm/F480nm).

2.6.4 Autofluorescence imaging of NAD(P)H and FAD

The cellular redox states can be estimated by measuring NAD(P)H and FAD autofluorescence as described in *(327)*. NAD(P)H has an autofluorescence characteristic of the nicotinamide ring at UV range of excitation, whilst FAD has a characteristic autofluorescence of the flavin ring excited at ~450nm. Autofluorescence imaging was performed on untransfected 2D monolayer cultures 2 days after seeding in 35mm^2 glass bottomed dishes. A phase contrast image of the cells was captured as a reference to identify cells/regions of interest. NAD(P)H and FAD autofluorescence were sequentially excited at 360±15nm and 465±10nm, respectively and images were acquired every 10 seconds. Background subtraction was performed using MetaFluor software and fluorescence measurements were transcribed in an excel spreadsheet. Data points were smoothened with a sliding average of 60 seconds. Changes in NAD(P)H and FAD autofluorescence (measured as arbitrary units) were calculated by subtracting the differences from the maximal fluorescence response during treatment to the maximal fluorescence 120 seconds prior to treatment (basal).

2.6.5 FRET imaging

Imaging of fluorescent-resonance energy transfer (FRET) sensors were performed on 2D monolayer cultures 2 days after seeding in 35mm^2 glass bottomed dishes and a day following transfection of the FRET sensor. Imaging was performed using an inverted fluorescence microscope (Olympus IX71, Olympus, Southend on Sea, UK) with a x40 oil-immersion objective lens. Cells were excited at 435±10nm using a 75W xenon arc lamp connected to a monochromator (Cairn Research, Faversham, UK), controlled by the MetaFluor software (Molecular Devices, Wokingham, UK). CFP or mTFP emissions at ~470nm and YFP or Venus emissions at ~535nm were simultaneously monitored using an Optosplit II beam splitter (Cairn Research) and Orca ER camera (Hamamatsu, Welwyn Garden City, UK). The following FRET sensors were used for live cell imaging experiments. Background subtraction was performed using MetaFluor software and fluorescence measurements were transcribed into an excel spreadsheet.

2.6.5.1 FLII12Pglu-700µδ6 Glucose sensor

The FLII12Pglu-700µδ6 cytosolic glucose sensor was initially generated by Wolf Frommer lab with an affinity range of 0.05 – 10mM *(328)*. The sensor contains a mutated bacterial glucose binding protein MglB combined with an mCitrine-eYFP and eCFP (Figure 2.8A) *(328)*. The application of glucose caused a simultaneous increase in eCFP fluorescence and decrease in mCitrine-eYFP fluorescence, leading to a decrease in FRET upon glucose binding to the sensor (Figure 2.8A and 2.8B). CFP and YFP fluorescence were acquired every 5 seconds, and real time changes in fluorescence of the glucose

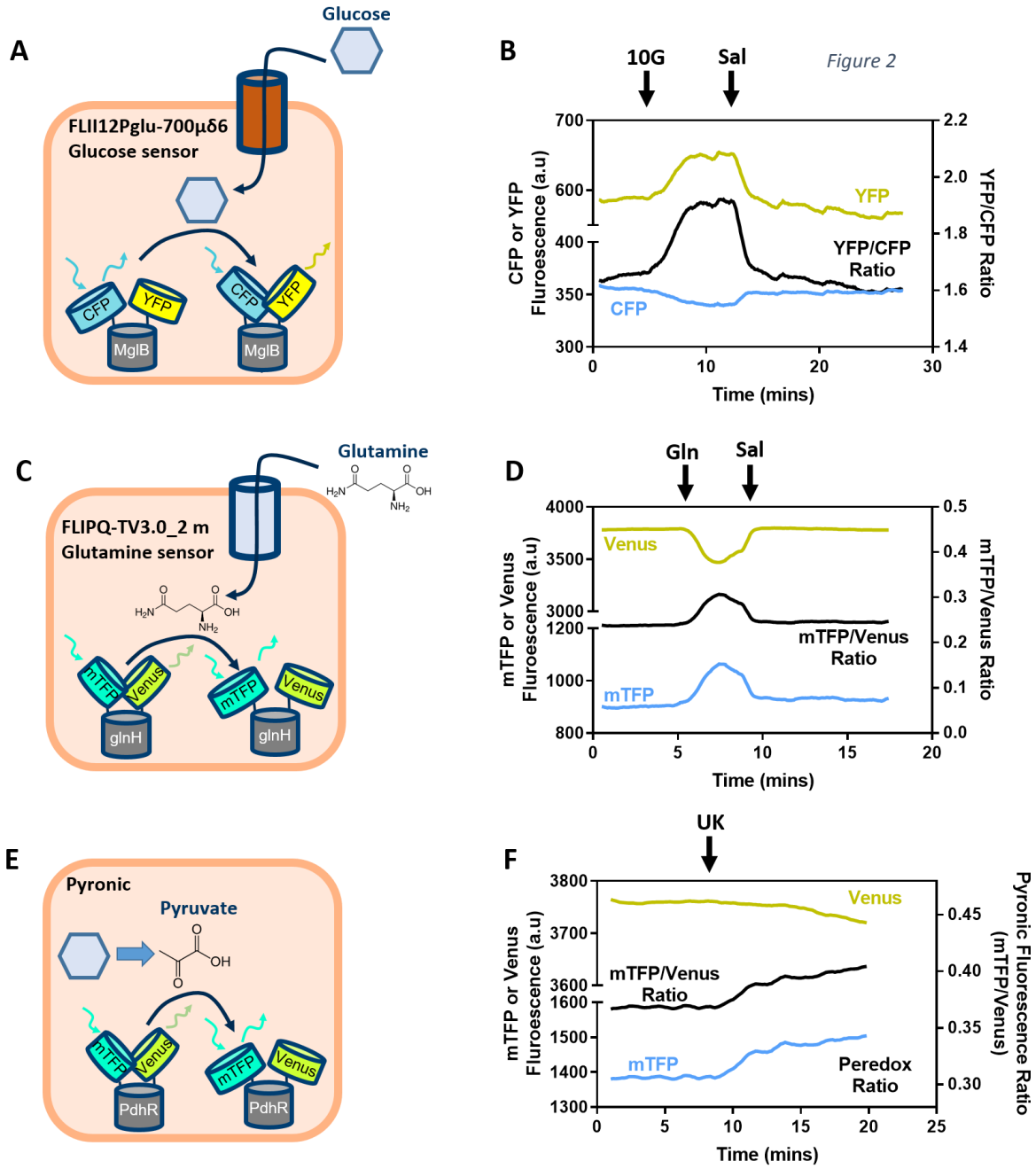

Figure 2.5. Measurement of intracellular metabolites by FRET imaging. (A) Diagram of intracellular glucose sensing using the FLII12Pglu-700µδ6 FRET sensor and (B) Changes in CFP and YFP fluorescence in response to 10mM glucose (10G), which are used to derive the YFP/CFP ratio as a measure of intracellular glucose levels. (C) Diagram of intracellular glutamine sensing using the FLIPQ-TV3.0_2 m FRET sensor and (B) Changes in mTFP and Venus fluorescence in response to 10mM glutamine (Gln). Fluorescent changes are used to derive the mTFP/Venus ratio as a measure of intracellular glutamine levels. (e) Diagram of intracellular pyruvate sensing using the Pyronic FRET sensor and (F) Changes in mTFP and Venus fluorescence in response to the mitochondrial pyruvate carrier inhibitor UK-5099 (UK), which elevates cytosolic pyruvate levels by inhibiting mitochondrial pyruvate uptake. Fluorescent changes are used to derive the mTFP/Venus ratio as a measure of intracellular pyruvate levels.

sensor were measured as the YFP/CFP ratio. Data points were smoothened with a sliding average over 30 seconds. Relative changes in intracellular glucose levels were calculated by dividing the differences from the maximal fluorescence response during glucose application to the maximal fluorescence 60 seconds prior to treatment (basal) and 60 seconds during washout (Figure 2.8B).

2.6.5.2 FLIPQ-TV3.0_2 m Glutamine sensor

The FLIPQ-TV3.0_2 m sensor has a cytosolic glutamine binding affinity of 1.6mM *(329)*. The sensor contains a mutated E.Coli glutamine binding protein glnH combined with mTFP and Venus proteins (Figure 2.8C) *(329)*. The application of glutamine caused a simultaneous increase in Venus fluorescence and decrease in mTFP fluorescence, leading to a decrease in FRET upon glutamine binding to the sensor (Figure 2.8C and 2.8D). mTFP and Venus fluorescence were acquired every 5 seconds, and real time changes in fluorescence of the glutamine sensor were measured as the mTFP/Venus ratio. Data points were smoothened with a sliding average over 30 seconds. Changes in intracellular glutamine levels were calculated by dividing the differences from the maximal fluorescence response during glutamine application to the maximal fluorescence 60 seconds prior to treatment (basal) and 60 seconds during washout (Figure 2.8D).

2.6.5.3 Pyronic sensor

The Pyronic sensor was initially generated by Felipe Barros lab with an affinity range of 10µM – 1mM for intracellular pyruvate *(330)*. The sensor contains an E.Coli pyruvate binding protein PdhR combined with mTFP and Venus proteins (Figure 2.8E) *(329)*. Increases in intracellular pyruvate levels by inhibiting endogenous pyruvate uptake by the mitochondria caused a simultaneous increase in Venus fluorescence and decrease in mTFP fluorescence respectively, leading to a decrease in FRET upon pyruvate binding to the sensor (Figure 2.8E and 2.8F). mTFP and Venus fluorescence were acquired every 10 seconds, and real time changes in fluorescence of the pyruvate sensor were measured as the mTFP/Venus ratio. Data points were smoothened with a sliding average over 60 seconds. Changes in intracellular pyruvate levels were calculated by dividing the differences from the maximal fluorescence response during glutamine application to the maximal fluorescence 120 seconds prior to treatment (basal).

2.7 Seahorse Measurements

The Seahorse XF24 bioanalyser (Agilent) measures in real time the proton (H^+) production/pH changes in the extracellular media to calculate the extracellular acidification rate (ECAR) and whilst detecting extracellular O_2 concentrations via a fluorescence-based oxygen sensor to calculate oxygen consumption rate (OCR) to measure oxidative phosphorylation *(331)*. The bioanalyser cartridge has 4 injection ports to enable sequential application of drug compounds per experiment.

The protocols for Seahorse measurements were followed according to manufacturer's instructions. Briefly, 20 of the 24 wells in the XF24 plates were used to establish 2D monolayer cultures at full confluency, with 4 wells used as blanks (no cell controls). The following day, the bioanalyser cartridge was hydrated with a calibrant and incubated overnight at 37°C in a non-CO_2 incubator. The cultures were treated with/without metformin in random order for 24 hours at 37°C in the humidifying chamber in 5% CO_2. On the day of the experiment, the cells were incubated with 525µl of Seahorse assay media (Phenol-red free media which does not contain glucose, glutamine, pyruvate, and low in bicarbonates) with the indicated compounds for 1 hour, 37°C in a non-CO_2 incubator. The cartridge was loaded with 75µl of the indicated drugs. After calibration, the calibrant plate was replaced with the culture plate and the experiment was performed at 37°C. At each measurement, each well was mixed for 3 minutes followed by measurements for another 3 minutes.

The mitochondrial stress test was performed to measure oxidative phosphorylation during incubation of 10mM glucose or 4mM glutamine. The basal OCR (before treatment) was monitored followed by addition of the ATP-synthase inhibitor oligomycin A (which decreases the OCR to measure ATP-linked mitochondrial respiration), the proton uncoupler FCCP (which maximises cellular respiration to measure the maximal capacity and respiratory reserve) and the respective complex I and III inhibitors rotenone and antimycin A to inhibit mitochondrial respiration (and calculate the uncoupled and non-mitochondrial respiration) (table 2.2, Figure 2.9A).

OCR parameter in mitochondrial stress test	**Biological meaning**	**Measurement**
Basal respiration	Mitochondrial respiration in the absence of any inhibitors, affected by substrate availability/oxidation.	OCR before injection – OCR non-mito respiration
Maximal respiration	Mitochondrial respiration in the presence of energy stress caused by FCCP.	OCR during FCCP application – OCR non-mito respiration
Spare reserve capacity	A measure of the ability for the cell to meet an increased energy demand.	OCR maximal respiration – OCR basal respiration
ATP-linked respiration	Mitochondrial respiration used for ATP synthesis	OCR basal respiration – OCR during oligomycin application
Uncoupled respiration	Mitochondrial respiration caused by H^+ leak independent of ATP synthesis	OCR non-mito respiration – OCR during oligomycin application
Non-mitochondrial respiration	Respiration not associated with mitochondria (eg. NADPH oxidases)	OCR during rotenone/antimycin A application

Table 2.6. Bioenergetic parameters to calculate the oxygen consumption rate (OCR) of the mitochondrial stress test using the Seahorse XF24 bioanalyser.

The glycolysis stress test was performed to measure the glycolysis bioenergetics in cells incubated with 2mM glutamine. The basal ECAR (before treatment) was monitored followed by the sequential addition of glucose (which increases ECAR due to glycolysis), oligomycin A (to maximise ECAR and calculate the glycolytic capacity and reserve by shifting the burden of ATP production towards glycolysis) and the glycolysis inhibitor 2-deoxyglucose (2-DG, table 2.3, Figure 2.9B).

ECAR parameter in mitochondrial stress test	**Biological meaning**	**Measurement**
Glycolysis	Medium acidification due to glycolytic turnover	ECAR during glucose application – ECAR before injection
Glycolytic Reserve	A measure of the ability for the cell to further maximise glycolysis in response to increased energy demand	ECAR during oligomycin A application – ECAR during glucose application
Glycolytic Capacity	Maximal glycolysis capacity of cells	ECAR during oligomycin A application – ECAR before injection
Non-glycolytic Acidification	Medium acidification not associated with glycolysis (e.g. TCA cycle activity).	ECAR before glucose injection

Table 2.7. Bioenergetic parameters to calculate the extracellular acidification rate (ECAR) of the glycolysis stress test using the Seahorse XF24 bioanalyser.

The Seahorse data were acquired using the Wave 2.0 software. The results were normalised to total protein content measured using BCA assay (Thermo Fisher) performed according to manufacturer's protocols.

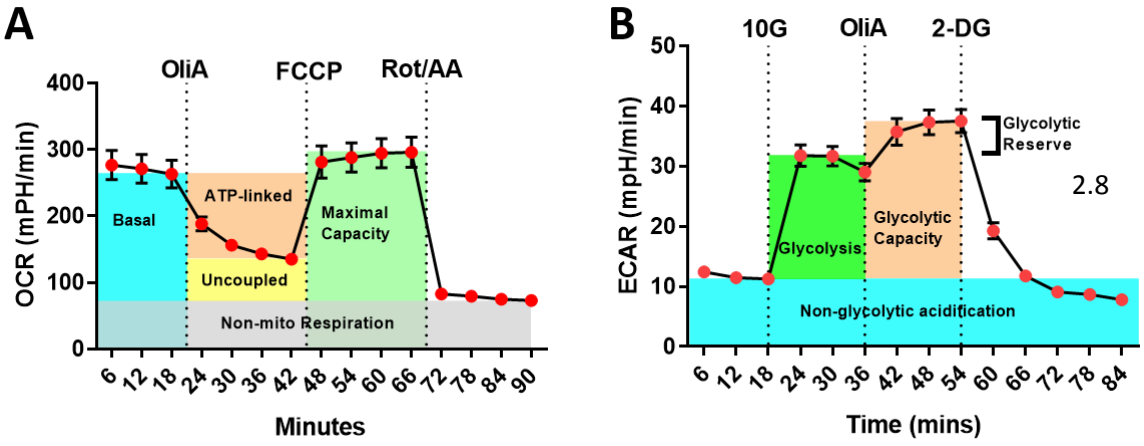

Figure 2.8. Diagram of the different parameters used to investigate oxidative phosphorylation and glycolysis using the Seahorse XF24 bioanalyser. (A) Example graph of the mitochondrial stress test, which measures the oxygen consumption rate (OCR). Mitochondrial respiration parameters such as Basal, ATP-linked, uncoupled respiration, maximal capacity and non-mitochondrial respiration can be calculated from the addition of three mitochondrial respiration inhibitors: ATP synthase inhibitor Oligomycin A (OliA), proton uncoupler FCCP and respective Complex I and III inhibitor Rotenone and Antimycin A (Rot/AA). Note the concentrations of inhibitors are all used at 1µM. (B) Example graph of the glycolysis stress test, which measures the extracellular acidification rate (ECAR). Parameters used to measure glycolysis, glycolytic capacity, glycolytic reserve and non-glycolytic acidification using the reagents glucose (10G, 10mM), Oligomycin A (OliA, 1µM) and 2-deoxyglucose (2-DG, 50mM).

2.8. Secretion and Enzyme Activity Assays

2.8.1 Lactate Secretion Assay

Lactate secretion was performed 2 days after seeding mouse intestinal organoids into 2D monolayers in 48 well plates. On the day of experiment, media was removed and cultures were washed 3 times with warm PBS. Cultures were incubated for 4 hours at 37°C in the humidifying chamber treated with 100µl of DMEM without phenol red, glucose, glutamine or pyruvate (Thermo Fisher) plus the indicated drugs. The medium was then collected and spun at 5,000 g for 5 minutes at 4°C to remove debris and dead cells. The supernatant was collected and lactate was measured at the Core Biochemical Assay Laboratory, University of Cambridge using the lactate assay kit (Siemens Healthcare, Germany). The lysates were treated with lysis buffer, and lysates were collected and spun at 10,000 g for 10 minutes at 4°C to remove debris. Secretion results were normalised to total protein content measured using BCA assay.

2.8.2 GDF-15 Secretion Assay

GDF-15 secretion was performed a day after seeding mouse intestinal organoids into 2D monolayers in 48 well plates. 2D organoid cultures were treated for 24 hrs at 37°C in the humidifying chamber

with 150µl of ENR and the indicated drugs. The medium was then collected and spun at 5,000 g for 5 minutes at 4°C to remove debris and dead cells. The supernatant was collected and GDF-15 was measured at the Core Biochemical Assay Laboratory, University of Cambridge using the mouse GDF-15 assay kit. Measurements were performed using a microtiter plate-based two-site electrochemiluminescence immunoassay using the MesoScale Discovery assay platform (MSD, Rockville, Maryland, USA). Unless stated, 2-3 wells were performed in parallel for each experiment. The secretion results were normalised to basal secretion (control) for each experiment to calculate the fold change.

2.8.3 LDH (Lactate dehydrogenase), AST (Aspartate transaminase) and ALT (Alanine transaminase) Assay

LDH, AST and ALT measurements in lysates were performed a day after seeding mouse intestinal organoids into 2D monolayers in 48 well plates. 2D organoid cultures were treated for 24 hrs at 37°C in the humidifying chamber with 150µl of ENR with and without 1mM metformin. The medium was then removed and the lysates were treated with Lysis buffer (see section 2.2) and spun at 10,000 g for 10 minutes at 4°C to remove debris and dead cells. The supernatant was collected and LDH, AST and ALT activity were measured using their respective kits (Siemens Healthcare, Germany) by the Core Biochemical Assay Laboratory, University of Cambridge. The lysate results were normalised to total protein content measured using BCA assay.

The basis for LDH, AST and ALT measurements are described in reference procedures *(332–335)*. Briefly, LDH measurements involve supplying L-lactate substrate to the sample, whilst measuring the 340nm absorbance formed due to increased NADH formation during the simultaneous reduction of lactate to pyruvate. ALT measurements involve supplying L-alanine substrate to the sample, which is metabolised to pyruvate. Pyruvate is then reduced to lactate via LDH, which simultaneously increases NADH oxidation to NAD+, the change of absorbance of which was then measured at 340nm. AST measurements involve supplying L-aspartate substrate to the sample, which is metabolised to α-ketoglutarate as well as forming oxaloacetate. Oxaloacetate is then reduced to malate via malate dehydrogenase, which simultaneously increases NADH oxidation to NAD+, the change of absorbance of which was then measured at 340nm.

2.9 Techniques to analyse Gene Expression

2.9.1 Real-time quantitative PCR (RT-qPCR)

Mouse intestinal 2D monolayer cultures plated in 48 well plates were lysed in RLT plus buffer and the RNA was extracted using the RNeasy Micro Plus kit (Qiagen) according to manufacturer's instructions. RNA-extraction from frozen intestinal tissues of HFD-fed mice was performed as described in *(321)*. Briefly, ~100mg of tissue was lysed in 1ml Qiazol lysis reagent (Qiagen 79306l) using a Lysing Matrix D homogenisation tube and Fastprep 24 Homogeniser (MP Biomedicals) according to manufacturer's instructions. RNA-extraction of homogenates was performed using RNeasy Micro Plus Kit.

300ng-1µg of RNA was used for cDNA synthesis using a reaction mixture detailed in table 2.1 according to manufacturer's instructions. The reverse transcription reaction was performed at 25°C for 10 minutes, 40°C for 50 minutes and 70°C for 15 minutes on the Thermo-Cycler. For RT-qPCR reactions, 5-25ng of cDNA/well was used, with TaqMan Universal master mix (Applied Biosystems) and TaqMan primer/probes (all from Fisher Scientific) added to the mixture. The RT-qPCR reaction was performed using the 7900 HT Fast Real-Time PCR system (Applied Biosystems, Fisher Scientific, Waltham, MA, USA) at 95°C for 20 seconds, followed by alternating between 95°C for 1 second and 60°C for 20 seconds for 50 cycles. The probes for the genes used for RT-qPCR experiments are detailed in Table 2.3.

The qPCR results were normalised by calculating the difference in cycle threshold values (ΔCT) between the housekeeper gene β-actin and the gene of interest ($CT_{\beta actin} - CT_{gene}$). Relative gene expression was expressed as $2^{\Delta CT}$ for the given gene.

Reagents	
RNA (diluted in Rnase free water)	14
Random primers	1
Anneal random primers to RNA at 65°C for 5 minutes in Thermal Cycler.	
Master Mix:	**Volume (µl)**
First Strand Buffer	5
DTT (100mM)	2.5
Rnase OUT (inhibitor)	0.625
dNTP (25mM)	0.5
Rnase free water	0.375
Superscript II enzyme	1
Total	10

Table 2.9. Composition of reagents used for reverse transcription using Superscript II.

2.9.2 RNA-Sequencing

Two intestinal organoid lines (GIP-cre tdRFP and SST-cre tdRFP) were used for RNA-seq experiments. Mouse intestinal 2D monolayer cultures plated in 24 well plates were lysed in RLT plus buffer and the RNA was extracted using the RNeasy Micro Plus kit (Qiagen) according to manufacturer's instructions. Removal of salt carryover was subsequently performed using RNeasy MinElute Cleanup kit (Qiagen). The quality of RNA was validated by Bioanalyser RNA Nano kit (Agilent) and Agilent Bioanalyser 2100 system with RIN values were between 8.1-9.4.

1µg of total RNA was used for library construction using Illumina's TruSeq Stranded mRNA Library Prep Kit according to the manufacturer's protocol at the Institute of Metabolic Science Genomics and Transcriptomics Core Facility (Cambridge, UK). Briefly, messenger RNA was enriched by poly-T oligo attached magnetic beads before reverse transcription. Addition of a single 'A' nucleotide (adenylation) after the synthesis of the double-stranded cDNA stopped the ligation of DNA fragments during the adapter ligation reaction. Unique barcodes were added to individual samples allowing multiplexing in sequencing. DNA fragments with successful adapters ligated were enriched with a limited amplification. The second strand cDNA, with the incorporation of dUTP, was quenched during amplification to allow strand-specific sequencing. Indexed libraries were purified, normalised, pooled and sequenced on the Illumina HiSeq 4000 platform at single read 50bp at the Genomics Core Facility, Cancer Research UK Cambridge Institute (Cambridge, UK).

All RNA sequencing analyses were performed using Bioconductor software packages in RStudio. The Ensembl code for each read count of the gene was annotated to the corresponding gene name in the mouse genome using BiomaRt package. Differential expression of genes were calculated using the DESeq2 package. A first DESeq analysis was performed to obtain a list of non-differentially expressed (non-DE) genes (P adjusted value >0.05) between control and metformin treated samples pooled from both organoid lines combined by fitting a negative binomial generalised linear model. A second DESeq analysis was performed by estimating the size factors using only the non-DE genes from the first analysis. A local dispersion estimation fit were performed in the second DESeq analysis. A threshold with log2FoldChange of 0.3 was selected and any genes with <0.3 log2FoldChange were classified as non-DE genes. The raw counts were normalised by variance stabilising transformation (VST), which divides the raw count data by the Size Factors. PCA analysis was performed on the VST-normalised count data using the plotPCA function.

Gene expression from the RNA-seq data were visualised using the following methods. Heatmaps were plotted using the Pheatmap package based on DE genes (filtered by P-adjusted value of <0.05, any gene with P adjusted value of >0.05 were excluded from the heatmap) which calculate the z-scores i.e. the relative expression of a VST-normalised gene in the sample compared to the calculated mean

expression of the gene in all 12 samples. Scatter plots were used to present the VST-normalised counts using the Geompoint function of the ggplot package. Volcano plots compare the Log2FoldChange (x-axis) and –log10 P-adjusted value (y-axis) using the Geompoint function of the ggplot package, with DE genes highlighted in red compared to non-DE genes (grey).

KEGG analysis was performed by mapping the KEGG pathway IDs to each gene associated with the pathway using the database extracted from the edgeR package. KEGG pathway enrichment analysis of DE genes were performed using the Clusterprofiler package, with a p-value cut-off of 0.05 and Benjamin-Hochberg corrections to account for false discovery rate. Gene Ontology (GO) analysis was performed in a subset of genes associated with the mitochondria, by mapping the GO terms for each gene using the Go.db package. GO enrichment analysis of DE genes were performed using the Goseq package, with a p-value cut-off of 0.05 and Benjamin-Hochberg corrections to account for false discovery rate. GO terms with over 300 DE genes in the category were automatically excluded from analysis.

2.10 Statistical Analysis

Results were analysed for normality distribution, and statistical differences between groups were analysed via GraphPad Prism 7.0 software. For RNA-seq data, statistical analysis of DE genes was performed via DE-Seq2 package using R Studio (Section 2.9). The specific statistical test used are stated in the Figure legends. All data were considered statistically significant when $P<0.05$.

Chapter 3: Transcriptomic characterisation of metformin responsive genes in intestinal cells

3.1 Summary

Although metformin is used in the clinic for the treatment of Type 2 Diabetes, the cellular mechanisms of metformin action are still being hotly debated. Whilst previous studies explaining cellular mechanisms of metformin action were based on the suppressing mitochondrial metabolism to inhibit ATP production and activation of the AMP-kinase signalling pathway downstream of increases in cellular AMP levels, other observations have suggested AMPK-independent mechanisms and the effects of metformin in other cellular processes *(210, 220)*. Transcriptomic studies could provide insights into metformin responsive genes and identify novel pathways of metformin action in different cells and tissues. This chapter examines the effects of metformin in metabolic pathways, signalling mechanisms and cellular processes in intestinal cells.

3.2 Background

3.2.1 AMPK-dependent mechanisms of Metformin

Previous studies into metformin action have centred on the role of AMPK in the regulation of cellular processes, particularly glucose and lipid metabolism *(210–214)*. Reported AMPK-dependent effects of metformin include the activation of fatty acid metabolism *(210, 211, 233, 336)*, suppressing adipogenesis *(337)*, skeletal muscle glucose uptake *(210, 336, 338–341)* and inhibiting hepatic gluconeogenesis *(210, 212, 342)* (see chapter 6 for detailed description of metabolic pathways); many of the enzymes involved are directly phosphorylated by AMPK. AMPK also regulate gene expression through the regulation of CREB co-transcription activators, CREB-binding protein (CBP), CRTC2 and SHP, which inhibits the ability of CREB to regulate the expression of gluconeogenic genes *(215–217)*. The activation of AMPK by metformin have been demonstrated to involve the inhibition of mitochondrial metabolism through increasing intracellular AMP levels *(209)*. Yet, metformin activates AMPK even at 50µM *(210)*; the concentrations are below its affinity of inhibiting mitochondrial complex I activity *(204)*. Metformin also increased serine/threonine kinase mediated phosphorylation of the α-subunit of AMPK *(210, 343)*. Experiments using mouse models with liver-specific knockout of the kinase LKB-1 reported a total loss of AMPK activity, which completely attenuated the glucose-lowering effects of metformin administration *(218)*.

3.2.2 Metformin and other signalling pathways

A seminal study by Foretz et al., argued that metformin also mediates its effects through AMPK-independent mechanisms *(220)*. They reported that liver-specific knockout of AMPK displayed comparable blood glucose levels, normal hepatic glucose production and expression of gluconeogenic genes compared to wild-type mice *(220)*. Metformin also achieved glucose-lowering effects despite the deletion of hepatic AMPK, whilst the allosteric AMPK activator A-769662 failed to achieve any noticeable physiological effects *(220)*. However, the AMP analogue AICAR (which is also a known activator of AMPK) was reported to mimic glucose-lowering effects of metformin in the liver-specific AMPK-/- mouse, leading to the speculation that AMP, as opposed to AMPK is important in regulating hepatic glucose production *(220)*. A more recent study confirmed this hypothesis by demonstrating that metformin (and phenformin) inhibited cAMP accumulation and PKA activity by increasing AMP concentrations in mouse primary hepatocytes *(224)*. This effect of metformin antagonised glucagon receptor signalling in vivo, which was dependent on cAMP signalling to stimulate hepatic gluconeogenesis *(224)*.

Other studies have argued for the role of mTOR signalling downstream of metformin effects *(221, 222, 344)*, although the role of AMPK in this pathway is uncertain. Mechanistic studies in mouse embryonic fibroblasts (MEFs) and prostate cancer cell lines demonstrated that metformin inhibits mTORC1 signalling independent of AMPK through activation of a Rag GTPase or the mTOR signalling inhibitor kinase REDD1 *(221, 344)*. By contrast, experiments in mouse primary hepatocytes have demonstrated that at 0.5mM metformin concentration, the mechanism is dependent on AMPK and the TSC1/2 complex *(222)*. The latter study also demonstrated that metformin consequently inhibited protein synthesis of primary hepatocytes via the mTOR signalling pathway *(222)*.

Metformin has also been reported to activate the tumour-suppressor gene ATM, which is involved in the DNA-damage response and cell cycle control *(125)*. This has been supported by the observations that the glycaemic responses of T2DM patients to metformin are linked to common genetic variants near the ATM locus *(125)*. Another study into the roles of metformin in pancreatic islets demonstrated that metformin induces the PPAR-α pathway, which is involved in the induction of GLP-1 receptor expression via a mechanism independent of AMPK *(223)*. Experiments in cancer cell lines have also shown that metformin, by reducing oxygen consumption which leads to increased oxygen tension and increased cellular oxygenation capacity, reduced protein levels of HIF-1α *(345, 346)*. Interactions between the PPAR-α and HIF-1α signalling pathways (whereby HIF-1α inhibits PPAR-α expression) during hypoxia have previously been reported *(347)*.

3.2.3 Metformin and cellular processes

Recent interest into the potential for metformin in cancer therapy owes to its ability to inhibit cancer cell proliferation *(219)*. Whether this is due to its indirect effects as a metabolic inhibitor is not known, although there is some evidence that metformin regulates cell cycle arrest genes. The mechanisms involved depend entirely on the cellular context and include; the activation of REDD1 (downstream of mTOR signalling) and P53 signalling pathways in prostate cancer cells *(344)*, activation of P27, P21 kinases in esophageal cancers *(348)* or downregulation of Cyclin D1 and E2Fs in breast cancer cell lines *(349)*. Other studies have also demonstrated that metformin decreases the expression of cell senescence markers *(350, 351)* and inhibits apoptosis *(351)*.

Metformin also induces autophagy *(352–354)*. Studies in primary hepatocytes have shown that metformin activates autophagy through the activation of the protein deacetylase Sirt1 and is associated with alleviating hepatosteatosis in Ob/Ob mice *(355)*. Metformin has also been reported to activate autophagy via an AMPK-dependent mechanism to mediate its cardioprotective effects against diabetic cardiomyopathy *(354)*. Similar studies in cancer cell lines have also shown that metformin induces AMPK and mTOR-dependent autophagy in lymphoma and melanoma cells *(352, 353)*.

Other effects of metformin include its role in the inflammasome *(356, 357)*, and the regulation of ER stress signalling pathways (see chapter 4) *(358, 359)*. Overall, there is growing evidence that metformin regulates cellular processes beyond mitochondrial metabolism.

3.2.4 Metformin and intestinal functions

Since the intestinal tract is the first site of exposure to high concentrations of orally administrated metformin, accumulating evidence investigate the role of metformin on intestinal function *(116, 312)*. Other than the effects of metformin on intestinal glucose transport and nutrient metabolism in intestinal cells (which are covered in subsequent chapters), metformin has been reported to directly influence various aspects of intestinal function. These include suppressing the expression of inflammatory markers *(360)*, promoting tight junction barrier function *(360–362)*, increasing GLP-1 secretion *(262, 263, 267)* and bile-acid homeostasis *(253, 257, 260)*. Activation of AMPK and regulation of mTOR signalling by metformin have also been confirmed in the intestine *(212, 360, 363, 364)*. Metformin also increases the length of villus but not crypts in the mouse ileum as well as increasing the expression of Paneth and goblet cell markers, suggesting a role of metformin in influencing differentiation of cells in the intestinal mucosa *(360)*. These studies provide some indication of the

vast effects of metformin action in the intestine, but systematic analysis into the cellular and metabolic pathways in the intestinal cells has yet to be reported to date.

3.2.5 Transcriptomic and genomic studies into metformin action

Recent studies using sequencing techniques and bioinformatics analysis have systematically investigated metformin action in various primary tissues and cancer cell lines to identify novel genes and mechanisms *(365–368)*. An influential study using RNA-sequencing of metformin treated human primary hepatocytes have identified metformin-responsive gene clusters associated with AMPK dependent and independent pathways *(365)*. The investigation was followed by ChIP-seq, which identified thousands of gene-regulatory elements associated with the metformin response, notably the cAMP-dependent transcription factor ATF3 and a potential regulatory element for the ATM gene *(365)*. A more recent study used RNA-seq to characterise pathways in skeletal muscle and subcutaneous adipose tissue biopsies from elderly participants taking metformin *(366)*. The study reported the effects of metformin in pathways that are unique to muscle and adipose tissue, whilst altering the expression of genes including *Mtor*, *Myc*, *Tnf*, *Tgfb1* and miRNA-29b *(366)*. Other studies have studied the transcriptomic responses to metformin in fibroblasts *(368)* and cancer cell lines *(367)*.

3.3 Aims

The aims of this study are:

1. To characterise transcriptomic changes to metformin in intestinal cells using bulk RNA-sequencing and DE-Seq analysis.
2. To investigate the metabolic pathways altered by metformin.
3. To examine the effect of metformin on signalling pathways and cellular processes.

3.4 Results

3.4.1 DE-Seq analysis of differentially expressed genes altered by metformin treatment

Note: RNA library preparation and Illumina sequencing of RNA samples were performed by Marcella Ma. Alignment analysis and raw count quantification of RNA-seq results were performed by Brian Lam, and preliminary DE-Seq analysis of data was performed by Pierre Larraufie.

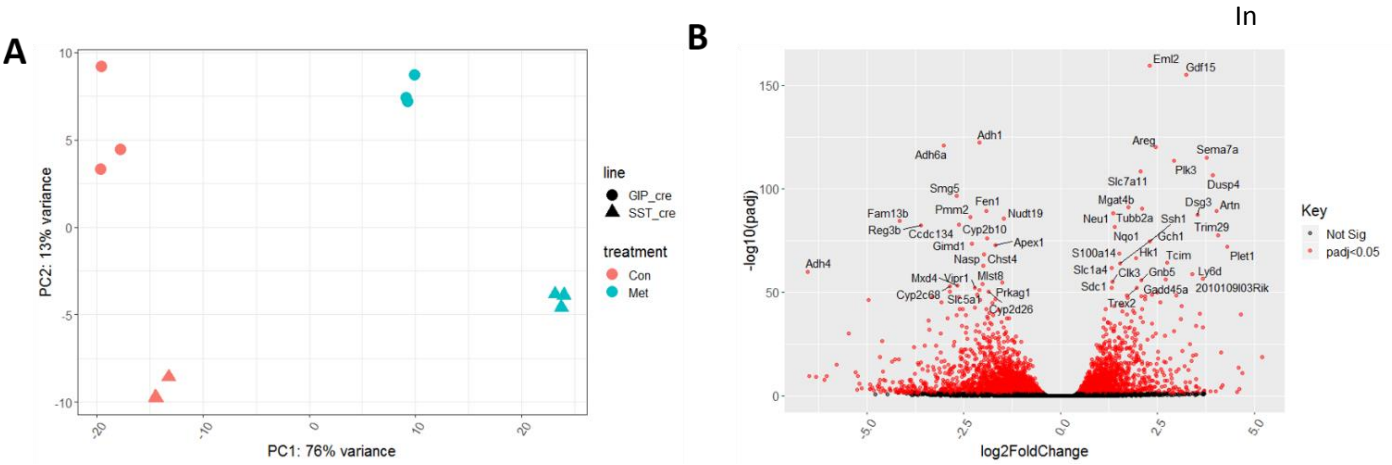

Figure 3.1. Gene expression profiling of duodenal organoid cells seeded into 2D monolayers following treatment of 1mM metformin or no treatment control.

(A) Principle component analysis (PCA) of subgroups from the RNA-seq output. Four subgroups were identified based on the drug treatment (PC1) and organoid line (PC2). (B) Volcano plot displaying the fold change (X-axis) compared to the P-adjusted values (Y-axis) of individual genes altered by metformin treatment. Red dots represent gene expression changes that were statistically significant (P<0.05), whilst black dots represent gene expression changes that were not statistically significant (Not Sig). Labelled genes represent the top 50 most differentially expressed genes (sorted by P values). Con; Control, Met; Metformin.

preparation of samples for RNA-sequencing, two transgenic organoid lines (called GIP-cre tdRFP and SST-cre tdRFP) were plated as 2D monolayer cultures in 3 separate 24-well plates on day 1 followed by treatment with or without 1mM metformin for 24 hours. RNA extraction was performed on day 3, followed by library preparation and RNA sequencing. Changes in the expression of genes altered by metformin were analysed using DE-Seq2. Cluster analysis of the bulk-seq output identified 4 distinct subgroups according to the organoid line and the treatment (Figure 3.1A). There is a 76% variance in gene expression (PC1) between control and metformin treatments, whilst only 13% variance in gene expression (PC2) is observed between the organoid lines. Of the 15,194 genes mapped to the database, 2,378 genes were significantly upregulated, and 1,660 genes were significantly downregulated by metformin treatment, respectively.

A volcano plot compares the genes based on the effect of metformin treatment on differential expression (Log2 of the fold change, x-axis) and the statistical significance of expression (-log10 of the P-adjusted value, y-axis), with the top 50 genes labelled (ranked based on statistical significance) (Figure 3.1B). Amongst the top genes significantly upregulated by metformin include the microtubule associated protein *Eml2*, growth factors *Gdf15* and *Areg*, membrane-bound protein *Sema7a*, protein kinase *Plk3* and the cysteine/glutamate transporter *Slc7a11*. Metformin decreased the expression of genes encoding for alcohol dehydrogenases *Adh1, Adh4* and *Adh6a* (see Figure 3.4),

phosphomannomutase *Pmm2* (see Figure 3.6), the glucose transporter *Slc5a1* (See chapter 5 and figure 3.13), the mRNA decay regulation gene *Smg5* and the FLAP endonuclease *Fen1*.

The effect of metformin on the expression of different intestinal epithelial markers were investigated to provide some suggestion into whether metformin alters the populations of different intestinal cell types. There were no significant changes in any markers for enteroendocrine cells, with the exception for increased glucagon gene (*Gcg*) expression (Figure 3.2A). There were no changes in the expression of goblet cell markers *Clca1* and *Tff3* (Figure 3.2B), whilst the expression of the mucin goblet cell marker Muc2 was too low for detection (data not shown). Metformin increased the expression of the Paneth cell marker *Lyz1*, but not *Defa22* or *Defa24* (Figure 3.2C). Metformin also altered the expression of different stem cell markers (Figure 3.2D). Metformin increased the expression of the tuft cell marker *Dclk1* (Figure 3.2E) and marginally altered the expression of enterocyte markers *Alfi1* and *Gstm3* (Figure 3.2F). Whether metformin changes the different intestinal epithelial cell populations remain inconclusive based on the transcriptomic data.

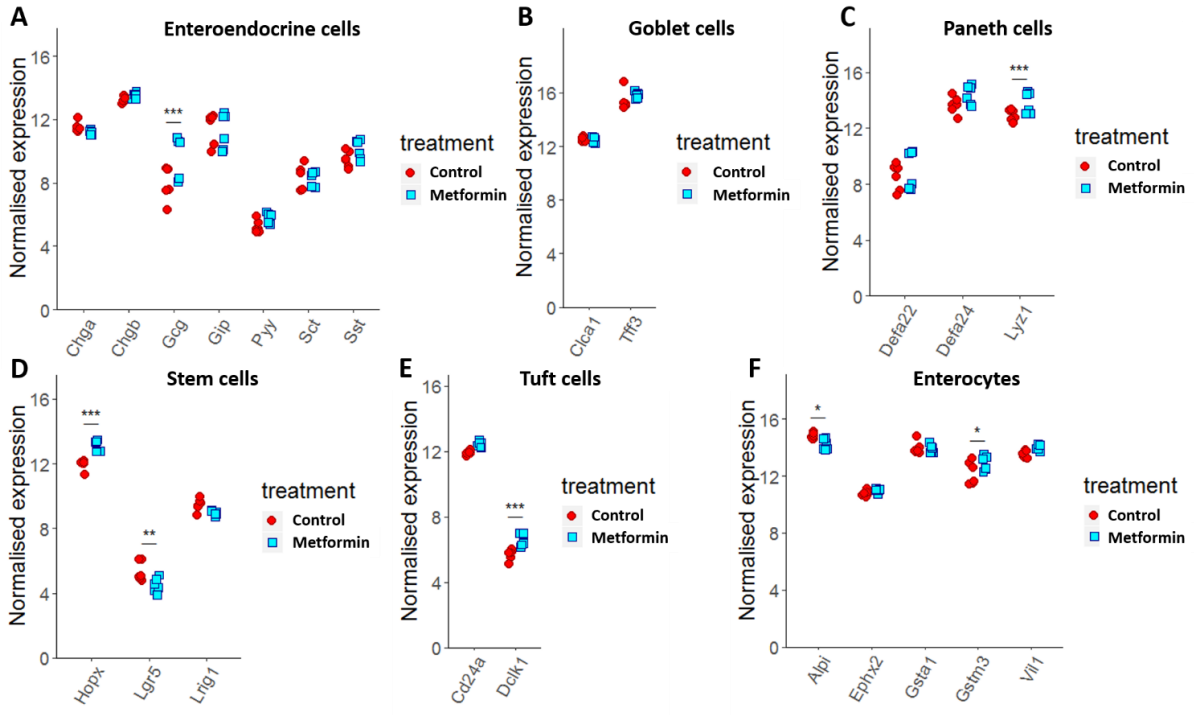

Figure 3.2. Expression of markers for the different intestinal cell types.
The effect of metformin on the expression of biomarkers for (A) enteroendocrine cells, (B) goblet cells, (C) paneth cells, (D) stem cells, (E) tuft cells and (F) enterocytes. The raw count data for each gene is normalised by the size factors and the library size. *, P<0.05, **, P<0.01, ***, P<0.001 (P-adjusted values calculated via DE-Seq analysis). Biomarkers were identified based on single-cell RNA-seq data from *(144, 369)*.

3.4.2 The effects of metformin on metabolic and signalling pathways in intestinal cells

Next, Kyoto-Encyclopedia of Genes and Genomes (KEGG) pathway enrichment analysis was performed. The dataset was mapped to a particular biological pathway from the KEGG database, and the KEGG enrichment analysis identifies cellular/biochemical processes altered in metformin-treated cultures based on the numbers of differentially expressed (DE) genes within each pathway. The metabolic pathways and cellular processes found in the KEGG enrichment analysis is shown in Figure 3.3A and 3.3B. The following sections cover gene expression profiles involved in many of these pathways highlighted from pathway analysis. Pathways known to be important to intestinal metabolism or are associated with metformin action, but have not been highlighted in the pathway analysis, were also studied in more detail. Other pathways identified from the analysis which play important roles in other tissues or with little previous evidence supporting their role in the intestine (such as adipocytokine signalling, insulin resistance, glycan degradation, drug metabolism and Fanconi anaemia pathway), were not investigated further.

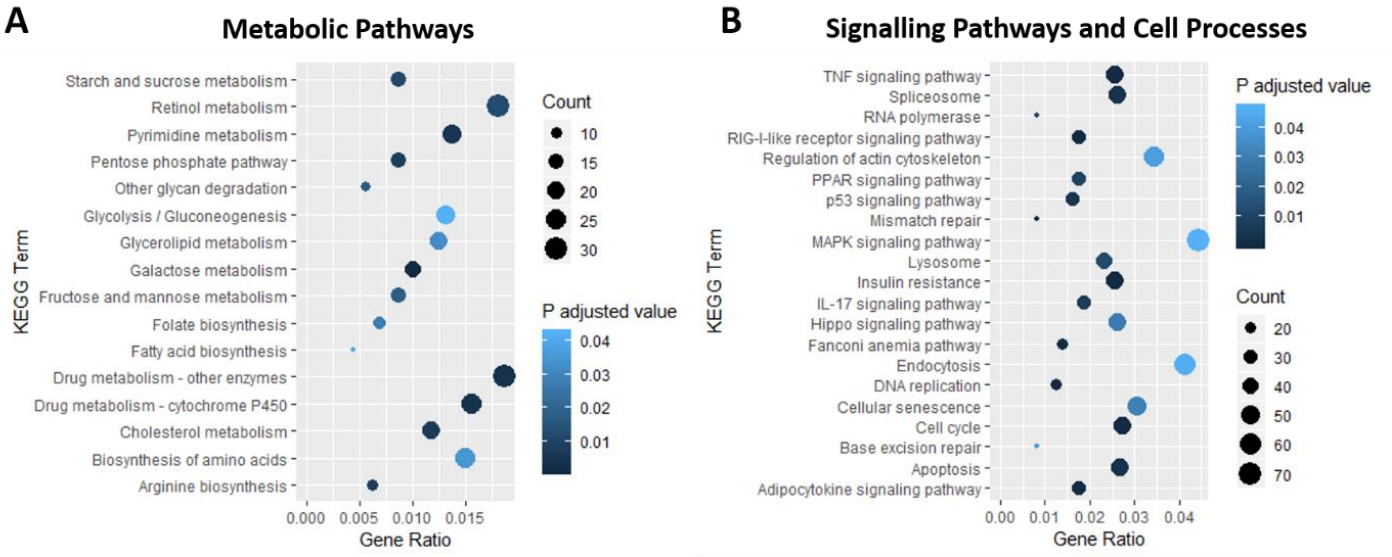

Figure 3.3. Scatterplot of KEGG enrichment statistical analysis of pathways altered by metformin treatment. Changes in (A) metabolic pathways and (B) signalling pathways and processes altered by metformin vs control. Gene ratio is the number of differentially expressed (DE) genes in a KEGG pathway divided by total number of genes in the pathway. Count represents the numbers of DE genes. P adjusted value is the P-value corrected for the false-discovery rate using the Benjamin-Hochberg method, with more statistically significant values representing greater shading intensity.

3.4.2.1 Metabolism of glucose and hexose sugars

Metformin has been reported to increase glycolytic production of lactate in the intestine *(64, 116, 207, 370)*. Glycolysis and gluconeogenesis were amongst the hexose sugar metabolism pathways highlighted in the KEGG enrichment analysis, with 21 out of 67 genes from the KEGG gene list being differentially expressed. Metformin increased the expression of all hexokinase isoforms (*Hk1, Hk2* and *Hkdc1*), phosphofructokinases (*Pfkm* and *Pfkp*), aldolase A (*Aldoa*) and aldehyde dehydrogenases (*Aldh1a3* and *Aldh3b2*) (Figure 3.4A, 3.4F). Metformin decreased the expression of enolase (*Eno3*), alcohol dehydrogenases (*Adh1, Adh4, Adh7*), and the gluconeogenesis glucose-6-phosphatase enzyme (G6pc). Starch and sucrose (glycogen) metabolism were also identified from the pathway analysis (14 DE genes out of 33 genes total genes) and was investigated further. Metformin increased the expression of phosphoglucomutases (*Pgm1* and *Pgm2*), genes promoting glycogen synthesis (*Ugp2* and *Gyg*) and the lysosomal glucosidase (*Gaa*), but decreased expression of phosphoglucomutase (*Pgm1l1*) (Figure 3.4B, 3.4F). Upregulated genes in the pentose phosphate pathway (enriched in the KEGG analysis, with 14 DE genes out of 32 genes total genes) include the rate-limiting enzyme glucose-6-phosphate dehydrogenase (G6pdx), ribulose-phosphate 3 epimerase (*Rpe*) and transaldolase (*Taldo1*); the latter is involved in the reversible, non-oxidative reactions to generate more NADPH and re-join with the glycolysis pathway by generating fructose-6-phosphate. Ribokinase (*Rbks*), the enzyme involved in ribonucleotide biosynthesis in the pathway, was downregulated in metformin treated cultures (Figure 3.4C and 3.4F).

Since glucose metabolism generates pyruvate and lactate, the expression of monocarboxylate transporters (MCTs) involved in their transport were investigated. Amongst the DE genes include *Mct6* and *Mct13* (Figure 3.4D). Metformin decreased the expression of cytosolic glycerolphosphate shuttle gene *Gpd1* but increased the expression of its mitochondrial counterpart *Gpd2*, both of which are involved in glycerol production and the transfer of reducing equivalents generated in glycolysis to the mitochondria (Figure 3.4E).

Pyruvate metabolism and tricarboxylic acid (TCA) cycle were also investigated as the genes involved in glycolysis and pyruvate metabolism markedly overlap with each other. Metformin increased the expression of pyruvate metabolism enzymes such as lactate dehydrogenase (*Ldhd*), malic enzymes (*Me1*, *Me3*) and dihydrolipoyl transacetylase involved in pyruvate dehydrogenase complex (*Dlat*) (Figure 3.5A, 3.5C). Metformin increased the expression of the mitochondrial phosphenolpyruvate carboxykinase (PEPCK) isoform *Pck2* but decreased the expression of its cytosolic counterpart *Pck1*. Amongst the genes involved in TCA cycle flux, isocitrate dehydrogenase 1 (*Idh1*), citrate synthase (*Cs*) and oxoglutarate dehydrogenases (*Ogdh, Ogdhl*) were induced in metformin-treated cultures (Figure

3.5B). Metformin did not significantly alter the expression of most mitochondrial metabolite transporters, with the exception of *Slc25a1* (the mitochondrial citrate transporter CIC) and *Slc25a15* (the mitochondrial ornithine translocase) (Figure 3.5C).

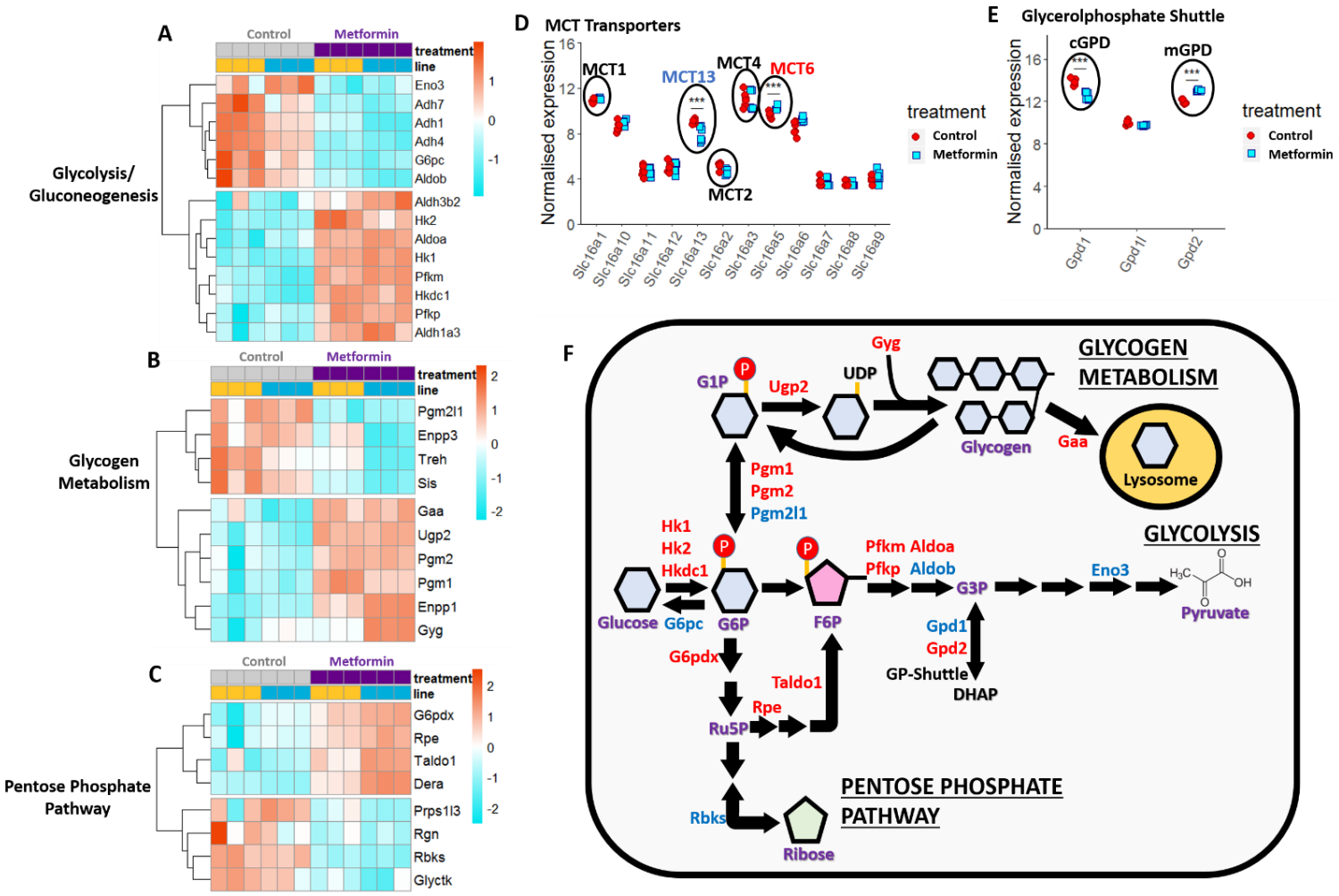

Figure 3.4. The effect of metformin on the expression of genes involved in glucose metabolism. (A, B and C) Heatmaps showing DE genes (filtered by p-adjusted value of <0.05, genes with p-adjusted value of >0.05 were not included in the heatmap) involved in glycolysis and gluconeogenesis (pathway ID: mmu00010), glycogen metabolism (pathway ID: mmu00500) and pentose phosphate pathway (pathway ID: mmu00030), affected by metformin treatment. Since some genes are involved in multiple pathways, they are shown only in a single pathway to avoid duplication. The colour key is shown on the right and depicts the expression z-scores for each gene. Red indicates higher than average expression and blue indicates lower than average expression for a particular gene in a sample. (D and E) The effect of metformin on the expression of monocarboxylate transporters (MCT) and components of the glycerolphosphate shuttle. (F) Schematic showing the expression changes of genes involved in the glycolysis, glycogen metabolism and pentose phosphate pathways. For D and F, red and blue shows the upregulated and downregulated genes, respectively.

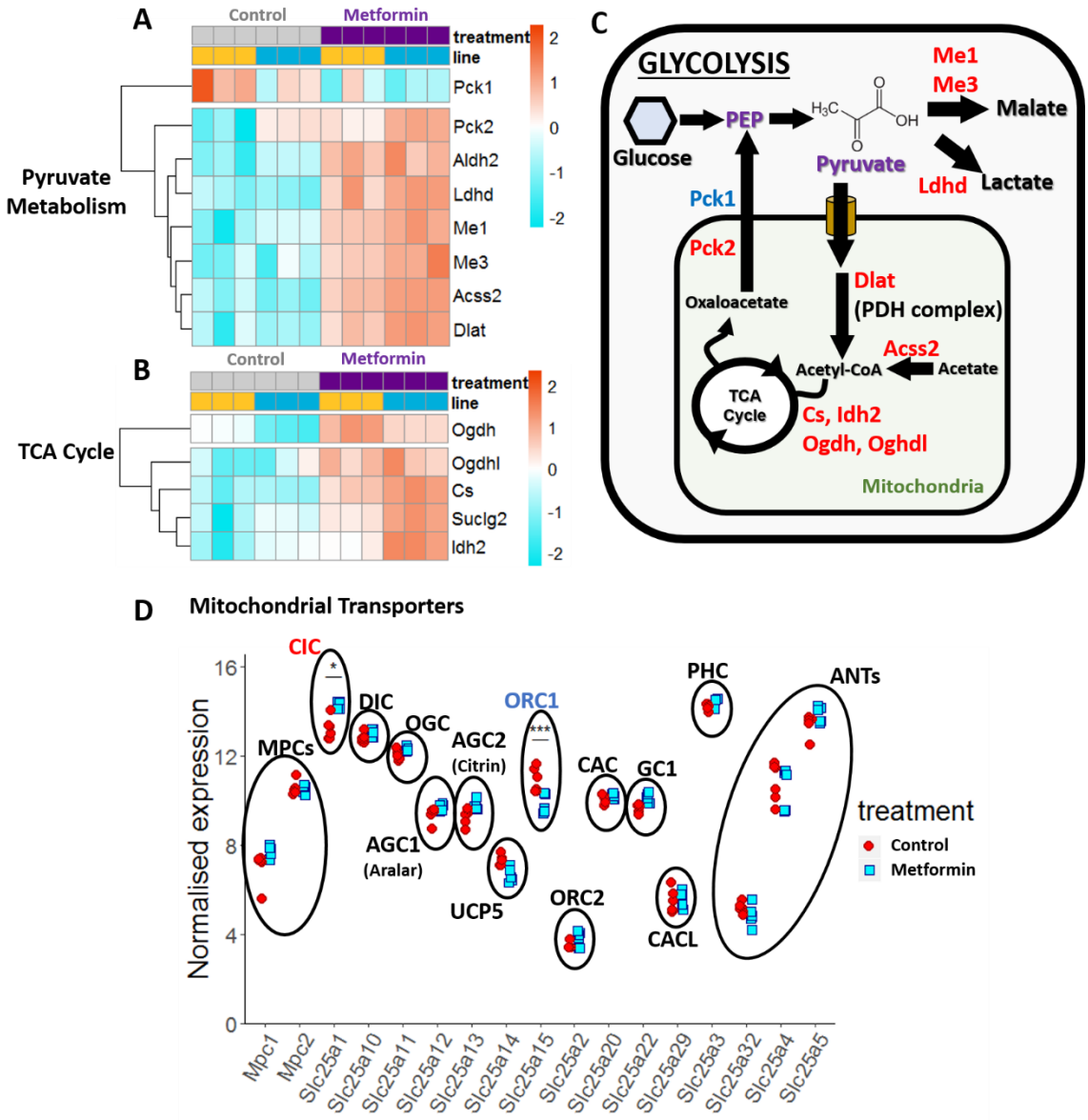

Figure 3.5. The effect of metformin on the expression of genes involved in mitochondrial metabolic transporters and pathways. (A and B) Heatmaps showing DE genes (filtered by p-adjusted value of <0.05, genes with p-adjusted value of >0.05 were not included in the heatmap) involved in pyruvate metabolism (pathway ID: mmu00620) and tricarboxylic-acid (TCA) cycle (pathway ID: mmu00020) affected by metformin treatment. Since some genes are involved in multiple pathways, they are shown only in a single pathway to avoid duplication. The colour key is shown on the right and depicts the expression z-scores for each gene. Red indicates higher than average expression and blue indicates lower than average expression for a particular gene in a sample. (C) Schematic showing the expression changes of genes involved in pyruvate metabolism and the TCA cycle. (D) The effect of metformin on the expression of pyruvate transporters and carriers. For C and D, red and blue shows the upregulated and downregulated genes, respectively.

Metformin decreased the expression of key genes involved in fructose metabolism, such as the rate-limiting enzyme ketohexokinase (*Khk*), aldolase B (*Aldob*), and triokinase/FMN cyclase (*Tkfc*) (Figure 3.6A, 3.6B). Genes involved in mannose metabolism include decreased expression of phosphomannomutase Pmm2 (involved in mannose metabolism to glycans) and increased expression of mannose-6-phosphate isomerase (*Mpi*), which connects mannose metabolism to glycolysis via interconversion of mannose-6-phosphate and fructose-6-phosphate (Figure 3.6A, 3.6B).

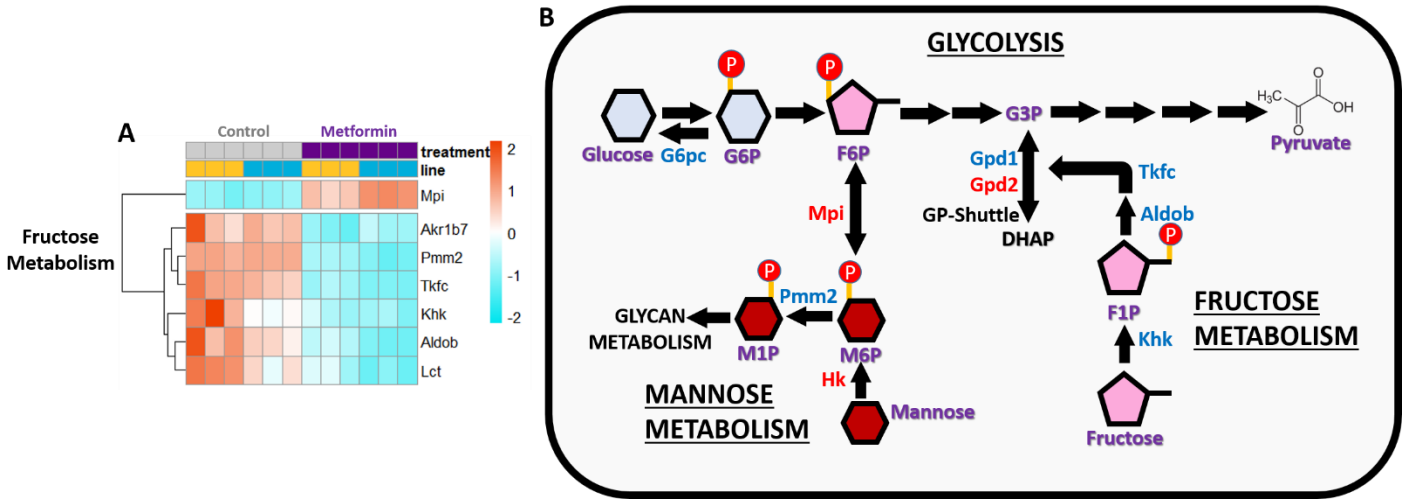

Figure 3.6. The effect of metformin on the expression of genes involved in fructose and mannose metabolism. (A) Heatmap showing DE genes (filtered by p-adjusted value of <0.05, genes with p-adjusted value of >0.05 were not included in the heatmap) involved fructose and mannose metabolism (pathway ID: mmu00051) affected by metformin treatment. The colour key is shown on the right and depicts the expression z-scores for each gene. Red indicates higher than average expression and blue indicates lower than average expression for a particular gene in a sample. Some of the genes are involved in glucose metabolism pathways and are shown in the heatmaps in other figures. (B) Schematic showing the expression changes of genes involved in fructose and mannose metabolism. Red and blue shows the upregulated and downregulated genes, respectively.

Overall, the RNA-seq evidence suggests that metformin promotes the expression of genes involved in glycolysis and pyruvate metabolism. Metformin also seemed to increase the expression of several key pentose phosphate pathway genes despite decreasing ribokinase expression, but the effect on glycogen metabolism are inconclusive. Metformin decreased the expression of genes involved in fructose metabolism.

3.4.2.2 Amino acid metabolism

The expression profiles of genes involved in the glutamate/aspartate/alanine metabolism pathway were investigated in detail, since these amino acids play important roles in intestinal epithelial cells *(178, 179, 183, 371)*. Metformin increased the expression of aspartate and alanine transaminases

(*Got1* and *Gpt*) respectively (Figure 3.7A, 3.7E). Additionally, metformin increased the expression of aspartate metabolism genes *Adss1, Adssl1, Ass1* and particularly *Asns*, which encodes asparagine

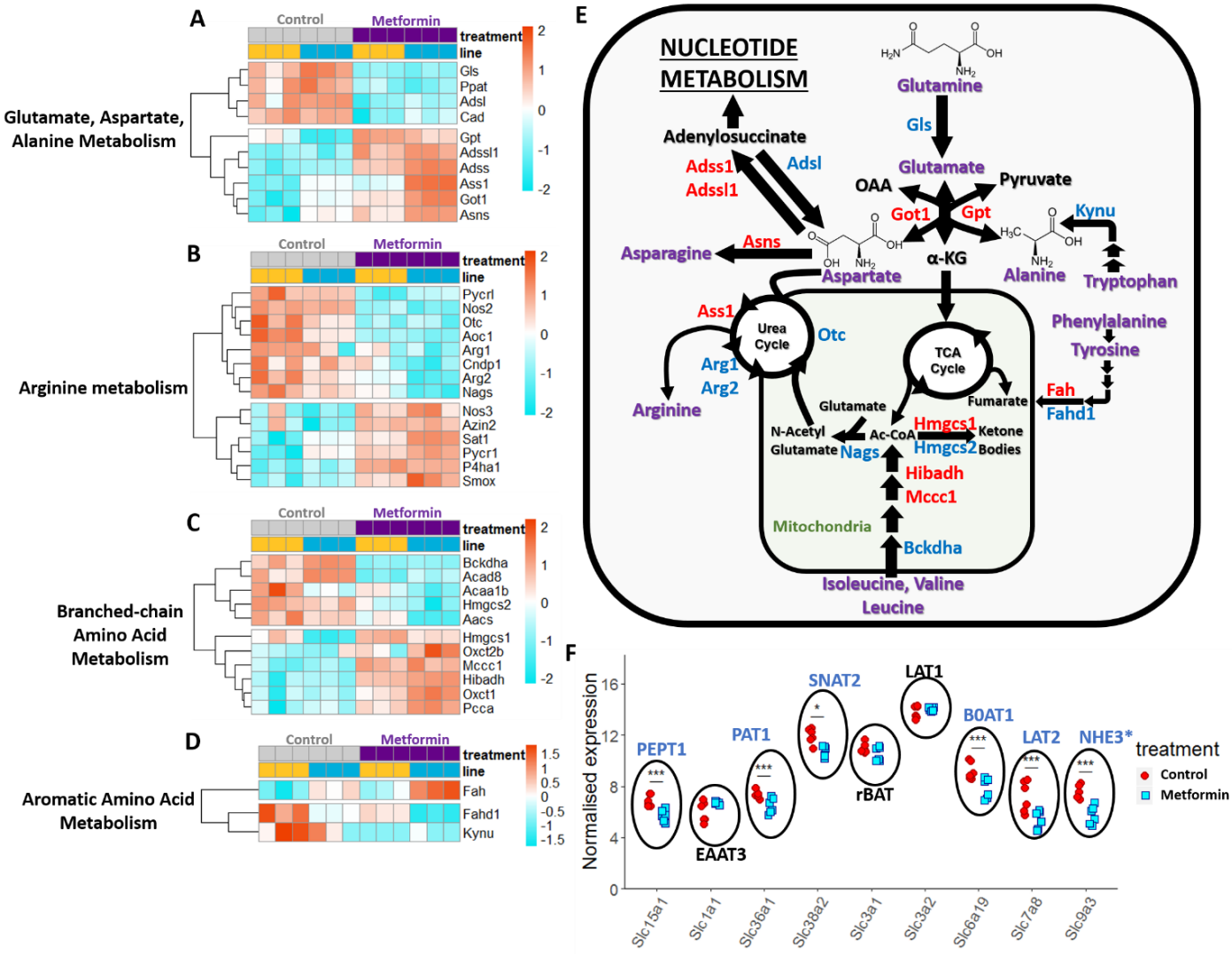

Figure 3.7. The effect of metformin on the expression of genes involved in amino acid metabolism and transporters. (A-D) Heatmaps showing DE genes (filtered by p-adjusted value of <0.05, genes with p-adjusted value of >0.05 were not included in the heatmap) involved in (A) Glutamate, Aspartate, Alanine metabolism (pathway ID: mmu00250), (B) Arginine metabolism (pathway ID: mmu00220 and 00330), (C) Branched-chain amino acid metabolism (pathway ID: mmu00280 and 00290) and (D) Aromatic amino acid metabolism (pathway ID: mmu00350, 00360 and 00380). Since some genes are involved in multiple pathways, they are shown only in a single pathway to avoid duplication. The colour key depicts the expression z-score and is shown on the right. Red indicates higher than average expression and blue indicates lower than average expression for a particular gene in a sample. (E) An integrated schematic showing the expression changes of genes involved in amino acid metabolism. (F) The effect of metformin on the expression of amino acid metabolism. *: NHE3 is not an amino acid transporter but is involved in maintaining the ion gradients necessary for electrogenic transport of amino acids. The transporters were identified from the protein digestion and absorption KEGG pathway (pathway ID: mmu04974). For E and F, red and blue shows the upregulated and downregulated genes, respectively.

synthetase, an indicator of amino acid deprivation *(372)*. Metformin decreased the expression of adenylosuccinate lyase (*Adsl*) associated with purine biosynthesis from aspartate, and glutaminase (*Gls*), the rate-limiting enzyme of glutamine metabolism. Because 20-55% of ingested branched chain amino acids (BCAAs- leucine, isoleucine and valine) are metabolised by the intestinal mucosa *(371)*, the effects of metformin in BCAA metabolism were investigated. Metformin decreased the expression of key genes *Bckdha* (the enzyme involved in the second step of BCAA catabolism) and *Hmgcs2*, but upregulated *Hibadh, Mccc1 and Hmgcs1*, which encode enzymes involved in Acetyl-CoA and ketone body metabolism (Figure 3.7BC, 3.7E). The KEGG enrichment analysis highlighted arginine biosynthesis as an enriched pathway in metformin treated cultures (16 DE genes out of 50 total genes). Metformin decreased the expression of key urea (arginine-citrulline) cycle genes such as *Otc, Arg1, Arg2* and *Nags* (Figure 3.7C, 3.7E). Metformin also altered the expression of some aromatic amino acid metabolism genes including fumarylacetoacetase (*Fah, Fahd1*) and kyneurinase (*Kynu*) (Figure 3.7D, 3.7E).

The effect of metformin on the expression of key amino acid transporters in intestinal epithelial cells were also investigated. From the transporters identified from the KEGG protein degradation and absorption pathway dataset, decreased expression of wide-spectrum amino acid transporters such as LAT1 (*Slc7a8*), B^0AT1 (*Slc16a9*), SNAT1 (*Slc38a1*) and SNAT2 (*Slc38a2*) were observed (Figure 3.8A). The oligo-peptide transporter PEPT1 (*Slc15a1*) and the imino-based amino acid transporter PAT1 (*Slc36a1*) were also downregulated, as well as the sodium/proton exchanger NHE3 (*Slc9a3*) involved in maintaining ion gradients for electrogenic activity to maintain amino acid transporter functions. To investigate whether decreased expression of the amino acid transporters would affect amino acid uptake, glutamine flux was monitored by live cell imaging of intestinal cells from Wild-type (Figure 3.8B), SNAT2 null (Figure 3.8C) and B^0AT1 null (Figure 3.8D) organoids transfected with a FRET-based glutamine sensor. No differences in glutamine flux were observed between the wild-type and knockout organoid lines, although SNAT2 null intestinal cells seemed to exhibit a reduced flux (P=0.123, Figure 3.8E). No differences were observed between control and metformin treated cells in any organoid line (Figure 3.8E). These results suggest that changes in amino acid transporter gene expression can be compensated by the functional activity of other glutamine transporters.

Folate dependent metabolism was highlighted from the KEGG enrichment analysis. This pathway was investigated in more detail, along with glycine/serine/threonine metabolism (since serine is a key 1-carbon substrate for the mitochondrial folate pool) and cysteine/methionine metabolism (the methionine cycle and folate metabolism pathways are interconnected). Metformin decreased the expression of many genes involved in folate dependent metabolism, with the exception of *Mthfd2*,

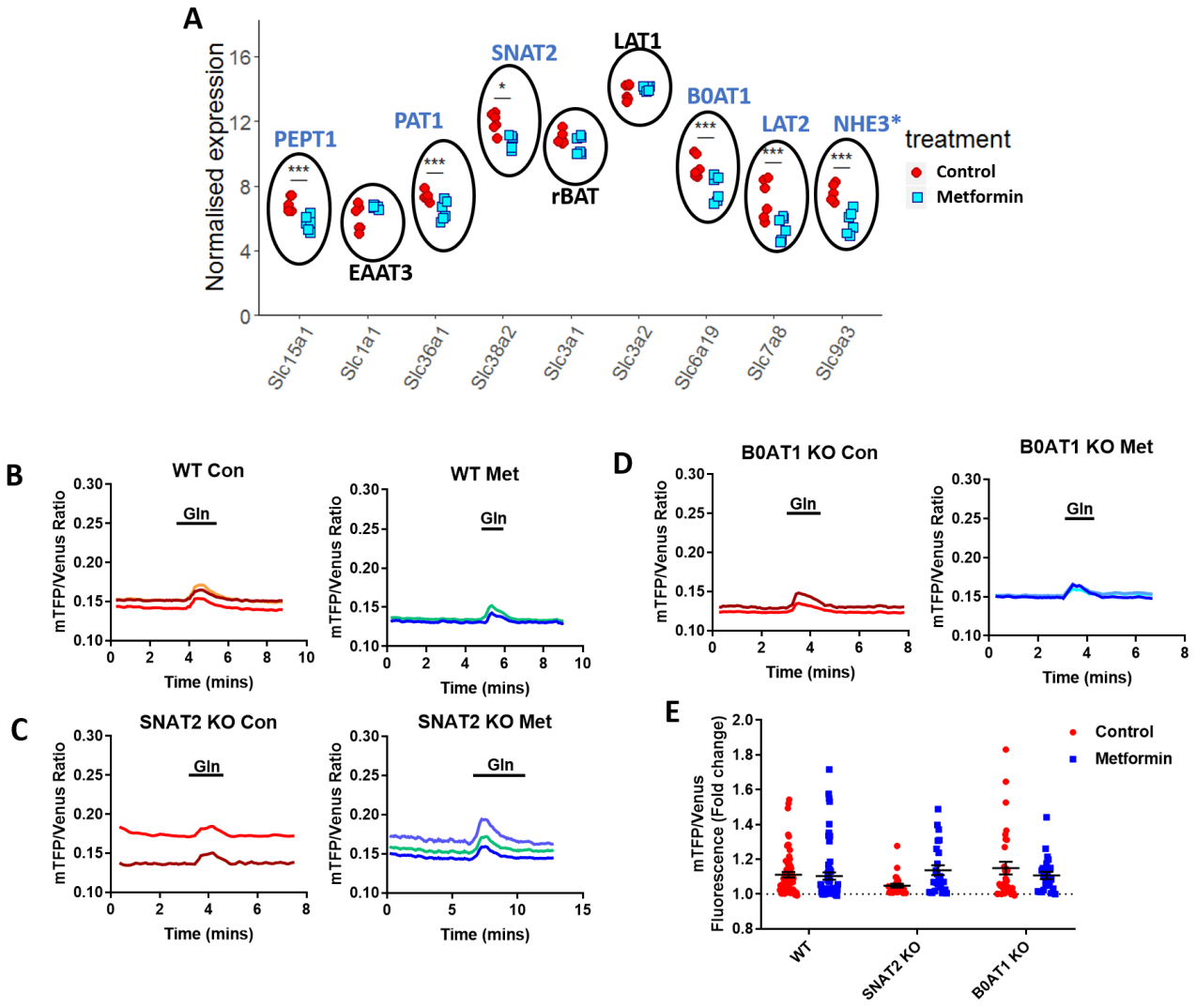

Figure 3.7. The effect of metformin on the expression of amino acid transporters and glutamine flux. (A) The effect of metformin on the expression of amino acid metabolism. *: NHE3 is not an amino acid transporter but is involved in maintaining the ion gradients necessary for electrogenic transport of amino acids. The transporters were identified from the protein digestion and absorption KEGG pathway (pathway ID: mmu04974). Red and blue shows the upregulated and downregulated genes, respectively. (B) Measurements of glutamine flux in intestinal cells from Wild-type organoids expressing a FRET-based glutamine sensor treated with control (Con) or metformin (Met). (C) Measurements of glutamine flux in intestinal cells from SNAT2 knockout organoids expressing a FRET-based glutamine sensor treated with control or metformin. (D) Measurements of glutamine flux in intestinal cells from B0AT1 knockout organoids expressing a glutamine sensor treated with control or metformin. (E) Changes in mTFP/Venus fluorescence of the glutamine sensor in control (red) or metformin (blue) treated intestinal cells from WT, SNAT2 KO and B0AT1 KO organoids. WT Control: N=62 cells from 18 dishes, WT Metformin: N=61 cells from 18 dishes, SNAT2 KO Control: N=27 cells from 9 dishes, SNAT2 KO Metformin: N=25 cells from 8 dishes, B0AT1 KO Control: N=32 cells from 7 dishes, B0AT1 KO Metformin: N=26 cells from 6 dishes. Bars are mean ± SEM. Two-way ANOVA and Bonferroni post hoc test.

which encodes for a multifunctional, rate-limiting enzyme of the mitochondrial folate cycle and has been associated with one-carbon pool imbalance in mitochondrial myopathies (Figure 3.9A, 3.9D) *(373, 374)*. Similarly, many of the genes involved in glycine, serine and threonine metabolism were downregulated by metformin treatment, except for aminolevulinic acid synthetase (*Alas1*) involved in glycine metabolism (Figure 3.9B). Metformin also decreased the expression of genes involved in cysteine and threonine metabolism (Figure 3.9C, 3.9D). This included DNA methyltransferases (*Dnmt1* and *Dnmt3a*) involved in DNA methylation. Other genes involved in cysteine/methionine metabolism such as glutamate-cysteine ligase (*Gclc*) (involved in cysteine metabolism to glutathione) and adenosylhomocysteinase-like 1 (*Ahcyl1*) (involved in methionine metabolism to homocysteine) were increased in metformin-treated cultures.

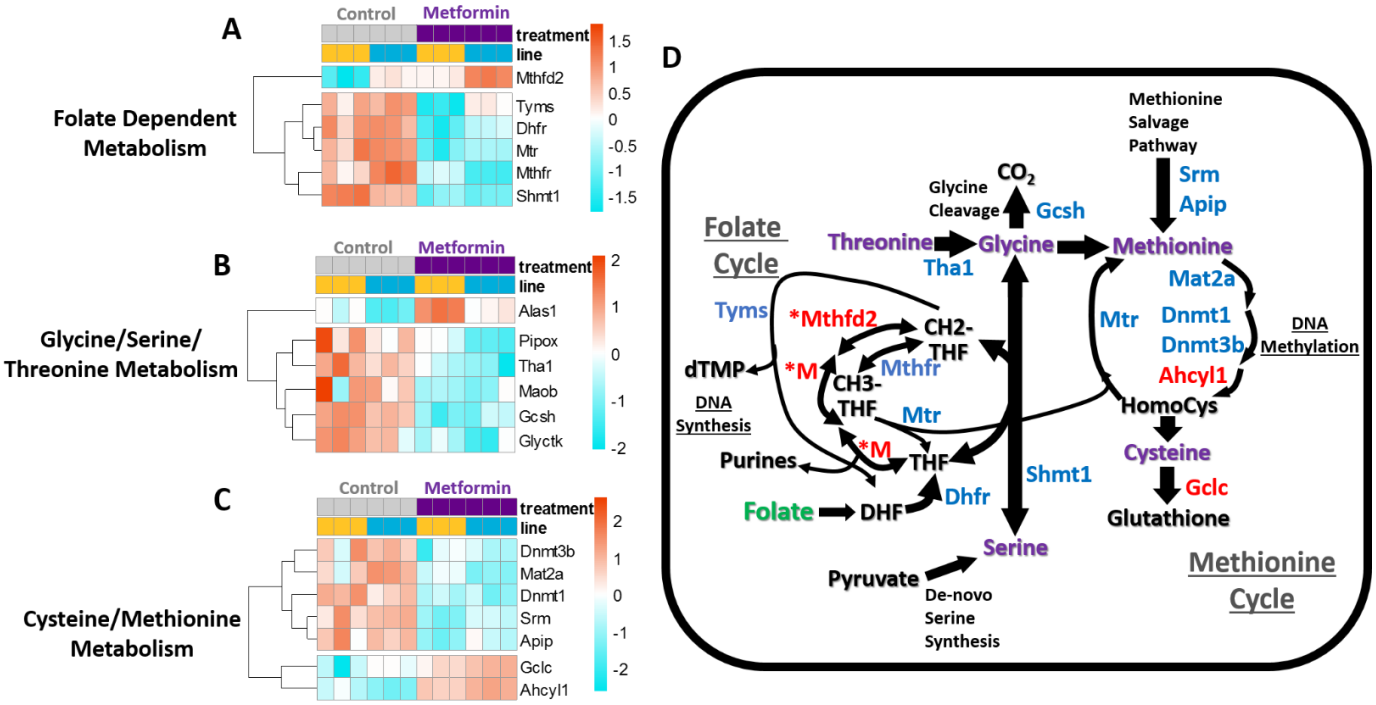

Figure 3.9. The effect of metformin on the expression of genes involved in the folate and methionine cycle. (A-C) Heatmaps showing DE genes (filtered by p-adjusted value of <0.05, genes with p-adjusted value of >0.05 were not included in the heatmap) involved in (A) Folate dependent Metabolism (pathway ID: mmu00790), (B) Glycine/Serine/Threonine metabolism (pathway ID: mmu00260) and (C) Glycine/Serine/Threonine metabolism (pathway ID: mmu00270). Colour key of the heatmap depicts the expression z-score. Red indicates higher than average expression and blue indicates lower than average expression for a particular gene in a sample. Since some genes are involved in multiple pathways, they are shown only in a single pathway to avoid duplication. (D) An integrated schematic showing the expression changes of genes involved in folate and methionine cycle. Red and blue shows the upregulated and downregulated genes, respectively. *M represents Mthfd2 (abbreviated), which catalyses multiple reactions in the mitochondrial folate cycle.

In summary, metformin increased the expression of genes involved in aspartate metabolism but decreased expression of genes involved in folate dependent metabolism, glycine/serine/threonine metabolism and cysteine/methionine metabolism. Many of the genes involved in the arginine-citrulline cycle were decreased by metformin. The expression of some of the amino acid transporters were also downregulated, although functional studies did not report differences in glutamine uptake.

3.4.2.3 Lipid metabolism, the PPAR signalling pathway, peroxisome and lysosome function

Since metformin has been reported to associate with cellular lipid metabolism and KEGG enrichment analysis highlighted increased fatty acid biosynthesis and cholesterol metabolism, the effects of metformin on lipid metabolism were investigated. In the fatty acid biosynthesis/elongation/degradation pathways, metformin increased the expression of acyl-CoA synthetases (*Acsl1, Acsl3* and *Acsl4*, but downregulated *Acsl6*), and fatty acid elongation enzyme Elovl4, but decreased the expression of fatty acid synthase (*Fasn*) and Acetyl-CoA thioesterase (*Acot4* and *Acot5*) (Figure 3.10A, 3.10B). Mitochondrial fatty acid oxidation genes such as *Echs1*, *Eci2*, *Mcat2* and *Oxsm* were increased in metformin treated cultures, whilst expression of the peroxisomal fatty acid oxidation gene *Acaa1b* was decreased.

Transporters involved in fatty acid and cholesterol uptake, such as *Cd36*, *Abcg5* and *Abcg8* were decreased in metformin treated cultures (Figure 3.10C, 3.10D). Amongst the cholesterol uptake receptors, the LDL uptake receptor (*Ldlr*) was increased, but the LDL receptor related protein (*Lrp2*) was decreased by metformin treatment. In the mitochondria, cholesterol transporters and metabolic enzymes *Tspo, Vdac2* and *Cyp27a1* were upregulated. Other DE genes include the lysosomal cholesterol trafficking genes (*Npc1* and *Npc2*- increased), the mitochondrial cholesterol uptake mediator (*Stard3* decreased), sterol O-acetyltransferase (*Soat2*- decreased) and lipoproteins (*Apoa1* and *Apoc3*- decreased) (Figure 3.10C, 3.10D).

The peroxisome proliferator-activated receptor (PPAR) pathway was also investigated, since activation of the pathway is closely associated with lipid metabolism and it is highlighted in the KEGG enrichment analysis (28 DE genes out of 85 total genes). Metformin increased the expression of *Pparg* but downregulated its transcriptional partner *Rxrb* (Figure 3.11A, 3.11B). Amongst the upstream PPAR pathway components, metformin increased the expression of long chain fatty acid transporter *Slc27a1*, but decreased the expression of very-LCFA and bile acid synthetases (*Slc27a2* and *Slc27a5* respectively), and fatty acid binding protein (*Fabp*). In addition to fatty acid metabolism genes (discussed in Figure 3.9), metformin increased the expression of PPAR target genes involved in glycerol metabolism/gluconeogenesis (*Gk* and *Aqp7*), and angiogenesis (*Agptl4* and *Sorbs1*).

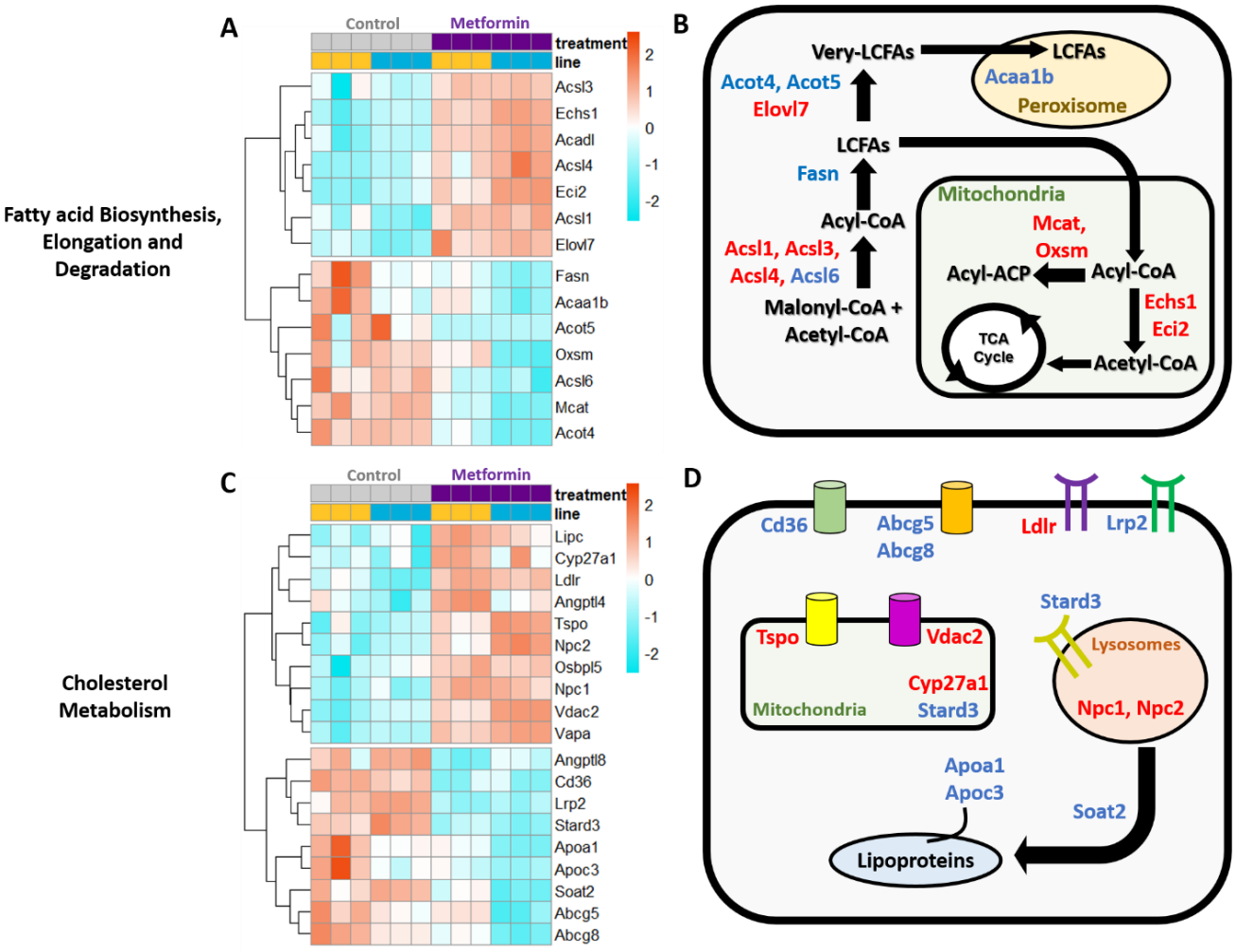

Figure 3.10. The effect of metformin on the expression of genes involved in fatty acid and cholesterol metabolism. (A and C) Heatmaps showing DE genes (filtered by p-adjusted value of <0.05, genes with p-adjusted value of >0.05 were not included in the heatmap) involved fatty acid (pathway ID: mmu00061, 00062 and 00071) and cholesterol metabolism (pathway ID: mmu04979). Since some genes are involved in multiple pathways, they are shown only in a single pathway to avoid duplication. The colour keys showing the expression z-scores are shown on the right. Red indicates higher than average expression and blue indicates lower than average expression for a particular gene in a sample. (B and D) Schematics showing the expression changes of genes involved in fatty acid and cholesterol metabolism. Red and blue shows the upregulated and downregulated genes, respectively.

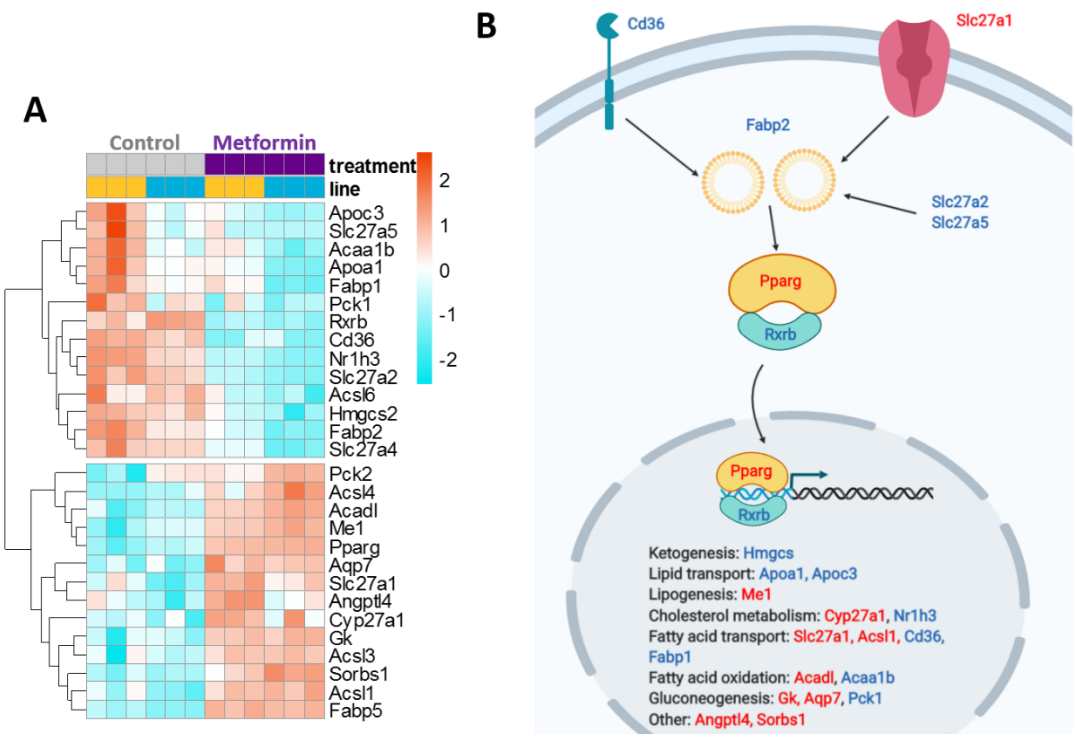

Figure 3.11. The effect of metformin on the expression of genes involved in the PPAR signalling pathway. (A) Heatmap showing DE genes (filtered by p-adjusted value of <0.05, genes with p-adjusted value of >0.05 were not included in the heatmap) involved in the PPAR signalling pathway (pathway ID: mmu03320). Some of the genes shown are involved in glucose and lipid metabolism pathways and are duplicated from previous figures to show their involvement in this pathway. The colour keys showing the expression z-scores are shown on the right. Red indicates higher than average expression and blue indicates lower than average expression for a particular gene in a sample. (B) Schematic showing the expression changes of genes involved in the PPAR signalling pathway. Red and blue shows the upregulated and downregulated genes, respectively. Schematic is adapted from the Pathview version of the pathway.

The peroxisome is closely associated with fatty acid and cholesterol metabolism and KEGG genesets associated with peroxisome function and was investigated further. Metformin decreased the expression of many peroxin subtypes (except *Pex11b*) involved in targeted peroxisomal transport, and purine/retinol metabolism genes (Figure 3.12A and 3.12B). Other peroxisome-targeted lipid metabolism genes such as *Nudt9, Amacr* and *Far2* were downregulated, and *Nudt7* was increased by metformin treatment. Amino acid metabolism genes spermine oxidase (*Paox*) was upregulated and sarcosine oxidase (*Pipox*) was downregulated, respectively. Metformin also increased the expression of the genes *Mpv17l* and *Gstk1* involved in peroxisomal ROS and antioxidant metabolism.

Within the genes involved in lysosome function (highlighted from KEGG enrichment analysis), Metformin increased the expression of most lysosomal peroxidases and membrane proteins (except lysosomal lipases *Acp2, Acp5* and the lysosomal sulfatase *Sgsh*, which were decreased in expression)

(Figure 3.12C, 3.12D). The ATP-dependent H^+ transporter subunits *Atp6v0d1*, *Atp6v0b* and *Atp6ap1*, which is essential for maintaining the acid environment of the organelle, was also upregulated by metformin. Genes involved in the transport of lysosomal proteins such as *Nagba, Ap3d1* and *Ap4s1* were decreased by metformin treatment, but expression of *M6pr* and *Cltc* were increased.

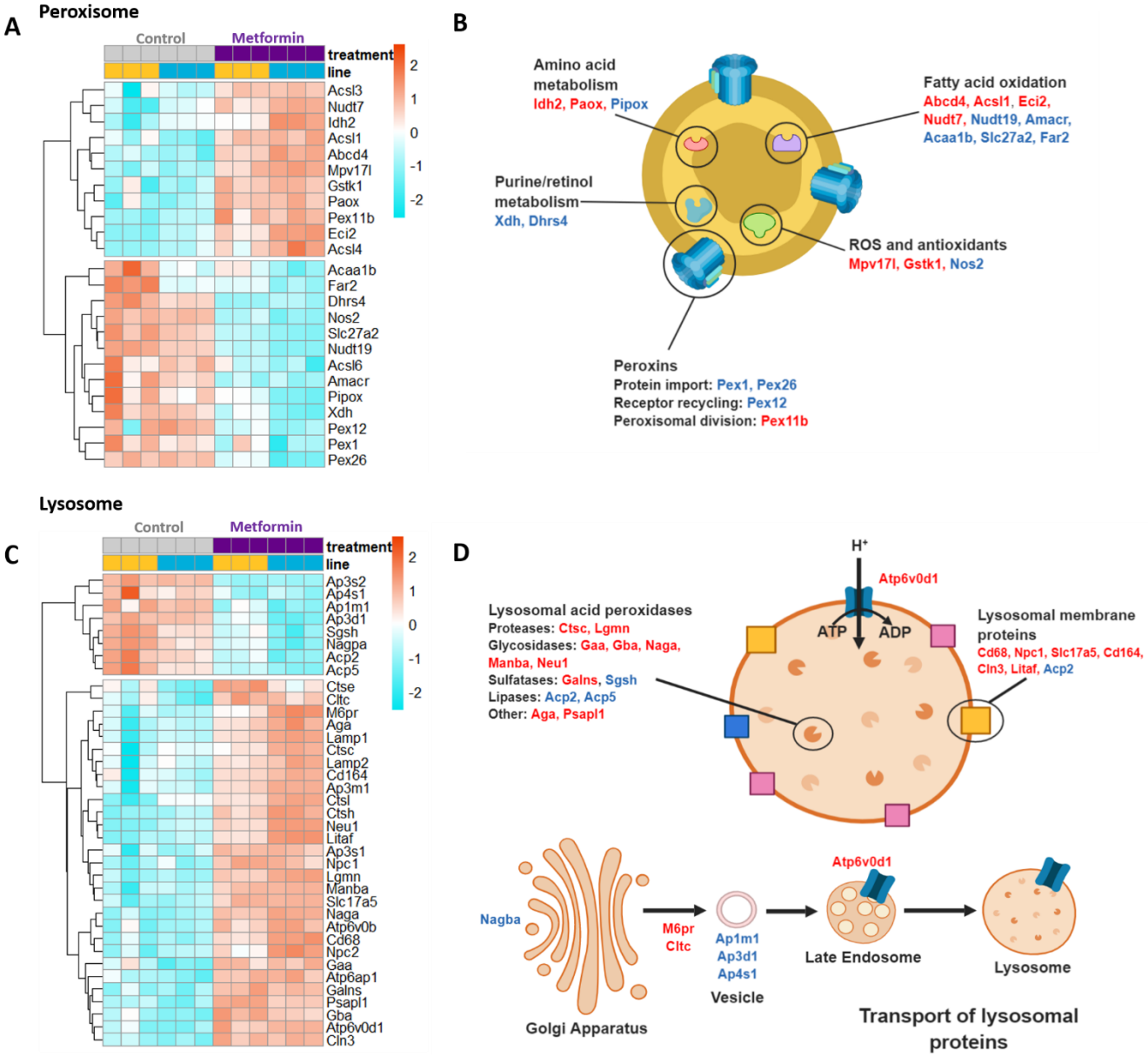

Figure 3.12. The effect of metformin on the expression of genes involved in peroxisome and lysosome processes. (A and C) Heatmaps showing DE genes (filtered by p-adjusted value of <0.05, genes with p-adjusted value of >0.05 were not included in the heatmap) involved in peroxisome (pathway ID: mmu04142) and lysosome (pathway ID: mmu04146) processes. Some of the genes shown are involved in other metabolism pathways and are duplicated from previous figures to show their involvement in this pathway. The colour keys showing the expression z-scores are shown on the right. Red indicates higher than average expression and blue indicates lower than average expression for a particular gene in a sample. (B and D) Schematics showing the expression changes of genes involved in peroxisome and lysosome processes. Red and blue shows the upregulated and downregulated genes, respectively. Schematic is adapted from the Pathview versions of the pathways.

Although KEGG enrichment analysis identified fatty acid biosynthesis, cholesterol metabolism and PPAR signalling pathways, detailed investigations did not reveal a conclusive pattern of expression. Most of the genes involved in lysosome function were upregulated under metformin treatment.

3.4.2.4 Signalling pathways involved in nutrient and energy sensing

Since metformin activates AMPK signalling, the transcriptomic responses of the AMPK signalling pathway were investigated in detail, despite that the AMPK signalling pathway was not highlighted in the KEGG pathway analysis. Whilst expression of the α-subunit (*Prkaa2*) was increased by metformin, expression of other subunits *(Prkab1*, β-subunit and Prkag1, γ-subunit) were downregulated (Figure 3.13A, 3.13B). The expression of inhibitory protein phosphatases of AMPK signalling (*Ppp2r5a, Ppp2r5b* and *Ppp2r5c*) were increased in metformin treated cultures. Although the effects of metformin in the expression profiles of other downstream AMPK signalling pathways were not particularly conclusive, the expression of vesicular transport genes (*Tdc1d1, Rab10* and *Rab14*) were induced by metformin.

Within the mTOR signalling complex, whilst *Mtor* and *Rictor* expression were both induced by metformin, the expression of *Mlst8* and *Telo2* were decreased (Figure 3.13C, 3.13D). Moreover, very few of the genes downstream of the mTOR signalling complex were differentially expressed (Figure 3.13D). Therefore, the effect of metformin on the transcriptomic expression profiles of mTOR signalling genes are inconclusive.

The HIF-1α pathway was also selected for investigation, as mitochondrial dysfunction caused by metformin treatment might be associated with HIF-1α signalling. *Hif1α* expression was increased by metformin, as well as its transcriptional co-activator HIF-1B (*Arnt*) and the ribosomal protein *Rps6* that regulates HIF-1A translation (Figure 3.14A, 3.14B). Genes that regulate targeted degradation of HIF-1a under normoxic conditions, such as the prolyl hydroxylase *Egln1* and the ubiquitin ligase *Vhl* were downregulated in metformin-treated cultures (the exception is the scaffold protein *Cul2* with upregulated expression). The effect of metformin on the expression of HIF-1a target genes was investigated using a catalogue of established HIF-1A target genes from *(375)*. From the catalogue, 20 out of 87 mapped genes were DE genes, with 16 upregulated and 4 downregulated genes, respectively (Figure 3.14C). Prominent genes involved in glycolysis as mentioned in Figure 3.4 and vascular associated genes (*Serpine1, Edn1, Nos3* and *Pdgfa*) were upregulated in metformin treated cultures (Figure 3.14C).

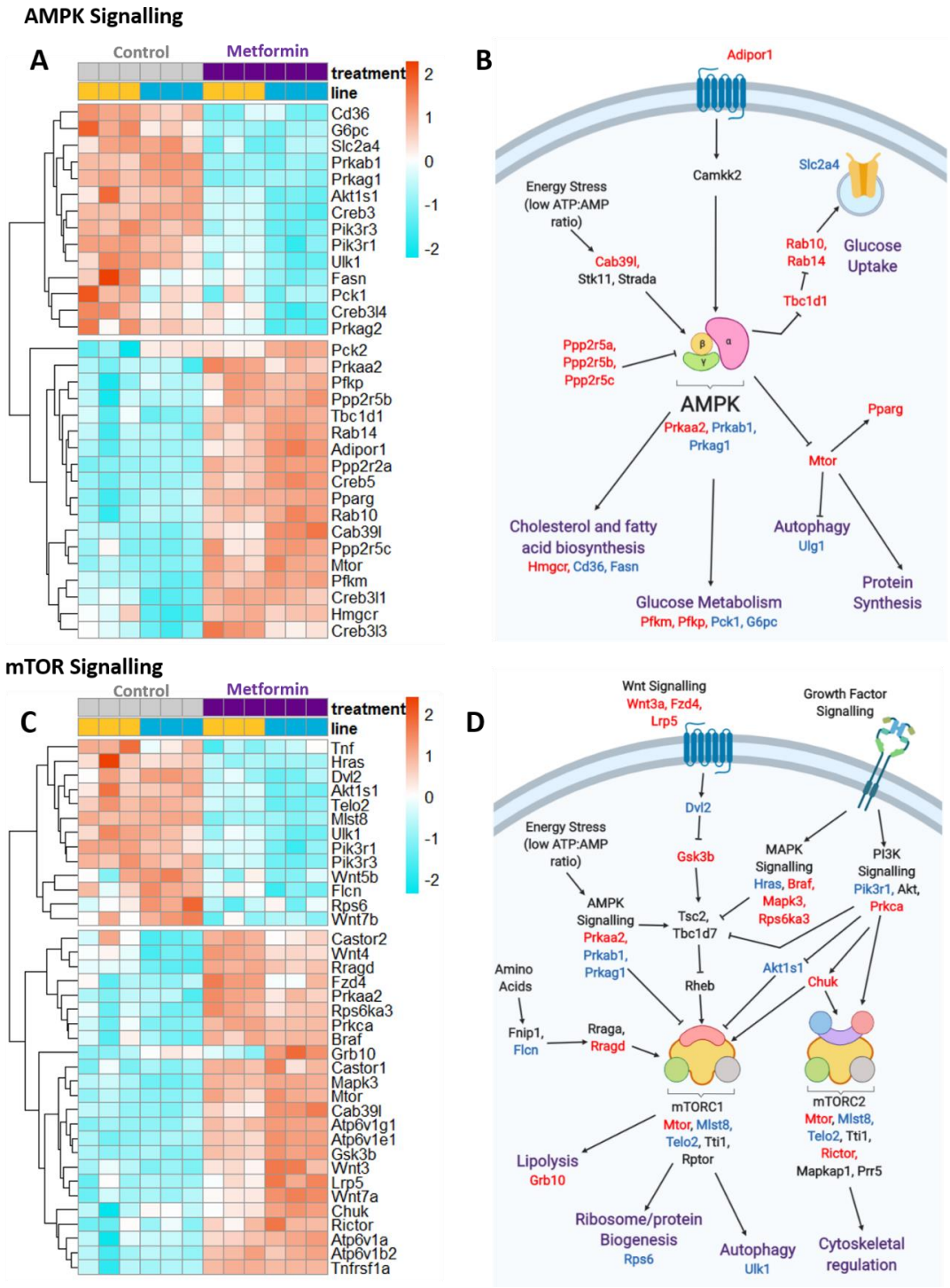

Figure 3.13. The effect of metformin on the expression of genes involved AMPK and mTOR signalling pathways. (A and C) Heatmaps showing DE genes (filtered by p-adjusted value of <0.05, genes with p-adjusted value of >0.05 were not included in the heatmap) involved in the AMPK (pathway ID: mmu04152) and mTOR signalling (pathway ID: mmu04150) pathways, respectively. Some of the genes shown are involved in other pathways and are duplicated from previous figures to show their involvement in this pathway. The colour keys showing the z-scores are shown on the right. Red indicates higher than average expression and blue indicates lower than average expression for a particular gene in a sample. (B and D) Schematics showing the expression changes of genes involved in AMPK and mTOR signalling pathways. Red and blue shows the upregulated and downregulated genes, respectively. Schematic is adapted from the Pathview versions of the pathways.

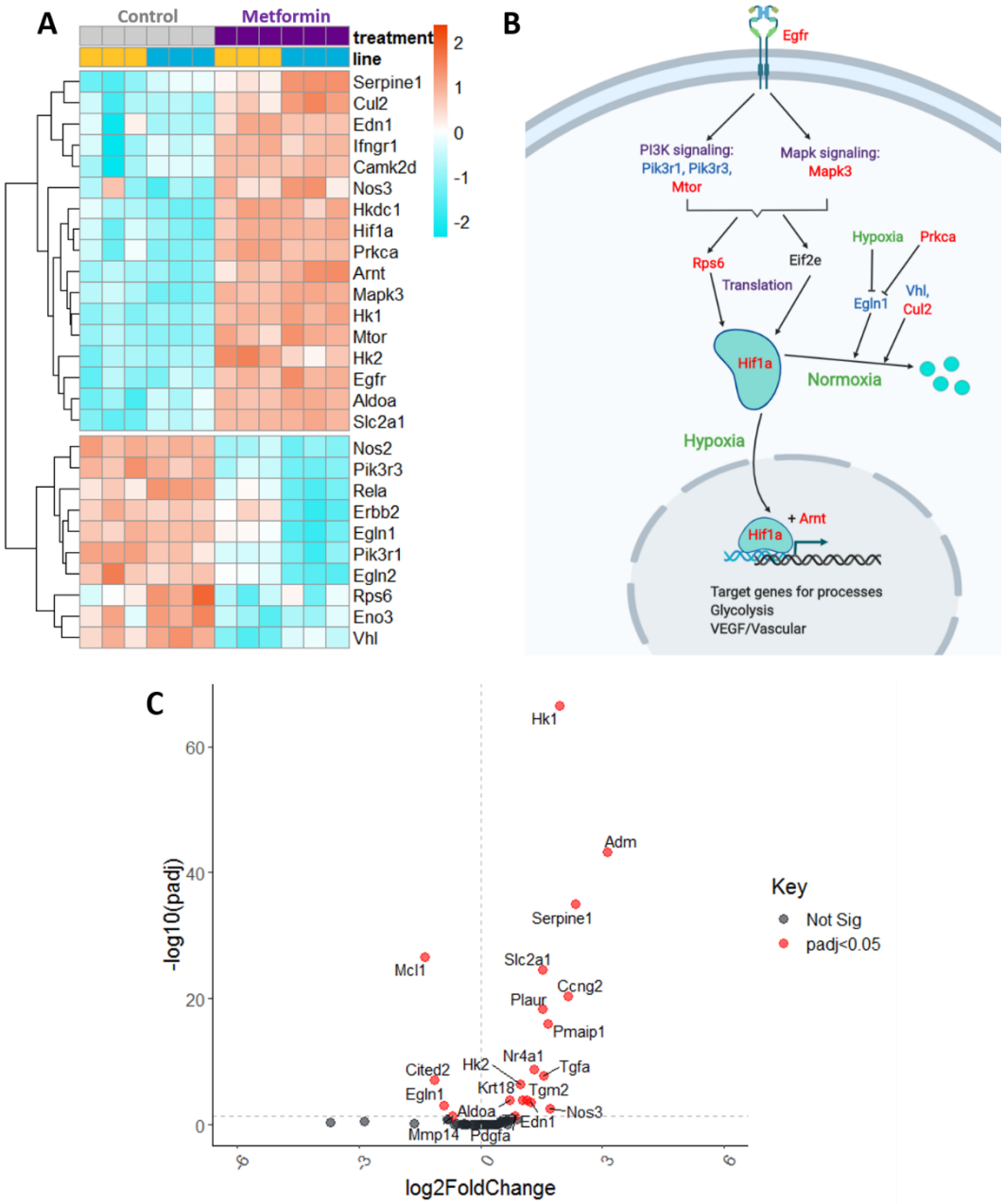

Figure 3.14. The effect of metformin on the expression of genes involved Hif1a signalling. (A) Heatmaps showing DE genes (filtered by p-adjusted value of <0.05) involved in the HIF1A signalling pathway identified from KEGG analysis (pathway ID: mmu04066). The colour keys showing the z-scores are shown on the right. (B) Schematics showing the expression changes of genes involved in HIF-1A signalling. Red and blue shows the upregulated and downregulated genes, respectively. Schematic is adapted from the Pathview version of the pathway. (C) Volcano plot showing the effects of metformin on the expression of HIF-1A signalling target genes, red shows significantly expressed genes (padj<0.05), black shows non-significant genes (Not Sig). The database is derived from *(375)*.

3.4.2.5 Growth factor signalling pathways

The KEGG enrichment analysis identified growth factor signalling pathways such as Hippo and MAPK signalling. There seems to be general upregulation of genes involved in the Hippo signalling pathway (Figure 3.15A). Metformin increased *Wwtr1* expression, which encodes the TAZ transcription factor central to the Hippo signalling pathway, as well as its co-transcription partners *Tc7* and *Tead1* (Figure 3.15A and 3.15B). Other upregulated genes include upstream regulatory proteins including *Stk3*, *Ppp2r2a, Ppp1cb, Rassf6* and *Actg1*. Casein kinase (*Csnk1e*), which is involved in the targeted degradation of TAZ, was also induced by metformin. Upstream signalling pathways that interact with Hippo pathway involve TGFβ, WNT and cell adhesion signalling. TGFβ signalling pathway genes *Tgfb2, Bmp2, Bmp8* and *Bmpr2* were upregulated by metformin; the pathway is involved in the activation of Smad transcription factors that associate with YAP or TAZ to coactivate transcription of a specific subset of genes. Genes involved in cell function *Cdh1* and *Ctnna1* were also increased by metformin, although they are involved the cytosolic retention of YAP and TAZ. Increased expression of downstream YAP/TAZ pathway genes, such as *Areg, Afp, Serpine1* and *Birc5* was also observed.

Since the MAPK signalling includes a broad spectrum of pathways activated by stress as well as growth factors, EGFR and TNFα signalling pathways were selected for further investigation as they activate MAPK signalling under different contexts. Various autocrine/paracrine growth factors involved in the EGFR signalling pathway, *Areg, Ereg, Btc, Hbegf* and *Tgfa*, and the EGF receptor (*Egfr*) were upregulated by metformin, although Erbb2 was downregulated and *Egf* expression remain unchanged (Figure 3.16A and 3.16B). The ERK arm of the EGFR signalling pathway seem to be increased by metformin, notably ERK gene *Mapk3* and upstream signalling component *Braf, Pak2* and *Pak4*, but the genes *Pak6* and *Hras* were also downregulated. In the PI3K arm of the EGFR pathway, the PI3K genes *Pik3r1* and *Pik3r3* genes were downregulated in metformin treated cultures whilst *Akt* expression was not significantly different. Genes involved in the Ca^{2+} dependent signalling arm of the *Prkca* and *Camk2d* of the EGFR signalling pathway were also upregulated by metformin.

In the TNFα signalling pathway, although the expression of MAPK signalling kinases (*Mapk3, Mapk8* and *Mapk13*), pro-apoptotic caspases (*Casp3, Casp7* and *Casp8*) and TNFα activated transcription factor *Creb3* were increased in metformin-treated cultures, TNF-receptor signalling *adaptors Ripk1, Traf2* and *Fadd* expression were downregulated (except *Tradd*, which was increased) (Figure 3.16C and 3.16D). Amongst TNFα signalling target genes affected by metformin include leukocyte recruitment, activation and cell adhesion/extracellular matrix genes (Figure 3.16D).

The transcriptomic evidence could potentially suggest that increased EGFR activation by growth factors might involve activation of the ERK-dependent signalling pathway in metformin treated

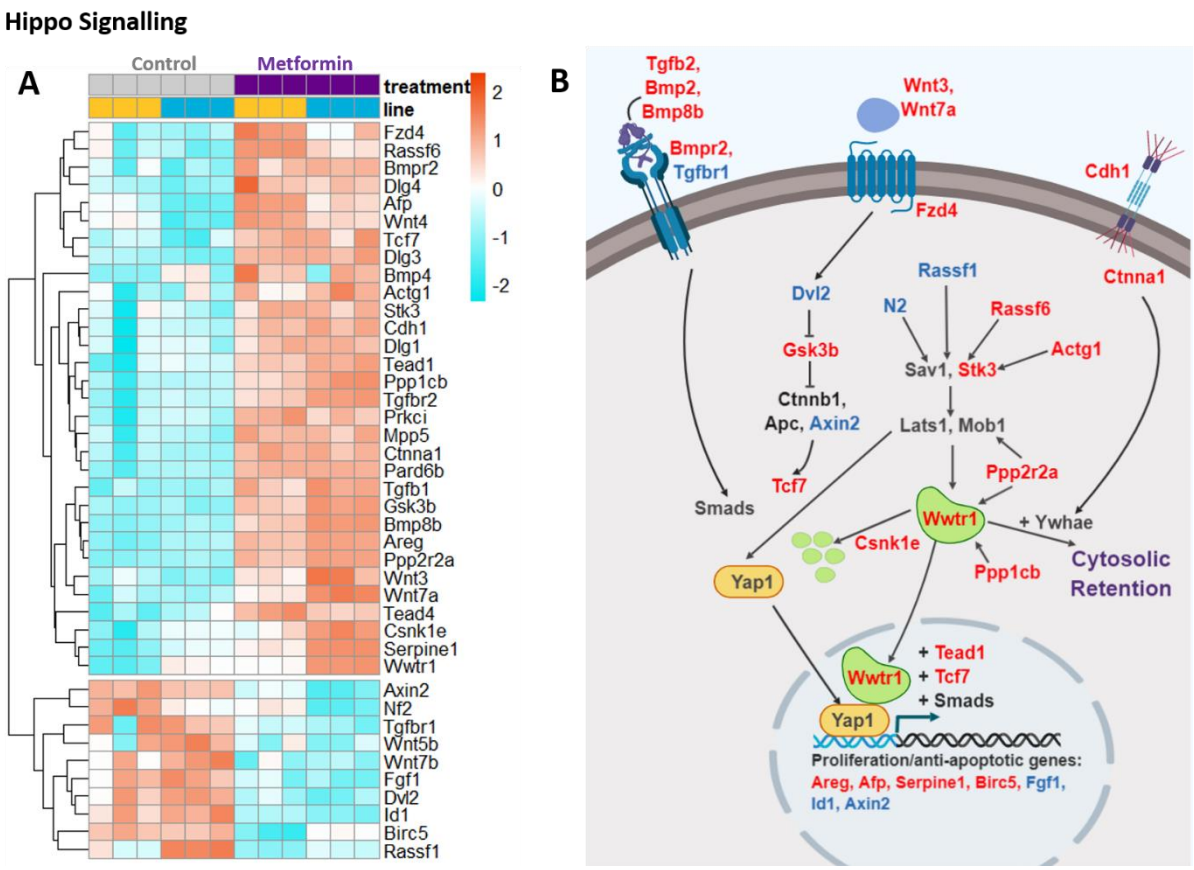

Figure 3.15. The effect of metformin on the expression of genes involved in the Hippo signalling pathway. (A) Heatmap showing DE genes (filtered by p-adjusted value of <0.05) involved in the Hippo signalling pathway (pathway ID: mmu04390). Some of the genes shown are involved in other pathways and are duplicated from previous figures to show their involvement in this pathway. The colour keys showing the z-scores are shown on the right. (B) Schematic showing the expression changes of genes involved in Hippo signalling pathway. Red and blue shows the upregulated and downregulated genes, respectively. Schematic is adapted from the Pathview versions of the pathway.

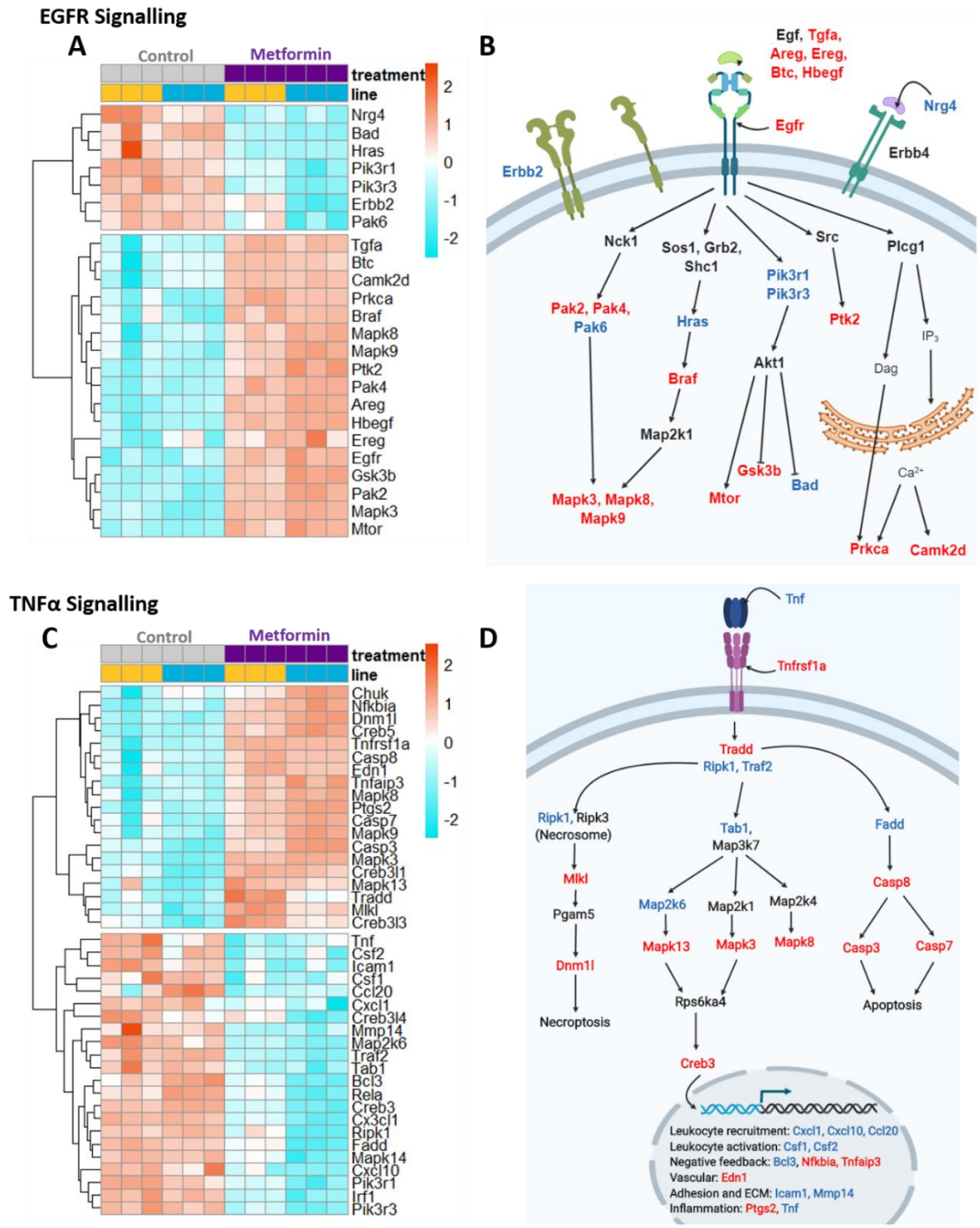

Figure 3.16. The effect of metformin on the expression of genes involved in TNFα and EGFR signalling. (A and C) Heatmaps showing DE genes (filtered by p-adjusted value of <0.05) involved in the EGFR (pathway ID: mmu04012) and TNFα (pathway ID: mmu044668) signalling pathways. Some of the genes shown are involved in other pathways and are duplicated from previous figures to show their involvement in this pathway. The colour keys showing the z-scores are shown on the right. (B and D) Schematics showing the expression changes of genes involved in EGFR and TNFα signalling pathways. Red and blue shows the upregulated and downregulated genes, respectively. Schematic is adapted from the Pathview versions of the pathways.

cultures, although this cannot be conclusive based on transcriptomic data alone. The effects of metformin in the TNFα signalling pathway is elusive.

3.4.2.6 P53 and the cell cycle

As well as TNFα, the P53 signalling pathway was also identified in the KEGG enrichment analysis. The gene *Trp53* was unexpectedly downregulated by metformin treatment, as well as its upstream DNA-damage kinase *Atr* (Figure 3.17A, 3.17B). However, prominent downstream P53 target genes involved in cell cycle arrest (*Sfn, Gadd45a, Gadd45b* and Gadd45g), apoptosis (*Casp3, Casp8, Pmaip1, Shisha5, Perp* and *Zmat3*), serpins (*Serpine1* and *Serpin5*), exosome (*Steap3*) were upregulated in metformin treated cultures. Other P53 target genes include downregulated apoptotic genes (*Siah1b* and *Pidd1*), P53 negative feedback genes (*Ccng, Ppm1d*) and DNA repair (*Sesn3, Rrm2*).

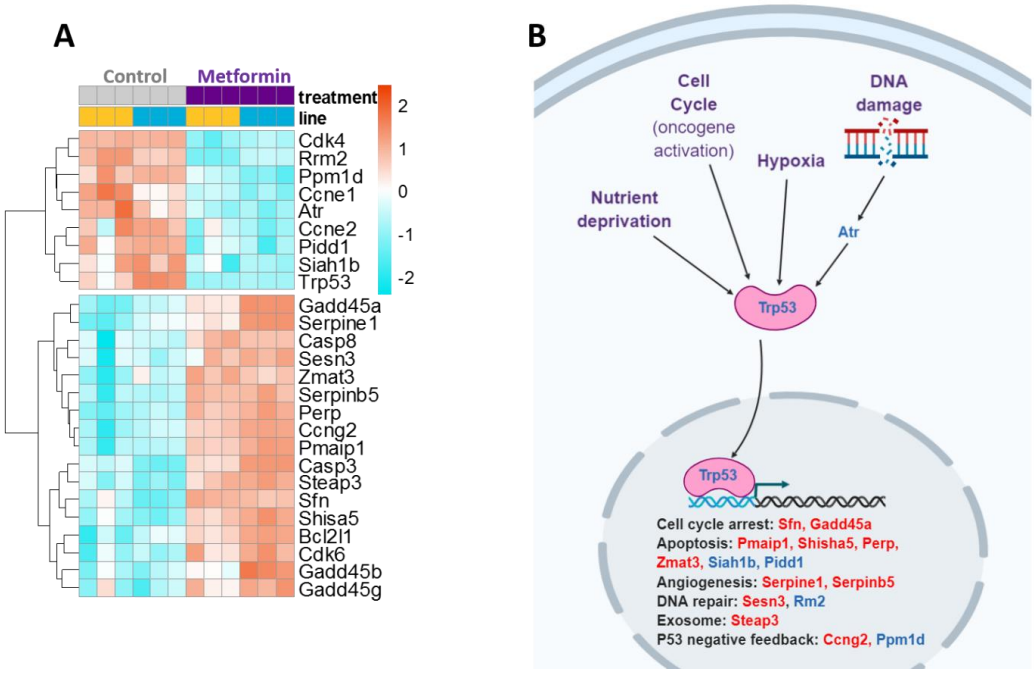

Figure 3.17. The effect of metformin on the expression of genes involved in the P53 signalling pathway. (A) Heatmap showing DE genes (filtered by p-adjusted value of <0.05) involved in the P53 signalling pathway (pathway ID: mmu04115). The colour keys showing the z-scores are shown on the right. (B) Schematic showing the expression changes of genes involved in the P53 signalling pathway. Red and blue shows the upregulated and downregulated genes, respectively. Schematic is adapted from the Pathview version of the pathway.

As well as P53 target genes involved in cell cycle arrest, other genes directly involved in cell cycle regulation was also differentially expressed in metformin treated cultures. In the G1 phase checkpoint, metformin decreased the expression of transcription factors *E2f1* and *Tfdp2* necessary to promote G1

progression, but increased the expression of G1 phase regulators *E2f5* and *Rb1*, and CDK inhibitors *Cdkn2b* and *Cdkn1c* (Figure 3.18A, 3.18B). Metformin also seemed to inhibit S phase progression by decreasing the expression of all minichromosome maintenance MCM complex genes, *Cdc6, Cdc7* and *Cdc45*, as well as origin recognition complex (ORC) genes *Orc5* and *Orc6* (although in the latter *Orc3* and *Orc4* were upregulated). *Cdc25a*, which promote both G1 and S phase progression, was downregulated in metformin cultures. In the G2 phase checkpoint, metformin decreased the expression of *Cdc25c*, which activate cyclins involved in G2 phase progression. Metformin decreased the expression of mitotic spindle assembly checkpoint genes such as *Mad1l1, Ttk, Cdc23, Cdc30*, Separase (*Espl1*) (which hydrolyses cohesins and triggers anaphase) and Cohesin (*Smc1a*) but increased the expression of *Mad2l2* and cohesion gene *Stag2*. The transcriptomic data suggests that metformin could stall cell cycle progression particularly during the G1 and S phases.

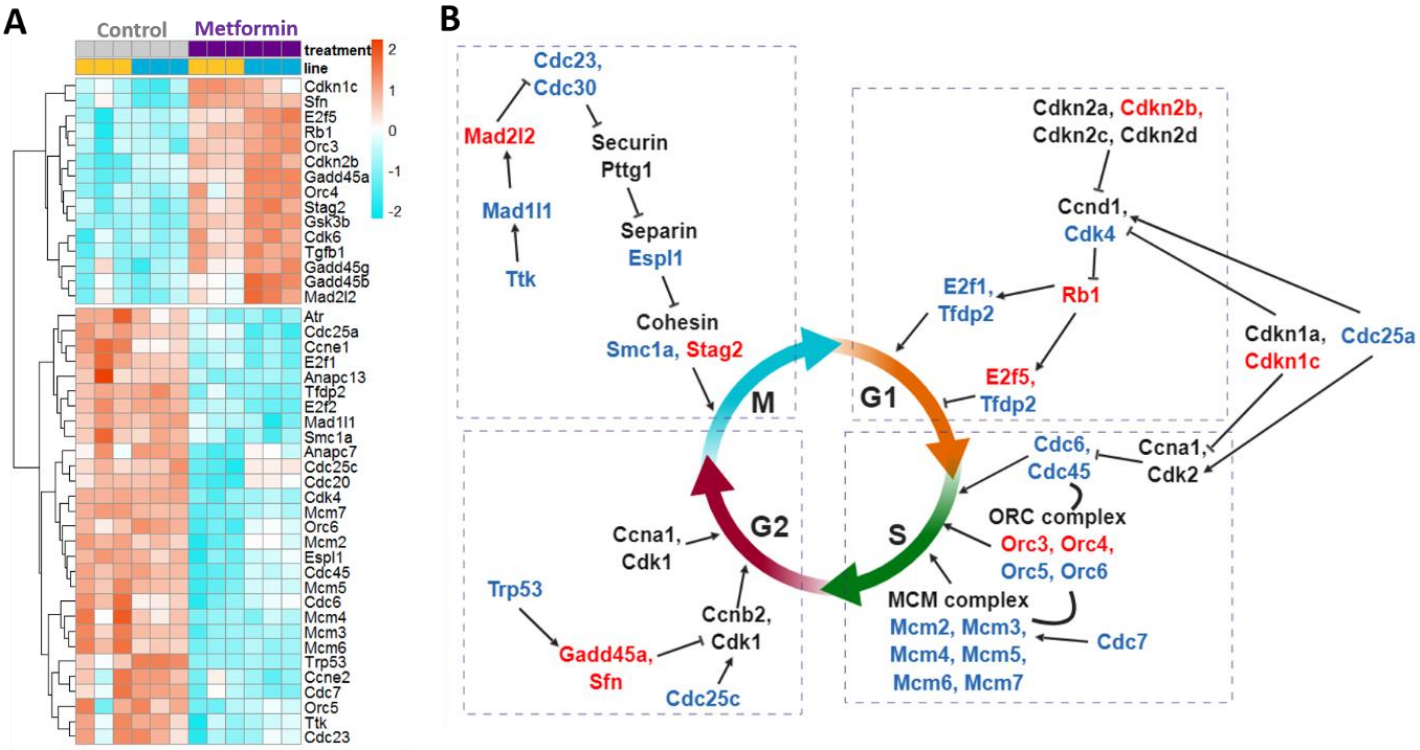

Figure 3.18. The effect of metformin on the expression of genes involved in cell cycle regulation. (A) Heatmap showing DE genes (filtered by p-adjusted value of <0.05) involved in cell cycle regulation (pathway ID: mmu04110). Some of the genes shown are involved in other pathways and are duplicated from previous figures to show their involvement in this pathway. The colour keys showing the z-scores are shown on the right. (B) Schematic showing the expression changes of genes involved in the P53 signalling pathway. Red and blue shows the upregulated and downregulated genes, respectively. Schematic is adapted from the Pathview version of the pathway.

3.4.2.7 Pyrimidine metabolism and DNA/RNA processes

Other pathways identified from KEGG enrichment analysis are nucleotide metabolism and DNA/RNA processes. 22 out of 58 genes were differentially expressed in the pyridine metabolism pathway, metformin downregulated genes favouring pyrimidine nucleotide biosynthesis include nucleotide kinases (*Nme6, Dtymk, Tk2* and *Uck1*), ribonucleotide reductase (*Rrm2*), dCMP deaminase (*Dctd*) and thymidylate synthetase (*Tyms*) (Figure 3.19A and 3.19B). The nucleotidases (*Nt5c2* and *Nt5m*) were also downregulated by metformin. Genes encoding enzymes involved in the catabolism of nucleotides, notably Ectonucleotide triphosphate diphosphohydrolase (*Entpd3*) and 5'-nucleotidase (*Nt5c1a*), were increased in metformin treated cultures (Figure 3.19A and 3.19B). These transcriptomic results suggest that metformin might favour nucleotide catabolism over biosynthesis.

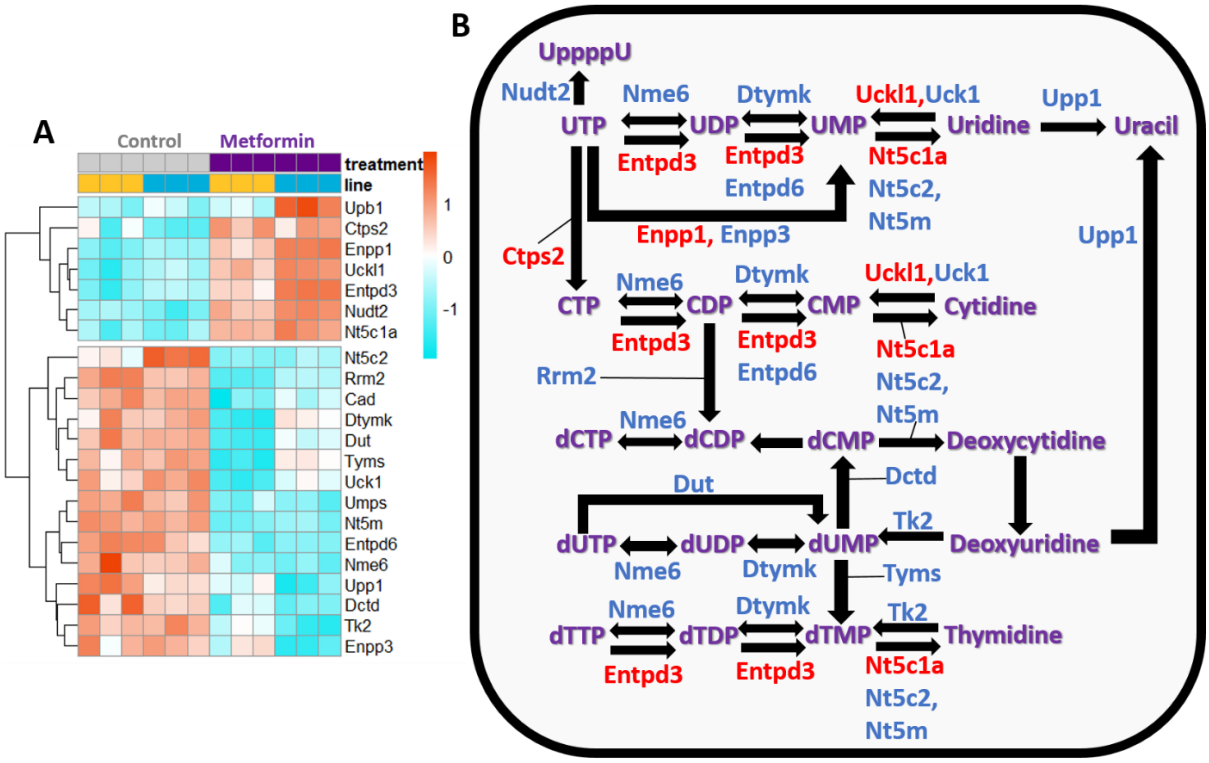

Figure 3.19. The effect of metformin on the expression of genes involved in pyrimidine metabolism. (A) Heatmap showing DE genes (filtered by p-adjusted value of <0.05) involved in pyrimidine metabolism (pathway ID: mmu00240). The colour keys showing the z-scores are shown on the right. (B) Schematic showing the expression changes of genes involved in pyrimidine metabolism. Red and blue shows the upregulated and downregulated genes, respectively.

With the exception of genes *Snrnp27, Prpf40b* and *Sf3b1*, metformin robustly decreased the expression of genes involved in the spliceosome, the machinery involved in regulating RNA splicing (42 out of 133 of genes in the pathway, Figure 3.20A). Metformin robustly downregulated the expression of RNA polymerases that regulate transcription (13 out of 30 genes), except *Polr2g* (Figure 3.20B). Moreover, metformin decreased the expression of genes involved in DNA replication, except DNA polymerase subunit *Pold4* (20 out of 35 genes, Figure 3.20C). Metformin also downregulated the expression of DNA repair genes except Endonuclease 8-like 1 *Neil1* (Figure 3.20D). The RNA-seq data provides evidence that metformin might be involved in downregulating the gene-expression machinery involved in DNA and RNA processes.

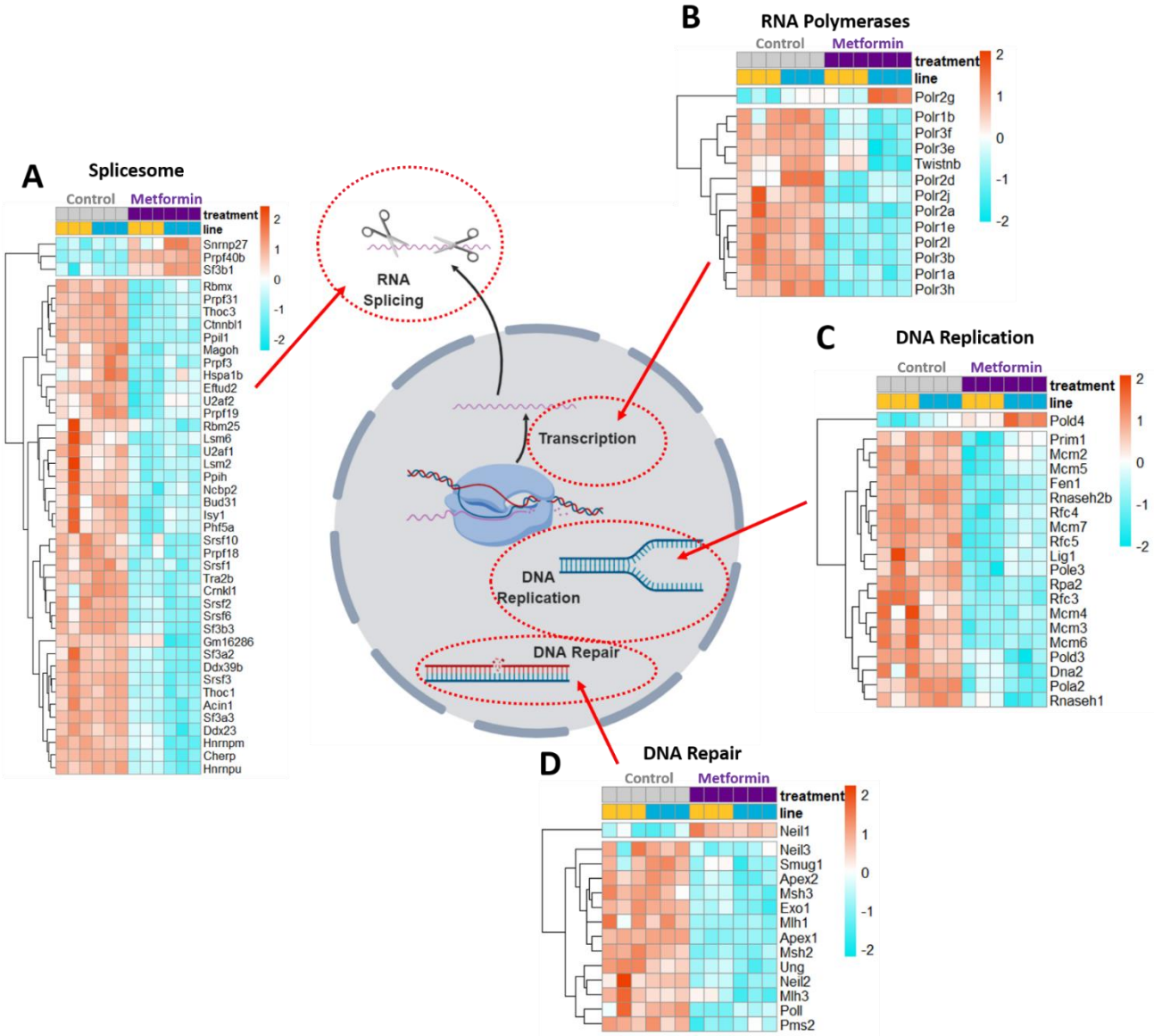

Figure 3.20. The effect of metformin on the expression of genes involved in DNA processes. (A-D) Heatmaps showing DE genes (filtered by p-adjusted value of <0.05) involved in (A) spliceosome assembly (pathway ID: mmu03040), (B) RNA polymerases (pathway ID: mmu03020), (C) DNA replication (pathway ID: mmu03030) and (D) DNA repair (pathway ID: mmu03410, 03420 and 03430). Some of the genes shown overlap with other pathways and may be duplicated. The colour keys showing the z-scores are shown on the right of each heatmap.

3.5 Discussion

3.5.1 Metformin and glucose/sugar metabolism

In this study, KEGG enrichment analysis highlighted glycolysis/gluconeogenesis as a key pathway altered by metformin treatment, by increasing the expression of hexokinases, phosphofructokinases and aldolase A (Figure 3.3, 3.4). Overexpression studies suggested that hexokinases and phosphofructokinases were rate-limiting enzymes of glycolysis flux *(376)*. Other studies have shown that metformin increased the activity of hexokinase and phosphofructokinase in diabetic cardiomyocytes *(377)*. The RNA-seq data in this study also demonstrated that metformin increased the expression of malic enzyme isoforms, alanine transaminase and lactate dehydrogenase D; all of these are involved in converting pyruvate to metabolites alternative to mitochondrial pyruvate oxidation (Figure 3.5). The RNA-seq data suggests that metformin could increase glycolytic flux by increasing the expression of these glycolytic enzymes, to generate alternative products such as malate, lactate and alanine in response to impaired mitochondrial function.

The mechanisms that explain how the expression of glycolytic enzymes are regulated by metformin is speculative, since this is the first study that shows the effects of metformin on the transcriptomic expression of glycolysis genes in intestinal cells. The mechanism might involve AMPK, although the transcriptomic data in this study did not identify a particular trend of DE genes within the AMPK pathway (Figure 3.13). This is despite substantial evidence demonstrating that metformin activates AMPK at the posttranslational level in intestinal tissues *(212, 360, 364, 378)*. A recent transcriptomic study into the effects of human hepatocytes investigating the AMPK-dependent and independent effects of metformin on transcriptomic responses, reported an upregulation of AMPK-signalling pathway components (including the AMPK subunit *Prkaa1* and CREB transcription factors); 6-phosphofructo-2 kinases (which convert fructose-6-phosphate to fructose-2,6-bisphosphate, the latter regulates the activity of PFKs) and GLUT1 transporter (*Slc2a1*) amongst the AMPK-dependent pathways activated by metformin, but that study did not report increased expression of glycolysis enzymes *(365)*. Moreover, AMPK has been reported to regulate glycolysis at the post-translational levels (such as phosphorylation of phosphofructokinases) *(379)*. The role of AMPK in the transcriptomic regulation of glycolysis enzyme expression could be investigated in future studies using a selective AMPK activator.

An alternative explanation for the upstream regulation of glycolysis enzyme expression is activation of the HIF-1A pathway, since many of the signalling components of the pathway (including *Hif1a* and *Arnt*) and many HIF-1A target genes were upregulated in metformin treated cultures (Figure 3.14).

Previous observations in cancer cell lines reported that metformin (and other electron transport chain inhibitors) suppressed HIF-1A signalling as a consequence of impairing oxygen consumption and increasing cellular oxygenation capacity in hypoxic conditions *(203, 345, 346)*. However, some studies in colorectal cancer cell lines report that metformin increases ROS generation which is known to stabilise HIF-1A activity *(380, 381)*. Alternatively, the TCA-cycle metabolite a-ketoglutarate is an essential substrate of prolyl hydroxylases that destabilise HIF-1a, thus reduced a-ketoglutarate levels associated with reduced TCA-cycle flux and impaired mitochondrial function by metformin could increase HIF-1a stability *(382)*. Increased pyruvate and lactate levels due to increased glycolysis associated with metformin treatment may also increase HIF-1a levels and stability, as reported in cancer cell lines *(383)*. Lactate has been reported as a signal in mediating changes in gene expression in response to metabolic changes *(384)*. A recent study reported increased HIF-1A expression in the small intestine of mouse models of Roux-en-Y gastric bypass surgery to enhance systematic glucose utilisation *(42)*. Therefore, HIF-1A could potentially be a general stress-activated signalling molecule activated by metformin in the intestinal cells to increase glucose utilisation by upregulating the expression of glycolytic enzymes.

In the liver, the effect of metformin in the expression of gluconeogenesis genes are well known *(215, 220, 385)*. DNA microarray analysis of liver samples from obese diabetic *db/db* mice have highlighted *G6pc* as one of the top genes downregulated by metformin treatment *(385)*. In this study, despite the reported downregulation of the gluconeogenesis genes *Pck1* and *G6pc* (Figure 3.4), *Pck2* was upregulated (Figure 3.4, 3.5) whilst none of the fructose-1,6-bisphosphatase (FBP) expression were differentially expressed (data not shown). Conclusions cannot be drawn on the effects of metformin on gluconeogenesis in intestinal cells based on the RNA-seq data alone. Indeed, the capabilities and contributions of the intestine as a gluconeogenic organ is not entirely clear, although the importance of the liver in gluconeogenesis is undisputed with a physiologically important impact on glucose homeostasis *(179, 386)*.

The RNA-seq data also identified transcriptomic changes in the pentose phosphate pathway (PPP) (Figure 3.3 and 3.4). The pentose phosphate pathway interacts with glycolysis and uses glucose-6-phosphate to generate NADPH and ribose as end products *(387)*. The RNA-seq data increased the expression of *G6pd*, the rate-limiting enzyme in the pentose phosphate pathway. Metformin also increased the expression of *Rpe* and *Taldo1*, enzymes involved in the non-oxidative phase of PPP and interacts with glycolysis through fructose-6-phosphate, but decreased the expression of ribokinase (*Rbk*), an enzyme important for ribonucleotide synthesis (Figure 3.4). Bias of the PPP in favouring NADPH production verses ribonucleotide generation has been demonstrated in metabolomic experiments of mouse livers deficient in Taldo1, which reported increased levels of ADP-ribose and

other nucleotides, but significantly lower levels of NADPH and marked oxidative stress *(388)*. The RNA-seq results suggest that metformin could potentially bias the PPP to favour NADPH production to protect against oxidative stress, over ribonucleotide biosynthesis. This needs to be clarified in the future by metabolic tracing studies into glucose-6-phosphate metabolism.

Metformin also changed the expression of genes involved in glycogen metabolism, particularly phosphoglucomutases and glycogen synthesis genes (*Ugp2* and *Gyg*) (Figure 3.3). However, the transcriptomic evidence is insufficient to suggest that metformin is increasing glycogen synthesis in the intestinal cells, since none of the key enzymes involved in glycogen metabolism- glycogen synthase (*Gys* family of genes) and glycogen phosphorylase (*Pyg* family of genes) are differentially expressed. Although glycogen stores have been reported in the intestine *(389, 390)*, their functions are unclear.

Decreased gene expression for key enzymes involved in fructose metabolism was also observed in metformin treated cells (Figure 3.6). There is increased evidence for the role of fructose metabolism in the intestine *(391, 392)*. Isotope tracing studies demonstrated that the rat intestine is capable of clearing ~90% of fructose at low levels, of which 40% is used for gluconeogenesis *(391)*. Since fructose metabolism for gluconeogenesis is an energy consuming process (ketohexokinase function is dependent on ATP hydrolysis in addition to other energy consuming steps in the gluconeogenesis pathway), decreased fructose metabolism may be a mechanism to conserve ATP expenditure.

3.5.2 Transcriptomic changes of amino acid sensing, transport and metabolism pathways by metformin

Metformin inhibits mitochondrial respiration; this is the main pathway of metabolism for amino acids such as glutamine and branched-chain amino acids (BCAAs) *(393)*. Although the RNA-seq data reports downregulation of the rate-limiting enzyme for glutamine metabolism glutaminase (*Gls*), many genes associated with aspartate metabolism were increased by metformin treatment (Figure 3.7). Previous studies have reported that metformin decreases glutamine metabolism in various cancer cell lines and in ovarian tumour biopsies from patients *(381, 394, 395)*. Emerging evidence also demonstrates that metformin, through inhibition of mitochondrial respiration and redox balance, reprograms aspartate metabolism towards nucleotide biosynthesis in cancer and other highly proliferative cells *(396, 397)*. Intestinal cells have a high turnover and metformin could increase the expression of aspartate metabolism genes as an adaptive survival mechanism to sustain the biosynthesis of some nucleotides (through adenylosuccinate). This should be investigated in the future by tracing aspartate metabolism using 13-Carbon labelled glutamine substrates.

Despite previous studies demonstrating that metformin disrupts BCAA metabolism in cancer cells *(394)*, the effect of metformin on BCAA metabolism is inconclusive based on the transcriptomic data alone. Since BCAA metabolism is oxidised in the mitochondria, metformin is likely to reduce BCAA oxidation as well through general impairment of mitochondrial function.

KEGG enrichment analysis also highlighted that the arginine biosynthesis pathway was altered by metformin (Figure Figure 3.3, 3.7). Detailed RNA-seq analysis revealed that metformin decreased the expression several citrulline biosynthesis genes (Figure 3.7) and the citrulline transporter ORC1 (Figure 3.5), which hints that metformin might also decrease citrulline biosynthesis. The intestine is a major source of citrulline from glutamine sources, which is used for renal arginine biosynthesis via the citrulline-arginine cycle *(398–400)*. Elevated citrulline levels have been implicated as a biomarker for intestinal inflammation and damage *(399, 401, 402)*. Decreased expression of citrulline biosynthesis enzymes by metformin could be a mechanism of ATP conservation.

The RNA-seq data has also shown that metformin decreased the expression of many broad-spectrum amino acid transporters and peptide transporters (Figure 3.8). However, metformin did not influence glutamine uptake based on live cell imaging studies using the FRET-based glutamine-sensor using duodenal organoids generated from B^0AT1 and SNAT2 null mice (Figure 3.8). This suggests that transcriptomic changes in glutamine transporters may not correlate with posttranslational/functional regulation, or the possibility that reduced transporter expression is compensated by increasing the membrane expression of other transporters. The functional studies into glutamine flux do not reflect upon the effect of metformin on the uptake of other amino acids, which are often dependent on transporters that differ from the ones used for glutamine uptake.

Detailed inspection of amino acid metabolism pathways in the RNA-seq data showed decreased expression of metabolic genes unique to glycine/serine/threonine metabolism and cysteine/methionine metabolism (Figure 3.9). These amino acids are involved in folate dependent metabolism (enriched in the KEGG analysis), which are important in DNA methylation, purine nucleotide biosynthesis and cell proliferation *(403–405)*. In the intestine, glycine and serine metabolism have been reported to play a role in DNA biosynthesis *(371, 400, 406)*. Previous studies using human cells and mitochondrial myopathy mouse models with defects in mtDNA replication causes an imbalance of the methyl cycle and impairs one-carbon metabolism by driving de-novo serine and glutathione biosynthesis *(373, 374, 407)*. Induced expression of the mitochondrial folate-metabolism enzyme Mthfd2 was observed in these mouse models (the gene was also upregulated by metformin in this study), causing an imbalance of nucleotide pools. Impaired mitochondrial function by metformin could affect flux through this metabolic pathway, which should be investigated in the

future using metabolic tracing studies. Decreased metabolism of these amino acids might provide one possible explanation for the general transcriptomic downregulation of DNA and RNA processes.

The mTOR signalling pathway is crucial to the regulation of amino acid metabolism and protein synthesis; disruption of mTOR affects intestinal differentiation and homeostasis *(408)*. Metformin has been reported to inhibit mTOR signalling and reduce protein synthesis in hepatocytes *(221, 222)*, whilst a recent study shows that constitutively activating mTOR in the small intestine of rats (by adenoviral delivery) decreased the glucose infusion rate (performed under euglycaemic clamp conditons) stimulated by metformin *(363)*. The RNA-seq data in this study does not provide conclusive evidence that metformin regulates mTOR signalling pathways in the intestinal cultures (Figure 3.13). It is likely that regulation of mTOR signalling by metformin could occur at the post-translational level; the effect of metformin on the expression of the various mTOR complex proteins should be investigated in future studies.

3.5.3 Metformin and intestinal lipid metabolism

Fatty acid biosynthesis, cholesterol metabolism and PPAR signalling were pathways highlighted from the KEGG enrichment analysis, although detailed examination showed that each pathway includes both upregulated and downregulated genes, even in the same enzyme isoforms (Figure 3.10 and 3.11). Based on the transcriptomic data alone, no conclusions could be drawn into the effects of metformin on intestinal lipid metabolism and PPAR signalling. This is by contrast to studies in other tissues such as adipocytes and hepatocytes, where the impact of metformin on lipid metabolism is more robust *(210, 211, 233, 366, 409)*. GO analysis of RNA-seq data of subcutaneous adipose tissue from elderly participants on metformin have similarly identified overrepresentation of pathways associated with lipid metabolism such as biosynthesis of unsaturated fatty acids, PPAR and SREBP signalling *(366)*. Metformin alters adipose tissue metabolism by decreasing the release of FFA from adipose tissue, promoting VLDL triglyceride clearance or increasing fatty acid oxidation *(233, 409)*. Metformin is known to reduce cholesterol synthesis and promote fatty acid oxidation via the AMPK pathway in liver hepatocytes *(210, 211)*. Furthermore, the PPARγ signalling pathway is an essential signalling pathway regulating metabolism in liver and adipose tissues *(410)*, but its role in intestinal metabolism is still elusive. This might suggest that most intestinal cells are probably less reliant on lipids as a source of fuel, whilst lipid storage and fatty acid oxidation are likely important metabolic functions in liver and adipose tissues that can be altered by metformin treatment.

3.5.4 Transcriptomic effects of metformin to signalling pathways and cellular processes

Autophagy is associated with nutrient deprivation and energy stress, and numerous studies have demonstrated the role of metformin in inducing autophagy *(352–355)*. The RNA-seq data shows that metformin induced the expression of genes encoding lysosomal hydrolases, lysosomal membrane proteins and the V-type H^+ ATP-ase (Figure 3.12), which may suggest increased activation of autophagy pathways in intestinal cells. AMPK is an essential regulator for autophagy, since knockout of AMPK causes defective autophagy in mouse hepatocytes *(411)*. AMPK has been reported to directly phosphorylate autophagy regulators such as the Beclin-1 complex and ULK-1 *(411–414)*, or via an indirect mechanism involving mTOR inhibition *(353)*. In the intestine, autophagy is an essential regulator of host defence and tissue homeostasis *(415, 416)*. Genetic variants of autophagy genes have been associated with the risk of inflammatory diseases, and mutations causing autophagy defects disrupt intestinal tissue integrity and functions of paneth cells *(417–420)*. Metformin induced autophagy in intestinal cells could be an adaptive response to preserve intestinal mucosal function in an energy-stress environment or to remove defective mitochondria (via mitophagy) caused by the inhibitory effects of metformin on mitochondrial metabolism *(411, 421)*. Further studies should functionally verify the induction of autophagy markers (such as LC3 or Beclin-1) in intestinal cells to confirm transcriptomic observations.

This study also reported the effects of metformin on new signalling pathways, which to our knowledge, have not previously been described in the literature. Metformin increased the expression of key Hippo signalling pathway genes, particularly *Wwtr1*, its upstream regulators and many Hippo signalling target genes (Figure 3.15). The Hippo signalling pathway is activated to control cell growth and organ size, and emerging evidence demonstrate its role in intestinal tissue regeneration and controlling stem cell fate by antagonising WNT signalling *(422–424)*. Direct evidence between metformin and the Hippo signalling pathway is unknown, although AMPK and LKB-1 has been reported to regulate Hippo signalling *(425–428)*.

Metformin also increased the expression of many EGF family of growth factors, EGFR and MAPKs (Figure 3.16). This is unexpected since mitochondrial and energy stress caused by metformin seemed to inhibit growth signalling pathways to limit proliferation, and EGFR is important for growth of intestinal stem cells and crypt expansion *(429–431)*. Whether metformin activates the EGFR signalling pathway at a posttranslational level is undetermined and should be investigated in the future. Since metformin causes the activation of stress pathways which can lead to growth arrest, senescence and apoptosis, concurrent activation of MAPK signalling may potentially be an adaptive counter-mechanism to ensure survival in intestinal cells.

The KEGG enrichment analysis highlighted stress and inflammatory pathways, such as TNFα, IL-17 and RIG-1 like receptor signalling altered by metformin treatment. However, detailed examination of the expression profiles within the TNFα signalling pathway, which also mediate its effects via MAPK albeit differences in other signalling components and transcriptional targets, are inconclusive (Figure 3.16). A recent study reported that metformin treatment did not alter TNFα, IFN-γ nor IL-1β mRNA expression in the ileum of wild-type mice, but attenuated the elevated expression of these cytokines in a IL-10 knockout mouse model of inflammatory bowel disease *(360)*. In that study, metformin treatment reduced the abundance of M1 macrophages in the ileum of the IL-10 knockout mice and improved barrier integrity in Caco-2 cells via activating an AMPK-dependent pathway *(360)*.

KEGG enrichment analysis highlighted the cell cycle and P53 signalling pathways. Although no conclusions could be drawn based on investigating the effects of metformin on the P53 signalling pathway, metformin alters the expression profiles of genes which promote cell cycle arrest (Figure 5.17 and 5.18). A previous study demonstrated that metformin regulates genes to promote cell cycle arrest in cancer cells *(348, 349, 432)*. In vivo morphological analysis of mouse ileum demonstrates that metformin administration increased villus length and staining for Paneth and goblet cells, without altering either the length of crypts or Ki67 proliferative marker expression *(360)*. The authors from the study suggested that metformin promoted intestinal differentiation *(360)*. Another study reported increased crypt proliferation, reduced expression of intestinal differentiation markers and decreased the height of mucosa in a villin-cre specific AMPKα knockout mouse model *(433)*. Perhaps by promoting cell cycle arrest of intestinal progenitors, metformin could alternatively increase the differentiation of the intestinal progenitors via an AMPK-dependent mechanism.

The RNA-seq analysis also decreased the expression of genes involved in RNA polymerases in gene transcription, DNA replication, repair and the spliceosome (Figure 5.20), which may suggest deactivation of these energetically expensive processes *(434)*. Analysis of pyrimidine metabolism pathways show that metformin generally downregulates genes involved in nucleotide biosynthesis but increase the expression of some genes that catabolise nucleotides, potentially causing an imbalance or reduction of the nucleotide pool for DNA processes (Figure 5.19). Other contributions to an imbalanced nucleotide pool could come from alterations in the PPP, folate dependent metabolism and aspartate metabolism. Perhaps reduced nucleotide metabolism could explain decreased DNA replication in metformin treated cultures and increased expression of cell cycle arrest genes in metformin treated cultures. Particularly, all of the genes encoding MCM complexes that initiate chromosome replication were downregulated in metformin treated cells, suggesting that reduced DNA replication prevents cell cycle progression beyond the S phase (Figure 5.18).

3.5.5 Conclusions

In this study, bulk RNA-seq provided detailed examination of the metabolic and signalling pathways affected by metformin in intestinal cells. The RNA-seq analysis complemented existing studies that metformin altered pathways associated with glycolysis/gluconeogenesis, autophagy, the cell cycle and DNA/RNA processes, which are likely to play important roles in intestinal homeostasis and regulate the metabolism of intestinal cells. The data also provided insights into the potential roles of metformin in novel pathways, such as amino acid metabolism, EGFR/MAPK, Hippo and HIF-1A signalling, which may suggest additional mechanisms of action in intestinal cells.

Transcriptomic analysis poses limitations in understanding the cellular processes that can also be influenced by translational and posttranslational control, or through compensatory mechanisms. For example, no difference in glutamine uptake was observed despite decreased mRNA expression of many amino acid transporters. A combination of transcriptomic, proteomic and metabolic analysis would be ideal to build a comprehensive picture to understand the effect of metformin in intestinal cells.

Chapter 4: Mechanisms of GDF-15 induction by metformin in intestinal cells

4.1 Summary

Growth differentiation factor 15 (GDF-15) is a well-established marker of cellular stress and is a recently discovered metabolic stress hormone associated with appetite regulation. Serum GDF-15 levels are highly elevated in patients receiving metformin treatment, which is speculated to contribute to weight loss effects of the drug *(76, 276, 295)*. The cellular mechanisms by which metformin induces GDF-15 secretion is unknown. The RNA-seq data identified GDF-15 as one of the most significantly upregulated genes in metformin treated intestinal cultures (see chapter 3). This is supported by experiments in HFD-fed mice orally administered with metformin, which reported induction of GDF-15 only in the proximal, distal small intestine and the colon, demonstrating the importance of the gastrointestinal tract in stimulating GDF-15 release *(321)*. This chapter examines the cellular mechanisms associated with GDF-15 secretion in intestinal cells.

4.2 Introduction

4.2.1 GDF-15 as a metabolic hormone

The first insights into the metabolic effects of GDF-15 were from studies by Johnen *et. al.,* who reported that mice bearing tumours overexpressing GDF-15 were cachexic and anorexic *(291)*. When GDF-15 was injected into mice, or using transgenic mice overexpressing GDF-15, reduced food intake and secondary weight loss were observed without any effects on energy expenditure *(291)*. GDF-15 null mice were reportedly more obese when exposed to standard chow or high fat diet (HFD) than wild-type mice *(292, 294)*. In human studies, GDF-15 levels were also elevated in obese patients, not just in patients with substantial weight loss, possibly due to increased adiposity during obesity and the ability of the adipose tissue to release GDF-15 *(435, 436)*.

Experiments in mice have demonstrated that GDF-15 administration directly results in conditioned taste aversion, whereby the animal associates the taste of a certain food with a toxic or aversive substance *(287)*. The results indicate that the effects of GDF-15 on food intake involves a central mechanism. Interventricular administration of GDF-15 in mice led to reduced food intake and body weight, whereas intraperitoneal injection of GDF-15 increased cFos activation in the Area Postrema (AP) and the Nucleus Tractus Solitarii (NTS) of the brainstem, brain regions associated with nausea

and vomiting *(293)*. Selective lesioning of these areas abolished the anorexigenic effects of GDF-15 *(293)*. Recent studies by Yang *et. al.*, used cell-surface display screening of 2,762 potential transmembrane domains and identified GDNF family α-receptor like A (GFRAL) as a high affinity cognate receptor for GDF-15 *(295)*. GFRAL associate with the receptor RET to form a heterodimer upon GDF-15 binding to facilitate signal transduction *(295)*. The importance of GFRAL were demonstrated in knockout mice, which abolished the anorexigenic and weight-loss effects of GDF-15 as well as sustained weight gain in response to HFD *(295)*. Analysis of tissue expression of GFRAL found that they are only expressed in a selective number of neurons located exclusively in the NTS and AP of the brainstem *(295)*. This reinforces the importance of GDF-15/GFRAL axis in the central regulation of food intake and body weight.

Interestingly, transgenic mice with elevated GDF-15 levels also showed improvements in glucose tolerance and insulin sensitivity following high fat diet (HFD) *(291)*. Some studies reported that GDF-15 levels are transiently elevated in response to an oral glucose tolerance test, whilst euglycaemic hyperglycaemic clamp studies in obese women reported transient elevations in GDF-15 *(437, 438)*. These studies suggest that acute changes in GDF-15 levels may correlate with insulin levels, although many of the patients in the study were also taking metformin, which could increase serum GDF-15 levels (see Section 4.2.3 below) *(437, 438)*. Furthermore, obese women with T2DM displayed elevated GDF-15 levels compared to obese women without diabetes *(439)*. However, the physiological role of GDF-15 in diabetes is not completely understood to date *(289)*.

4.2.2 Mechanisms of GDF-15 induction

GDF-15 was initially reported as a stress-responsive hormone elevated in various animal models of tissue injury, such as chemically induced liver and lung injury, surgical nephrectomy, ischaemic reperfusion injury and dilated cardiomyopathy *(284, 285, 440, 441)*. GDF-15 is also elevated in response to tissue inflammation, as in rheumatoid arthritis or liver cirrhosis *(442, 443)*. GDF-15 has been reported to limit the extent of tissue damage, but its physiological role during injury and inflammation are incompletely understood *(441, 443)*. Inflammatory markers such as C-reactive protein (CRP) have been reported to induce GDF-15 expression via the P53 pathway, which directly interacts with the *Gdf15* promoter *(444, 445)*. Activation of the NF-kB signalling pathway have also been reported to trigger GDF-15 induction by tumour cells to suppress the activity of inflammatory macrophages *(446)*.

GDF-15 is especially elevated in patients with mitochondrial diseases, a heterogeneous spectrum of genetically inherited disorders caused by mutations in proteins localised in the mitochondria which cause mitochondrial dysfunction *(447, 448)*. Transcriptomic studies of skeletal muscle biopsies from

patients with mitochondrial encephalomyopathy caused by mutations of the thymidine kinase (Tk2) gene demonstrated substantial overexpression of GDF-15 amongst other genes associated with the P53 signalling pathway *(449)*. Subsequent studies have identified elevated serum levels of GDF-15 and a similar stress-responsive hormone FGF-21 in patients with various mitochondrial disorders *(447, 448)*.

Various *in vivo* and cellular models demonstrate that GDF-15 induction by cellular stressors are associated with the integrated stress response (ISR) *(286, 374)*. Using a mouse model of mitochondrial myopathy caused by muscle specific mutations of the Twinkle mtDNA helicase (associated with mtDNA replication), Khan *et. al.*, demonstrated induction of GDF-15 and FGF21 coinciding with ISR genes and mitochondrial unfolded protein response (mtUPR) genes downstream of mTORC1 activation *(374)*. Similarly, mouse models of mitochondrial myopathy due to mutations of the *Crif1* gene causing defective ribosomal translation, and global knockout of *Polg* (mitochondrial targeted DNA polymerase) caused GDF-15 overexpression and elevated serum levels associated with mtUPR and ISR genes *(286)*. Inhibitors that disrupt mitochondrial dysfunction all associate with general ISR activation via induced ATF4 and CHOP expression *(450)*. Recent studies by Patel *et. al.*, demonstrated that other stressors that activate the ISR pathway, such as defective ER glycosylation, protein misfolding and hypoxia also caused an overexpression of GDF-15 in Mouse Embryonic Fibroblast (MEF) cells *(287)*. CHOP has been demonstrated to bind directly to the promoter of GDF-15 to elicit gene expression, demonstrating that GDF-15 induction is directly regulated by ISR *(451)*.

4.2.3 Metformin and GDF-15

A large scale clinical study (called the ORIGIN trial) involving 8,401 T2DM patients (and from this cohort 2,317 patients on metformin) identified GDF-15 as a novel biomarker from a panel of 237 potential biomarkers that is strongly linked to the use and dosage of metformin *(276)*. A recent study from the SUMMIT cohort of 1,438 patients with a history of T2DM and cardiovascular disease, revealed that metformin use was associated with a 40% elevation of serum GDF-15 levels that is independent of other factors *(277)*. In a recent transcriptomic analysis of human hepatocytes pre-treated with metformin, *Gdf15* was amongst the top upregulated genes associated with an AMPK-independent pathway of metformin action *(365)*.

As mentioned in chapter 3, *Gdf15* is one of the most significantly upregulated genes in metformin treated intestinal 2D monolayer cultures (Figure 3.1). In a collaboration with Steve O'Rahilly and others, we have reported that metformin use in obese non-diabetic patients from the CAMERA clinical trial was associated with elevated GDF-15 levels *(321)*. Metformin prevented weight gain in HFD mice but not in GDF15 and GFRAL knockout mice, demonstrating that the modest anorexigenic effects of

metformin are associated with GDF-15 *(321)*. To investigate the site of metformin action, oral administration of metformin (single dose for 6 hours or long-term dosage for 11 days) elicited *Gdf15* mRNA expression in the small intestine, the colon and the kidneys, suggesting the potential involvement of these organs in the elevations of GDF-15 in response to metformin administration *(321)*.

4.3 Aims

This chapter expands the investigation into the cellular mechanisms by which metformin causes GDF-15 induction in the intestine. The aims of this study are:

1. To examine the mechanisms of mitochondrial stress caused by metformin in stimulating GDF-15 secretion in intestinal organoids.
2. To identify metformin responsive genes and pathways associated with mitochondria function to better understand the link between metformin and GDF-15 release.
3. To elucidate the role of ISR in metformin stimulated GDF-15 secretion in intestinal cells.

4.4 Results

Note: Experiments involving metformin oral dosing in HFD-fed mice and RNA-extraction of organs were performed by Tony Coll, Irene Cimino and Debra Rimmington.

4.4.1. Mitochondrial stress and GDF-15 induction in intestinal cells

The effects of Gdf15 induction was compared with other GDF family growth factors, FGF family of growth factors and other known stress activated growth factors to investigate whether metformin treatment causes a general upregulation of stress hormones. Compared to other growth factors, the induction of *Gdf15* expression by metformin was the most robust (Figure 4.1A). Metformin also, to a lesser extent, increased the expression of *Fgf15*, a hormone released in the GI tract involved in bile-acid synthesis, and *Tgfb1*, the cytokine involved in inflammatory stress (Figure 4.1A). Metformin modestly increased the expression of *Fgf21*, another hormone that is induced by stress, although the expression of *Fgf21* is very low compared to *Gdf15* and other growth factor genes. Metformin treatment downregulated *Gdf9* but was without effect on the expression of *Gdf11* and other TGF-β growth factors. Confirming RNA expression studies, metformin also significantly increased the

secretion of GDF-15 in mouse duodenal organoids (between 2-6-fold) and ileal organoids (between 2-3 fold) over a 24-hour period (Figure 4.1B and 4.1C).

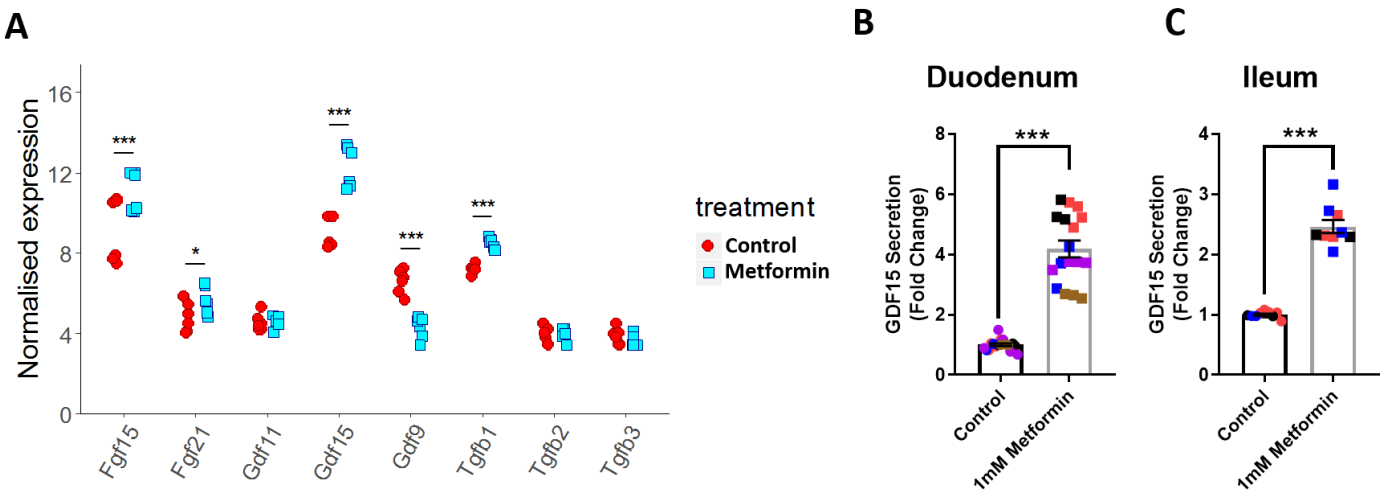

Figure 4.1. Metformin stimulates Gdf15 expression and secretion in intestinal cultures. (A) The effect of metformin on the expression of *Gdf15*, other GDF family of growth factors, FGF family of hormones and TGF family of paracrine factors. The raw count data for each gene is normalised by the size factors and the library size. *, P<0.05, **, P<0.01, ***, P<0.001 (P-adjusted values calculated via DE-Seq analysis). N=6 plates from 2 different organoid lines. (B and C) Metformin (1mM) pre-treatment stimulates GDF-15 secretion in intestinal cultures generated from (B) mouse duodenal organoids (Control: N= 18 wells, Metformin: N=17 wells, 3-5 wells assessed in parallel from 5 independent experiments) and (C) mouse ileal organoids (N=9 wells from 3 independent experiments). Secretion normalised to the control. Results presented as mean ± SEM. Different colours represent different experiments. ***, P<0.001. Two-tailed t-test.

To provide some insight into how metformin elicited GDF-15 secretion, intestinal 2D monolayer cultures generated from mouse duodenal organoids were incubated with various inhibitors for 24 hours. Rotenone, which like metformin inhibits Complex I of the electron transport chain, induced GDF-15 secretion response by 3.2 fold at a similar magnitude as metformin (4.1 fold) (Figure 4.2A and 4.2B). Interestingly, the complex III inhibitor Antimycin A induced a more marked GDF-15 secretion response by 15.5 fold (Figure 4.2A and 4.2B). Other mitochondrial inhibitors such as the proton uncoupler FCCP (which dissipates the mitochondrial membrane potential) and the mitochondrial pyruvate carrier inhibitor UK-5099 (to investigate the effects of mitochondrial pyruvate oxidation from glucose metabolism) did not significantly increase GDF-15 secretion (Figure 4.2A and 4.2B). The AMPK activator Az-991 (to mimic the AMPK-dependent signalling arm of metformin) did not significantly increase GDF-15 secretion either (Figure 4.2B). Since other mitochondrial electron transport chain inhibitors in addition to metformin also stimulates GDF-15 secretion, the results suggest that metformin stimulates GDF-15 secretion through a mitochondrial dependent mechanism, but was independent to AMPK activation.

Given that metformin inhibits Complex I activity (which oxidises NADH to NAD+ in the mitochondria), GDF-15 secretion could be associated with the mitochondrial NADH/NAD+ redox state. This was

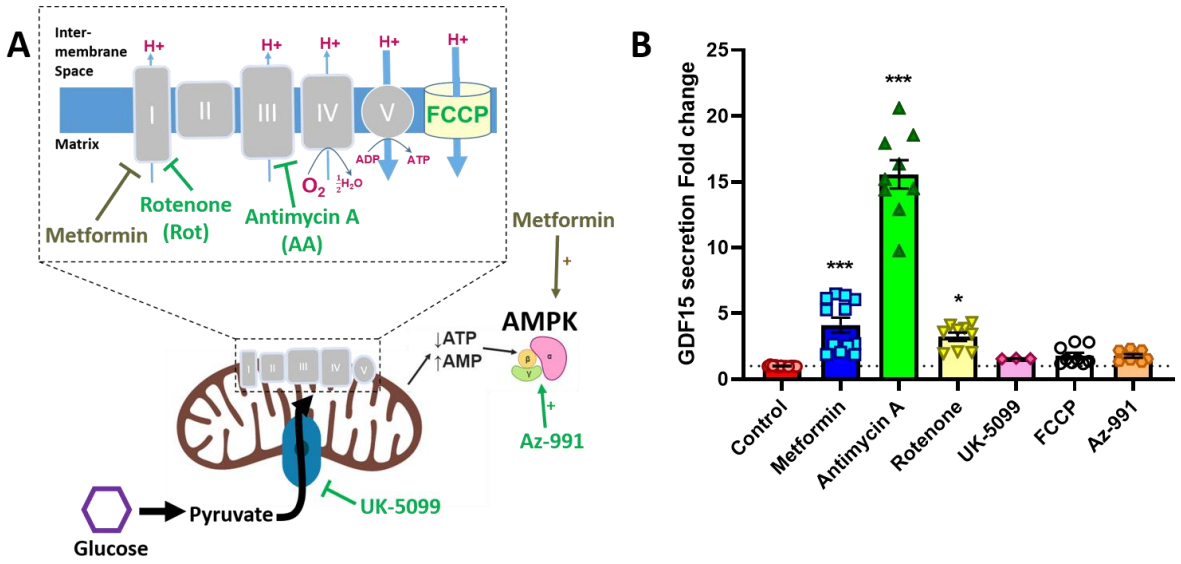

Figure 4.2. Inhibitors of the electron transport chain stimulate GDF-15 secretion in intestinal cells. (A) Schematic showing the mechanisms of action of metformin and different mitochondrial respiration inhibitors. (B) GDF-15 secretion in mouse duodenal 2D monolayer cultures pre-treated with metformin (1mM, N=12 wells, 3 wells assessed in parallel from 4 independent experiments), antimycin A (10µM, N=9 wells, 3 wells from 3 independent experiments), rotenone (10µM, N=9 wells, 3 wells assessed in parallel from 3 independent experiments), UK-5099 (10µM, N=3 wells from 1 experiment), FCCP (10µM, N=9 wells, 3 wells from 3 independent experiments) and Az-991 (10µM, N=9 wells, 3 wells assessed in parallel from 3 independent experiments) for 24 hours. Secretion is normalised to the control (N=9 wells, 3 wells assessed in parallel from 3 independent experiments). Results presented as mean ± SEM. *, P<0.05, ***, P<0.001. One-way ANOVA and Bonferroni post-hoc test.

investigated by supplementing 2D organoid cultures with nicotinamide mononucleotide (NMN) to stimulate NAD+ biosynthesis via the nicotinamide mononucleotide adenylyltransferase NMNAT in the NAD+ salvage pathway (Figure 4.3A). Since NMN affects both mitochondrial and cytosolic NADH/NAD+ redox states, the effects of the compound duroquinone, which elicits NAD+ synthesis as a substrate for the cytosolic quinone reductase NQO1 was investigated in metformin treated cultures (Figure 4.3A) *(452, 453)*. NMNATs and NQO isoforms are all expressed in intestinal cells, and metformin induced *Nqo1* expression (Figure 4.3B and 4.3C). NMN supplementation reduced metformin stimulated GDF-15 secretion in both of the experiments, whilst duroquinone was without effect (Figure 4.3D). The results implicate the role of mitochondrial NADH/NAD+ redox state in metformin stimulated GDF-15 secretion.

Metformin has been shown to stimulate ROS generation in cancer cell lines *(381)*. The role of ROS in metformin stimulated GDF-15 secretion in intestinal cells were investigated by treatment with

mitochondrial targeted ROS inducers and antioxidants. Co-treatment with MitoTEMPO, a mitochondrial antioxidant which functions as a superoxide dismutase mimetic to scavenge

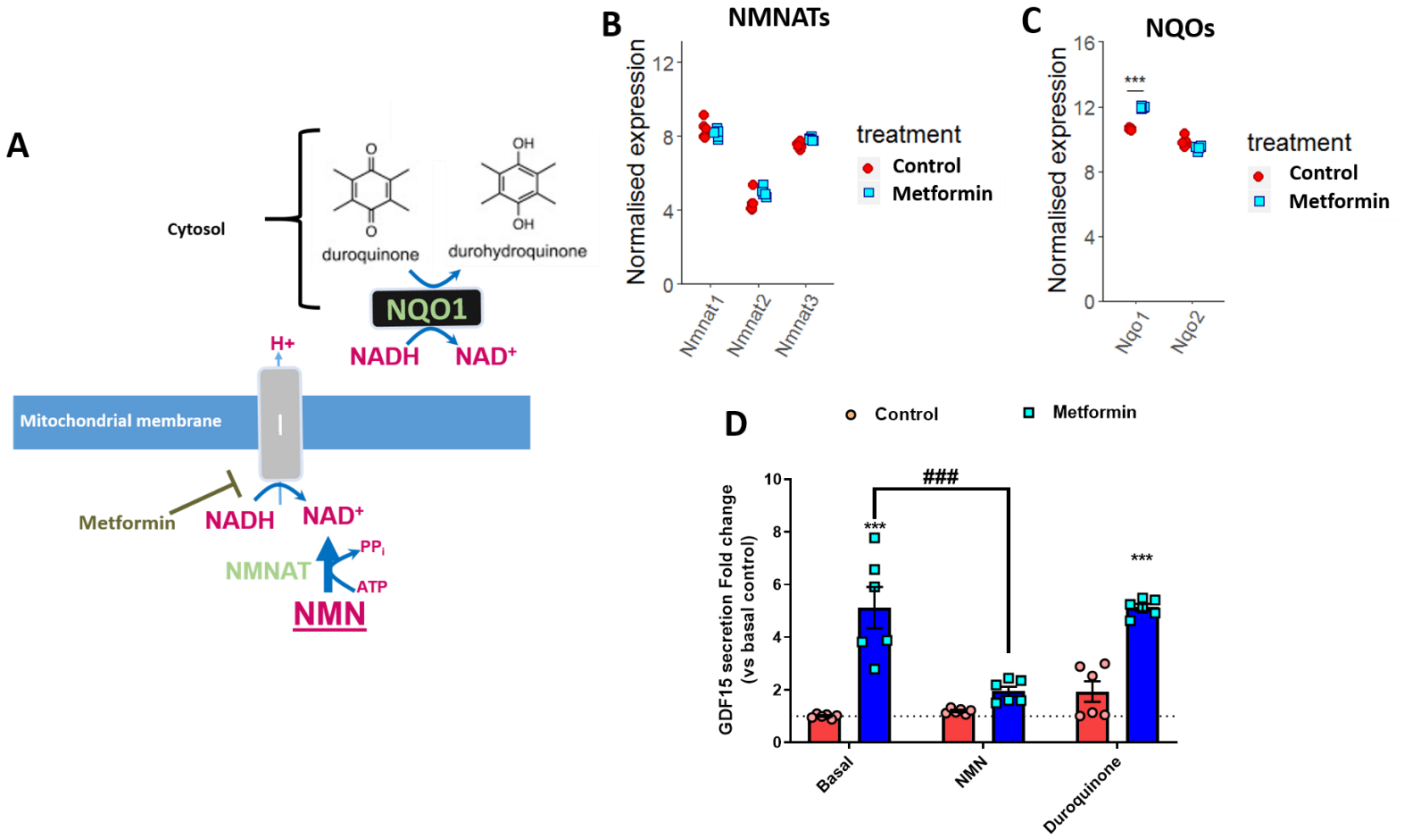

Figure 4.3. Restoring mitochondrial NADH/NAD+ redox balance reduces metformin-stimulated GDF-15 secretion. (A) Schematic showing the mechanisms of action of metformin, nicotinamide mononucleotide (NMN) and duroquinone. (B and C) The effect of metformin on the expression of (B) NMNATs and (C) NQOs. The raw count data for each gene is normalised by the size factors and the library size. ***, P<0.001 (P-adjusted values calculated via DE-Seq analysis). (D) GDF-15 secretion in mouse duodenal 2D monolayer cultures co-treated with control or metformin (1mM) for 24 hours with NMN (5mM) and Duroquinone (50µM). Cultures were pre-treated with NMN or Duroquinone for an hour prior to co-treatment with or without metformin. Secretion is normalised to the control. Results presented as mean ± SEM. N=6 wells, 3 wells assessed in parallel from 2 independent experiments. ***, P<0.001. Two-way ANOVA and Bonferroni post-hoc test.

superoxides *(454)*, modestly decreased metformin-stimulated GDF-15 secretion (in 3 out of 4 experiments) but also modestly increased basal GDF-15 secretion in one experiment (Figure 4.4A and 4.4B). Elevation of mitochondrial ROS using MitoParaquat (MitoPQ), a mitochondrial targeted redox cycler that elevates superoxide production *(455)*, and MitoCDNB1, which disruption of thiol redox state by inhibiting glutathione-S-transferases (GSTs) and deplete mitochondrial glutathione *(456)*, both modestly stimulated basal GDF-15 secretion (Figure 4.4B). The results suggest that mitochondrial ROS may make a small contribution to GDF-15 secretion and may be involved in metformin-stimulated GDF-15 secretion. It is unknown whether cytosolic ROS could play a more important role (since

MitoTEMPO may not eliminate all superoxide released from to the cytosolic side of Complex III), and this should be tested using some other non-mitochondrial targeted antioxidants.

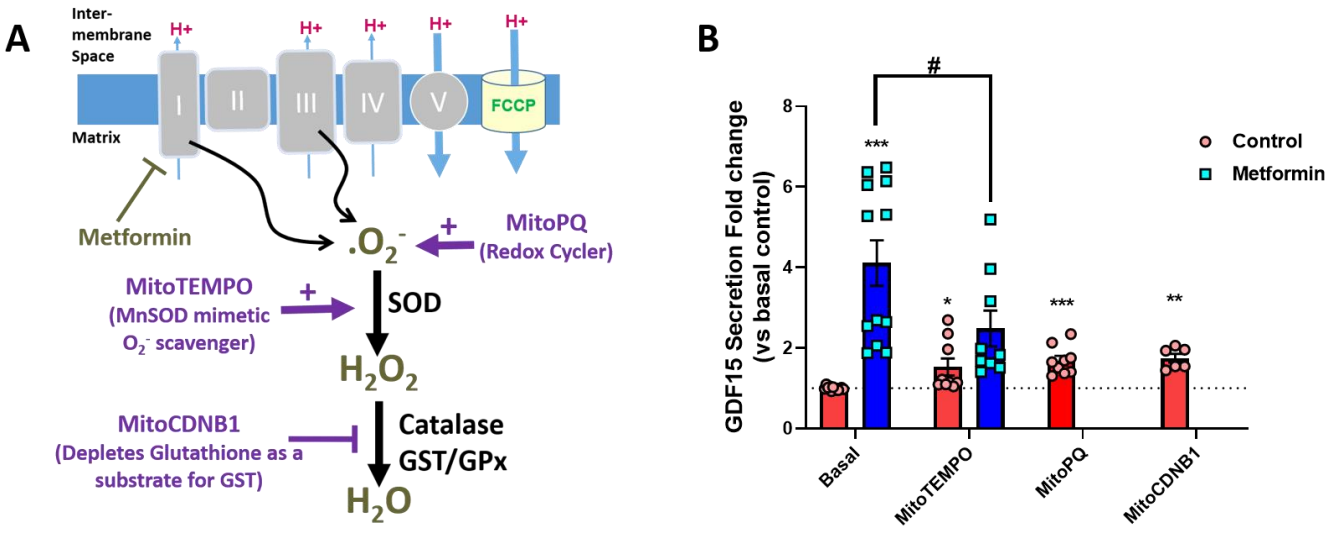

Figure 4.4. The effect of ROS in metformin-stimulated GDF-15 secretion. (A) Schematic showing the mechanisms of action of metformin, and different mitochondrial ROS stimulators. (B) GDF-15 secretion in mouse duodenal 2D monolayer cultures pre-treated with MitoPQ (5µM, N=9 wells, 3 wells assessed in parallel from 3 independent experiments), MitoCDNB1 (5µM, N=6 wells, 3 wells assessed in parallel from 2 independent experiments) or metformin (1mM, N=12 wells, 3 wells assessed in parallel from 4 independent experiments) with MitoTEMPO (100µM N=9 wells, 3 wells assessed in parallel from 3 independent experiments). Secretion is normalised to the control (N=12 wells, 3 wells assessed in parallel from 4 independent experiments). Cultures were pre-treated with MitoTEMPO for an hour prior to co-treatment with or without metformin. Results presented as mean ± SEM. Basal control: N=12 wells, 3 wells assessed in parallel from 4 independent experiments. *, P<0.05, **, P<0.01, ***, P<0.001. Two-way ANOVA and Bonferroni post-hoc test.

The effects of the drugs that alter mitochondria protein homeostasis (proteostasis) were also investigated, since they have previously been shown to induce the mtUPR response which was linked to GDF-15 secretion *(450)*. Co-treatment with doxycycline, an inhibitor of mitochondrial translation *(457)*, stimulated GDF-15 secretion in control cultures, but did not further stimulate GDF-15 secretion in the presence of metformin in 3 out of 4 experiments, whereas there seems to be an additive effect in one experiment (Figure 4.5A and 4.5B). Actinonin, which affects the de novo turnover of mitochondrial proteins *(458)*, further stimulated GDF-15 secretion in metformin co-treated cultures, and seemed to increased basal GDF-15 secretion, although not statistically significant (P=0.1644, Figure 4.5A and 4.5C). Co-treatment with mitoBloCK6, an inhibitor of mitochondrial protein import through TIM22 and Mia40/Erv1 pathways *(459)*, stimulated additional GDF-15 secretion in control and metformin treated cultures (Figure 4.5A and 4.5D). Ciprofloxacin, which inhibits mtDNA replication by inhibiting mitochondrial topoisomerases from relaxing its supercoil structure also further stimulated GDF-15 secretion in both control and metformin treated cultures (Figure 4.5A and 4.5E). These results

suggest that mitochondrial translation, and not mitochondrial protein import or protein turnover, may form a part of the mechanism of metformin stimulated GDF-15 secretion.

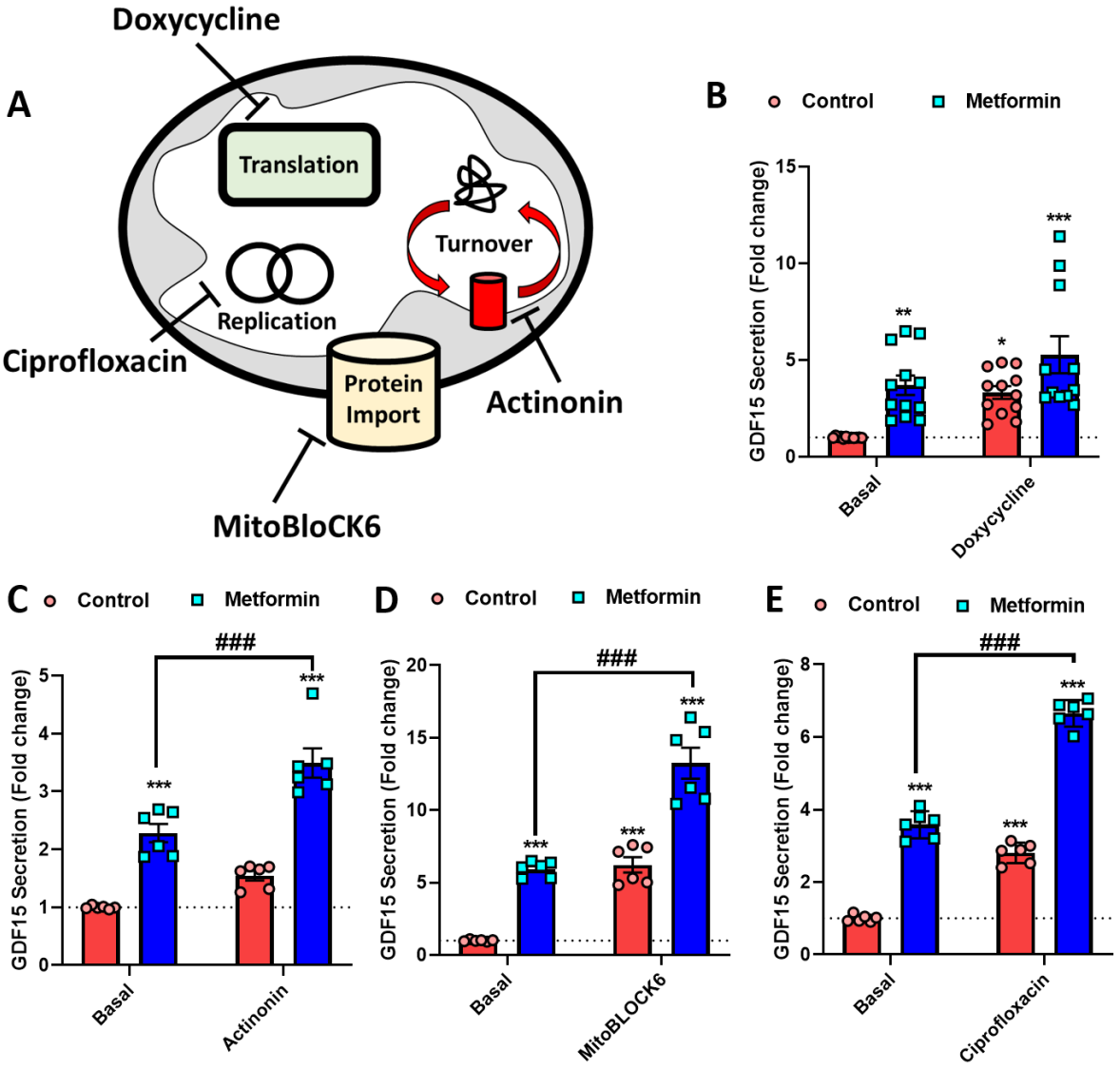

Figure 4.5. The effect of mitochondrial proteostasis inhibitors in GDF-15 secretion. (A) Schematic showing the mechanisms of action of doxycycline, actininonin and MitoBloCK6 in the mitochondria. (B-D) GDF-15 secretion in mouse duodenal 2D monolayer cultures pre-treated with metformin (1mM) with (B) doxycycline (50µM, N=12 wells, 3 wells assessed in parallel from 4 independent experiments), (C) actinonin (100µM, N=9 wells, 3 wells assessed in parallel from 3 independent experiments), (D) MitoBloCK6 (50µM, N=6 wells, 3 wells assessed in parallel from 2 independent experiments) and (E) ciprofloxacin (100µg/ml, N=6 wells, 3 wells assessed in parallel from 2 independent experiments). Cultures were pre-treated with doxycycline, actinonin, MitoBloCK6 or ciprofloxacin for an hour prior to co-treatment with or without metformin. Secretion is normalised to the control. Results presented as mean ± SEM. *, P<0.05, ***, P<0.001 compared to control. ###, P<0.001 compared to metformin. Two-way ANOVA and Bonferroni post-hoc test.

4.4.2. The effect of metformin on the expression of mitochondria-associated genes

Further insights into mechanisms of metformin stimulated GDF-15 secretion could be gained from investigating the expression profiles of genes assoaciated with the mitochondria function. Sub-analysis of expression profiles from 1,158 nuclear-encoded genes associated with or localised to the mitochondria were performed using the MitoCarta 2.0 database *(460)*. 1,056 out of 1,158 genes were mapped to the database, and 289 DE genes (27.3%) were identified. The most statistically significant DE genes from the MitoCarta 2.0 database are shown as a volcano plot (Figure 4.6A). Gene ontology (GO) enrichment analysis was conducted to identify the mitochondrial processes altered in the metformin treated cultures. The top 30 GO terms associated with upregulated genes mostly involve

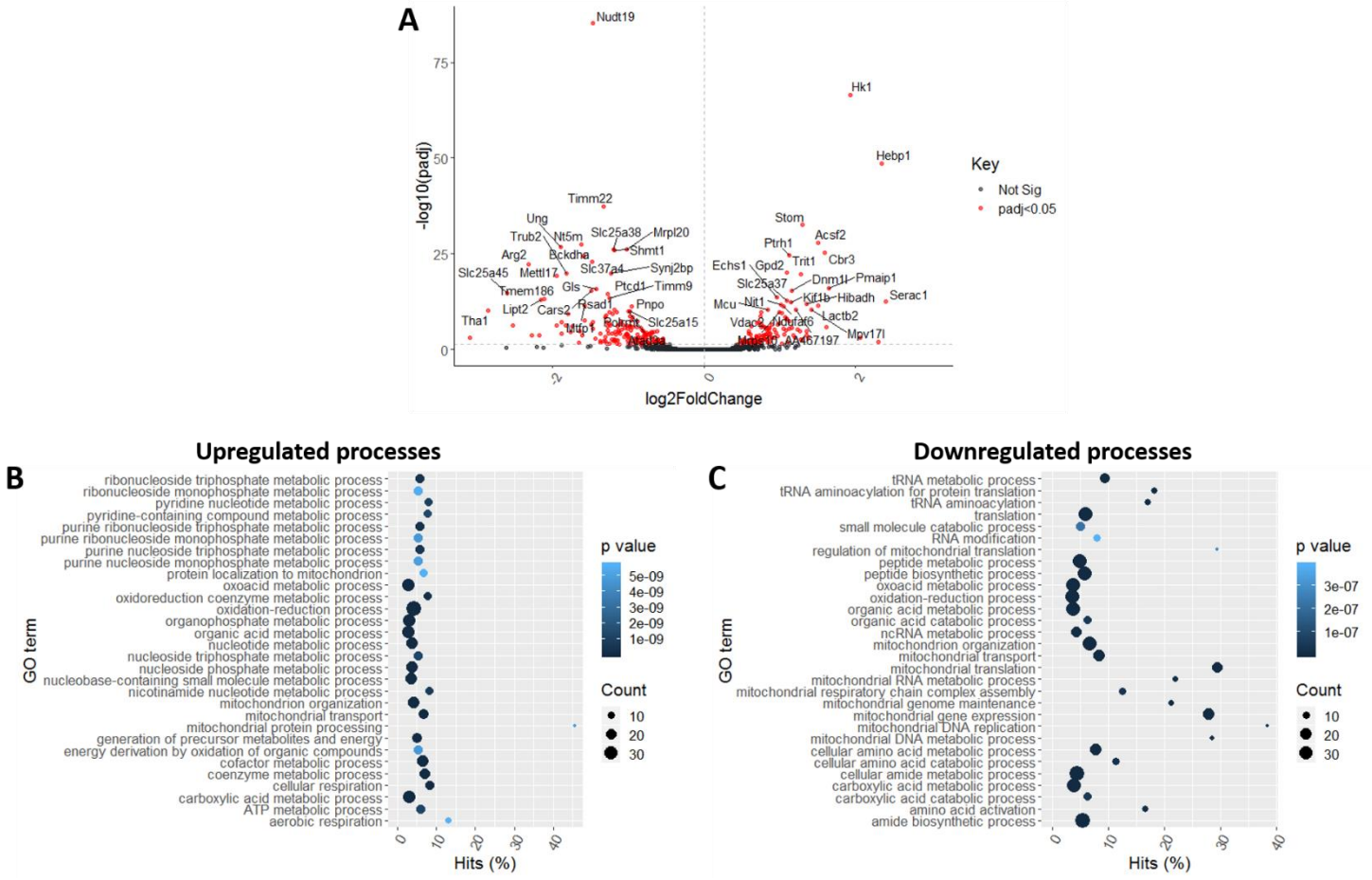

Figure 4.6. RNA-seq analysis of mitochondria associated genes based on the MitoCarta 2.0 database. (A) Volcano plot displaying the fold change (X-axis) compared to the P-adjusted values (Y-axis) of individual genes altered by metformin treatment. Red dots represent gene expression changes that were statistically significant (P<0.05), whilst black dots represent gene expression changes that were not statistically significant (Not Sig). Labelled genes represent the top 50 most differentially expressed genes (sorted by P-adjusted values). Con; Control, Met; Metformin. (B and C) Gene ontology (GO) analysis of (B) upregulated and (C) downregulated genes altered by metformin. Hits (%) is the number of differentially expressed (DE) genes in a particular GO term divided by total number of genes in the pathway. Count represents the numbers of DE genes in the GO term. P adjusted value is the P-value corrected for the false-discovery rate using the Benjamin-Hochberg method, with more statistically significant values representing greater shading intensity.

metabolic processes, although the terms were <15% hit, except for mitochondrial protein processing (Figure 4.6B). The top 30 GO terms associated with downregulated genes particularly include RNA processes and genome maintenance (Figure 4.6C). The hit % of downregulated GO processes were much more dispersed (between 5%-40% hit), which may suggest more notable influences of metformin on mitochondrial DNA and RNA processes (Figure 4.6C).

The effect of metformin on the expression profiles of mitochondrial and cytosolic translation machinery were investigated since many of the downregulated GO terms were tRNA processes and translation. 8 out of 17 genes encoding mitochondrial aminoacyl tRNA synthetases were DE genes, with 7 downregulated and 1 upregulated by metformin (Figure 4.7A). In comparison, only 2 out of 25 cytosolic aminoyacyl tRNA synthetases were DE genes (aminoacyl tRNA synthetase complex interacting protein *Aimp2* and cysteinyl tRNA-synetase *Cars*) (Figure 4.7B). Similarly, 18 out of 78 genes encoding mitochondrial ribosomes were DE genes, with 15 downregulated genes and 3 genes induced by metformin (Figure 4.7C). This was compared to only 7 out of 94 cytosolic ribosomes identified as DE genes (Figure 4.7D). Metformin also markedly decreased the expression of essential genes involved in mitochondrial DNA replication, particularly mitochondrial DNA polymerases (*Polg* and *Polg2*), mitochondrial RNA polymerase (*Polrmt*), mtDNA helicases (*Twnk*, *Dna2*), mtDNA ribonuclease (*Rnaseh*) and mitochondrial nucleotide metabolism enzymes (*Mgme1, Ung, Apex2* and *Tk2*) (Figure 4.7E). These results indicate that metformin downregulates the expression of genes involved in mitochondrial translation and mtDNA replication.

The effect of metformin on other aspects of mitochondrial function were also explored. The effects of metformin on the expression of mitochondrial import proteins were mixed- downregulation of inner membrane translocases (*Timm8a1, Timm9* and *Timm22*), upregulation of mitochondrial peptidases (*Pmpca* and *Pmpcb*), as well as altered expression of outer membrane translocases (*Tomm40l* increased, *Tomm5* decreased) and inner mitochondrial membrane proteases (*Immp2l* increased, *Immp1l* decreased) (Figure 4.8A). Amongst the genes associated with mitochondrial protein folding, metformin increased the expression of key genes encoding proteases involved in the mtUPR response (*Lonp1, Yme1l1* and *Oma1*) and mitochondrial chaperones (*Hspa9, Grpel2* and *Dnajc2*, although *Dnajc11* was downregulated) (Figure 4.8B). The effects of metformin in the expression of oxidative phosphorylation genes were inconclusive, with up- and down-regulation of some complex enzyme subunits such as cytochrome c oxidases (*Cox18* increased, *Cox10* decreased) and NADH dehydrogenases (*Ndufc2* and *Ndufaf6* increased, *Ndufaf4* decreased) (Figure 4.8C). Furthermore, no conclusions could be drawn on the effects of metformin on mitochondrial dynamics; whilst the mitochondrial fission protein *Mtfp5*, the mitophagy GTPase *Rab35* and the mitophagy kinase *Pink1* were downregulated by metformin, the mitophagy protein *Snap29*, mitochondrial fission proteins

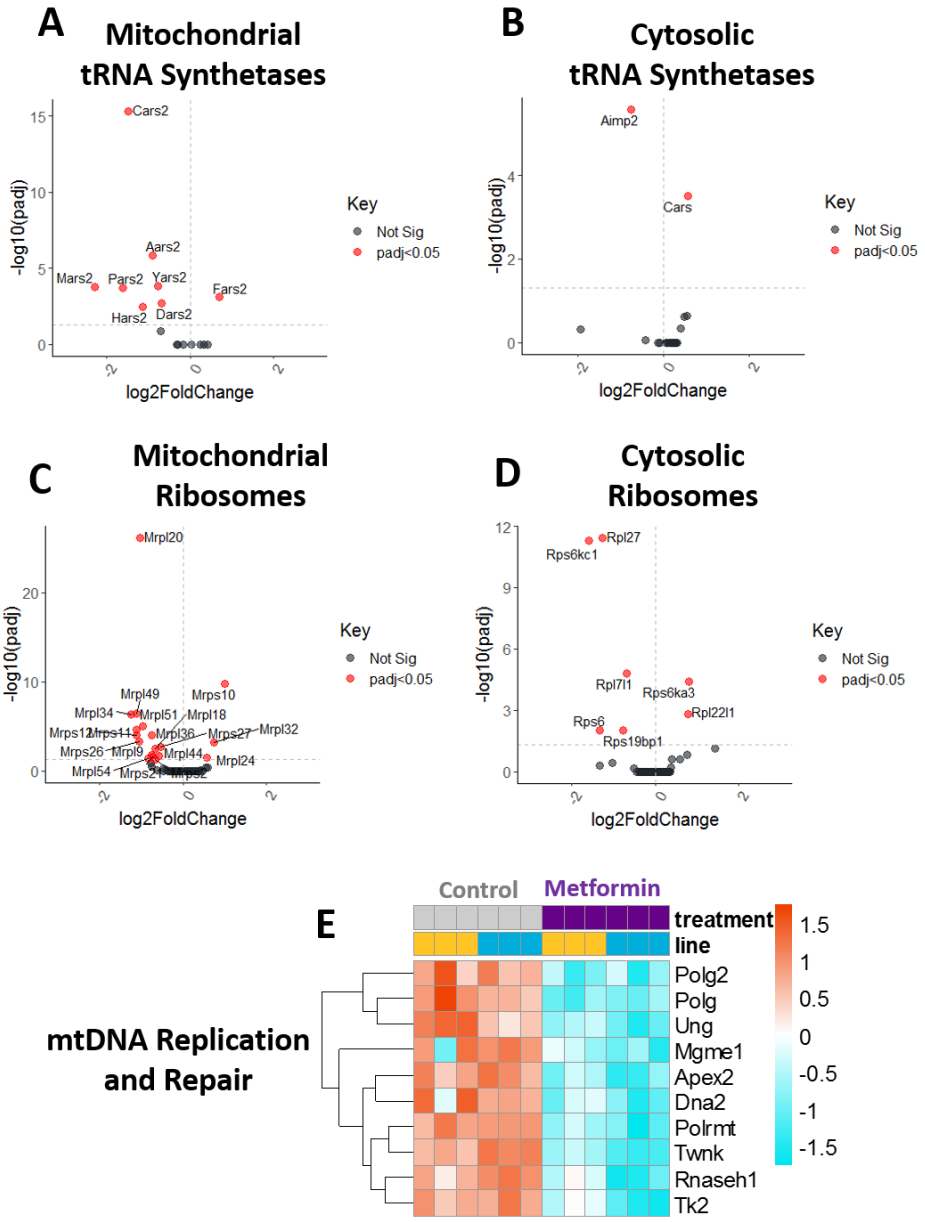

Figure 4.7. Metformin decreased the expression of genes involved in mitochondrial translation and mtDNA replication. (A-D) Volcano plot displaying the fold change (X-axis) compared to the P-adjusted values (Y-axis) of genes encoding (A) mitochondrial tRNA aminoacyl synthetases (B) cytosolic tRNA aminoacyl synthetases (C) mitochondrial ribosomal proteins and (D) cytosolic ribosomal proteins. Red dots represent gene expression changes that were statistically significant (P<0.05), whilst black dots represent gene expression changes that were not statistically significant (Not Sig). Labelled genes represent DE genes. (E) Heatmap showing DE genes (filtered by p-adjusted value of <0.05) involved in mtDNA replication, transcription and repair affected by metformin treatment. The colour key depicts the z-score and is shown on the right. N=6 plates from 2 different organoid lines.

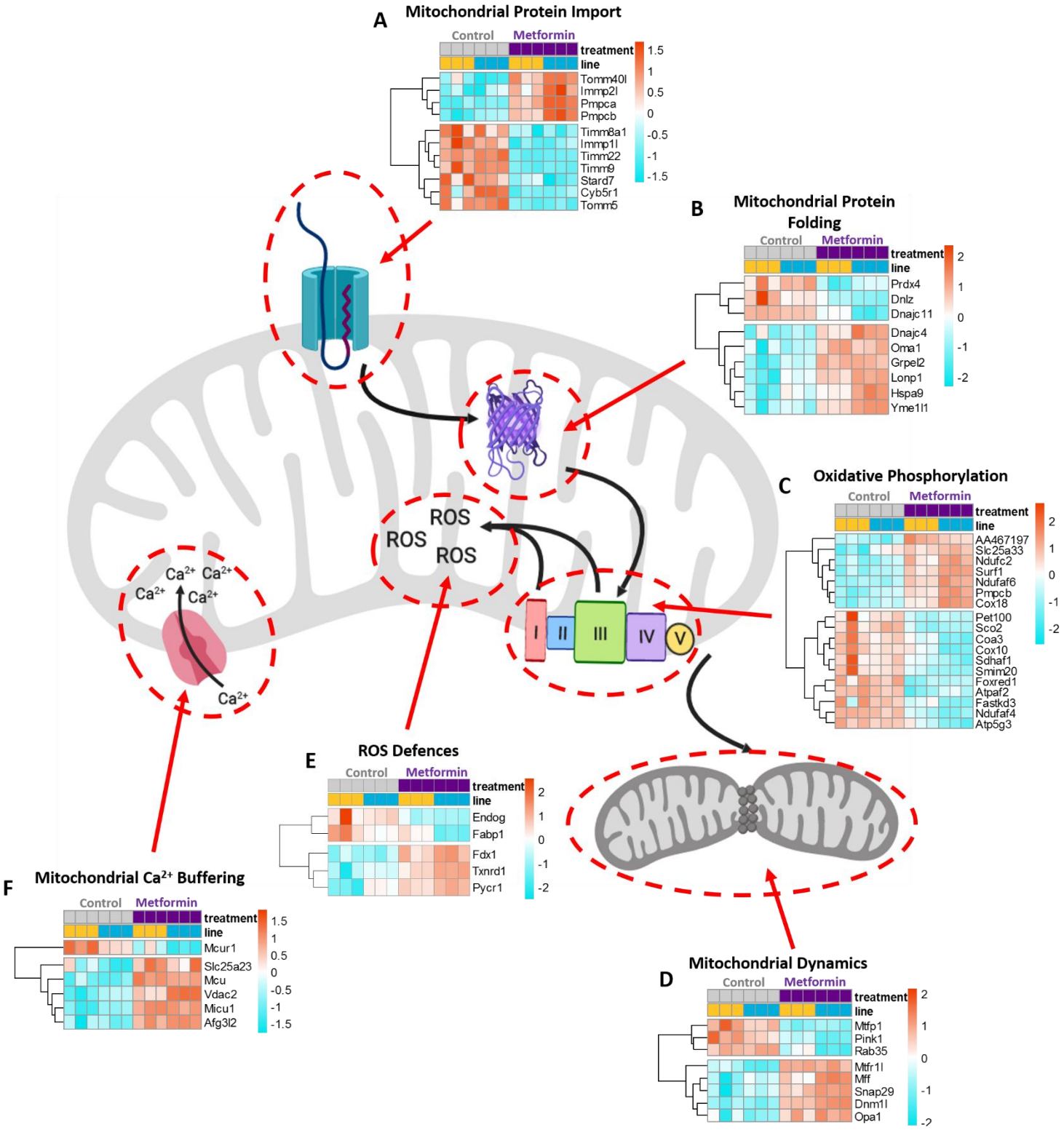

Figure 4.8. The effect of metformin on the expression of genes involved in mitochondrial processes. (A-E) Heatmaps showing DE genes (filtered by p-adjusted value of <0.05) involved in (A) mitochondrial protein import (B) Mitochondrial protein folding, , (C) oxidative phosphorylation (D) mitochondrial dynamics, (E) ROS defences and (F) mitochondrial Ca^{2+} signalling. The colour key depicts the z-score and is shown on the right of each heatmap. N=6 plates from 2 different organoid lines.

Mff, Mtfr1l, Dnm1l and mitochondrial fusion protein *Opa1* were also upregulated (Figure 4.8D). Metformin did not cause marked changes in the expression of genes involving ROS defences (Figure 4.8E), Metformin increased the expression of genes associated with mitochondrial Ca^{2+} signalling, including the mitochondrial Ca^{2+} uptake transporter complex *Mcu, Micu1* and *Afg3l2* (although the regulatory protein *Mcur1* was downregulated), the mitochondrial Ca^{2+} transport channel *Vdac1* and the Ca^{2+} dependent mitochondrial phosphate carrier *Slc25a33* (Figure 4.8E).

4.4.3. Metformin activates ISR and the HIF-1A signalling pathway to stimulate GDF-15 induction

Since GDF-15 induction is associated with activation of ISR in response to a number of stressors including mitochondrial dysfunction *(287, 450)*, the possibility of ISR activation as part of metformin stimulated GDF-15 secretion were explored. From the intestinal tissues in HFD-fed mice, oral dosing of metformin for 6 hours elicited an increase in *Ddit3* expression (which encodes the CHOP

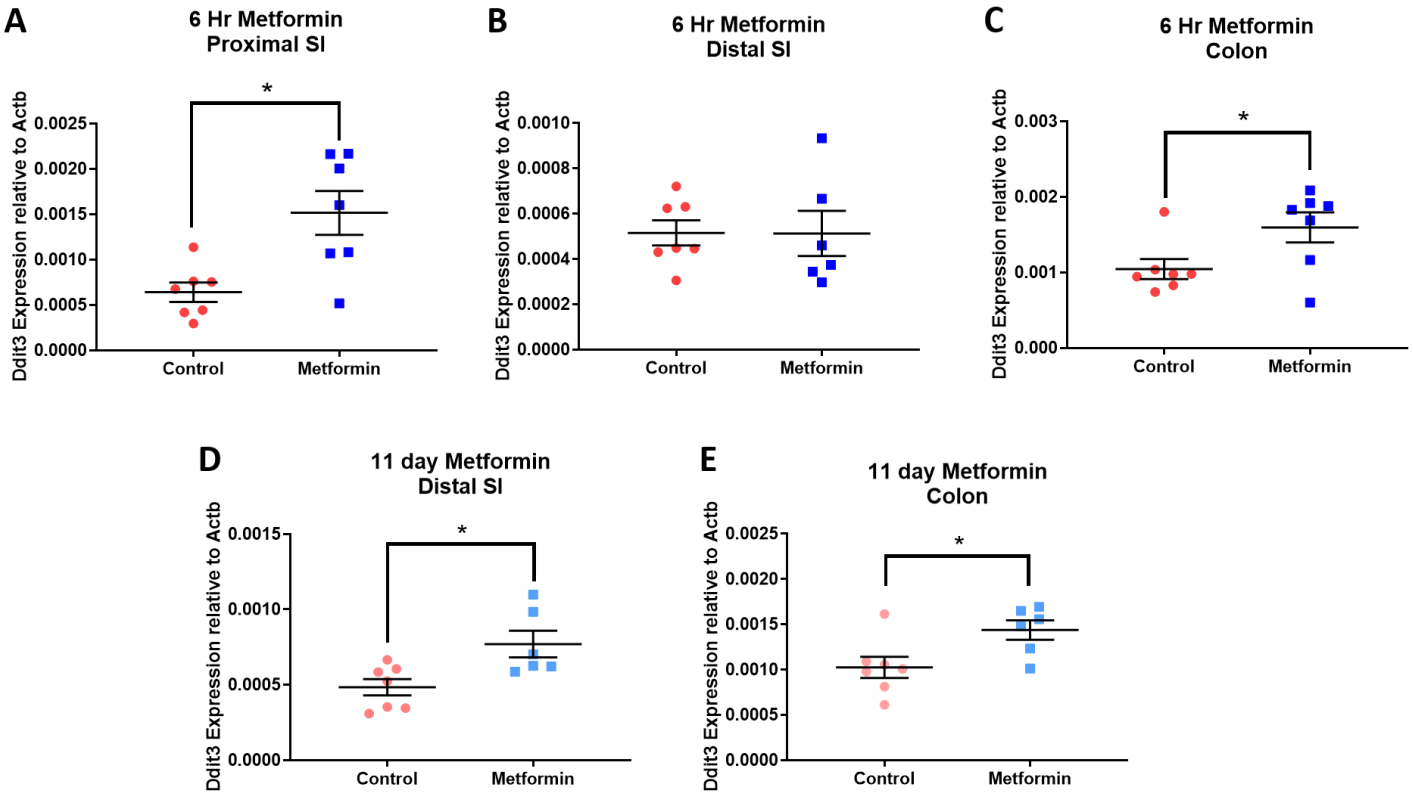

Figure 4.9. Metformin induces Ddit3 (CHOP) expression in the intestines of HFD-fed mice. (A-C) HFD-fed mice fed with a single dose of 600mg/kg metformin for 6 hours induced Ddit3 expression in (A) proximal small intestine (SI) and (C) colon, but not (B) distal SI. mRNA analysis of fresh frozen tissue normalised to expression levels of b-actin (Actb). N=6-7 mice per group. *, P<0.05. Two-tailed independent t-test. (D and E) HFD-fed mice fed with 300mg/kg metformin for 11 days induced Ddit3 expression in (D) distal SI and (E) colon. mRNA analysis of fresh frozen tissue normalised to expression levels of b-actin (Actb). N=6 mice per group. *, P<0.05. Two-tailed independent t-test.

transcription factor activated during ISR) in the proximal small intestine and colon, but not the distal small intestine (Figure 4.9A-4.9C). These segments of the intestine coincided with induction of *Gdf15* mRNA expression by metformin treatment *(321)*. Similarly, long-term oral treatment of metformin for 11 days also increased *Ddit3* mRNA expression in the distal small intestine and colon (Figure 4.9D and 4.9E), which correlates with the induction of *Gdf15* expression *(321)*. This suggests that metformin activates ISR to elicit *Gdf15* expression in the intestine.

To confirm the observations in the mouse intestine, the effects of ISR on GDF-15 secretion were confirmed using 2D monolayer cultures from intestinal organoids. ISR is activated by the phosphorylation of translation initiation factor eIF2α by serine/threonine kinases, which are in turn activated by various cellular stressors (Figure 4.10A) *(461, 462)*. Phosphorylated eIF2α preferentially translates transcription factors with specific upstream open reading frames (uORFs) such as ATF4 and ATF5 over general protein synthesis, leading to induction of a transcriptional cascade such as upregulation of *Ddit3* (CHOP) and *Atf3*, amongst others *(463)*. The contribution of ISR to metformin stimulated GDF-15 secretion was investigated by co-treatment with ISRIB, an inhibitor which prevents the phosphorylation of the translation initiation factor eIF2α. ISRIB co-treatment significantly diminished metformin stimulated GDF-15 secretory response at 1µM but was without effect at 0.1µM concentrations and no differences were found on basal secretion (Figure 4.10B and 4.10C). Co-treatment with the PERK inhibitor GSK-2606414 (associated with the ER stress arm of ISR) modestly reduced metformin-stimulated GDF-15 secretion and increased basal secretion in one experiment (Figure 4.10D), suggesting some contribution of PERK in metformin elicited ISR. Co-treatment with the GCN2 inibitor A-92 (activated by amino acid deprivation in the ISR pathway) did not alter metformin-stimulated GDF-15 secretion but inhibited GDF-15 secretion stimulated by the histidyl-tRNA synthetase inhibitor Histidinol to mimic amino acid deprivation (Figure 4.10E).

RNA-sequencing analysis demonstrate that metformin did not alter the expression of *Eif2a*, *Eif2ak3* (PERK) or *Eif2ak4* (GCN2), but increased the expression of *Eif2ak2* (PKR) and downregulated *Eif2ak1* (HRI) (Figure 4.10F). This likely reflects the importance of posttranslational regulation as opposed to transcriptomic changes in *Eif2a* and stress-activated kinases during ISR. The effects of metformin on the expression of confirmed ATF4 target genes were also investigated (Figure 4.10F). Only *Asns* and *Pck2* expression were increased by metformin treatment (associated with asparagine and glucose metabolism, respectively), whilst *Atf3* and *Atf5* were downregulated by metformin treatment (Figure 4.10F). Notably, metformin did not alter the expression of *Atf4, Ddit3, Chac1* (involved in UPR and glutathione biosynthesis), *Psph* (serine metabolism) and *Trib3* (involved in NF-kB and cytokine signalling responses) (Figure 4.10F). These results do not provide conclusive evidence that metformin elicits the expression of ATF-4 dependent genes.

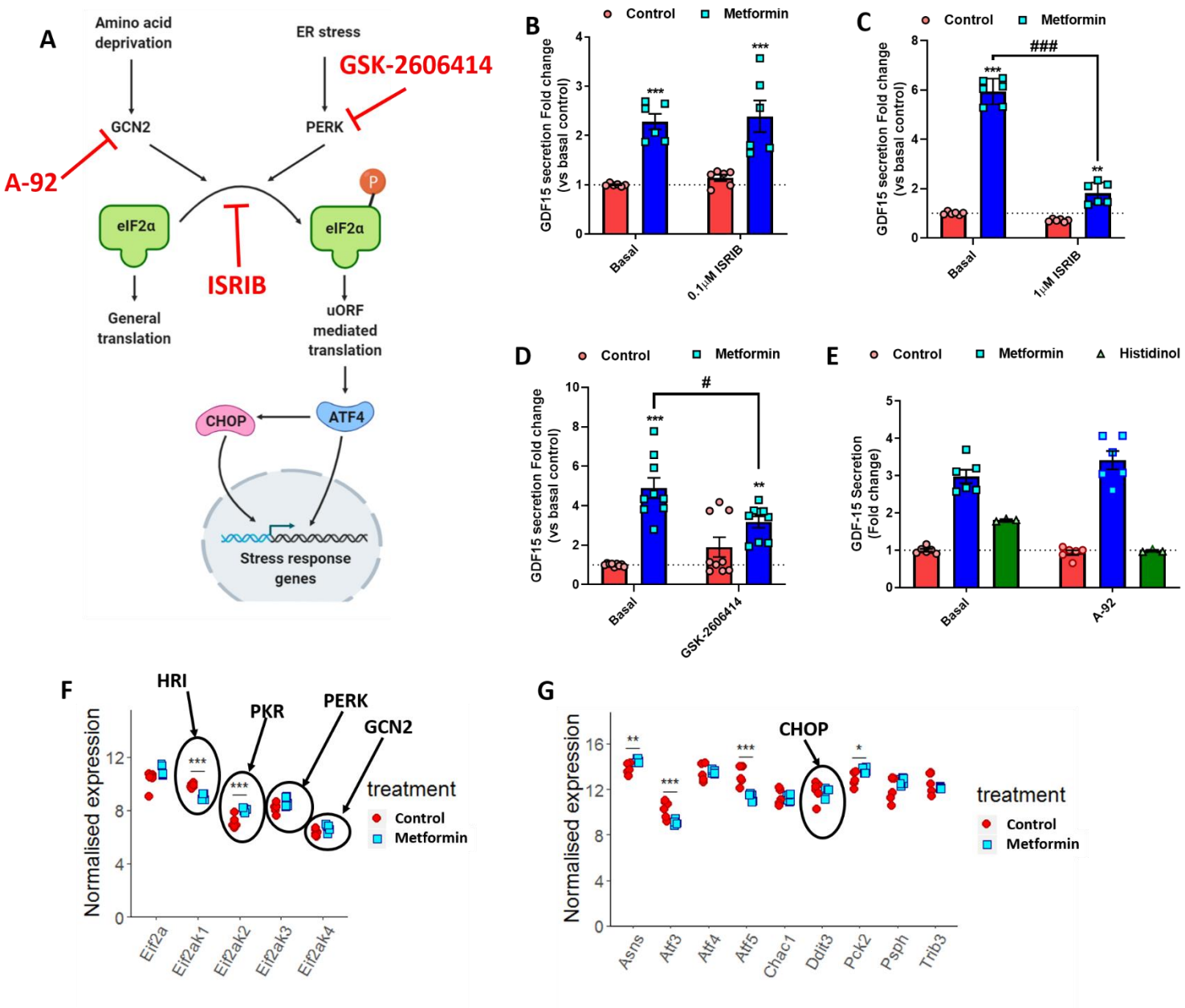

Figure 4.10. Metformin activates ISR to stimulate GDF-15 secretion. (A) Schematic showing the ISR pathway and mechanisms of action of ISRIB, A-92 and GSK-2606414. (B-D) GDF-15 secretion in mouse duodenal 2D monolayer cultures pre-treated with metformin (1mM) with (B and C) ISRIB (0.1μM and 1μM respectively), (D) GSK-2606414 (0.2μM) and (E) A-92 (20μM). Cultures were pre-treated with ISRIB, GSK-2606414 or A-92 for an hour prior to co-treatment with or without metformin. ISRIB: N=6 wells, 3 wells assessed in parallel from 2 independent experiments. GSK-2606414: N=6 wells, 3 wells assessed in parallel from 3 independent experiments. A-92: N=6 wells, 3 wells assessed in parallel from 2 independent experiments except for Histindol, where N=3 wells from 1 experiment. For (B-E), *, P<0.05, **, P<0.01, ***, P<0.001 vs control, #, P<0.05, ###, P<0.001 vs metformin. Two-way ANOVA and Bonferroni's post hoc test. (F and G) The effect of metformin on the expression of (F) Eif2a and stress-activated kinases and (G) ATF target genes from the RNA-seq data. The raw count data for each gene is normalised by the size factors and the library size. *, P<0.05, **, P<0.01, ***, P<0.001 (P-adjusted values calculated via DE-Seq analysis).

Previous studies reported that overexpression of CHOP, but not ATF4, ATF5 or ATF6 was associated with increased *Gdf15* promoter activity *(286)*, the effects of CHOP in the downstream ISR pathway was examined. Duodenal organoids generated from CHOP null mice were still able to elicit GDF-15 secretion in response to metformin comparable to wild-type organoids (when normalised to control of the organoid line) (Figure 4.11A). However, when the results were normalised to wild-type control, GDF-15 secretion in CHOP-KO organoids were lower, but metformin was able to still elicit GDF-15 secretion (Figure 4.11B). The results suggests that metformin-stimulated GDF-15 secretion might be partially dependent on CHOP in intestinal cultures.

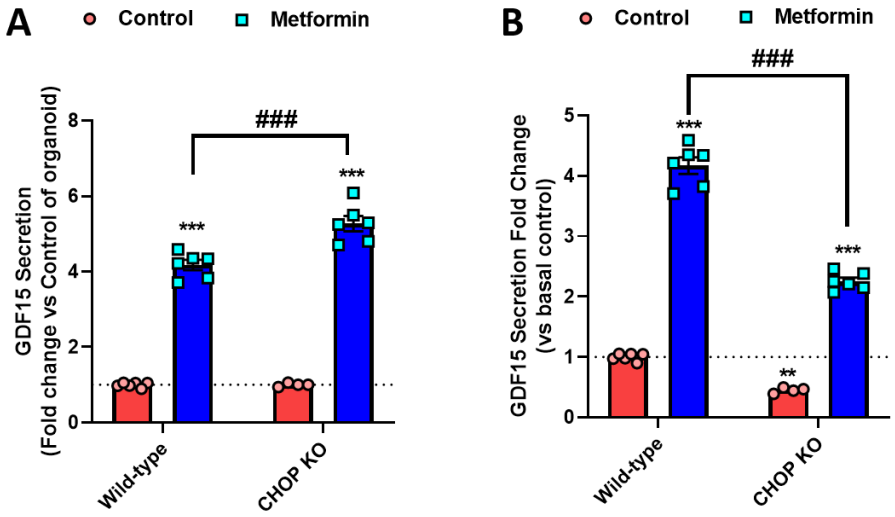

Figure 4.11. Metformin-stimulated GDF-15 secretion in CHOP knockout mouse duodenal organoids. (A) GDF-15 secretion in mouse duodenal 2D monolayer cultures generated from wild-type and CHOP-null (CHOP KO) mice pre-treated with metformin (1mM). Wild-type organoids control and metformin: N=6 wells, CHOP KO control: N=4 wells, CHOP KO metformin: N=6 wells, 1-3 wells assessed in parallel from 2 independent experiments. Metformin-stimulated GDF-15 secretion was normalised to the control of the organoid line. (B) The same set of data generated in A, but all of the data was normalised to basal control of the wild-type line only. ***, P<0.001 vs wild-type control, ###, P<0.001 vs wild-type metformin. Two-way ANOVA and Bonferroni's post hoc test.

Since Hif1a gene expression and target genes in the HIF-1A signalling pathway were upregulated in the RNA-seq data (chapter 3, Figure 3.14), the effects of HIF-1A inhibitors on GDF-15 secretion were investigated using two inhibitors, KC7F2 (an inhibitor of HIF-1A translation) and NSC-134754 (an inhibitor of HIF-1A activity and protein levels) *(464, 465)*. Metformin-stimulated GDF-15 secretion was completely abolished when co-treated with KC7F2, and NSC-134754 in all of the experiments (Figure 4.12A and 4.12B). The inhibitors modestly reduced basal GDF-15 secretion (Figure 4.12A and 4.12B). The results suggest that activation of the HIF-1A signalling pathway is indispensable for metformin-stimulated GDF-15 secretion.

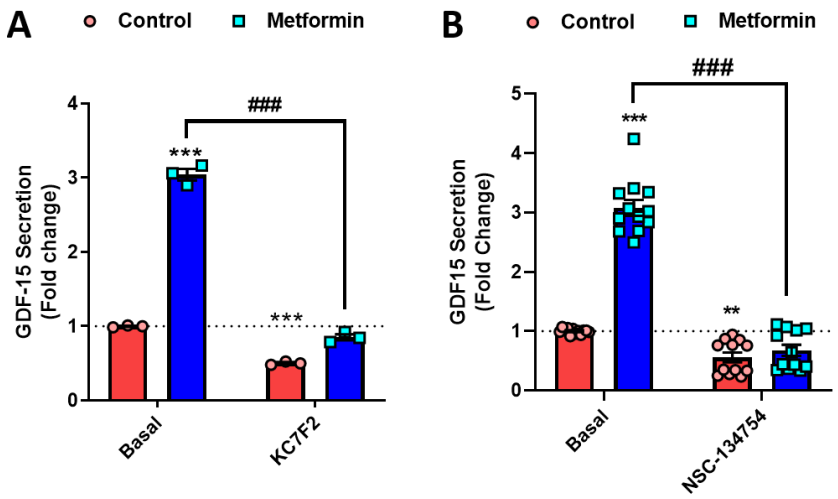

Figure 4.12. HIF-1A inhibitors inhibited GDF-15 secretion. (A) GDF-15 secretion in mouse duodenal 2D monolayer cultures pre-treated with metformin (1mM) HIF-1A inhibitors KC7F2 (50uM, A) and NSC-134754 (10uM, B). N=3 wells from 1 experiment. Cultures were pre-treated with KC7F2 or NSC-134754 for an hour prior to co-treatment with or without metformin. (b) GDF-15 secretion in mouse duodenal 2D monolayer cultures generated from wild-type and CHOP-null (CHOP KO) mice pre-treated with metformin (1mM). N=12 wells, 3 wells assessed in parallel from 4 independent experiments. For (B-E), **, P<0.01, ***, P<0.001 vs control, ###, P<0.001 vs metformin. Two-way ANOVA and Bonferroni's post hoc test.

4.5 Discussion

4.5.1 Mechanisms of metformin-stimulated GDF-15 secretion in intestinal cells

This study characterised the mechanisms of metformin stimulated GDF-15 secretion in cells seeded in 2D monolayer cultures from intestinal organoids, using pharmacological compounds and analysis of mitochondrial genes by RNA-seq. The experiments were a follow up investigation based on the RNA-seq data from intestinal organoids (chapter 3) and analysis of *Gdf15* expression in intestinal tissues of HFD-mice treated with metformin *(321)*, which revealed the importance of the intestine in GDF-15 induction by metformin.

This study provides two lines of evidence to show that metformin stimulated GDF-15 secretion is dependent on the inhibition of mitochondria Complex I activity, and not by AMPK activation (Figure 4.2 and 4.3). First, metformin stimulated significant GDF-15 secretion in a comparable manner to rotenone, but the AMPK activator Az-991 failed to elicit significant GDF-15 secretion (Figure 4.2). Second, the NAD+ biosynthesis precursor NMN, which has been shown to reduce Complex I dependency of cancer cells treated with metformin *(396)*, decreased GDF-15 secretion elicited by metformin (Figure 4.3). These observations complemented a similar RNA-seq study performed on

metformin treated human hepatocytes, revealing that *Gdf15* induction occurs via an AMPK independent pathway *(365)*. Moreover, inhibitors that directly impair electron transport chain function (Antimycin A and oligomycin) induced *Gdf15* expression in C2C12 myotubes, whilst various mouse models with other impaired mitochondrial processes also induced *Gdf15* expression, as discussed later *(286, 374)*. The strongest evidence comes from observations in patients with mitochondrial diseases, who were reported to have elevated serum GDF-15 levels *(447, 448)*. This study supports the accumulating literature in confirming that metformin stimulated GDF-15 secretion via a direct mitochondrial mechanism in cells, mice and humans.

Although metformin is known to inhibit mitochondrial metabolism, the mechanisms involving other mitochondria processes are less known. RNA-seq analysis was used to investigate the effect of metformin on mitochondrial genes to suggest which mitochondrial processes were disrupted in intestinal cells and further interpret the mechanisms of metformin stimulated GDF-15 secretion. The RNA-seq data showed downregulation of GO processes involving RNA processes and translation, and decreased expression of many genes encoding mitochondrial ribosomes and aminoacyl tRNA synthetases, but not a general shutdown of the cellular translation machinery (Figure 4.6 and 4.7). This is also supported by the observations that inhibition of mitochondrial translation by doxycycline did not elicit additive GDF-15 secretion upon co-treatment with metformin, in contrast to other mitochondrial proteostasis and mtDNA replication inhibitors (Figure 4.5). This is consistent with a recent study by Quiros *et. al.*, who reported consistent downregulation of mitochondrial ribosomes at the proteomic level in response to different mitochondrial inhibitors, including FCCP *(450)*. Whether this reflects decreased mitochondria numbers in the cells needs to be determined in the future. Doxycycline and muscle-specific *Crif1* deleted mice also reported GDF-15 induction in muscle cells *(286)*. These experiments suggest that metformin impairs OXPHOS and disrupting mitochondrial translation as a mechanism to stimulate GDF-15 secretion.

Evidence from mitochondrial encephalomyopathy patients with a mutation of the gene encoding pyrimidine synthesis enzyme thymidine kinase (*Tk2*), and experiments in a mouse model with deletions of Twinkle mtDNA helicase, shows the importance of mtDNA replication in GDF-15 induction *(374, 449)*. This study revealed that genes involved in mtDNA replication were downregulated by metformin treatment (Figure 4.7). However, unlike mitochondrial translation, metformin also downregulated genes involved in DNA transcription, replication and repair in the nucleus (see chapter 3, Figure 3.20). Impaired mitochondrial respiration have been reported to decrease de novo nucleotide biosynthesis and nucleotide pools, which could affect mtDNA (as well as nuclear DNA) maintenance processes *(466–470)*. However, co-treatment of ciprofloxacin, which inhibits mtDNA replication, increased GDF-15 secretion in both control and metformin-treated cultures (Figure 4.5),

suggesting that metformin stimulated GDF-15 secretion is unlikely to be dependent on decreased mtDNA replication.

Metformin, as well as complex I inhibitor Rotenone and complex III inhibitor Antimycin A, has been reported to alter mitochondrial ROS production *(381, 471–473)*. Mitochondrial targeted compounds that stimulate ROS production, MitoPQ and MitocDNB1, only elicited a modest GDF-15 secretory response, whilst high concentrations of MitoTEMPO also weakly decreased metformin stimulated GDF-15 secretion (Figure 4.4). Whether the partial inhibition observed in response to MitoTEMPO is due to the contribution of non-mitochondrial ROS should be considered in future studies. Furthermore, whether these compounds were influencing GDF-15 secretion at their optimal concentrations should be examined. RNA-seq analysis did not show any marked changes in the expression of ROS defence genes (Figure 4.8). Other studies using C2C12 myotubes have shown that the antioxidant Trolox did not affect *Gdf15* mRNA expression induced by Antimycin A and Oligomycin, demonstrating that the mechanism might be ROS independent *(448)*. This study shows that ROS signalling probably plays a minor role in metformin stimulated GDF-15 secretion.

Perturbed mitochondria function activates the mtUPR, a mechanism associated with accumulation of misfolded and unfolded proteins which leads to the induction of mitochondrial proteases and chaperone expression to restore mitochondrial function *(450, 474–476)*. The RNA-seq data revealed upregulation of mtUPR proteases such as *Lonp1*, *Yme1l1*, *Oma1*, *Grpel* and the chaperone *Hspa9*, suggesting that metformin might also activate mtUPR in intestinal cells (Figure 4.8). The mtUPR response, such as that elicited by doxycycline or inhibiting LONP1 proteases by CDDO, also activates ISR via the induction of the master regulator ATF4 *(286, 450)*. This response may also be mediated by the eIF2α kinases GCN2 or PKR, although this is not completely understood *(477, 478)*. However, the GCN2 inhibitor suppressed GDF-15 secretion elicited by histidinol but not metformin, suggesting that GCN2 function is redundant to metformin-stimulated GDF-15 secretion (Figure 4.10).

As well as mitochondrial stress, metformin has also been reported to initiate ER stress via the activation of PERK-ATF4 signalling pathway in rat primary cardiomyocytes *(479)*. Inhibition of PERK activity via GSK-2606414 modestly decreased metformin-stimulated GDF-15 secretion in intestinal 2D monolayer cultures (Figure 4.10). This contrasts with experiments in MEF cells, in which the same concentrations of GSK-2606414 had no effect on phenformin stimulated *Gdf15* mRNA expression *(321)*. The differences in effect could be time-dependent (6 hours in MEFs compared to 24 hours in organoids) or dependent on a cellular context *(321)*. Perhaps depletion of cellular ATP levels by high dose metformin treatment could disrupt protein folding and trigger ER stress in intestinal cells, although the importance of this pathway remains to be elucidated.

Despite the modest effect (if at all) of the GCN2 and PERK inhibitors on metformin-stimulated GDF-15 secretion, the eIF2a phosphorylation inhibitor ISRIB mostly inhibited metformin stimulated GDF-15 secretion (Figure 4.10), demonstrating the importance of ISR and supporting other studies showing the importance of ISR in *Gdf15* induction *(286, 287, 374, 451)*. Other eIF2a kinases such as PKR or HRI could be involved in the upstream mechanisms of the ISR pathway, which should be investigated in future experiments with selective inhibitors. Similarly, metformin treatment induces the expression of ISR transcription factors ATF4 and CHOP in the colon (Figure 4.9 and *(321)*), although this is not reflected in the RNA-seq data in duodenal organoids (Figure 4.10). This could be due to a temporary induction of ISR genes at the transcriptomic level in the intestinal cells at an earlier time point, or increased abundance of the transcription factors at protein level, which should be confirmed in future studies.

CHOP has been reported to bind directly to the promoter of *Gdf15*, and studies in MEF cells demonstrate that siRNA-mediated knockdown of CHOP reduced the induction of *Gdf15* expression by Phenformin *(286, 321, 451)*. Metformin pre-treatment still elicited significant GDF-15 secretion in CHOP knockout mouse intestinal cells despite that GDF-15 secretion were already lower in CHOP knockout compared to wild-type organoids (Figure 4.11). However, we acknowledge that no form of normalisation has been performed to account for differences in cellular content between different organoid lines. CHOP could be partially involved in metformin-stimulated GDF-15 secretion, whilst CHOP independent pathway such as activation of IRE1-XBP-1 signalling (as XBP-1 also binds to the promoter of GDF-15) could be involved *(480, 481)*.

Described in a recent study by Loubiere *et. al.*, metformin stimulates mitochondrial Ca^{2+} uptake as an indirect result of triggering ER Ca^{2+} release in prostate cancer cells, which promotes mitochondrial swelling and disorganisation of cristae *(482)*. In the study, metformin treatment for 24 hours increased the expression of MCU mRNA and VDAC protein levels *(482)*. The RNA-seq data reported increased expression of many key mitochondrial Ca^{2+} signalling genes (including Mcu and Vdac1), which may suggest a role of mitochondrial Ca^{2+} signalling in mitochondrial stress or dysfunction in intestinal cells. This could have an impact on metformin stimulated GDF-15 secretion and should be tested in the future using MCU inhibitors.

The RNA-seq data highlighted that metformin increased the expression of *HIF-1A*, its co-transcriptional partners and many known HIF pathway target genes, whilst decreasing the expression of HIF regulatory factors (Chapter 3, Figure 3.14). The observations that HIF-1A inhibitors abolished metformin-stimulated GDF-15 secretion suggests that the mechanism is dependent on the HIF-1A signalling pathway (Figure 4.12). A previous study by Lakhsal *et al.,* reported that chelation of iron with

2,2-Bipyridyl (BiP) induced *Gdf15* gene expression in numerous human cell lines, but siRNA knockdown of *Hif1a* exhibited modest reduction on the induction response, by contrast to the effects of the HIF-1A inhibitors *(483)*. The mechanisms by which HIF-1A could be activated by metformin in this study is not known. This study contradicts with the results from previous studies which reported that metformin, via the inhibition of complex I of the electron transport chain, inhibited HIF-1A activity through decreasing oxygen consumption and increasing the cellular oxygenation ability in various cancer cells *(203, 345, 346)*. Therefore, the alternative explanation for why Metformin could increase HIF-1A signalling is by an indirect mechanism, such as by increasing ROS production which could increase mRNA expression levels and stability of HIF-1A *(484)*. Indeed as discussed above, MitoTEMPO modestly decreased metformin-stimulated GDF-15 secretion, although the effects were not as potent compared to the HIF-1A inhibitors. Future studies should measure the effects of metformin on ROS production in intestinal cells, such as measurements of superoxide production via MitoSOX indicator.

4.5.2 The gastrointestinal tract in metformin-stimulated GDF-15 secretion

This study, supporting collaborative *in vivo* observations in HFD-fed mice, suggests that the gastrointestinal tract is an important site for GDF-15 release in response to oral metformin treatment *(321)*. The only other organ with elevated *Gdf15* mRNA expression to metformin was the kidneys, the site by which metformin is excreted in urine *(321)*. Other organs with putative metformin action, such as the liver and adipose tissues, did not report induction of *Gdf15* expression despite previous evidence demonstrating that these tissues were capable of inducing *Gdf15* expression under stress *(279, 443)*.

Studies involving oral gavage of C14-labelled metformin tracer by Wilcock and Bailey have demonstrated that the gastrointestinal tract accumulates metformin at the highest (millimole/kg) concentrations compared to other organs after a single oral gavage in wild type and STZ diabetic rats, which was followed by the kidney (~400µmol/kg) *(312)*. Metformin concentrations in the liver and adipose tissues were always lower by comparison at these same time points *in vivo* *(312)*. Furthermore, intestinal enterocytes have been reported to express various metformin transporters (PMAT, SERT, OCT1 and OCT3), particularly biased expression of transporters at the apical side rather than the basolateral side, which enables enterocytes to accumulate metformin at high concentrations and only permitting ≤60µmol/kg concentrations to be absorbed in the blood *(263, 312, 315)*. Since metformin could only disrupt mitochondrial function at high concentrations inside cells *(204)*, and GDF-15 induction occurs via a mitochondrial dependent mechanism, this study suggests that gastrointestinal tract is likely to be the main organ of GDF-15 release into the blood in response to oral metformin treatment.

Interestingly, in situ hybridisation studies demonstrate that *Gdf15* expression is only localised in the crypts of a subset of enterocytes and colonocytes in mouse intestinal sections in response to metformin *(321)*. Although the identity of these cell types were not clarified in the study, the abundance of these cells and their location in the intestinal mucosa likely represent transit amplifying cells, which are known to rely on mitochondrial function to determine cell fate *(189, 485)*. Future studies should investigate the functional identity of these *Gdf15* positive cells and whether selective ablation of *Gdf15* in these intestinal cells can sufficiently reduce the effect of metformin on GDF-15 levels in the serum.

4.5.3 Comparing the effects of metformin on GDF-15 and other stress hormones/metabolic growth factors

Similar to GDF-15, FGF21 is also elevated in children with mitochondrial disorders and in mouse models of defective mtDNA replication *(374, 448)*. FGF21 levels are also elevated in the serum of patients on metformin therapy, and metformin induce FGF-21 mRNA expression and secretion in hepatocytes via an ISR-dependent mechanism (although an involvement of AMPK is debateable) *(297, 471)*. The induction of FGF21 seems to occur via a pathway which relies on oxidative stress, since MitoTEMPO suppressed metformin induced *Fgf21* expression in hepatocytes and the antioxidant Trolox inhibited induction of *Fgf21* by Antimycin A and Oligomycin in C2C12 myotubes *(297, 448)*. Metformin increased *Fgf21* expression in intestinal cells within the RNA-seq database, although the expression levels are low (Figure 4.1). This is not unexpected since FGF21 is known to be released primarily by the liver, where it mediates metabolic effects on adipose tissues to improve insulin sensitivity, as well as regulating food intake and energy expenditure *(304, 306–308)*.

In addition to FGF21, metformin also increased *Fgf15* expression (the feedback hormone involved in bile acid homeostasis) in intestinal cells (Figure 4.1). This is in contrast to a recent study reporting that metformin treatment in T2DM patients decreased serum FGF19 (the human homologue of FGF15) levels *(260)*. Perhaps these different observations could be due to species differences in metformin regulated Fgf15/19 expression, or comparisons between the 2D monolayer cultures to the human studies where human intestinal enterocytes are regularly exposed to an environment of high bile acid levels.

The RNA-seq data also highlighted downregulation of *Tgfb1* expression, a paracrine growth factor induced by cellular stress which is also involved in intestinal inflammation *(486)*. This observation also supports a different study reporting that metformin inhibits TGF-B1 signalling and may explain putative inflammation protective effects of metformin *(360, 487)*.

4.5.4 Conclusions

The results from this chapter connects the findings presented from previous studies to suggest a working mechanism to explain metformin stimulated GDF-15 secretion, which are presented in Figure

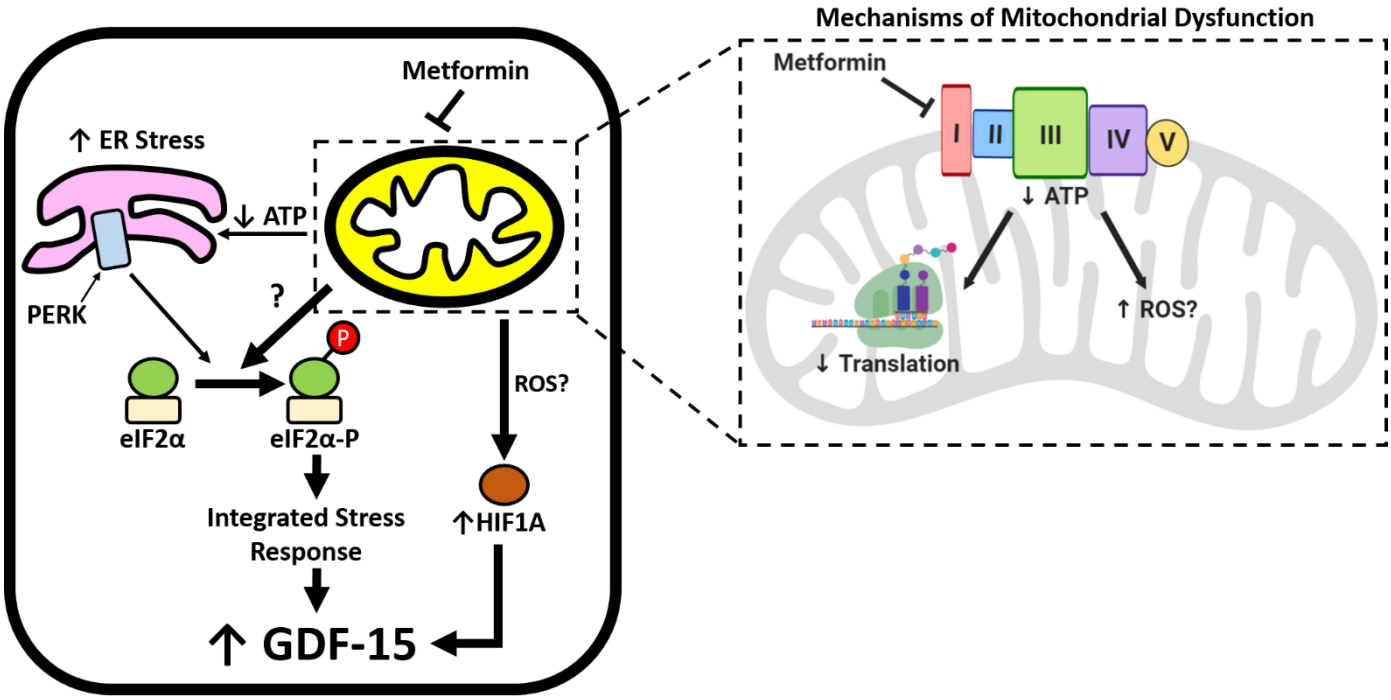

Figure 4.13. Working model describing the effects of metformin on GDF-15 induction.

4.13. In response to the inhibition of mitochondrial respiration by metformin, the mitochondria attenuate protein translation. This activates ISR via eIF2α phosphorylation to stimulate GDF-15 secretion. Metformin also activates HIF-1A signalling pathway via an unknown mechanism (the most plausible candidate is oxidative stress) to stimulate GDF-15 secretion. ER stress could also contribute to metformin stimulated GDF-15 secretion to some extent. This chapter implicates the role of the gastrointestinal tract as an endocrine organ to stimulate GDF-15 release in response to metformin treatment.

Chapter 5: Mechanisms of metformin action on glucose uptake in intestinal cells

5.1 Summary

Despite clinical application of metformin for the treatment of type 2 diabetes mellitus for over 50 years, the mechanisms explaining the glucose lowering effects of metformin are not completely understood. Recent studies have identified glucose uptake and transport in the gut as targets of metformin action *(116)*. Whilst some studies demonstrate that metformin could directly alter intestinal glucose absorption, metformin has also been reported to increase intestinal glucose utilisation from the blood *(207, 236, 237, 488–490)*. However, the cellular mechanisms that explain the effects of metformin on glucose transport are unclear. This chapter examines the effects of metformin on glucose uptake and transporter expression in intestinal enterocytes.

5.2 Introduction

5.2.1 Glucose transport in intestinal enterocytes

In the gastrointestinal tract, glucose transporters play essential roles in the uptake and absorption of glucose in intestinal epithelial cells. Glucose absorption involves the uptake of glucose mediated by the sodium-dependent glucose transporter SGLT1 incorporated into the apical (brush border) membrane of epithelial cells *(491, 492)*. This glucose transporter utilises the electrochemical gradient of sodium ions to transport glucose into cells *(493)*. The predominant role of SGLT1 in glucose absorption was demonstrated from observations in patients with the potentially fatal condition of glucose and galactose malabsorption caused by loss-of-function mutations in the transporter *(494–496)*. Similarly, *Sglt1* knockout mice displayed impaired glucose absorption and a decreased rate of glucose appearance in the blood following an oral glucose tolerance test *(491)*.

It has been generally accepted that the facilitative transporter GLUT2 is involved in the basolateral exit of intracellular glucose via facilitated diffusion from enterocytes. GLUT2 is a low affinity but high capacity glucose transporter also capable of transporting fructose and glucosamine *(497, 498)*. The evidence supporting GLUT2 in glucose absorption was based on the observations of GLUT2 localisation in the basolateral membrane of enterocytes, and of GLUT2 mediated glucose and fructose transport in vesicles derived from basolateral membranes *(492, 498, 499)*. Some evidence also suggests that GLUT2 vesicles could be recruited to the apical membrane under high glucose conditions, or in

response to taste receptor or GLP-2 receptor activation to further facilitate luminal glucose absorption, although evidence supporting this mechanism has been inconsistent *(491, 492, 500–505)*. Unlike SGLT1 however, patients with Fanconi-Bickel syndrome (caused by inactivating mutations in the gene encoding GLUT2) and GLUT2 knockout mice showed normal intestinal glucose absorption and glucose appearance in the blood following glucose tolerance tests *(506–508)*. This suggests a redundant role of GLUT2 in glucose absorption and possible compensation by other mechanisms, such as exocytosis mediated by glucose-6-phosphate translocase as was previously reported *(506)*.

The high affinity and low capacity glucose transporter GLUT1 is also expressed in the basolateral membrane of intestinal cells, although GLUT1 was detectable in the stomach and the colon but was barely expressed in the small intestine *(509)*. The contributions of GLUT1 in intestinal glucose transport under physiological conditions is unknown. However, GLUT1 expression was induced in the basolateral membranes of the small intestine in mice with streptozocin-induced diabetes *(510)*. Interestingly, GLUT1 was also overexpressed in the alimentary limbs of rats and patients after Roux-en-Y gastric bypass, which was associated with intestinal hyperplasia and increased intestinal serosal to mucosal glucose transport in mice and patients with RYGB (RYGB) *(42, 43)*. GLUT1 has also been shown to be upregulated in rats after sleeve-gastrectomy with duodenojejunal bypass, but not after sleeve-gastrectomy alone *(43, 511)*.

GLUT5 is also expressed in the apical membrane of the small intestine and transports solely fructose *(512, 513)*. Experiments in GLUT5 knockout mice demonstrate reduced dietary fructose absorption in the jejunum by 75% and negligible appearance of fructose in the plasma following oral fructose administration *(514)*. Moreover, the glucose transporter GLUT7 is expressed in the apical membrane of the jejunum, ileum and colon, although functional studies into its contribution to intestinal glucose transport are still lacking *(515)*.

5.2.2 Metformin and intestinal glucose absorption

Several studies demonstrate that oral metformin administration alters intestinal glucose absorption, which may contribute to the glucose lowering effects of metformin *(234–236, 488, 489, 516)*. Early studies using isolated hamster and rat intestine models demonstrated that following pre-treatment with various biguanides *(234, 235)* or 2 hours after oral metformin administration *(489)* intestinal glucose transport was inhibited. Similarly, intraduodenal, but not intravascular administration of metformin inhibited glucose transport in the perfused small intestines *(488)*.

A recent study using PET/CT scan imaging demonstrated that oral metformin administration delayed intestinal transit of orally administered F-2DG in HFD-fed mice *(236)*. The authors performed ex vivo examination of glucose transport using everted gut sacs from HFD-fed mice treated with oral metformin and observed that mucosal to serosal transport of F-2DG in the proximal jejunal and proximal ileal intestinal segments were decreased *(236)*. Furthermore, the rate of glucose appearance in the blood following intraduodenal administration of glucose was lower in metformin treated mice compared to vehicle treated mice, providing direct evidence that metformin reduced glucose absorption *(236)*.

Metformin has also been reported to decrease intestinal glucose absorption in one clinical study involving 12 patients with T2DM *(516)*. The study involved administering metformin to the patients for 30 minutes followed by introducing a non-metabolisable glucose analogue 3-O-methylglucose (3-OMG) via an intraduodenal catheter over the course of 120 minutes *(516)*. The results demonstrated that metformin administration was associated with reduced serum 3-OMG levels, which correlated with increased serum GLP-1 levels, possibly due to increased intestinal transit of glucose to the distal small intestine to stimulate GLP-1 secretion from L cells *(516)*.

5.2.3 The "glucose sink" model of metformin action in the intestines

Metformin has also been reported to increase glucose utilisation in the mouse and human intestine *(116)*. Multiple observations from position-emission tomography – computed tomography (PET-CT) imaging involving intravenous injection of a non-metabolisable glucose analogue tracer ^{18}F-fluorodeoxyglucose (^{18}F-DG) demonstrated that long-term oral metformin administration was associated with accumulation of the tracer in the small intestine and the colon *(237, 364, 490, 517–519)*. Additionally, the tracer stops accumulating in the GI tract in patients who have ceased taking metformin *(238, 490, 520, 521)*. The phenomenon of increased intestinal glucose uptake in patients on metformin has been reported to interfere with radiological assessments of gastrointestinal and genitourinary malignancies, leading to false-negative diagnoses *(490, 522)*. Similar results have also been reported in metformin treated HFD-fed mice administered [3H]-2DG, which showed increased uptake only in the small intestines and the brain, but to a lesser extent in the liver *(236)*.

A recent phase 2 clinical trial in T2DM patients reported that under euglycaemic hyperinsulinaemic conditions (which maintain constant blood glucose levels), metformin increased F-DG uptake in the small intestine and colon, demonstrating that the mechanism is independent of insulin *(237)*. The observed increase in F-DG uptake in the colon positively correlated with reduced fasting plasma

glucose levels in patients *(237)*. The authors proposed that the gastrointestinal tract acts as a "sink" in depositing glucose from the circulation as a mechanism to explain the glucose-lowering effects of metformin *(237)*. Studies in rodents and patients with type 2 diabetes demonstrate that glucose is most likely to be metabolised by intestinal enterocytes *(64, 207)*. However, some studies demonstrated that AMPK activation (a pathway activated by metformin) increases the abundance of GLUT2 in the brush border membrane, which is associated with improved glucose homeostasis and could potentially facilitate glucose efflux into the lumen *(523, 524)*. The molecular mechanisms underlying the effects of metformin in glucose utilisation are therefore still elusive.

5.3 Aims

This chapter investigates the cellular mechanisms of action of metformin on glucose uptake and expression of glucose transporters in the gastrointestinal tract. The aims of this study are:

1. To examine the effects of metformin on the expression of glucose transporters in intestinal enterocytes from organoids and intestinal tissues from HFD-fed mice administered with metformin.
2. To investigate the effects of metformin on glucose uptake in enterocytes in vitro and identify the transporters and mechanisms involved.

5.4 Results

5.4.1 The effect of metformin on the mRNA expression of glucose transporters in intestinal cultures

To identify a lead into studying the molecular mechanisms of metformin on glucose transport in intestinal cells, the RNA-seq database obtained from murine intestinal 2D monolayer cultures treated for 24 hours with 1mM metformin was initially used to investigate the effects of metformin on the mRNA expression of the GLUT family of facilitative transporters (*Slc2aX*) and the sodium-dependent glucose transporter SGLT1 in mouse 2D monolayer cultures generated from duodenal organoids. Metformin treatment decreased the expression of GLUT transporters *Slc2a2* (GLUT2), *Slc2a4* (GLUT4), *Slc2a5* (GLUT5), *Slc2a7* (GLUT7) and the SGLT1 transporter *Slc5a1* (Figure 5.1A). *Slc2a1* (GLUT1) was the only glucose transporter transcript that was upregulated by metformin treatment from the list of transporters investigated (Figure 5.1A). The glucose transporter genes *Slc5a1*, *Slc2a1*, *Slc2a2* and

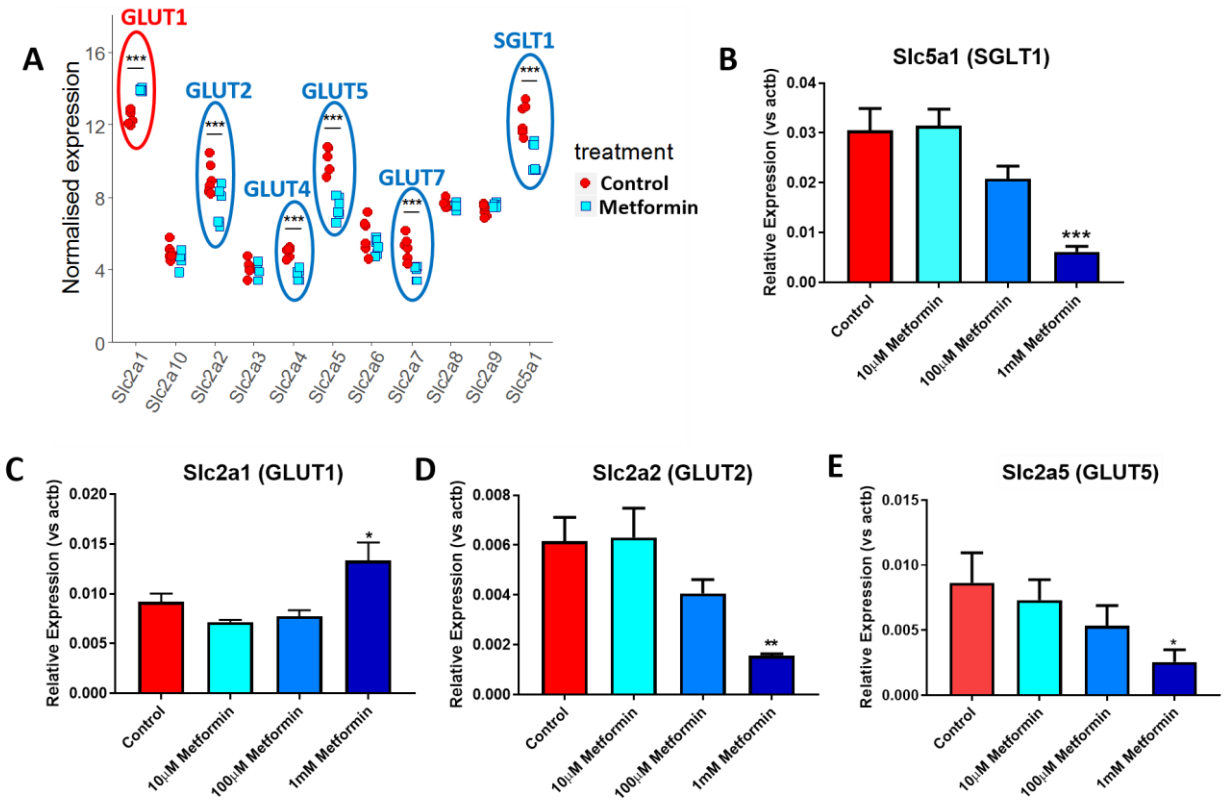

Figure 5.1. The effect of metformin on the expression of GLUT and SGLT transporters in duodenal organoid cells seeded into 2D monolayer cultures. (A) RNA-sequencing analysis of the mRNA transcript expression of all GLUT (Slc2a) transporter isoforms and the SGLT1 (Slc5a1) transporter in duodenal organoid 2D monolayer cultures in response to 1mM metformin pre-treatment for 24 hours. ***, P<0.001 (p-adjusted value). DE-seq analysis and Benjamin-Hochberg corrections. Each point represents a plate (N=6 plates from 2 organoid lines). Red and blue labels surrounding each DE gene shows the up- and down-regulated genes, respectively. (B-E) qPCR analysis of expression of select glucose transporters in duodenal organoid 2D monolayer cultures; (B) *Slc5a1* (SGLT1), (C) *Slc2a1* (GLUT1), (D) *Slc2a2* (GLUT2) and (E) the fructose transporter *Slc2a5* (GLUT5) in response to metformin pre-treatment from 10μM to 1mM for 24 hours. N=9 wells, with 3 wells assessed from 3 independent experiments except for SGLT1 where N=15 wells with 3 wells assessed in parallel from 5 independent experiments. *, P<0.05, **, P<0.01, ***, P<0.001. One way ANOVA and Bonferroni post-hoc test.

Slc2a5 were selected for further investigation since the expression levels for these genes were the highest in the RNA-seq data and previous literature confirmed their importance in intestinal cells *(43, 491, 492, 510, 514)*. RT-qPCR analysis demonstrated that treatment of metformin at 1mM, but not at any lower concentrations, significantly altered the expression of these transcripts in duodenal 2D monolayers that replicated the observations from the RNA-seq data (Figure 5.1B-E). These results demonstrate that the effects of metformin could only be observed at high concentrations.

The effects of metformin on the mRNA expression of the glucose transporters were also examined in 2D monolayer cultures generated from mouse ileal organoids. Metformin treatment at 1mM (but not at any lower concentrations) caused a trend towards lower expression of *Slc5a1* (Figure 5.2A), *Slc2a2* (Figure 5.2C) and *Slc2a5* (Figure 5.2D), although the results were not statistically significant. Similar to duodenal organoid 2D monolayers, metformin (only at 1mM concentration) significantly increased the expression of *Slc2a1* (Figure 5.2B). These results suggest that the effects of metformin were not exclusive to duodenal organoids/cells. The effects of the different metformin treatments on the mRNA expression of suspended 3D duodenal organoids in matrigel domes were also investigated.

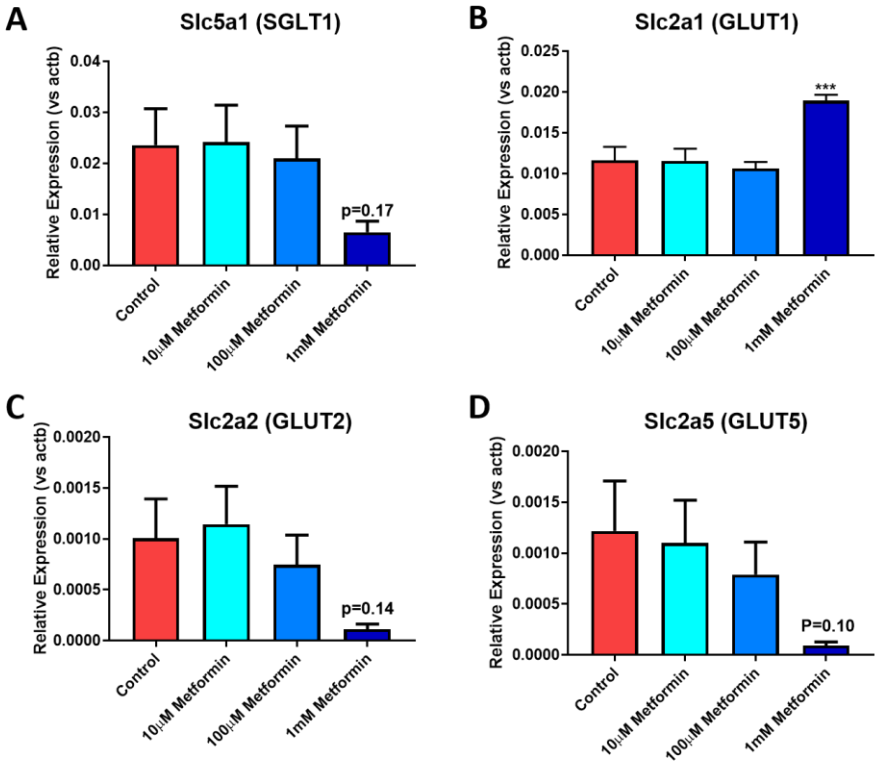

Figure 5.2. The effect of metformin on the expression of GLUT1, GLUT2, GLUT5 and SGLT transporters in ileal organoid cells seeded into 2D monolayers. (A-D) qPCR analysis of expression of select glucose transporters in ileal organoid 2D monolayer cultures; (B) Slc5a1 (SGLT1), (C) Slc2a1 (GLUT1), Slc2a2 (GLUT2) and the fructose transporter Slc2a5 (GLUT5) in response to metformin pre-treatment from 10uM to 1mM for 24 hours. N=9 wells, with 3 wells assessed in parallel from 3 independent experiments. *, P<0.05, **, P<0.01, ***, P<0.001. One way ANOVA and Bonferroni post-hoc test.

Unlike 2D monolayer cultures, metformin treatment did not alter the mRNA expression levels of *Slc5a1* (Figure 5.3A) or *Slc2a2* in 3D organoids (Figure 5.3B). This likely suggests that the "inside-out" conformation of 3D organoids (i.e. the apical face of intestinal cells facing the inside of the organoid lumen) prevents metformin uptake into intestinal cells in a 3D organoid model.

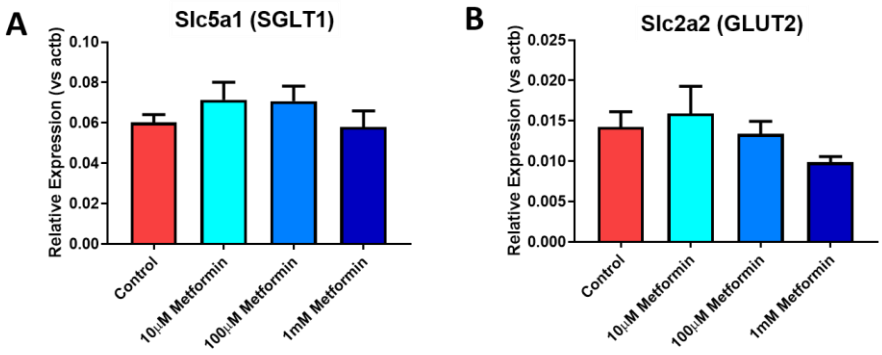

Figure 5.3. The effect of metformin on the expression of SGLT1 and GLUT2 transporters in 3D duodenal organoids. (A and B) qPCR analysis of expression of glucose transporters (A) Slc5a1 (SGLT1) and (B) Slc2a2 (GLUT2) in 3D duodenal organoids in response to metformin pre-treatment from 10μM to 1mM for 24 hours. N=9 wells, with 3 wells assessed in parallel from 3 independent experiments.

5.4.2 Metformin increases glucose uptake in intestinal cells mediated by a GLUT transporter

The effects of metformin on glucose uptake in intestinal 2D monolayer cultures were investigated via fluorescence imaging of cells transfected with the intracellular FRET glucose sensor, FLII12Pglu-700μδ6. Duodenal 2D organoid cultures were treated overnight prior to analysis with either 1 mM metformin or vehicle control. Application of glucose at 10mM concentration increased the YFP/CFP ratio (a relative measure of increased glucose uptake) in control and metformin treated cells (Figure 5.4A and 5.4B). Application of glucose at 1mM concentration increased the YFP/CFP ratio in all of the metformin-treated, but only 4/27 control cells (Figure 5.4A and 5.4B). Metformin treatment increased the uptake of glucose when applied at 1mM and 10mM concentrations (Figure 5.4C). Since different glucose concentrations were often applied sequentially in the same experiment, whether the function of the FRET sensor was saturated by repeated glucose exposure was investigated by monitoring the YFP/CFP ratio following two repeated applications of 10mM glucose. As expected, changes in the YFP/CFP ratio after applying 10mM glucose for a second time did not significantly differ from the first glucose application (Figure 5.4D and 5.4E).

To explore the functional identity of the glucose transporter(s) involved in metformin stimulated glucose uptake, changes in the YFP/CFP ratio were monitored in response to 10mM glucose following pre-application of different glucose transport inhibitors. Application of the broad-spectrum SGLT

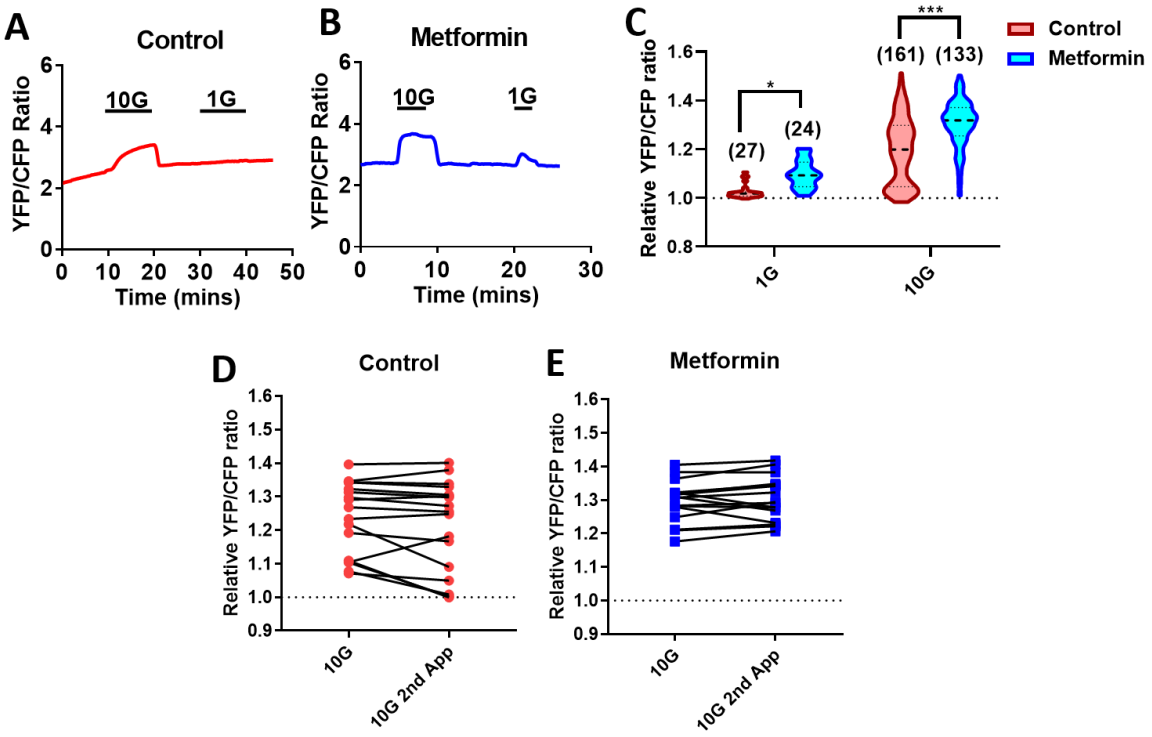

Figure 5.4. Metformin increase glucose uptake in intestinal cells from duodenal organoid 2D monolayers. (A and B) Example traces of YFP/CFP fluorescence ratios from Control (A) and Metformin (B) treated cells. Glucose treatments at 1mM (1G) and 10mM (10G) concentrations were applied as indicated. (C) The effect of 1mM and 10mM glucose on the YFP/CFP fluorescence ratios in control (red) and metformin-treated (blue) cells normalised to the baseline (*; P<0.05, ***; P<0.001, Two-way ANOVA and Bonferroni post-hoc test). Results shown as a violin plot with the median and confidence intervals indicated as dotted lines. Numbers of cells studied for each condition are indicated in the graph. (D and E) The effect of repeated 10mM glucose application on the YFP/CFP fluorescence ratio (control: N= 17 cells from 7 dishes, metformin: N=16 cells from 5 dishes, paired t-test). Abbreviations: 10G; 10mM glucose, 1G; 1mM glucose.

inhibitor phloridzin at 5µM, which has been reported to inhibit SGLT1 and SGLT2-mediated glucose transport in previous studies *(525)*, did not alter glucose uptake in either control or metformin treated cells (Figure 5.5A-5.5C). This suggests that the SGLT family of transporters (such as SGLT1) do not play a major role in glucose uptake in intestinal cells in the 2D monolayer cultures. Pre-treatment with the broad-spectrum GLUT transport inhibitor phloretin at both 10µM and 100µM reduced glucose uptake in control and metformin treated cells (Figure 5.6A-5.6F). This suggests that a GLUT transporter is responsible for the observed glucose uptake. In an attempt to examine which GLUT transporter isoform was involved in mediating glucose uptake, cytochalasin B was applied at 1µM, which had previously been reported to completely inhibit GLUT1, GLUT3 and GLUT4 dependent transport at that concentration but partially inhibits GLUT2 (as the Ki for GLUT2 was 2µM whereas the Ki for GLUT1, GLUT3 and GLUT4 were 0.1µM) *(526)*. Application of cytochalasin B completely inhibited glucose

transport in 11/13 of control cells and 14/15 of metformin treated cells (Figure 5.6G-5.6I). Forskolin, which had previously been reported to preferentially inhibit glucose uptake mediated by GLUT1 and GLUT4 over GLUT2 *(527, 528)*, also reduced glucose uptake in control and metformin treated cells (Figure 5.6J-5.6L).

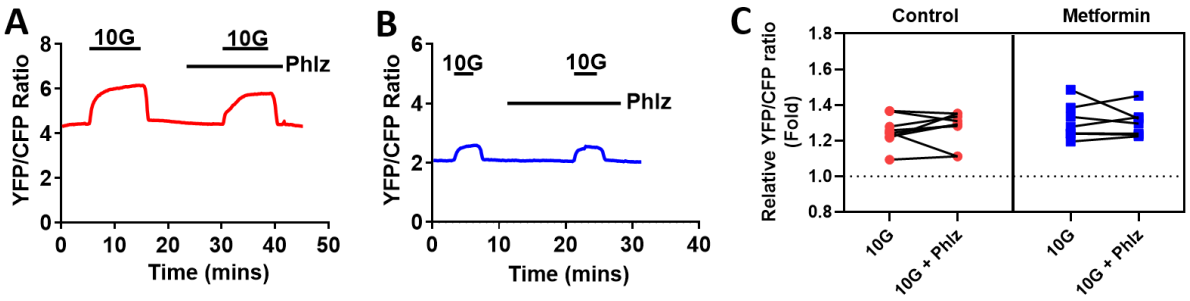

Figure 5.5. The SGLT inhibitor Phloridzin did not affect glucose transport in enterocytes. (A and B) Example traces of YFP/CFP fluorescence ratios from (A) Control and (B) Metformin treated cells. Glucose (10mM, 10G) and phloridzin (5µM) were applied as indicated. (C) The effect of glucose with and without 5µM phloridzin on the YFP/CFP fluorescence ratios in control (red) and metformin-treated (blue) cells normalised to the baseline. Control: N= 9 cells from 4 dishes, metformin: N=7 cells from 3 dishes. Paired t-test. Abbreviations: 10G; 10mM glucose, Phlz; Phloridzin.

To examine the contribution of GLUT2 over other glucose transporters, the GLUT2 substrate glucosamine was co-applied with glucose in an attempt to inhibit glucose transport via competitive inhibition (since transport studies previously showed that glucosamine exhibited a Kd of ~1.5mM compared to a Kd of ~17mM for glucose) *(497)*. Application of glucosamine (10mM) did not affect glucose transport in either control or metformin treated cells (Figure 5.7A-5.7C). Similarly, other studies have reported that fructose is transported via GLUT2 at a similar transport affinity compared to glucose, which could be used to inhibit GLUT2-dependent glucose transport through competitive inhibition *(498)*. Co-application of fructose at 100mM (which should otherwise saturate GLUT2 mediated transport) did not affect glucose uptake (Figure 5.7D-5.7F). The observations that glucosamine and fructose did not influence glucose uptake could suggest that glucose uptake in intestinal cells may not be dependent on GLUT2, although there are no positive controls to show that glucosamine or fructose could influence glucose transport in this study.

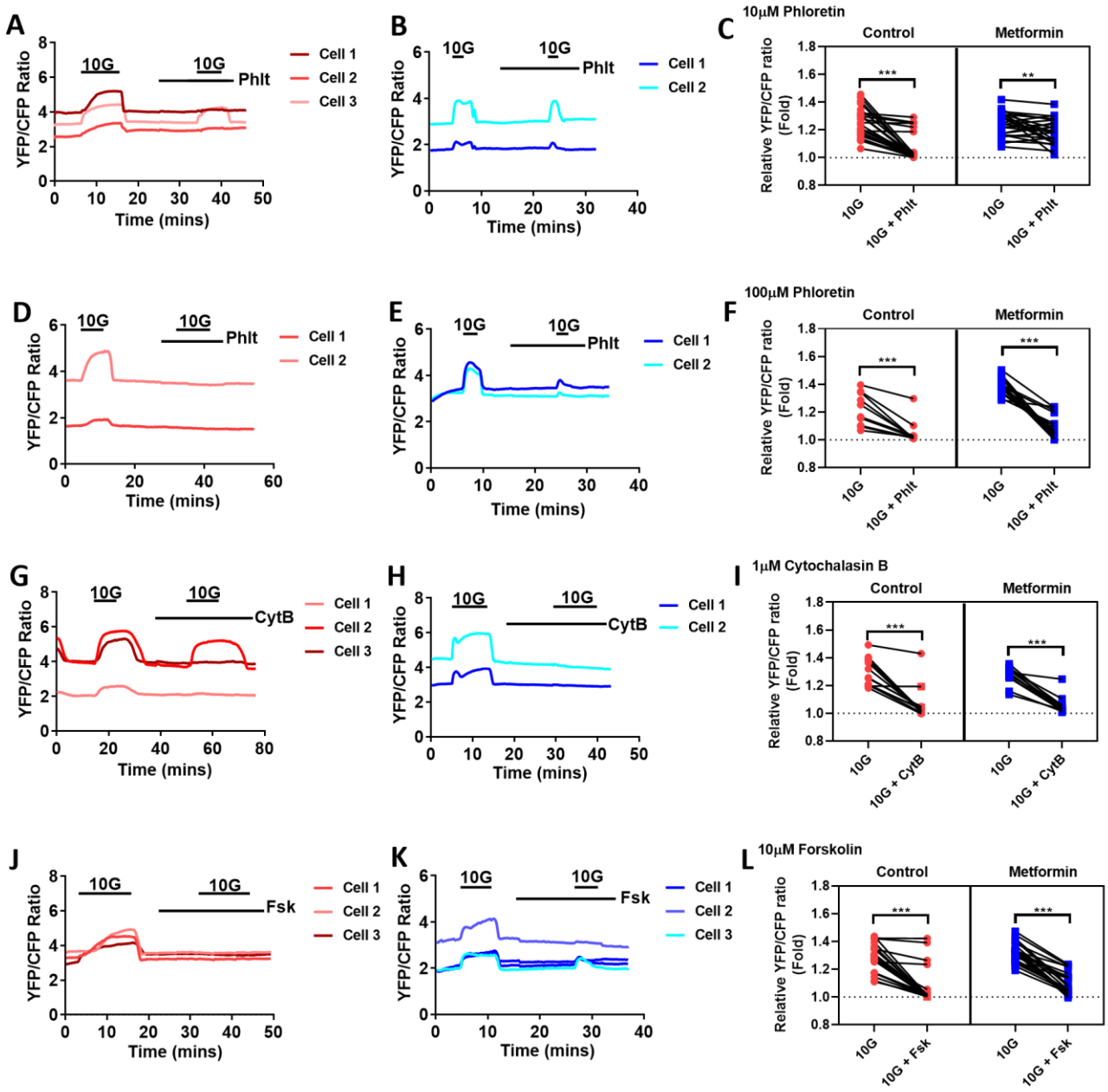

Figure 5.6. GLUT transporter inhibitors reduced glucose uptake in enterocytes. (A-B) Example traces of YFP/CFP fluorescence ratios from Control (A) and Metformin (B) treated cells. Glucose (10mM, 10G) and phloretin (10uM) were applied as indicated. (C) The effect of glucose with and without 10µM phloretin on the YFP/CFP fluorescence ratios in control (red) and metformin-treated (blue) cells normalised to the baseline (**; P<0.01, ***; P<0.001, paired T-test). Control: N= 23 cells from 9 dishes, metformin: N=24 cells from 8 dishes. (D-F) Same as A-C except where phloretin was applied at 100µM instead (***; P<0.001, paired-t-test). Control: N= 11 cells from 5 dishes, metformin: N=16 cells from 6 dishes. (G-I) Example traces of YFP/CFP fluorescence ratios from Control (A) and Metformin (B) treated cells. Glucose (10mM, 10G) and the GLUT transport inhibitor Cytochalasin B (1µM) were applied as indicated. (I) The effect of glucose with and without 1µM cytochalasin B on the YFP/CFP fluorescence ratios in control (red) and metformin-treated (blue) cells normalised to the baseline (***; P<0.001, paired T-test). Control: N= 13 cells from 4 dishes, metformin: N=15 cells from 5 dishes. (J-K) Example traces of YFP/CFP fluorescence ratios from Control (A) and Metformin (B) treated cells. Glucose (10mM, 10G) and the putative GLUT transport inhibitor Forskolin (10uM) were applied as indicated. (L) The effect of glucose with and without 10µM Forskolin on the YFP/CFP fluorescence ratios in control (red) and metformin-treated (blue) cells normalised to the baseline (***; P<0.001, paired T-test). Control: N= 23 cells from 8 dishes, metformin: N=24 cells from 9 dishes. For the example traces, different colours denote different cells as shown in the legends. Abbreviations: 10G; 10mM glucose, Phlt; Phloretin, CytB; Cytochalasin B, Fsk; Foskolin.

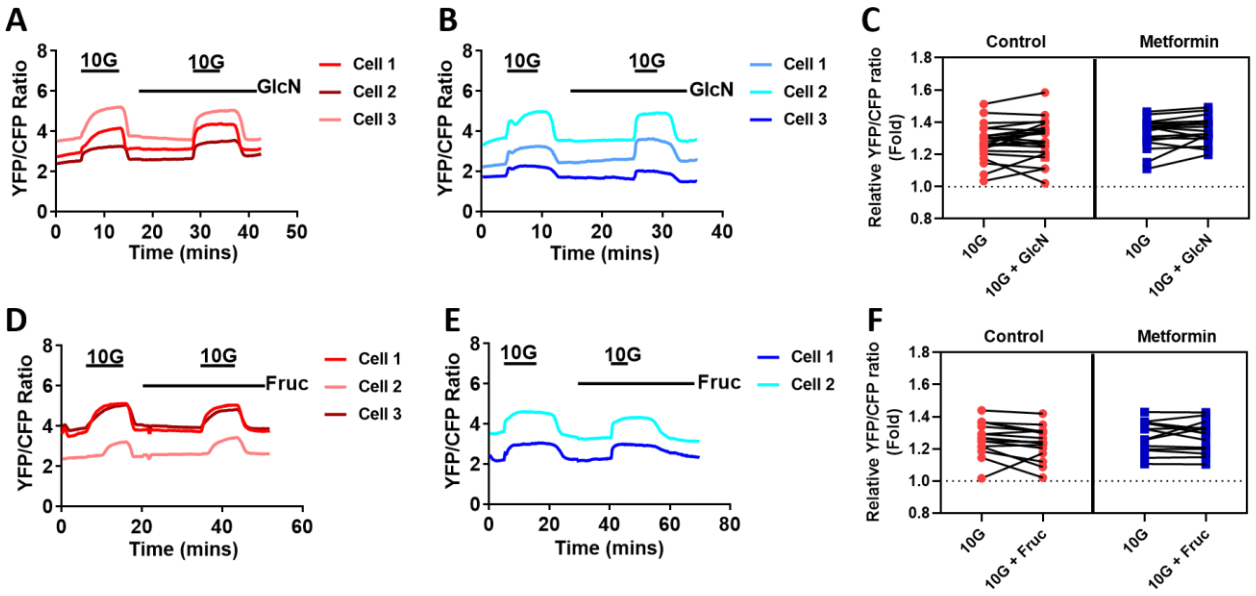

Figure 5.7. Co-application of GLUT2 substrates with glucose does not affect glucose transport. (A-B) Example traces of YFP/CFP fluorescence ratios from Control (A) and Metformin (B) treated cells. Glucose (10mM, 10G) and the high-affinity GLUT2 transporter glucosamine (10mM) were applied as indicated. (C) The effect of glucose with and without 10mM glucosamine on the YFP/CFP fluorescence ratios in control (red) and metformin-treated (blue) cells normalised to the baseline Control: N= 22 cells from 7 dishes, metformin: N=17 cells from 9 dishes. Paired T-test. (D-F) Same as A-C except where fructose was applied at 100mM instead. Control: N= 16 cells from 6 dishes, metformin: N=15 cells from 6 dishes. For the example traces, different colours denote different cells as shown in the legends. Abbreviations: 10G; 10mM glucose, GlcN; Glucosamine, Fruc; Fructose.

5.4.3 Signalling pathways involved in the regulation of glucose uptake and expression of glucose transporters by metformin

The effects of different candidate signalling pathways on the expression of glucose transporters and glucose uptake were also examined. As discussed in chapter 3, AMPK and HIF-1A signalling were identified as the candidate pathways that were most likely to influence glucose metabolism based on the RNA-seq data. The role of the AMPK signalling pathway on glucose transporter expression and glucose transport was examined by investigating the effects of treating intestinal monolayer cultures with the AMPK activator Az-991 at 1µM or 10µM concentrations for 24 hours, concentrations which have previously been reported to activate AMPK *(529, 530)*. Az-991 treatment at either concentration did not affect the expression of either *Slc5a1*, *Slc2a1*, *Slc2a2* or *Slc2a5* (Figure 5.8A-5.8D). However, the YFP/CFP ratio was modestly increased in Az-991 treated cells compared to control cells in response to 10mM glucose (Figure 5.8E-5.8G). These observations suggest that AMPK activation mediated by

metformin may increase glucose uptake at a post-translational but not at a transcriptomic level, which might be a downstream mechanism of metformin action.

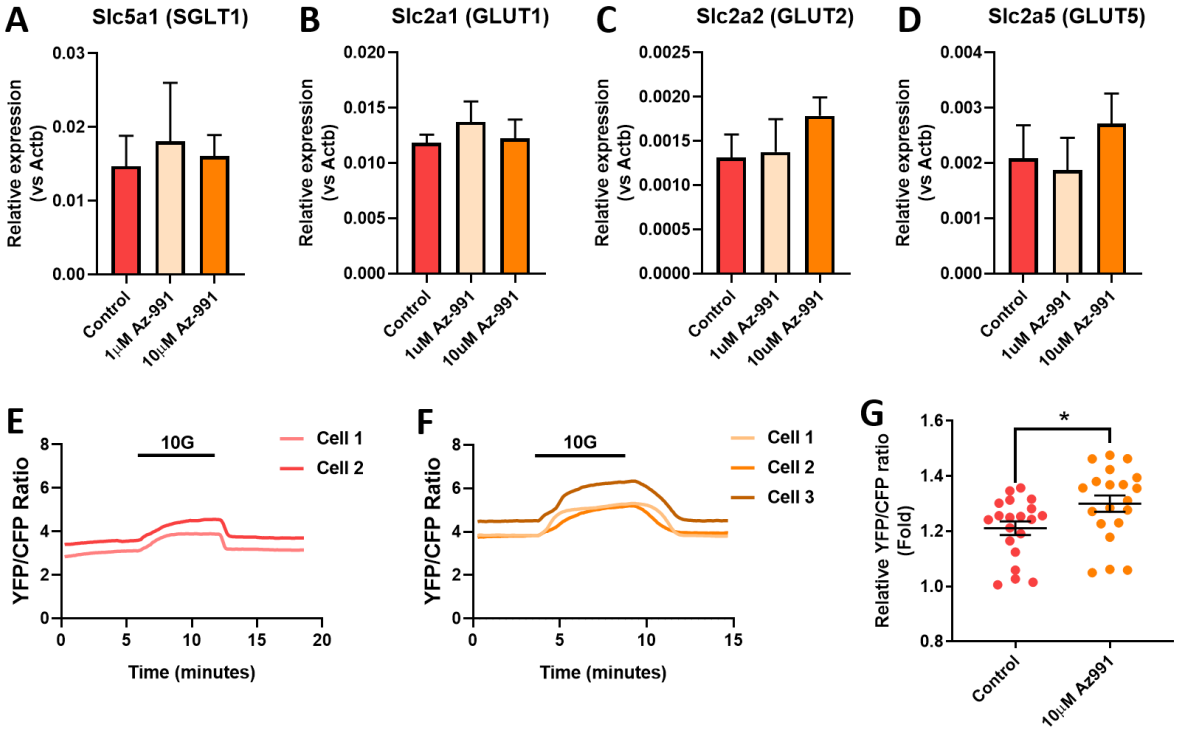

Figure 5.8. The AMPK activator AZ-991 does not affect the expression of glucose transporters but modestly increased glucose uptake. (A-D) qPCR analysis of expression of select glucose transporters in 2D duodenal organoid monolayers; (a) *Slc5a1* (SGLT1), (b) *Slc2a1* (GLUT1), (C) *Slc2a2* (GLUT2) and (D) fructose transporter *Slc2a5* (GLUT5) in response to AZ-991 pre-treatment at 1μM and 10μM for 24 hours. N=6 wells, with 3 wells assessed in parallel in 2 independent experiments. (E and F) Example traces of YFP/CFP fluorescence ratios from Control (A) and 10μM AZ-991 (B) pre-treated cells. Glucose (10mM, 10G) was applied as indicated. (G) The effect of AZ-991 on the YFP/CFP fluorescence ratios in control (red) and AZ-991-treated (orange) cells normalised to the baseline Control: N= 20 cells from 7 dishes, AZ-991: N=20 cells from 7 dishes. *, P<0.05, Two-tailed independent t-test.

The role of the HIF-1A signalling pathway on the expression of the glucose transporters was investigated using the two inhibitors, KC7F2 and NSC-134754 previously reported to inhibit metformin-stimulated GDF-15 secretion (Chapter 4, Figure 4.12). KC7F2 treatment alone decreased the expression of *Slc5a1* (Figure 5.9A), *Slc2a1* (Figure 5.9B) and *Slc2a2* (Figure 5.9C). Treatment of KC7F2 abolished the effects of metformin in inducing *Slc2a1* expression (Figure 5.9B). The expression of *Slc5a1* and *Slc2a2* were lower in metformin treated cells compared to control cells in the presence of the inhibitor (Figure 5.9A and 5.9C). Similar to KC7F2, application of NSC-134754 also decreased the expression of *Slc5a1* (Figure 5.9D), *Slc2a1* (Figure 5.9E) and *Slc2a2* (Figure 5.9F) and abolished the

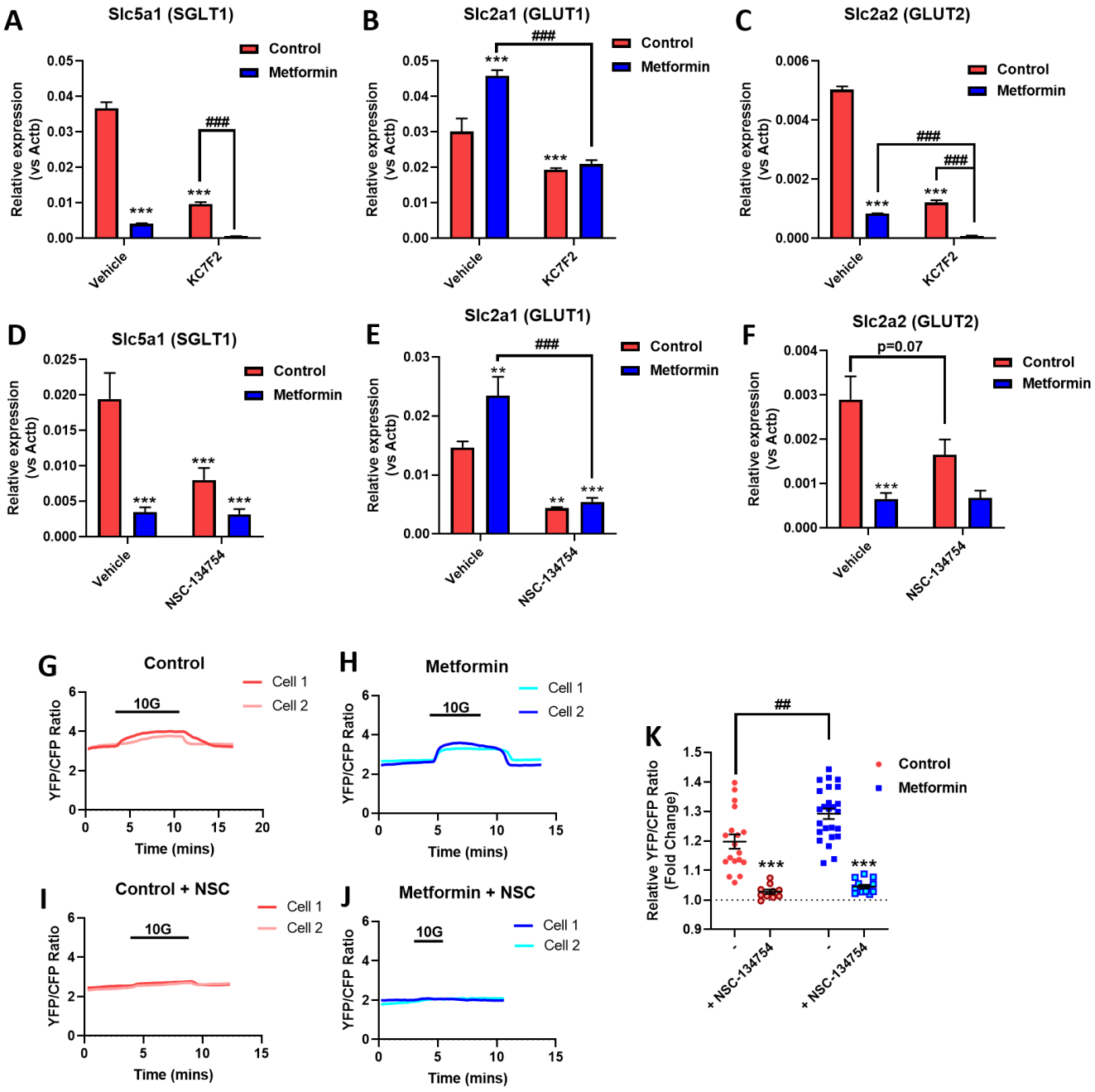

Figure 5.9. Inhibition of HIF1A decreased the expression of glucose transporters and inhibited glucose uptake. (A-F) The effect of metformin and HIF-1A translation inhibitors (A-C) 50μM KC7F2 or (D-F) NSC-134754 on *Slc5a1* (SGLT1), *Slc2a1* (GLUT1) and *Slc2a2* (GLUT2) mRNA expression in 2D duodenal organoid monolayers. KC7F2: N=3 wells from 1 experiment. NSC-134754: N=8-9 wells, with 2-3 wells assessed in parallel from 3 independent experiments. Cells were pre-treated with vehicle, KC7F2 or NSC-134754 for 1 hour, followed by co-treatment with control or 1mM metformin for 24 hours. ***, P<0.001 vs vehicle control. ###, P<0.001 vs metformin and KC7F2 or NSC-134754 co-treatment. (G-J) Example traces of YFP/CFP fluorescence ratios from Control (G), Metformin (H), Control + 10μM NSC-134754 (I) and Metformin + 10μM NSC-134754 (J) pre-treated cells. The effect of NSC-134754 on the YFP/CFP fluorescence ratios in control (red) and metformin treated (blue) cells normalised to the baseline Control: N= 18 cells from 4 dishes, Control + NSC-134754: N=10 cells from 4 dishes, Metformin: N=25 cells from 5 dishes, Metformin + NSC-134754: N=13 cells from 5 dishes. ##, P<0.01 control vs metformin vehicle. ***, P<0.001 vs vehicle control, Two-way ANOVA and Bonferroni post hoc test. Abbreviations: 10G; 10mM glucose, NSC; NSC-134754.

effects of metformin in eliciting *Slc2a1* expression (Figure 5.9E). Unlike KC7F2, NSC-134754 did not affect the expression of *Slc5a1* or *Slc2a2* in the presence of metformin (Figure 5.9D, 5.9F). This could suggest that KC7F2 might be less selective as KC7F2 is known also to affect the S6 kinase and EIF2B pathways *(464)*. These results suggest that the HIF-1A pathway plays a role in inducing *Slc2a1* expression by metformin, but the changes in the expression of *Slc5a1* or *Slc2a2* mediated by metformin might be mediated by other, as yet to be identified pathways.

To investigate the effects of the HIF-1A signalling on glucose uptake, intestinal cultures transfected with the FRET-based glucose sensor were pre-treated with and without metformin and/or NSC-134754 for 24 hours. NSC-134754 markedly reduced glucose uptake in both control and metformin treated cells and abolished the differences in glucose uptake between control and metformin treated cells (Figure 5.9G-5.9K). These observations suggest that glucose uptake is controlled by the HIF-1A signalling pathway.

5.4.4 The effects of metformin on the mRNA expression of glucose transporters in intestinal tissues of HFD-fed mice

To confirm that the effects of metformin on the expression of glucose transporters were not exclusive to an intestinal monolayer culture system, the effects of metformin on the mRNA expression of glucose transporters in different tissue segments of the small intestine and colon were investigated using the HFD-fed mouse model. Oral dosing of metformin for 6 hours decreased the expression of *Slc5a1* in the lower small intestine, but not the upper or middle small intestinal tissues (Figure 5.10A-5.10C). Metformin also increased *Slc2a1* expression in the lower small intestine ($p=0.05$) but no significant changes were observed in the upper or middle small intestine or the colon (Figure 5.10D-5.10G). Similarly, metformin decreased *Slc2a2* expression in the upper and lower small intestine, although there was a trend towards decreased expression in the middle small intestine, and the expression was very low in the colon (Figure 5.10H-5.10K).

Similarly, long-term oral treatment with metformin for 11 days also reduced *Slc5a1* mRNA expression in the lower, but not the upper or middle small intestine segments (Figure 11A-5.11C). Metformin also significantly increased the expression of *Slc2a1* in the lower small intestine but not in the small intestinal tissues from other regions (Figure 5.11D-5.11G). Metformin decreased the expression of *Slc2a2* in the middle small intestine, and there was a trend towards decreased expression in the lower small intestine, whereas transcript expression was not affected in the upper small intestine or the colon (Figure 5.11H-5.11K).

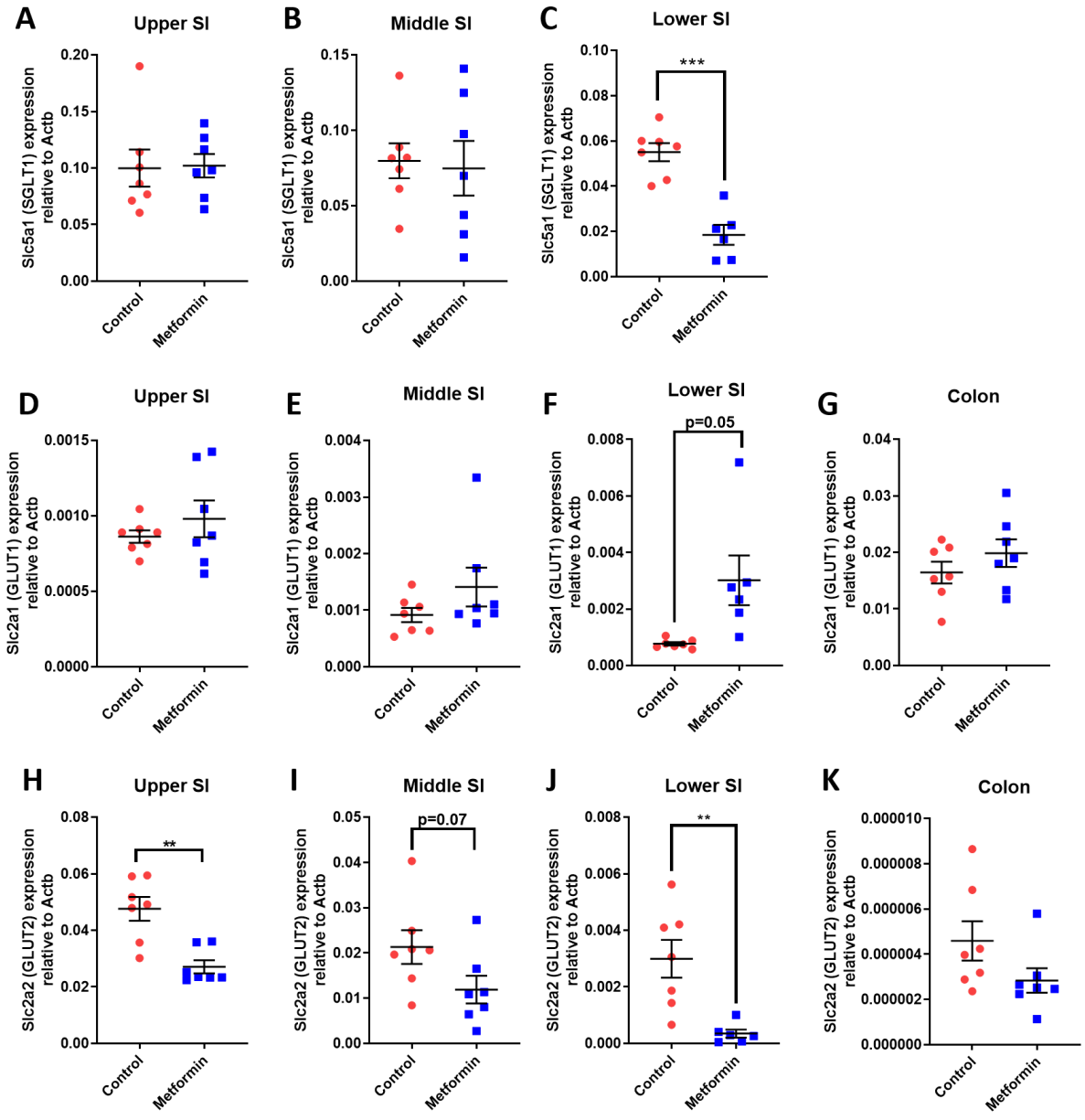

Figure 5.10. The effects of a single dose of metformin (600mg/kg) on the expression of glucose transporters in the small intestinal tissues of HFD-mice after 6 hours. (A-C) The effects of metformin on the mRNA expression of *Slc5a1* (SGLT1) in the (A) upper small intestine (SI), (B) middle SI and (C) lower SI. (D-G) The effects of metformin on the mRNA expression of *Slc2a1* (GLUT1) in the (D) upper SI, (E) middle SI, (F) lower SI and (G) colon. (H-K) The effects of metformin on the mRNA expression of *Slc2a2* (GLUT2) in the (H) upper SI, (I) middle SI, (J) lower SI and (K) colon. mRNA analysis of fresh frozen tissue normalised to expression levels of b-actin (Actb). N=6 mice per group. *, P<0.05, **, P<0.01, ***, P<0.001. mRNA analysis of fresh frozen tissue normalised to expression levels of b-actin (Actb). Abbreviations: SI; Small Intestine.

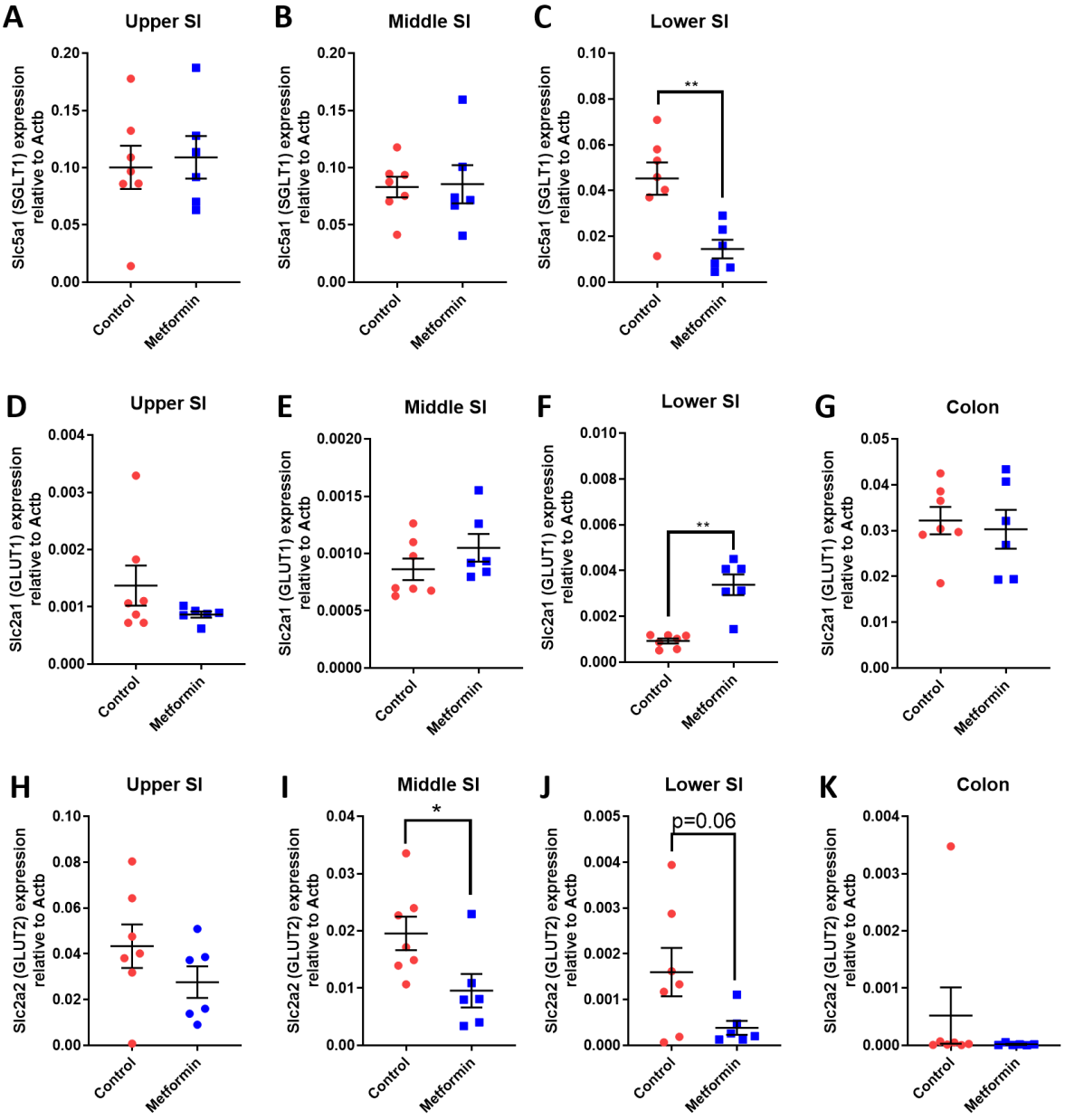

Figure 5.11. The effects of once daily oral metformin administration (300mg/kg) on the expression of glucose transporters in the small intestinal tissues of HFD-mice after 11 days. (A-C) The effects of metformin on the mRNA expression of *Slc5a1* (SGLT1) in the (A) upper small intestine (SI), (B) middle SI and (C) lower SI. (D-G) The effects of metformin on the mRNA expression of *Slc2a1* (GLUT1) in the (D) upper SI, (E) middle SI, (F) lower SI and (G) colon. (H-K) The effects of metformin on the mRNA expression of *Slc2a2* (GLUT2) in the (H) upper SI, (I) middle SI, (J) lower SI and (K) colon. mRNA analysis of fresh frozen tissue normalised to expression levels of b-actin (Actb). N=6-7 mice per group (7 control, 6 metformin). *, P<0.05, **, P<0.01. mRNA analysis of fresh frozen tissue normalised to expression levels of b-actin (Actb). Abbreviations: SI; Small Intestine.

The results demonstrated that metformin treatment for either 6 hours or 11 days altered the expression of glucose transporters in the distal intestine in a similar manner to that observed in intestinal 2D monolayer cultures.

5.5 Discussion

5.5.1 Does metformin increase basal glucose uptake by upregulating GLUT1 transporters?

To date, the number of studies reporting the cellular effects of metformin on glucose uptake have been limited, even though observations from multiple studies established that oral metformin administration dramatically increased intestinal glucose uptake and utilisation in rodents and humans *(237, 364, 490, 517–519)*. This study examines the cellular mechanisms by which metformin increases glucose uptake and changes the expression of glucose transporters in the small intestine.

The expression and functional studies presented in this study suggest that metformin increases GLUT1 mediated glucose transport. These were supported by several lines of evidence. First, from the RNA-seq and qPCR studies of the different expression of glucose transporters, the *Slc2a1* gene encoding GLUT1 was amongst the highest in expression and was the only gene from the GLUT family of transporters upregulated by metformin treatment in both duodenal and ileal organoids, whereas the expression of other glucose transporters were either decreased or not affected by metformin treatment (Figure 5.1 and 5.2). Second, live-cell imaging studies using a FRET-based glucose sensor demonstrated that metformin increased the uptake of glucose that was inhibited by multiple GLUT transport inhibitors, particularly inhibitors with a preferential inhibition for GLUT1, GLUT3 and GLUT4 over GLUT2, whereas inhibition of SGLT1 did not affect glucose uptake (Figure 5.4 and 5.6). Finally, glucosamine and fructose previously reported to be transported by GLUT2 did not alter glucose uptake, which could suggest that glucose uptake mediated by GLUT2 in intestinal cells is relatively unimportant (Figure 5.7). However, it should be acknowledged that there were no positive controls available to confirm that these GLUT2 co-substrates exhibit any competitive inhibition of glucose uptake, which could be confirmed in the future by using cell lines that overexpress GLUT2. Future experiments could involve transgenic knockout of GLUT1 in intestinal organoids to verify the role of GLUT1 in glucose uptake.

A recent study investigating the arterial-venous exchange of metabolites in pigs demonstrated that the gut consumes the largest quantities of glucose compared with other organs, establishing the importance of the gut as a "glucose sink" *(186)*. However, the mechanisms involved in the basolateral uptake of glucose from the blood into intestinal epithelial cells are not known, despite well-established knowledge that SGLT1 and GLUT2 are involved in the transepithelial absorption of glucose. Two key glucose transporters are expressed in the basolateral membrane of intestinal epithelial cells; GLUT1 and GLUT2, whereas SGLT1 is only expressed in the apical membrane of enterocytes that have apical-basolateral polarity *(492, 509, 510)*. This could explain why the SGLT transport inhibitor phloridzin did not affect glucose uptake in the intestinal 2D monolayers, which loses its apical-basal polarity when seeded onto a matrigel-coated surface. Alternatively, the transport capacity of SGLT1 could be much lower than GLUT1. Previous experiments demonstrated that expression of GLUT1 transporters in the GI tract is low in comparison with the expression of the transepithelial glucose transporters GLUT2 and SGLT1 in the small intestine, although no functional studies were performed in that study regarding the contribution of GLUT1 on basolateral glucose uptake *(509)*. However, it should be noted that GLUT1 is a high affinity (with a Km value of ~1.5mM) but low capacity transporter, whereas GLUT2 is a low affinity (with a Km value of ~17mM) and high capacity transporter *(497)*. This seems to suggest that GLUT1 could play a more important role in mediating glucose transport from the blood into intestinal epithelial cells compared to GLUT2, considering that the physiological concentrations of glucose in the blood are ~5-6mM.

Furthermore, GLUT1 is overexpressed in the alimentary limb after RYGB surgery and has been reported to mediate increased intestinal glucose utilisation, along with adaptive changes such as hypertrophy and transcriptomic changes in glucose metabolism genes *(42, 43)*. Similarly, GLUT1 gene expression was also increased in rats following sleeve-gastrectomy with duodenojejunal bypass *(511)*. From the experiments performed on HFD-fed mice, oral metformin administration for 6 hours or 11 days increased the expression of *Slc2a1* in the distal small intestine, which could provide further evidence that metformin increases glucose uptake by upregulating GLUT1 transporters (Figure 5.10 and 5.11). These experiments suggest that upregulating the GLUT1 transporter and increasing basal uptake of glucose in the intestine may be shared mechanisms of bariatric surgery and metformin in achieving the glucose lowering effects.

5.5.2 The effect of metformin on the expression of other glucose transporters

Although metformin has been reported to affect intestinal glucose absorption, the cellular mechanisms that explain this effect are unclear and often contradictory. An early study investigated

the effects of metformin on the expression of intestinal glucose transporters, revealing that oral metformin treatment in rats for 3 days increased the abundance of SGLT1 in the duodenum and jejunum, and GLUT5 in the jejunum, whilst the expression of GLUT2 was unaltered *(531)*. A separate study demonstrated that acute administration of metformin (for 3 minutes) in intraluminal intestinal loops decreased the abundance of SGLT-1 protein associated with AMPK activation and decreased short circuit currents in acute metformin treated tissues as measured by Ussing chamber experiments *(523)*. Observations reported by other groups studying the effects of the AMPK activator AICAR also argued that AMPK activation by metformin increases the abundance GLUT2 protein in the brush border membranes associated with AMPK activation *(523, 524)*. Similarly, studies in insulin-resistant animal models argue for the case that GLUT2 is translocated to the brush border of enterocytes to allow glucose flux from the blood into the intestinal lumen *(505, 523)*. However, the evidence regarding apical GLUT2 translocation is by itself conflicting as other studies could not replicate these observations *(491, 492)*. A recent investigation by Bauer *et al.,* reported that metformin increases SGLT-1 mediated glucose sensing in the small intestine by altering the composition of the microbiota, which was associated with improved glucose sensing and increased GLP-1 secretion, further complicating the molecular mechanisms of metformin action on glucose absorption *(251)*.

The data presented in this study demonstrated that metformin treatment decreased the expression of both *Slc5a1* (SGLT1) and *Slc2a2* (GLUT2) in intestinal cells from the 2D organoid monolayer model system (Figure 5.1 and 5.2) and the distal small intestinal tissues of HFD-fed mice treated with metformin for 6 hours or 11 days (although *Slc2a2* expression was also decreased in the tissues from the middle small intestine as well) (Figure 5.10 and 5.11). The limitation of the intestinal 2D monolayer culture model should be acknowledged, as the lack of apical-basolateral polarity of intestinal cells in culture limits the ability to study transepithelial glucose transport. However, numerous other studies in mice have also reported that oral metformin use decreases the absorption of glucose and increases the transit of glucose down the small intestine *(234–236, 488, 489)*. Furthermore, various pharmacogenetic studies demonstrate that a "reduced function" genetic variant for *Slc2a2* (rs8192675) was associated with a modestly greater effect of metformin on glycaemic control *(129, 130)*. Although *Slc2a2* is the predominant glucose transporter in hepatocytes (involved in release of glucose produced from gluconeogenesis) and was therefore the main focus in one of the studies *(129)*, reduced *Slc2a2* function could also affect the ability of the gut to absorb glucose which may also contribute to the effects of metformin on glycaemic control. Future studies should examine the effect of metformin on transepithelial glucose transport in cells plated in transwell inserts, which have the advantage of retaining apical-basolateral polarity of intestinal cells.

It should be acknowledged from the experiments in HFD-fed mice that metformin only altered the expression of the glucose transporters (especially *Slc5a1* and *Slc2a1*) in the distal small intestine, whereas the effects in other intestinal regions were highly variable (Figure 5.10 and 5.11). These regional differences are likely to be explained by variations of metformin biodistribution in the GI tract as opposed to differences in metformin action in different regions of the intestinal tract. Studies by Wilcock and Bailey demonstrated that metformin accumulates at the highest concentrations in the distal small intestine compared to other intestinal regions after metformin oral gavage in mice *(312)*. The observations that metformin can also induce similar expression changes in duodenal organoids from 2D monolayers at millimolar concentrations also suggest that metformin concentrations in the intestinal tissues underlie the expression changes in glucose transporters.

In the RNA-sequencing data and confirmation from RT-qPCR in intestinal cultures, metformin also decreased the expression of *Slc2a5* (GLUT5), the predominant transporter for fructose *(514)*. As discussed in chapter 3, metformin also decreased the expression of fructose metabolism genes, *Khk*, *Aldob* and *Tkfc* (Figure 3.6). This provides further evidence from the expression data that fructose uptake and metabolism could be decreased by metformin treatment, which requires functional validation in future studies. Furthermore, metformin also decreased the expression of *Slc2a7* (GLUT7), a recently characterised glucose transporter expressed in the apical membranes of the small intestine which has a high affinity for glucose and fructose, although its role in intestinal glucose uptake is not known *(515)*.

5.5.3 The contributions of the AMPK and HIF-1A signalling pathways to glucose transport changes mediated by metformin

Metformin is known to cause the activation of AMPK, which was postulated to be the initial candidate signalling pathway that regulates glucose uptake by metformin *(210)*. Indeed, studies in skeletal muscle have reported that metformin increases glucose uptake via an AMPK-dependent mechanism involving the translocation of GLUT4 vesicles to the cell membrane *(340)*. This study reports that treatment with the AMPK activator AZ-991 for 24 hours did not alter the mRNA expression of the glucose transporters that were altered in expression by metformin, but modestly increased glucose uptake (Figure 5.8). Although *Slc2a1* has previously been identified as a target gene that was upregulated by the AMPK-dependent arm of metformin in hepatocytes *(365)*, this study and others suggest that the effects of AMPK are translational or post-translational in intestinal cells. Furthermore, our RNA-seq data demonstrated that genes encoding vesicle trafficking proteins potentially responsible for the translocation of glucose transporters to the cell membrane, *Rab10* and *Rab14*,

were upregulated in metformin treated cultures (Chapter 3, Figure 3.13). Of note, this study did not investigate whether metformin increases AMPK activation in the intestinal cultures, although previous studies have reported that metformin increases AMPK phosphorylation in intestinal cells/tissues in vitro and ex vivo *(264, 378, 523)*.

Since HIF-1A signalling activation is associated with transcriptional upregulation of genes encoding glucose transporters and glycolysis, this prompted further investigations into the effects of inhibiting HIF-1A on the expression of glucose transporter transcripts. Supporting the RNA-seq data, the results showed that pharmacological inhibition of HIF-1A abolished the effects of metformin on *Slc2a1* expression, but not *Slc2a2* or *Slc5a1* expression (Figure 5.9). Similarly, imaging studies of intracellular glucose concentrations demonstrate that the HIF-1A inhibitor NSC-134754 markedly attenuated glucose uptake in both control and metformin treated cells, suggesting that the HIF-1A signalling pathway is essential for maintenance of glucose uptake pathways (Figure 5.9). This also provides another indirect line of evidence that glucose uptake is mediated by GLUT1, since NSC-134754 abolished any effects of metformin on glucose uptake, similar to its effects on *Slc2a1* expression. Also, *Slc2a1* is the bona fide target gene of the HIF-1A signalling pathway, upregulation of which drives glycolysis in cancer cells *(532, 533)*.

Interestingly, inhibition of HIF-1A also decreased the expression of *Slc5a1* and *Slc2a2* in control cultures (Figure 5.9). Although reduced *Slc2a2* expression has previously been reported in isolated islets derived from HIF-1A knockout mouse (and therefore pharmacological inhibition of HIF-1A in this study achieved the same effect in intestinal cells) *(534)*, the mechanisms that regulate *Slc5a1* transcript expression are unclear. The observations that metformin altered the mRNA expression of transporters at millimolar concentrations could potentially suggest a mitochondrial dependent mechanism, since metformin is known to only inhibit complex I activity at millimolar concentrations *(204, 205)*.

A role of HIF-1A was also demonstrated in experiments involving bariatric surgery *(42, 43)*. Mouse models that had undergone RYGB surgery exhibited transcriptomic changes in HIF-1A and many of its target genes in the alimentary limb, which was responsible for the effects of increased glucose utilisation and intestinal hypertrophy post-surgery *(43)*. The results from this study suggest that the HIF-1A signalling pathway is important in the effects of metformin and may share a similar mechanism to RYGB surgery in increasing intestinal glucose utilisation.

5.5.4 Conclusions

This study describes a potential cellular mechanism that supports the effects of metformin on glucose utilisation and absorption in the GI tract. High concentrations of metformin increased the expression of Slc2a1 (GLUT1) and increased glucose uptake in intestinal cells, which may explain the increased glucose utilisation by the small intestine in mice and humans. This mechanism could be mediated by the AMPK and especially HIF-1A signalling pathways. Future experiments should investigate the functional effects of AMPK and HIF-1A modulators in mouse models via glucose tolerance tests. In addition, metformin also decreased the expression of *Slc2a2* (GLUT2) and *Slc5a1* (SGLT1) by an unknown mechanism, which could potentially contribute to the effects of metformin in decreasing intestinal glucose absorption in other studies.

Chapter 6: Metformin and nutrient metabolism in intestinal cells

6.1 Summary

Intestinal nutrient metabolism has a major influence on whole-body energy expenditure *(175)*. Since orally administered metformin is more effective at glycaemic control than intravenous administration *(319)*, and metformin accumulates at high concentrations inside intestinal cells *(312, 315)*, it is speculated that the actions of metformin on intestinal metabolism would greatly contribute to its effects as a glucose-lowering agent. However, knowledge into effects of metformin and nutrient metabolism in intestinal cells is still limited, since much of the existing literature were previously reported in liver and cancer cells *(116, 240)*. This chapter examines the effects of metformin on nutrient metabolism in intestinal cells using extracellular flux analyser assays and live-cell imaging of metabolites.

6.2 Background

6.2.1 Nutrient metabolism in intestinal cells

The small intestine is highly metabolically active to sustain the energy demanding processes of nutrient digestion and absorption *(175, 176)*. Earlier studies have identified glucose and glutamine as the main sources of fuel utilised by intestinal cells *(177–185)*. Intestinal glucose metabolism is responsible for 15% and 30% of CO_2 production from luminal and arterial sources, respectively *(180)*. Carbon tracer studies demonstrated that intestinal cells are highly glycolytic, with most of the glucose metabolised to produce lactate or alanine *(535)*, whilst only ~10% of glucose is oxidised in the mitochondria *(177)*. Glutamine is reported to be a more important fuel; its oxidation is responsible for 35% and 52-70% of total CO_2 production during postabsorptive and fasting states, respectively *(177, 180)*. Glutamine is an important substrate for the generation of alanine through alanine aminotransferases, as well as other amino acids such as proline and citrulline *(178, 179, 536)*, with some studies arguing that glutamine is an important substrate for intestinal gluconeogenesis *(179, 386, 535)*. The intestine has been demonstrated to also be capable of metabolising ketone bodies *(177, 181, 182, 536)* , fatty acids *(177, 537–539)* and fructose *(391)*.

Recent studies demonstrated that nutrient metabolism is heterogeneous amongst different cell types along the crypt-villus axis *(150, 187–189)*. Intestinal organoids grown under high Wnt conditions (to model intestinal stem cells) were more reliant on glycolysis than organoids grown in standard medium

(150). Inhibitors of mitochondrial function *(150)* or using an intestine-selective HSP60 knockout mouse model that causes mitochondrial dysfunction *(485)* disrupted intestinal differentiation, demonstrating that mitochondrial respiration is a feature of more differentiated cells. Measurements of NADH lifetime distribution of cells along the crypt-villus axis similarly confirmed that intestinal stem cells are highly glycolytic, whilst terminally differentiated villus cells require mitochondrial oxidation *(189)*. Intestinal organoids with impaired mitochondrial pyruvate metabolism *(187)*, impaired fatty acid oxidation *(188)* or glutamine deprivation *(540)* displayed reduced intestinal crypt expansion and organoid formation. These observations were also supported by proteomic analyses of the crypt-villus axis in the intestines of neonatal piglets, which demonstrated increased expression of proteins involved in the tricarboxylic acid (TCA) cycle, fatty acid and amino acid oxidation in the villus factions compared to the crypts *(541)*. These studies highlighted that, in contrast to earlier studies, fuel metabolism are heterogeneous and defines different intestinal cell types along the crypt-villus axis.

6.2.2 Cellular mechanisms of metformin on nutrient metabolism

At the cellular level, metformin accumulates at high concentrations in the mitochondria compared to other cellular compartments *(201)*. Previous studies extensively focussed on the inhibition of complex I (NADH dehydrogenase) of the mitochondrial electron transport chain to attenuate oxidative phosphorylation, although much of these effects were studied at high concentrations of metformin *(201–204)*. Other studies also reported that metformin inhibited other aspects of mitochondrial bioenergetics such as uncoupled respiration *(205)* or ATP-synthase activity *(201)*. Metabolic tracing studies from cancer cells demonstrated that metformin reduced flux of TCA cycle intermediates responsible for oxidative metabolism *(205, 206)*. As a result of inhibiting mitochondrial respiration, metformin indirectly increases lactate production from glycolysis in a variety of cell types *(59, 64, 207, 208)*. A recent study of whole-body metabolism in HFD-fed mice reported reduced whole-body glucose oxidation (calculated as the changes in respiratory quotient values as measured by indirect calorimetry in response to oral gavage) during an early response to a single oral metformin gavage, whilst increasing the amount of non-oxidised glucose *(236)*. This translates the cellular effects of metformin in inhibiting mitochondrial respiration/glucose oxidation to an in vivo setting.

The evidence associating metformin and hepatic gluconeogenesis is controversial. Earlier studies in rodent and humans support the hypothesis that metformin mediates its glucose-lowering effects by inhibiting hepatic gluconeogenesis *(220, 225–227)*. The mechanisms involved is still disputed. Madiraju *et al.,* demonstrated that low-dose metformin directly inhibited the mitochondrial glycerolphosphate dehydrogenase involved in the glycerolphosphate shuttle, which suppressed hepatic gluconeogenesis from lactate and glycerol (but not pyruvate or alanine) sources in a redox dependent manner *(225, 226)*. Other studies demonstrate that metformin decreased hepatic

gluconeogenesis by inhibiting fructose 1,6-bisphosphatase (FBP-1) *(542)*, or by decreasing glycogen cycling *(389, 543, 544)*. However, some of the recent studies challenge this mechanism to show that metformin increases endogenous glucose production in Carbon-14 tracer experiments on liver samples from HFD-fed mouse models and in patients with recent onset type-2 diabetes *(207, 228)*.

Due to AMPK activation, metformin also suppresses lipogenesis and increase fatty acid oxidation (FAO) *(210, 211, 229, 230)*. Several studies have demonstrated that metformin inhibits the activity of Acetyl-CoA carboxylase (ACC) to promote FAO, as well as inhibiting the expression of SREBP-1 and fatty acid synthase (Fasn) to suppress lipogenesis in hepatocytes *(210, 211, 233, 545)*. The effects of metformin in promoting FAO despite inhibiting mitochondrial respiration seem paradoxical (since FAO is dependent on mitochondrial respiration). However, Gonzalez-Barroso *et al.,* demonstrated that metformin did not inhibit palmitate oxidation in 3T2-L1 adipocytes, despite inhibiting basal oxygen consumption, increasing extracellular acidification and activating AMPK *(545)*. The mechanisms underlying the permissive effect of metformin on FAO remain elusive.

6.2.3 Metformin and intestinal nutrient metabolism

Metformin accumulates at milimole concentrations within intestinal cells despite micromolar concentrations present in plasma *(312, 315, 394)*. Metformin decreases mitochondrial function in intestinal cells, as oral administration decreased the NADH/NAD+ ratio in the intestinal mucosa of HFD mice *(207)* and reduced oxygen consumption in intestinal organoids *(546)*. Several ex vivo and in vivo studies performed in rodents demonstrated that metformin increased intestinal glucose utilisation and lactate release into the splanchnic bed as a result from inhibiting mitochondrial respiration *(64, 116, 207, 239–242, 312)*.

6.3 Aims

This chapter investigates the effects of metformin on nutrient metabolism to complement the observations that metformin increases glucose uptake in intestinal cells from the previous chapter. The aims of this study are:

1. To examine the role of metformin in glycolysis and glucose oxidation in intestinal cells
2. To investigate the mechanisms of metformin in maintaining glycolysis
3. To examine the role of the mitochondria in pyruvate and glutamine oxidation in intestinal cells
4. To assess the effect of metformin on the endogenous metabolism of glycogen and fatty acids

6.4 Results

All metformin (1mM) treatments were overnight (18-28 hours) prior to imaging experiments or for 24 hours prior to Seahorse and lactate measurements.

6.4.1 Metformin decreases glucose oxidation but maximises glycolysis in intestinal cells

To assess the effects of metformin on glucose oxidation and confirm that metformin inhibits mitochondrial respiration in intestinal cells, the mitochondrial stress test was performed using the Seahorse flux bioanalyser in the presence of glucose (10mM) in the Seahorse media. Oxygen consumption was consistently lower in metformin treated cells in comparison to control cells, even in the presence of mitochondrial respiration inhibitors; oligomycin (ATP-synthase inhibitor), FCCP (proton uncoupler) and Rotenone/Antimycin A (Complex I and III inhibitors, respectively) (Figure 6.1A). Metformin treatment reduced basal, maximal, ATP-linked and uncoupled oxygen consumption rate, whilst the respiratory reserve was unaffected (Figure 6.1B). This confirms that metformin inhibits mitochondrial glucose metabolism (Figure 6.1B).

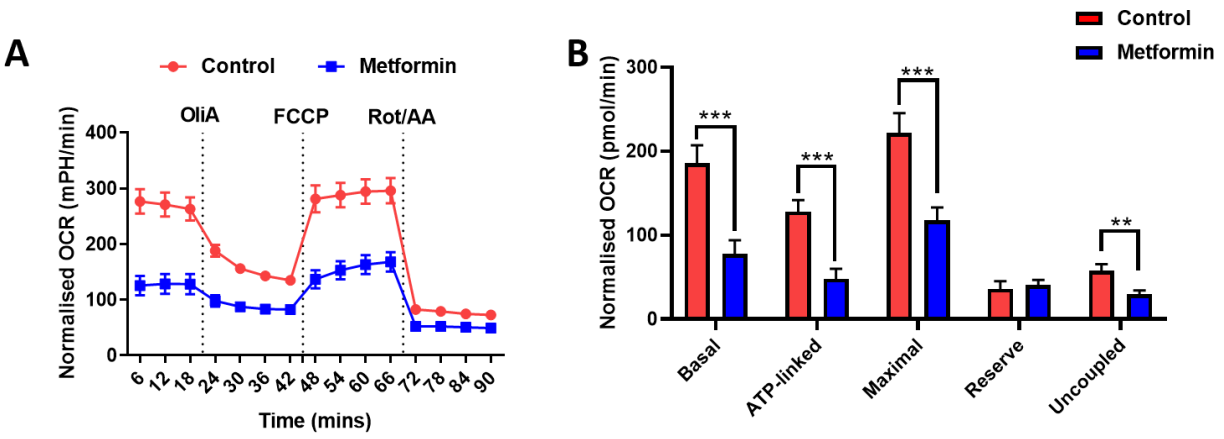

Figure 6.1. Metformin decreases glucose oxidation in intestinal cells. (A) Changes in oxygen consumption rate (OCR) over time during the mitochondrial stress test in which intestinal cells were previously treated with control or without metformin for 24 hours. Cells were incubated with glucose (10mM) in XF basal media for 1 hour prior to measurements. Dotted lines indicate when a compound was added. Oligomycin-A (OliA, 1µM), FCCP (1µM), Rotenone/Antimycin A (Rot/AA, 1µM each). (B) The effect of metformin on the measured parameters. The methods on how the parameters were calculated are described in detail in chapter 2, section 2.7. N=4-5 wells from 4 independent experiments. ***; P<0.001. Two-way ANOVA and Bonferroni post-hoc test.

To support the observations from the mitochondrial stress test, the effects of metformin on the cellular redox state was studied by live-cell imaging of NAD(P)H and FAD autofluorescence. Previous studies have demonstrated that NAD(P)H autofluorescence is dominated by mitochondrial, as opposed to cytosolic NADH *(547–550)*. Glucose increases NADH generation through TCA-cycle oxidation, whilst decreasing FAD autofluorescence mediated by succinate metabolism in the TCA cycle *(551, 552)*. The proton uncoupler FCCP was used as a positive control, as depletion of the mitochondrial membrane potential by FCCP maximises fuel oxidation and electron transport chain activity, thereby forcing the mitochondria to oxidise NADH to NAD+ and oxidise FADH2 to FAD *(327, 553)*. Glucose simultaneously increased NAD(P)H and reduced FAD autofluorescence in control cells, respectively, which was reversed in the presence of FCCP (Figure 6.2A, 6.2C 6.2D). Metformin pre-treatment significantly diminished the effects of glucose and FCCP on NAD(P)H and FAD autofluorescence (Figure 6.2B, 6.2C and 6.2D). This is consistent with metformin impairing mitochondrial function through redox metabolism.

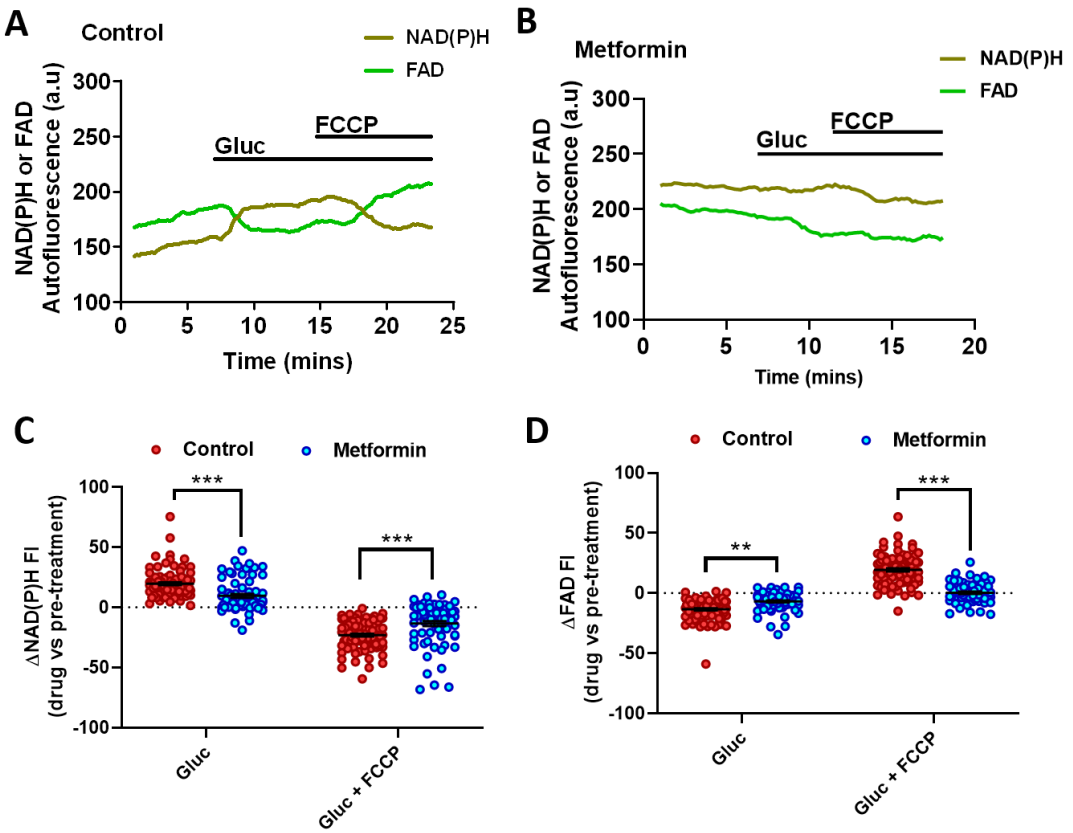

Figure 6.2. The effect of metformin on the redox state in intestinal cells. (A and B) Example traces of NAD(P)H (yellow) and FAD (green) autofluorescence measurements in control (A) and metformin (B) treated cells. (C and D) The effect of control (red dots) and metformin (blue dots) on NAD(P)H (C) and FAD (D) autofluorescence in the presence of glucose (Gluc, 10mM) with or without FCCP (1µM). Each dot denotes one cell. N= 92 cells (control) and 70 cells (metformin), experiments from 4 dishes. **; P<0.01, ***; P<0.001, Two-way ANOVA and Bonferroni post-hoc test.

A glycolytic stress test was performed to assess the glycolysis parameters of intestinal cells by measuring pH changes in the media to calculate the extracellular acidification rate (ECAR) (see chapter 2, section 2.7 for methods). Metformin treated cultures increased glycolysis, and abolished the glycolytic reserve, suggested by the fact that they were unable to further increase glycolytic flux as measured by ECAR upon oligomycin addition (Figure 6.3A and 6.3B). Metformin also modestly increased the glycolytic capacity; the maximum cellular capacity to undergo glycolysis (Figure 6.3B) *(554)*. Note that this appeared in part to be a consequence of a lower non-glycolytic acidification (changes in ECAR prior to glucose addition, thus not attributed to glycolysis and thought to be a consequence of CO_2 production in the citric acid cycle) in the metformin-treated cells compared to control cells, although this did not reach statistical significance (Figure 6.3B). The results suggest that metformin increased glycolysis consequent to inhibiting mitochondrial respiration.

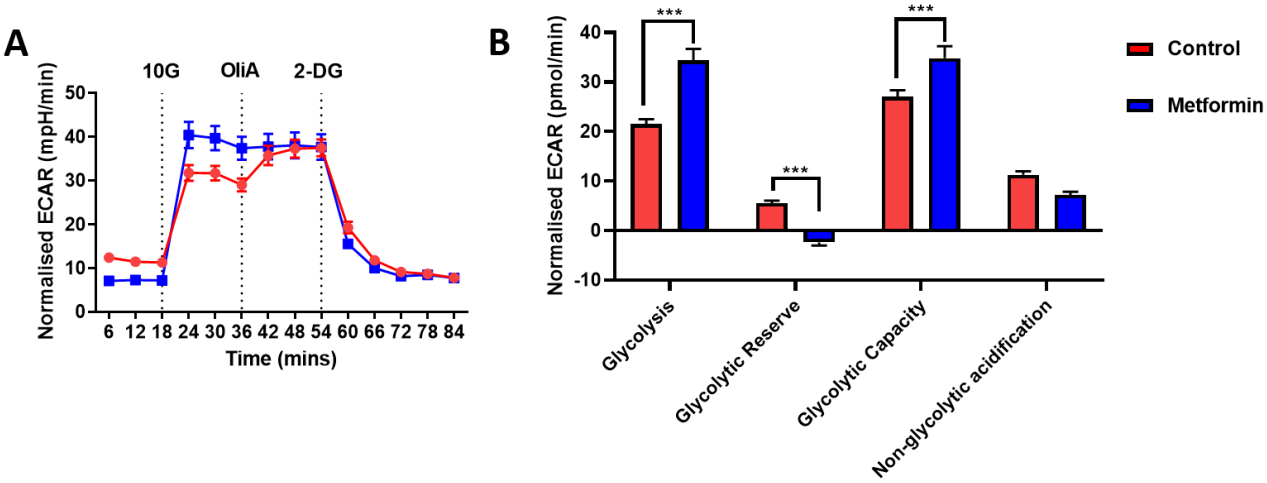

Figure 6.3 Metformin increases intestinal glycolysis to its maximal capacity. (A) Changes in extracellular acidification rate (ECAR) over time during the glycolytic stress test wherein intestinal cells were previously treated with control or with 1mM metformin for 24 hours. Dotted lines indicate when a compound was added: Gluc; glucose (10mM), OliA; oligomycin-A (1µM), 2-DG; 2-deoxyglucose (50mM). (B) The effect of metformin on the measured parameters of the glycolysis stress test. The methods on how the parameters were calculated are described in detail in Chapter 2, section 2.7. N=10 wells from 3 independent experiments. NS; not significant. ***; P<0.001. Two-way ANOVA and Bonferroni post-hoc test.

The effects of metformin on ATP generation from glucose metabolism was monitored via live-cell imaging of intestinal cells transfected with the fluorescent ATP sensor PercevalHR. Each glycolysis reaction produces a net 2 molecules of ATP for each molecule of glucose, whilst glucose oxidation produce ~36 molecules of ATP (Figure 6.4A). Changes in Perceval fluorescence was observed only in 21/26 of control cells in response to washout of glucose with saline (Figure 6.4B-6.4D), whilst all of the cells treated with metformin responded, indicating that metformin pre-treatment robustly

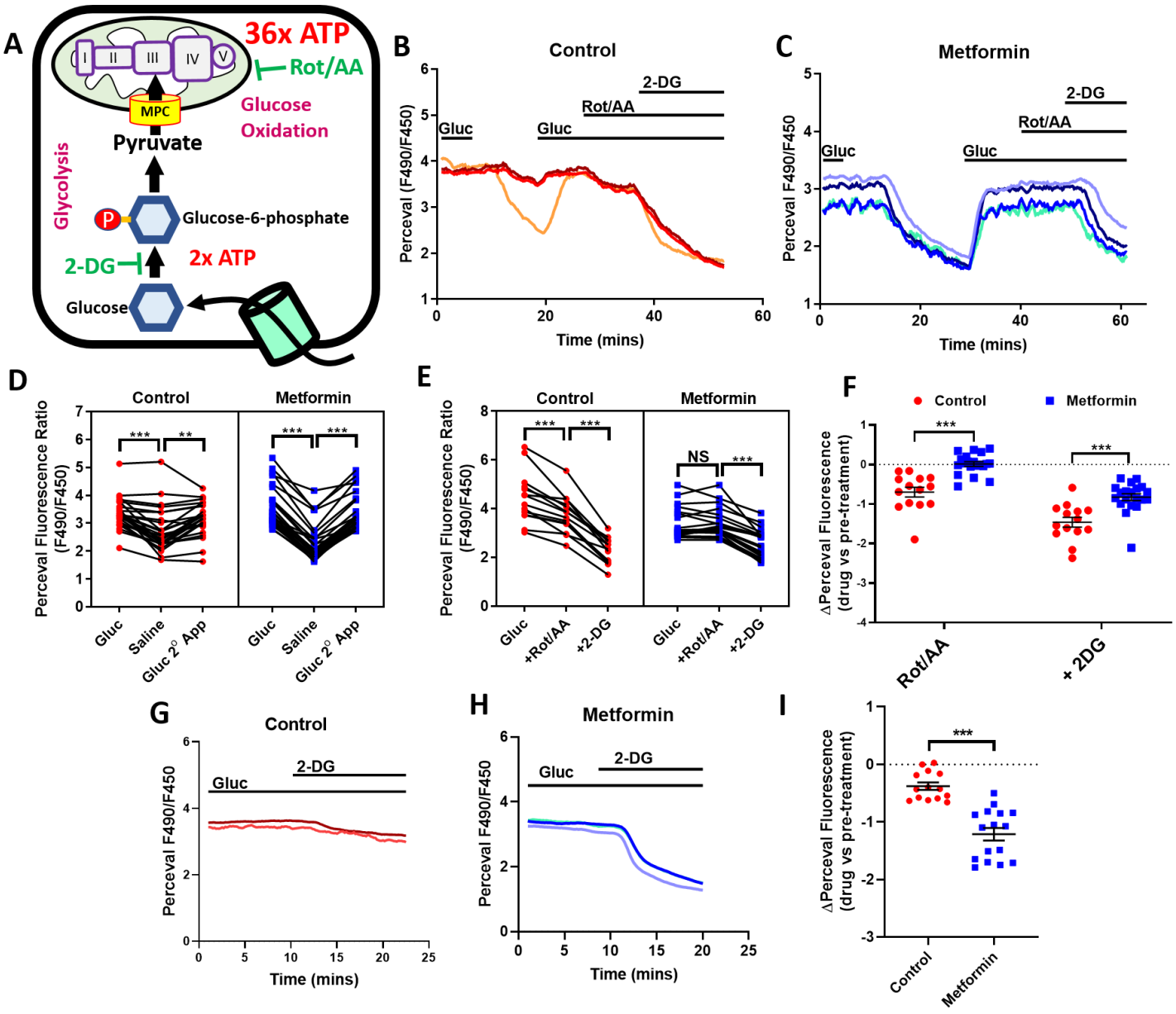

Figure 6.4. Metformin inhibits ATP generation from glucose oxidation but increases glycolytic ATP production.
(A) Schematic showing the effects of rotenone and antimycin A (Rot and AA respectively) and 2-deoxyglucose (2-DG) on cellular ATP generation. (B and C) Example traces of Perceval fluorescence ratios from Control (B) and Metformin (C) treated cells. The treatments glucose (Gluc, 10mM), Rot/AA (1µM) and 2-DG (50mM) were applied as indicated. Different coloured lines denote responses from different cells. (D) Measured Perceval fluorescence ratios in control (red) and metformin-treated (blue) cells where glucose was switched to saline and re-applied. **; P<0.01, ***; P<0.001, control: Friedman test and Dunn's post-hoc test, N=24 cells from 9 dishes, metformin: Repeated-measures ANOVA and Bonferroni post-hoc test, N=24 cells from 8 dishes). (E) The effect of 10mM glucose (Gluc), Rot/AA and 2-DG on the Perceval fluorescence ratios in control (red) and metformin-treated (blue) cells (***; P<0.001, Repeated-measures ANOVA and Bonferroni post-hoc test. Control: N=14 from 5 dishes, metformin: N=20 cells from 4 dishes). (F) Rot/AA decreased Perceval fluorescence in control cells, not metformin-treated cells. (***; P<0.001, Repeated measures Two-way ANOVA.). (G and H) Example traces of Perceval fluorescence ratios from Control (G) and Metformin (H) treated cells in response to 2-DG alone. Different coloured lines denote responses from different cells. (I) 2-DG significantly decreased Perceval fluorescence in metformin treated cells relative to control cells. ***; P<0.001, student's t-test. Control; N=14 from 4 dishes and metformin; N=17 from 4 dishes).

increased ATP generation from glucose metabolism (Figure 6.4B-6.4D). The contribution of glucose oxidation in glycolytic ATP generation was assessed with rotenone and antimycin A (Rot/AA). Rot/AA decreased Perceval fluorescence ratio in control cells but was without a significant effect on metformin treated cells (Figure 6.4E and 6.4F). Subsequent exposure to 2-DG on top of Rot/AA markedly decreased Perceval fluorescence, to a larger extent in control than in metformin treated cells (Figure 6.4E-6.4F). Exposure to 2-DG alone in the presence of glucose decreased the Perceval fluorescence in metformin treated cells more than the control (Figure 6.4G-6.4I), confirming that metformin treated cells rely on glycolytic ATP production, whereas control cells show greater metabolic flexibility, presumably oxidising an alternative fuel to buffer ATP production through mitochondrial respiration.

6.4.2 Metformin increases glycolytic metabolism of pyruvate towards lactate and alanine

Lactate production could influence glycolysis in two ways: (1) The forward lactate dehydrogenase reaction regenerates NAD+ that is required to maintain glycolysis and (2) lactate production causes intracellular acidification which reduces the glycolysis rate by inhibiting phosphofructokinase, thus necessitating functional monocarboxylate transporters (MCTs) for lactate efflux *(549, 555, 556)*. The competitive LDH inhibitor Oxamate, and high affinity MCT inhibitors AR-C155858 (MCT1/2 blocker) *(557)* and Syrosingopine (MCT1/4 blocker) *(556)* were used to study the pyruvate-lactate metabolism pathway (Figure 6.5A). Metformin pre-treatment increased lactate secretion in the intestinal cultures in the presence of 10mM glucose, whilst inhibition of LDH by Oxamate or inhibition of MCTs by AR-C155858 and Syrosingopine partially reduced the lactate secretion response elicited by metformin (Figure 6.5B). Unexpectedly, metformin treatment significantly, but modestly decreased LDH activity, which likely reflects lower LDH levels (Figure 6.5C). The effects of these inhibitors on the cytosolic NAD+/NADH ratio was also investigated by live-cell imaging of cells transfected with the Peredox sensor. In control cells, Oxamate application did not elicit notable changes in the Peredox fluorescence, but significantly increased Peredox fluorescence in metformin pre-cultured cells (Figure 6.5D). Similarly, application of MCT inhibitors AR-C155858 and Syrosingopine elicit increased Peredox fluorescence in metformin pre-cultured cells than control cells, although this did not reach statistical significance (Figure 6.5E).

Similar observations were also observed in the Perceval imaging experiments to observe the effects of the inhibitors on intracellular ATP. Oxamate did not affect Perceval fluorescence in the presence of glucose in control cells, but significantly decreased Perceval fluorescence in metformin treated cells (Figure 6.6A). Combined AR-C155858 and Syrosingopine treatment modestly decreased Perceval

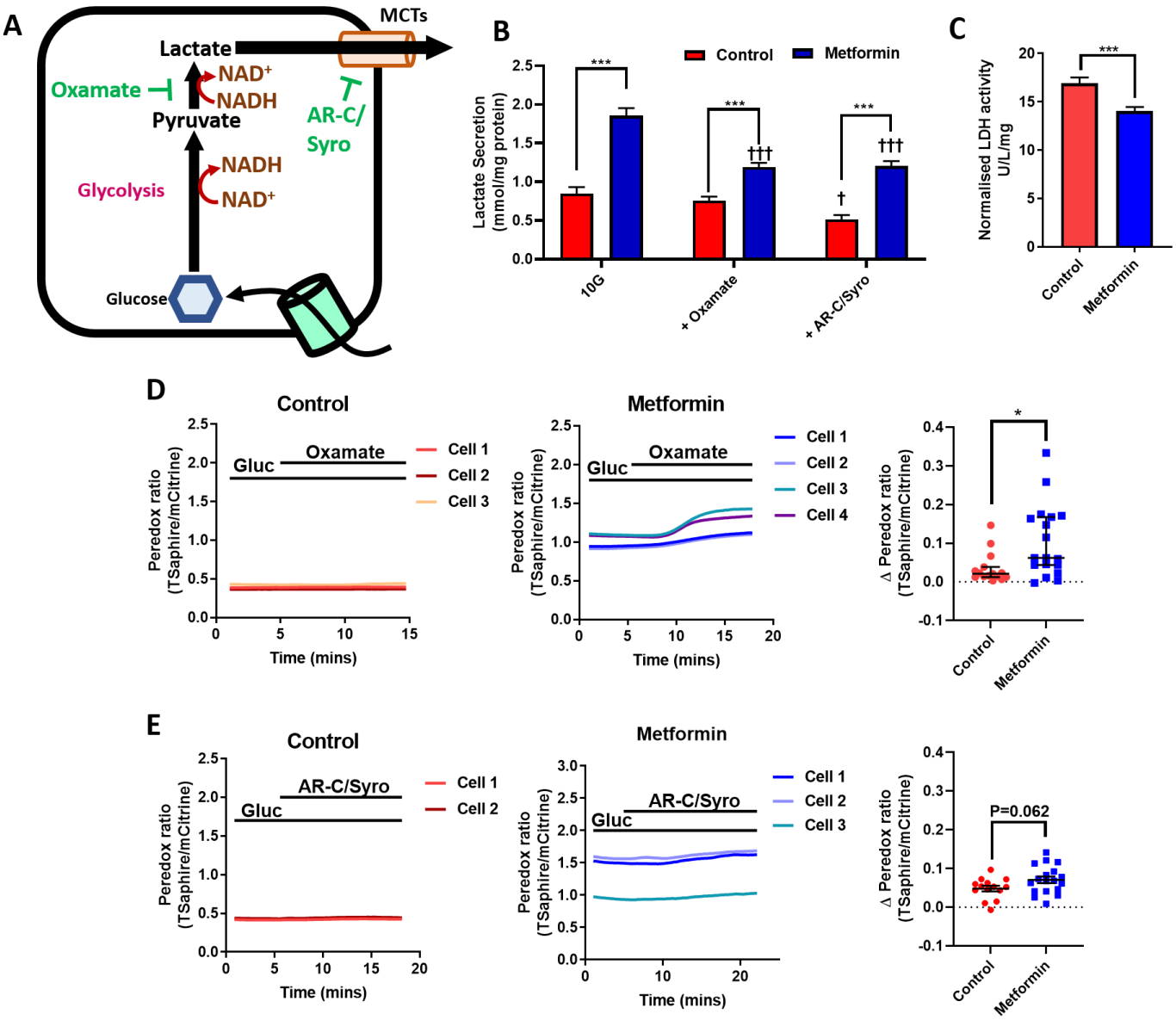

Figure 6.5. The effect of metformin on lactate production, LDH activity and Peredox fluorescence elicited by lactate metabolism/transport inhibitors (A) Schematic showing the effects of the LDH inhibitor Oxamate and MCT inhibitors AR-C155858 (MCT1 and MCT2) and Syrosingopine (MCT1 and MCT4) on glycolysis pathway. (B) Lactate secretion levels in control and metformin pre-treated cultures in glucose (10mM, 10G), with oxamate (50mM) or AR-C155858 (AR-C, 10µM) and Syrosingopine (Syro, 50µM). Error bars are mean ± SEM. *; P<0.05, **; P<0.01, ***; P<0.001, vs control. †††; P<0.001 vs pre-treated conditions in 10G. Two-way ANOVA and Bonferroni post-hoc test. N=2-3 wells from 4 independent experiments except AR-C/Syro, where 3 independent experiments were performed. (C) LDH activity in control and metformin treated cultures. Error bars are mean ± SEM. ***; P<0.001, vs control. Independent t test. N=3 wells from 4 independent experiments. (D) The effects of oxamate on Peredox fluorescence in Control (red) and Metformin (blue) treated cells. Glucose (Gluc, 10mM) and oxamate (50mM) were applied as indicated. Different coloured lines denote responses from different cells. Error bars are median ± confidence intervals. *; P<0.05, Mann-Whitney test. Control: N= 15 cells from 4 dishes; Metformin: N=18 cells from 4 dishes. (E) The effects of AR-C155858 and Syrosingopine on Peredox fluorescence in Control (red) and Metformin (blue) treated cells. Glucose (Gluc, 10mM), AR-C155858 (10µM) and Syrosingopine (50µM) were applied as indicated. Different coloured lines denote responses from different cells. Error bars are mean ± SEM. Control: N= 14 cells from 4 dishes; Metformin: N=19 cells from 4 dishes. Independent t-test.

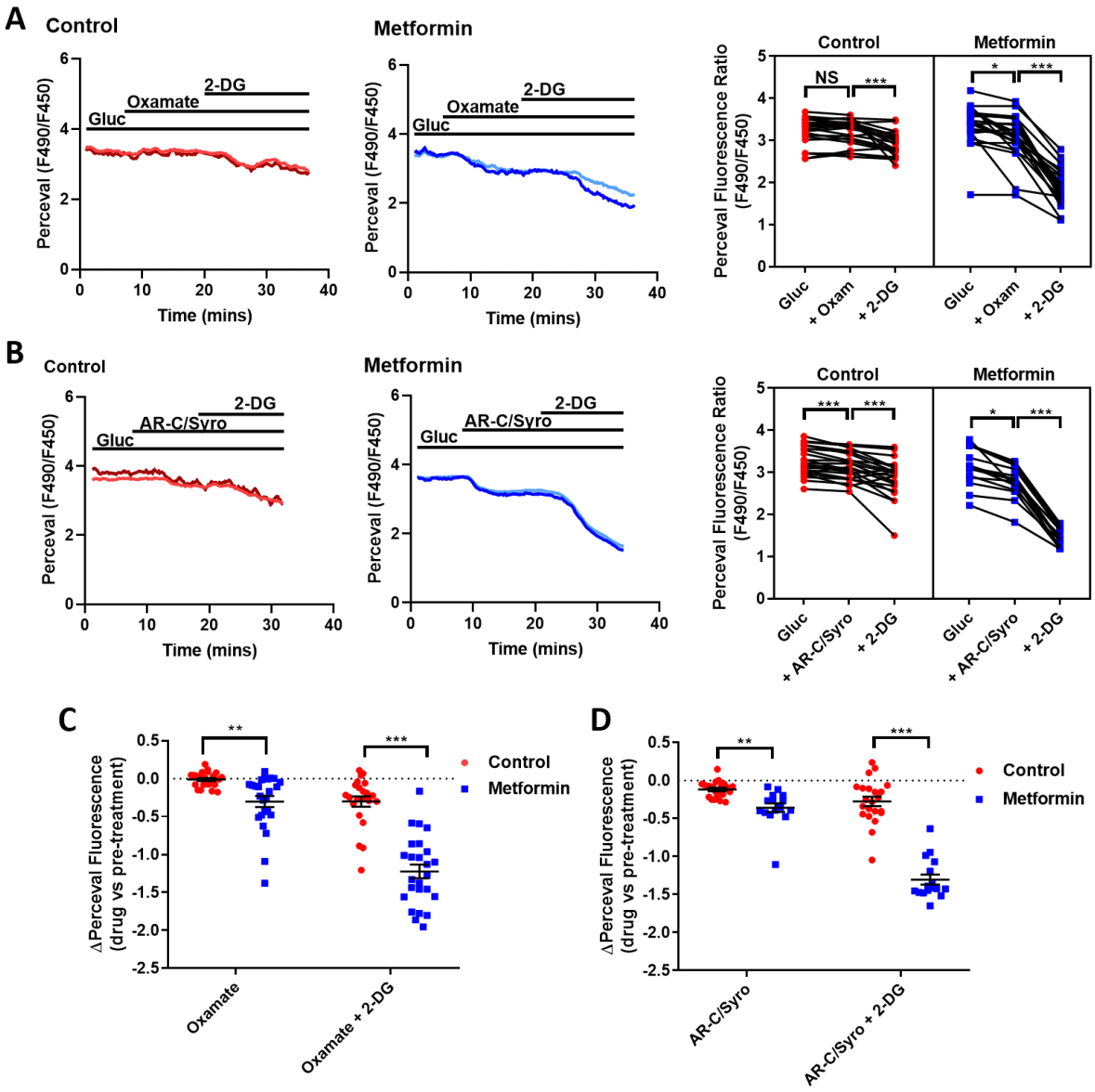

Figure 6.6. Inhibiting lactate production and transport decreases Perceval fluorescence but does not completely inhibit glycolysis in metformin treated cells. (A) The effects of oxamate on Perceval fluorescence in Control (red) and Metformin (blue) treated cells. Glucose (Gluc, 10mM), oxamate (50mM) and 2-DG (50mM) were applied as indicated. Different coloured lines denote responses from different cells. Control: N=23 cells from 6 dishes; metformin: N=25 cells from 6 dishes. (B) The effects of MCT inhibitors AR-C155858 and Syrosingopine on Perceval fluorescence in Control (red) and Metformin (blue) treated cells. The treatments glucose (Gluc, 10mM), AR-C155858 (AR-C, 10µM), Syrosingopine (Syro, 50µM) and 2-DG (50mM) were applied as indicated. Different coloured lines denote responses from different cells. Control: N=22 cells from 6 dishes; metformin: N=16 cells from 5 dishes. For A and B: repeated measures ANOVA and Bonferroni post hoc test or Friedman test with Dunn's post-hoc test (if normality is not passed) for before-after comparisons. (C and D) Oxamate (C) and MCT inhibitors (D) decreased Perceval fluorescence more profoundly in metformin treated cells than control cells. For C and D, Error bars are mean ± SEM. **; P<0.01, ***; P<0.001, two-way ANOVA and Bonferroni post-hoc test.

fluorescence in control cells, but the effects were more profound in metformin treated cells (Figure 6.6B). 2-DG further decreased Perceval fluorescence in both control and metformin treated cells independent of the inhibitors (Figure 6.6C, 6.6D). This could be due to incomplete inhibition of glycolysis by the LDH and MCT inhibitors, or that glycolysis could be sustained by the metabolism of pyruvate to alanine or other alternative pathways.

Aspartate and alanine transaminases are also involved in glycolysis; aspartate transaminases are involved in the malate aspartate shuttle, another mechanism that regenerates cytosolic NAD+ (whilst mitochondrial NAD+ is simultaneously reduced), whereas alanine transaminases are involved in the metabolism of pyruvate to alanine. Particularly, alanine aminotransferases are expressed and functionally important in intestinal cells *(535, 558)* and both transaminases were upregulated by metformin treatment in monolayer cultures (See chapter 3). The activities of aspartate (AST) and alanine (ALT) transaminases were increased in metformin pre-treated cultures (Figure 6.7A and 6.7B). Aminooxyacetate (AOA), a broad-spectrum aminotransferase inhibitor, was used to examine changes in perceval fluorescence in metformin-treated cells (Figure 6.7C). Application of AOA decreased Perceval fluorescence in metformin-treated cells more so than control cells, although this was not statistically significant (Figure 6.7D, P=0.06). To distinguish the contribution of alanine transaminases from aspartate transaminases, Perceval fluorescence was monitored upon application of the selective alanine-aminotransferase inhibitor β-chloro-L-alanine (βCLA) and AOA sequentially (see Figure 6.7C for schematic). βCLA similarly decreased Perceval fluorescence in metformin, but not control cells (Figure 6.7E). Subsequent AOA application weakly reduced Perceval fluorescence, whilst 2-DG further decreased Perceval fluorescence independent of the inhibitors (Figure 6.7E). These observations suggest that despite increased activity of alanine and aspartate transaminases, alanine aminotransferases but not aspartate transaminases may contribute to glycolytic ATP production despite not being essential to maintain glycolysis.

Further evidence against an important role of the malate-aspartate shuttle in glycolytic ATP production was demonstrated by Perceval fluorescence measurements involving the oxoglutarate-glutamate transporter inhibitor phenylsuccinate. Application of phenylsuccinate did not differently affect the Perceval fluorescence between control and metformin pre-treated cells (Figure 6.8A and 6.8C). The roles of the glycerolphosphate shuttle in Perceval fluorescence was also investigated, since the conversion of glycerol-3-phosphate (G3P) to dihydroxyacetone phosphate (DHAP) by cytosolic glycerolphosphate dehydrogenase (GPDH) also regenerates cytosolic NAD+ (but also requiring mitochondrial FAD metabolism). 100μM concentrations of the putative glycerolphosphate shuttle inhibitor iGP-1 did not affect the Perceval fluorescence produced from glycolysis in control and

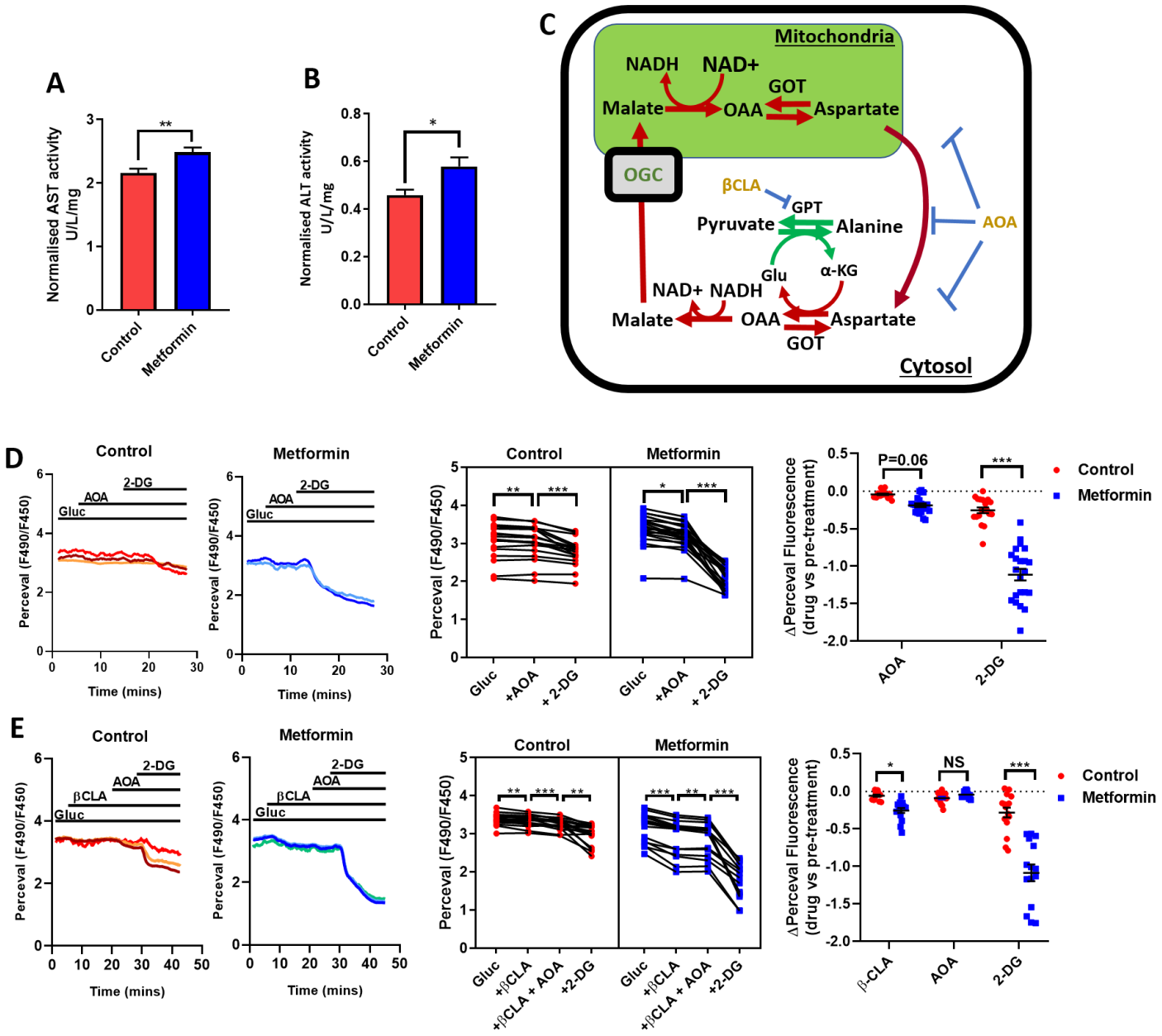

Figure 6.7. The effect of metformin on alanine and aspartate transaminases in intestinal cells. (A) Aspartate transaminase (AST, or GOT) and (B) Alanine transaminase (ALT or GPT) activity in control and metformin treated cultures. Error bars are mean ± SEM. **; P<0.01, *; P<0.05, vs control. Independent t test. N=3 wells from 4 independent experiments. (C) Schematic showing the effects of transaminase inhibitors Aminooxyacetate (AOA) and β-chloro-L-alanine (βCLA) on metabolic pathways. (D) The effects of AOA on Perceval fluorescence in Control (red) and Metformin (blue) treated cells. Glucose (Gluc, 10mM), AOA (10mM) and 2-DG (50mM) were applied as indicated on the traces. Different coloured lines denote responses from different cells. Control: N=19 from 4 dishes, metformin: N=22 cells from 3 dishes. (E) Distinguishing alanine aminotransferase from aspartate aminotransferase activity on Perceval fluorescence in control (red) and metformin (blue) treated cells. Glucose (Gluc, 10mM), βCLA (1mM), AOA (10mM) and 2-DG (50mM) were applied as indicated. Control: N=16 from 3 dishes, Metformin: N=15 cells from 3 dishes. *; P<0.05, **; P<0.01, ***; P<0.001. Error bars are means ± SEM. Repeated measures ANOVA and Bonferroni post hoc test or Friedman test with Dunn's post-hoc test (if normality is not passed) for before-after comparisons between different treatments, two-way ANOVA and Bonferroni post-hoc test for ΔPerceval Fluorescence comparisons between control and metformin.

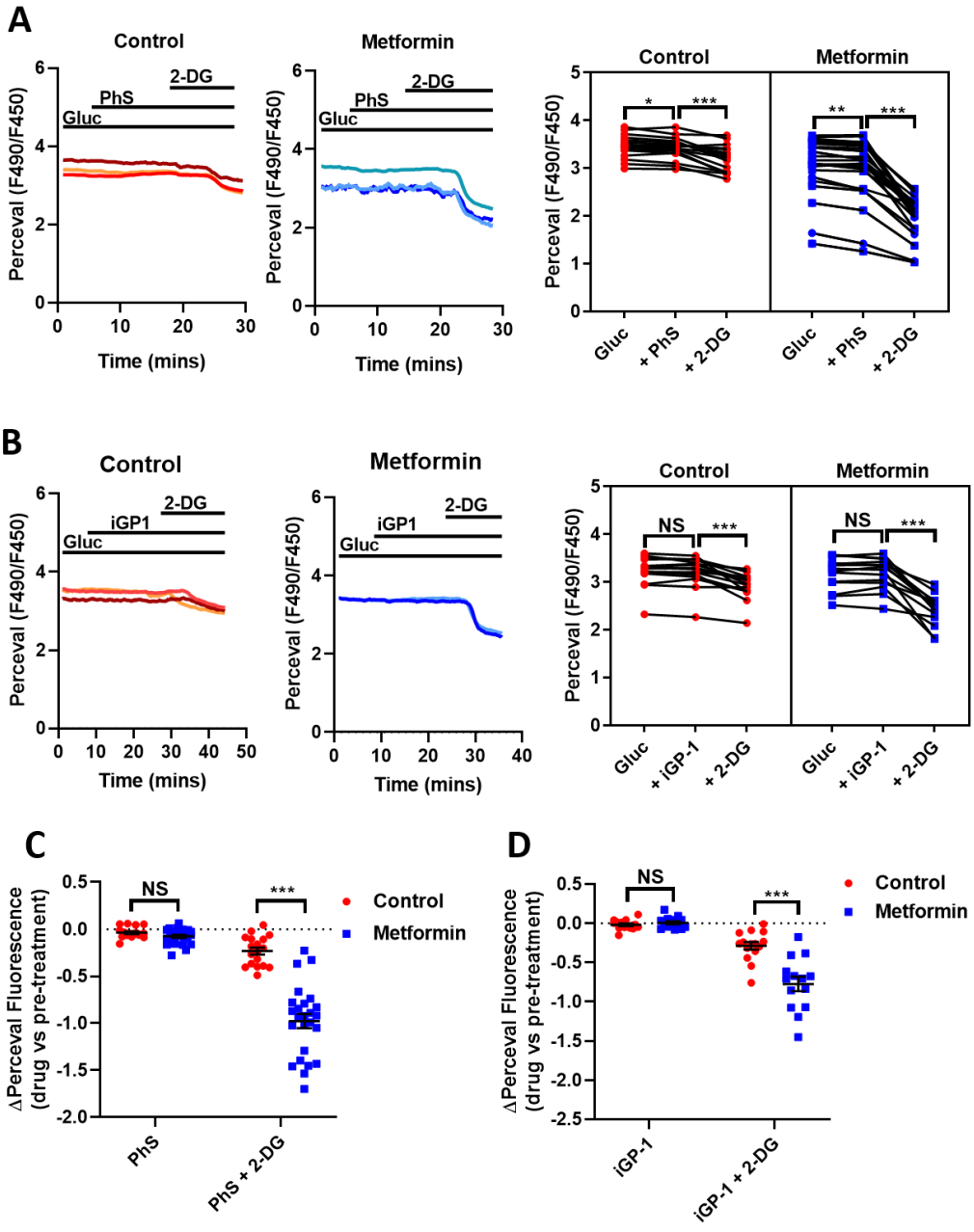

Figure 6.8. Inhibitors of the malate aspartate shuttle and glycerolphosphate shuttle does not affect Perceval fluorescence. (A) The effects of the oxoglutarate-glutamate transport inhibitor Phenylsuccinate (PhS) on Perceval fluorescence in Control (red) and Metformin (blue) treated cells. Glucose (Gluc, 10mM), Phenylsuccinate (10mM) and 2-DG (50mM) were applied as indicated. Control: N=18 from 4 dishes, metformin: N=33 cells from 5 dishes. Repeated-measures ANOVA and Bonferroni post-hoc test.(B) The effects of the mitochondrial glycerolphosphate dehydrogenase inhibitor iGP1 on Perceval fluorescence in Control (red) and Metformin (blue) treated cells. Glucose (Gluc, 10mM), iGP1 (100µM) and 2-DG (50mM) were applied as indicated on the traces. Different coloured lines denote responses from different cells. Control: N= 15 cells from 5 dishes, metformin: N=14 cells from 4 dishes. NS; not significant. ***; P<0.001, Repeated-measures ANOVA and Bonferroni post-hoc test. (C and D) Changes in Perceval fluorescence in control and metformin treated cells to PhS (C) or iGP-1 (D) and 2-DG. NS; not significant, ***; P<0.001, Two-way ANOVA and Bonferroni post-hoc test.

metformin treated cells, despite reported effects on other cell types and animal models at the same concentrations *(559–563)* (Figure 6.8A-6.8D).

6.4.3 The effect of metformin on pyruvate and glutamine metabolism

Following glycolysis, pyruvate enters the mitochondria where it is converted into acetyl-CoA and joins the TCA cycle for oxidative metabolism. The contributions of endogenous mitochondrial pyruvate oxidation in control and metformin pre-treated cultures were investigated using the mitochondrial pyruvate carrier inhibitor UK-5099 (which inhibits mitochondrial uptake of pyruvate) in the presence of 10mM glucose. Application of UK-5099 (10µM) significantly decreased OCR in control cultures compared to DMSO, but the drug did not affect OCR in metformin treated cultures compared to DMSO (Figure 6.9A and 6.9B). This suggests that cells are not actively oxidising the pyruvate generated from glycolysis in metformin-treated cultures. UK-5099 also modestly decreased Perceval fluorescence in control but not metformin treated cells (Figure 6.9C-6.9E), but the changes in Perceval fluorescence were indistinguishable between treatments (Figure 6.9F). This might suggest that intestinal cells are not dependent on endogenous pyruvate oxidation for glycolytic ATP production. UK-5099 application also abolished the different effects of 2-DG on the Perceval fluorescence in control and metformin treated cells (Figure 6.9F). This probably indicates that at least in 5 out of 17 control cells, its metabolic flexibility is compromised in the presence of UK-5099 and is therefore more dependent on glycolysis for ATP production (Figure 6.9F). The other 12 of 17 cells are still resistant to the effects of 2-DG on Perceval fluorescence (compared to metformin treated cells), which could be that these control cells were able to utilise pyruvate from another source to sustain mitochondrial respiration and TCA-cycle metabolism (and therefore maintain their metabolic flexibility).

Since intestinal cells express MCTs (see Chapter 3) which exports lactate generated from glycolysis (Figure 6.3), the effects of exogenous pyruvate (1mM) application, a substrate of MCTs, was also investigated using Perceval imaging. Perceval fluorescence in control intestinal cells did not change despite switching the perfusion from pyruvate to saline (Figure 6.10A-6.10B), although subsequent application of Rot/AA decreased Perceval fluorescence in control cells (Figure 6.10D). None of the treatments (not even Rot/AA) altered Perceval fluorescence in metformin treated cells (Figure 6.10C-6.10D), except for 10mM glucose (Figure 6.10D). This observation also confirms the effects of UK-5099 in demonstrating that intestinal cells are not dependent on pyruvate oxidation for ATP synthesis, whereas metformin treated cells are highly dependent on glucose as a fuel for ATP-production.

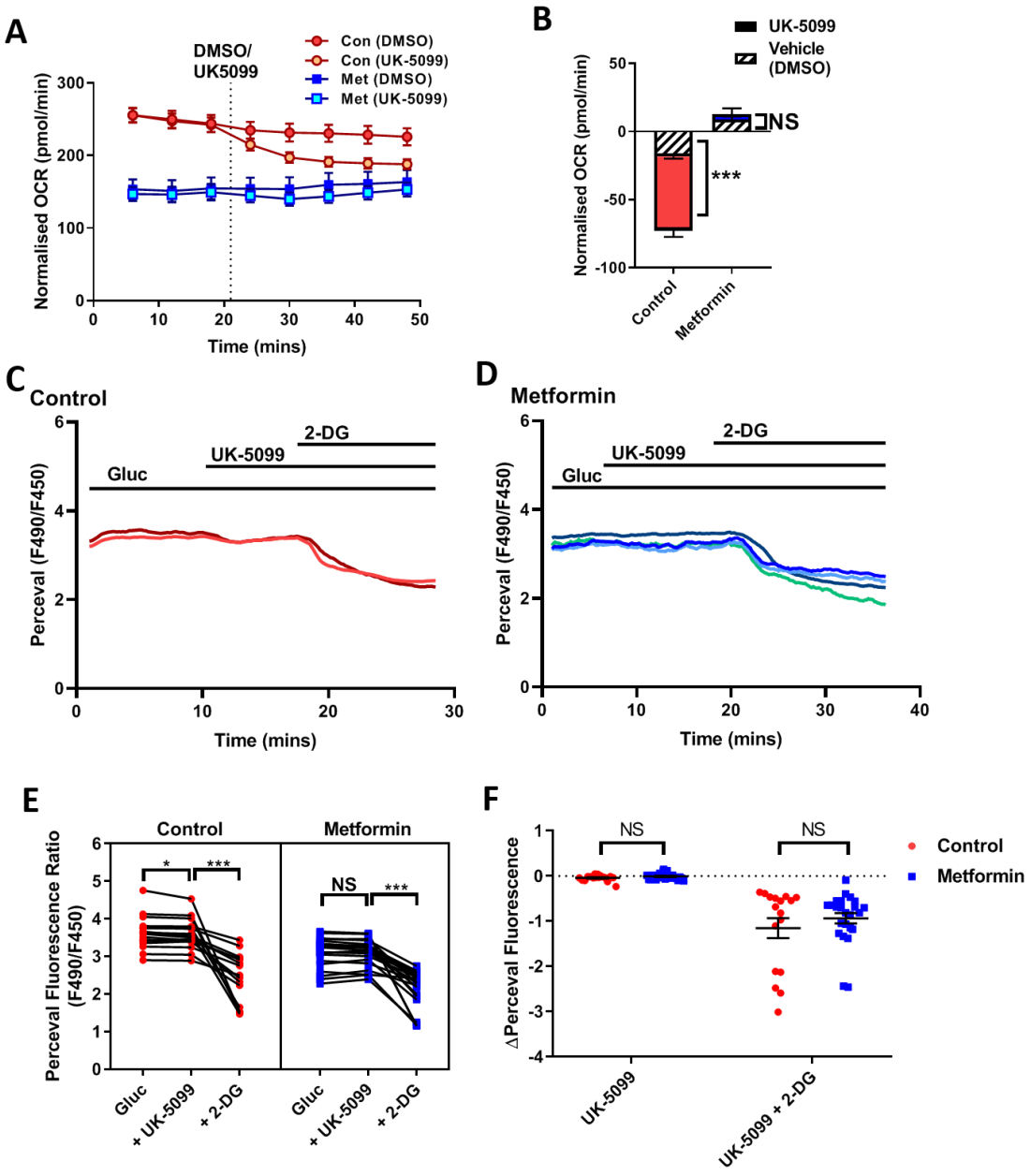

Figure 6.9. Inhibiting mitochondrial pyruvate transport decreases oxygen consumption in control cells, but does not remarkably affect Perceval fluorescence in control and metformin treated cells.

(A and B) The effects of the mitochondrial pyruvate carrier inhibitor UK-5099 compared to DMSO on oxygen consumption of control and metformin cultured cells as measured by the seahorse bioanalyser. For B, normalised OCR was calculated as differences after drug application and third time point measured before application ***, P<0.001 compared to DMSO in control cultures. N=4-5 wells from 4 independent experiments. (C and D) The effects of the mitochondrial pyruvate carrier inhibitor UK-5099 on Perceval fluorescence in Control (red, C) and Metformin (blue, D) treated cells. Glucose (Gluc, 10mM), UK-5099 (10µM) and 2-deoxyglucose (2-DG, 50mM) were applied as indicated on the traces. Different coloured lines denote responses from different cells. (E) Measured Perceval fluorescence ratios in control (red) and metformin-treated (blue) cells in the presence of UK-5099. Control: N= 17 cells from 3 dishes, metformin: N=24 cells from 3 dishes. NS; not significant. ***; P<0.001, Repeated-measures ANOVA and Bonferroni post-hoc test. (F) Changes in Perceval fluorescence in control and metformin treated cells to iGP-1 and 2-DG. NS; not significant, Two-way ANOVA and Bonferroni post-hoc test.

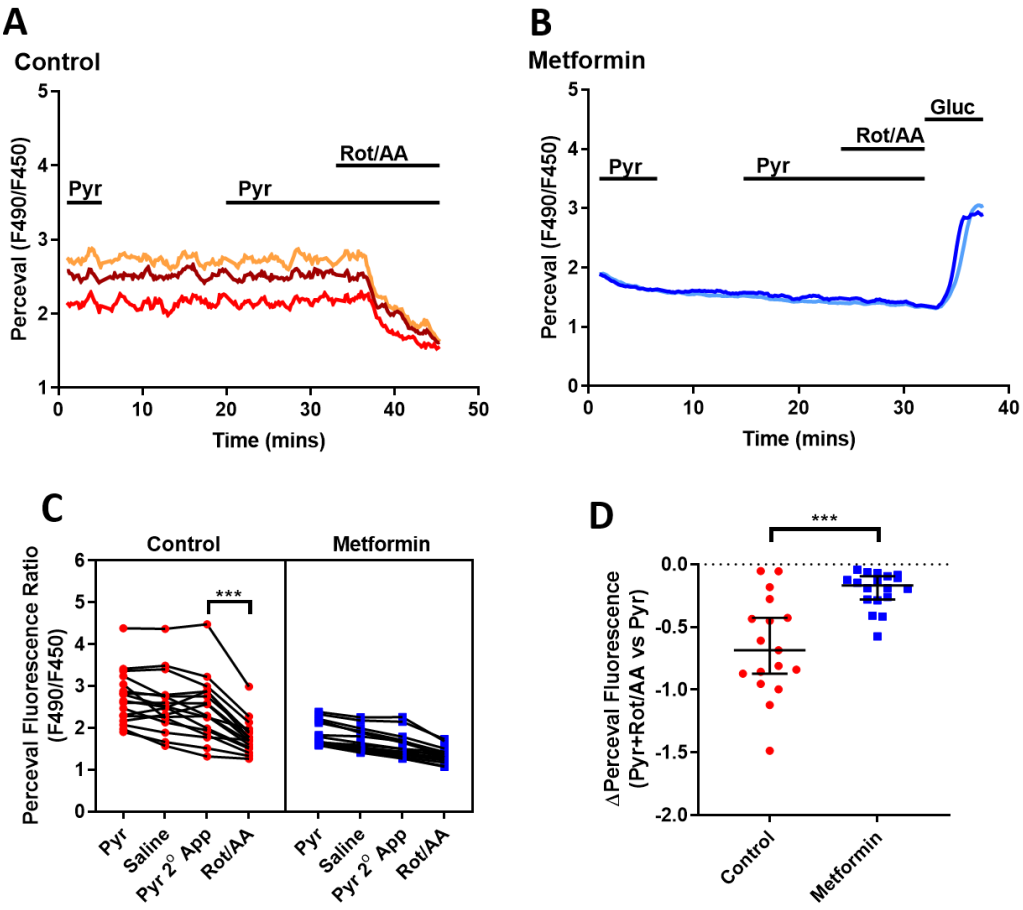

Figure 6.10. Exogenous pyruvate exposure does not affect Perceval fluorescence.
(A and B) The effects of pyruvate exposure on Perceval fluorescence in Control (red, A) and Metformin (blue, B) treated cells. For metformin treated cells, glucose (Gluc, 10mM) was applied as a positive control, but not included for analysis. Pyruvate (Pyr, 1mM) and Rotenone/Antimycin A (Rot/AA, 1µM each) were applied as indicated on the traces. Different coloured lines denote responses from different cells. (C) Measured Perceval fluorescence ratios in control (red) and metformin-treated (blue) cells to pyruvate, saline and Rot/AA. Control: N= 17 cells from 6 dishes, metformin: N=16 cells from 5 dishes. NS; not significant. ***; P<0.001, Friedman test and Dunn's post-hoc test. (D) Changes in Perceval fluorescence in response to Rot/AA in control and metformin treated cells. Bars are median ± 95% confidence interval. ***, P<0.001. Mann-Whitney test.

Live cell imaging of intracellular pyruvate generated from glycolysis were also performed by using the genetically encoded FRET-based fluorescent pyruvate sensor Pyronic. Inhibition of mitochondrial pyruvate uptake using UK-5099 in the presence of glucose (10mM) modestly increased pyruvate levels in control cells, but not metformin treated cells (Figure 6.11A). However, inhibiting the mitochondrial electron transport chain using rotenone and antimycin A in the presence of glucose did not increase

pyruvate levels in either control or metformin treated cells (Figure 6.11B). This suggests that under conditions where mitochondrial electron transport is blocked, pyruvate is not accumulating in the cytosol but instead metabolised through alternative pathways.

The effects of glutamine metabolism on oxygen consumption and ATP generation was also studied, since glutamine is highly metabolised in intestinal cells, and like pyruvate can only generate ATP via oxidative phosphorylation. In the presence of glutamine (4mM), metformin treated cells displayed lower basal, ATP-linked, maximal and uncoupled oxygen consumption (Figure 6.12A, 6.12B). The respiration in the presence of FCCP was lower than basal respiration in control cells

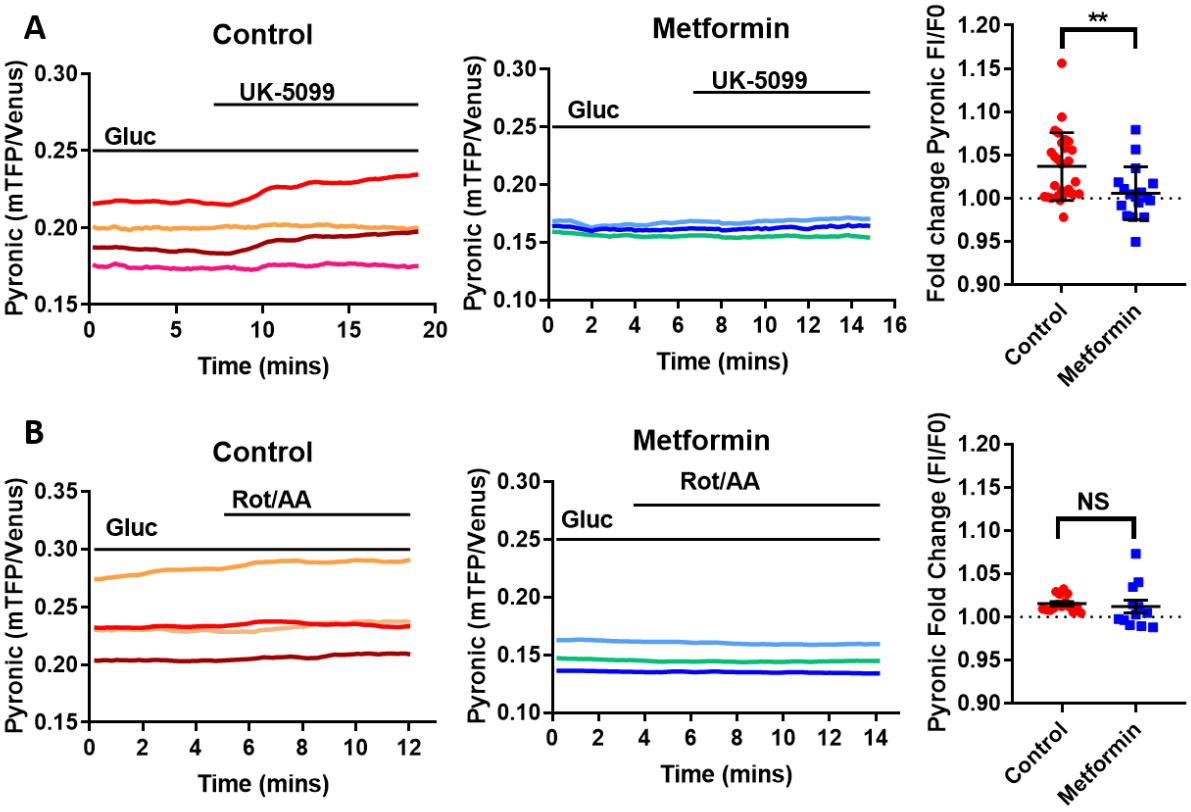

Figure 6.11. The effects of UK-5099 and electron transport chain inhibitors on Pyronic fluorescence. (A) The effects of the mitochondrial pyruvate carrier inhibitor UK-5099 (10µM) on Pyronic fluorescence in Control (red) and Metformin (blue) treated cells. Different coloured lines denote responses from different cells. Changes in Pyronic fluorescence expressed as fold change. Data expressed as Bars are median ± 95% confidence interval. Control: N= 27 cells from 4 dishes, metformin: N=17 cells from 3 dishes. **, P<0.01. Mann-Whitney U test. (B) The effects of rotenone and antimycin A (Rot/AA, 1µM each) on Pyronic fluorescence in Control (red) and Metformin (blue) treated cells. Different coloured lines denote responses from different cells. Changes in Pyronic fluorescence expressed as fold change. Data expressed as Bars are mean ± SEM. Control: N= 15 cells from 2 dishes, metformin: N=12 cells from 2 dishes. NS; not significant. Student's t-test.

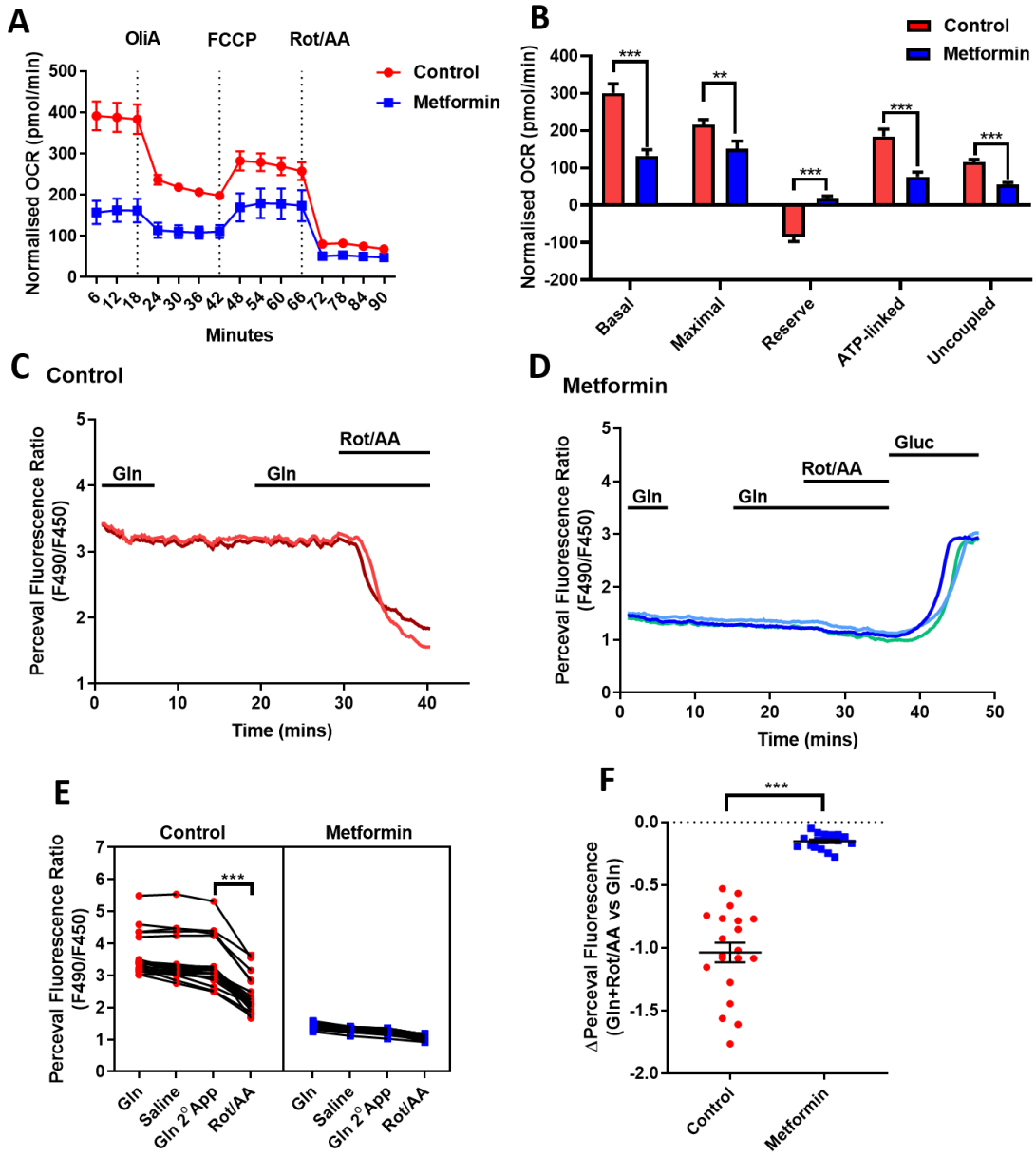

Figure 6.12. Metformin decreases glutamine oxidation in intestinal cells, but glutamine is not a dependent fuel for ATP production. (A) Changes in oxygen consumption rate (OCR) over time during the mitochondrial stress test in intestinal cells previously treated with control or without metformin for 24 hours. Cells were incubated with glutamine (4mM) for 1 hour prior to measurements. Dotted lines indicate when a compound was added. Oligomycin-A (OliA, 1µM), FCCP (1µM), Rotenone/Antimycin A (Rot/AA, 1µM each). (B) The effect of metformin on the parameters measured during the mitochondrial stress test. N=4-5 wells from 4 independent experiments. ***; P<0.001. Two-way ANOVA and Bonferroni post-hoc test. (C and D) The effects of glutamine on Perceval fluorescence in Control (red, C) and Metformin (blue, D) treated cells. For metformin treated cells, glucose (Gluc, 10mM) was applied as a positive control, but was not included for analysis. Glutamine (Gln, 4mM) and Rotenone/Antimycin A (Rot/AA, 1µM each) were applied as indicated on the traces. Different coloured lines denote responses from different cells.(E) Measured Perceval fluorescence ratios in control (red) and metformin-treated (blue) cells to glutamine, saline and Rot/AA. Control: N= 20 cells from 4 dishes, metformin: N=18 cells from 4 dishes. NS; not significant. ***; P<0.001, Friedman test and Dunn's post-hoc test. (F) Changes in Perceval fluorescence in response to Rot/AA in control and metformin treated cells. Bars are mean ± SEM. ***, P<0.001. Student's t-test.

(Figure 6.12B). This observation was also previously reported for palmitate metabolism in neonatal cardiomyocytes *(564)*. This could suggest that basal glutamine oxidation is already at maximal levels and intestinal cells might be running out of glutamine before the addition of FCCP. Abolition of the mitochondrial membrane potential via FCCP could also disrupt the transport of glutamate into the mitochondria via the aspartate-glutamate carrier (AGC), which is dependent on H^+ co-transport *(565)*. Alternatively, prior inhibition of mitochondrial ATP synthesis by oligomycin could also perturb the functions of Na^+/K^+ ATP-ase, which maintains Na^+ electrochemical gradient and suppress electrogenic transport of glutamine across the plasma membrane. Perceval fluorescence imaging demonstrated that glutamine exposure was without effect on Perceval fluorescence in control and metformin treated cells (Figure 6.12C-6.12F). Rot/AA application consistently attenuated Perceval fluorescence in control but not metformin treated cells (Figure 6.12E and 6.12F).

6.4.4 The effect of metformin on ATP generation from glycogen and lipid sources in intestinal cells

Although the mitochondrial fuels pyruvate and glutamine did not affect Perceval fluorescence, decreased Perceval fluorescence was observed in control treated intestinal cells in the presence of Rotenone and Antimycin A, suggesting that intestinal cells are able to metabolise an endogenous energy store to sustain intracellular ATP levels in the absence of these fuels. The role of glycogen metabolism was explored by measuring the Perceval fluorescence of cells exposed to saline buffer and the sequential exposure of: (1) glycogen phosphorylase inhibitor GPi-688, (2) glycolysis inhibitor 2-DG (inhibits glucose phosphorylation via hexokinase) to inhibit other pathways of glycogen mobilisation such as debranching enzyme activity or lysosomal α-glucosidases which produce glucose from glycogen and (3) Rotenone and antimycin A as a positive control (Figure 6.13A). GPi-688 treatment alone decreased Perceval fluorescence in 26/31 control cells and 11/27 metformin-treated cells incubated in saline, although the changes in metformin treated cells were small and not statistically significant. 2-DG and Rot/AA treatments further reduced Perceval fluorescence in control cells (Figure 6.13B, 6.13C). 2-DG modestly but significantly alter the Perceval fluorescence in metformin treated cells (Figure 6.13D, 6.13E). The changes in Perceval fluorescence to all the treatments was consistently lower in metformin treated cells compared to control cells (Figure 6.13F). This suggests that there were less glycogen stores in metformin treated cells at the start of the imaging experiment. It should also be noted that Perceval fluorescence was markedly lower in metformin treated cells from the beginning of the experiment, which is likely to be due to low intracellular ATP levels and metabolism in the absence of glucose to ensure survival (Figure 6.13B-6.13E).

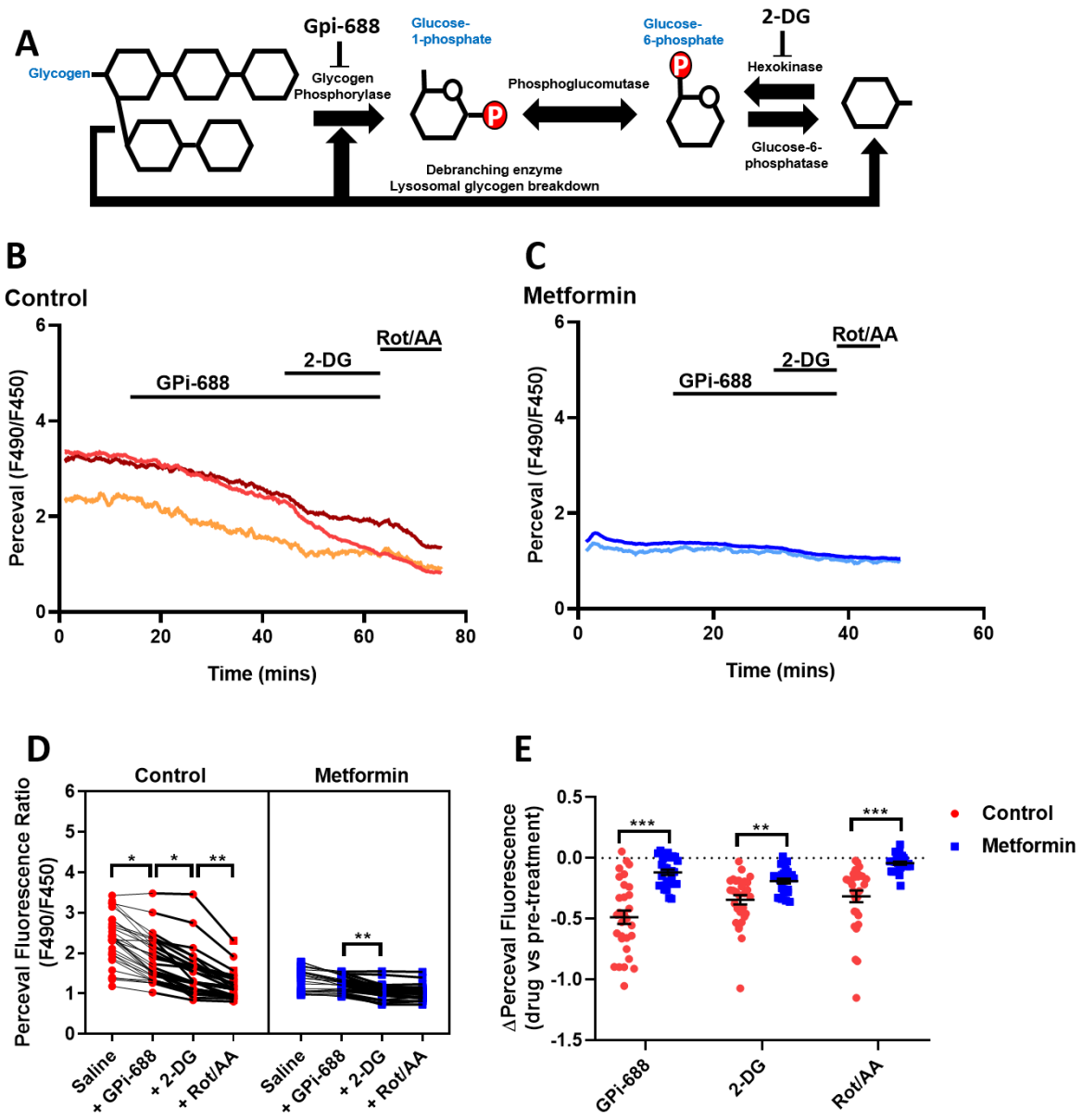

Figure 6.13. Metformin decreases glycogen mobilisation in intestinal cells. (A) Diagram showing the actions of glycogenolysis inhibitors used in the experiments. (B and C) The effects of glycogenolysis inhibitors on Perceval fluorescence in Control (red, B) and Metformin (blue, C) treated cells. GPi-688 (20µM), 2-deoxyglucose (2-DG, 50mM) and Rotenone/Antimycin A (Rot/AA, 1µM each) were applied as indicated on the traces. The cells were incubated with 4mM glutamine prior to experiments, before switching to saline during the first 3 minutes of imaging. Different coloured lines denote responses from different cells. (D) Measured Perceval fluorescence ratios in control (red) and metformin-treated (blue) cells to GPi-688, 2-DG and Rot.AA. Control: N=30 cells from 8 dishes, metformin: N=27 cells from 7 dishes. NS; not significant. *; P<0.05, **; P<0.01, ***; P<0.001, Friedman test and Dunn's post-hoc test. (E) Changes in Perceval fluorescence in control and metformin treated cells to GPi-688, 2-DG and Rot/AA. **; P<0.01, ***; P<0.001. Two-way ANOVA and Bonferroni post-hoc test.

Endogenous lipid mobilisation was also considered as a candidate internal fuel source since fatty acid oxidation has previously been reported in intestinal cells *(177, 537–539)*. Contributions of fatty acid oxidation were investigated by measuring the effect of the mitochondrial carnitine palmitoyltransferase 1 (CPT1) shuttle inhibitor etomoxir (which prevents fatty acid transport into the mitochondria) on Perceval fluorescence in cells exposed to saline. Rotenone/antimycin A was used as positive control. When used at 20µM concentrations, etomoxir was without effect in control cells, but modestly reduced Perceval fluorescence in metformin treated cells (Figure 6.14A-6.14E). Considering that the Perceval fluorescence in metformin treated cells were already low at the beginning of the experiments, whether the changes in perceval fluorescence was due to the genuine effects of etomoxir, or a false positive effect due to the gradual decline in intracellular ATP levels in the absence of glucose, is unknown. 100µM etomoxir decreased Perceval fluorescence in both control and metformin treated cells, but the differences between treatments were not observed (Figure 4.14F). This is likely due to the reported off-target effects of etomoxir on mitochondrial respiration when used at ≥100µM concentrations, such as complex I inhibition and disruption of CoA homeostasis, in addition to inhibiting FAO *(566–568)*. The observations do not suggest that stored lipids are an important fuel source in intestinal cells.

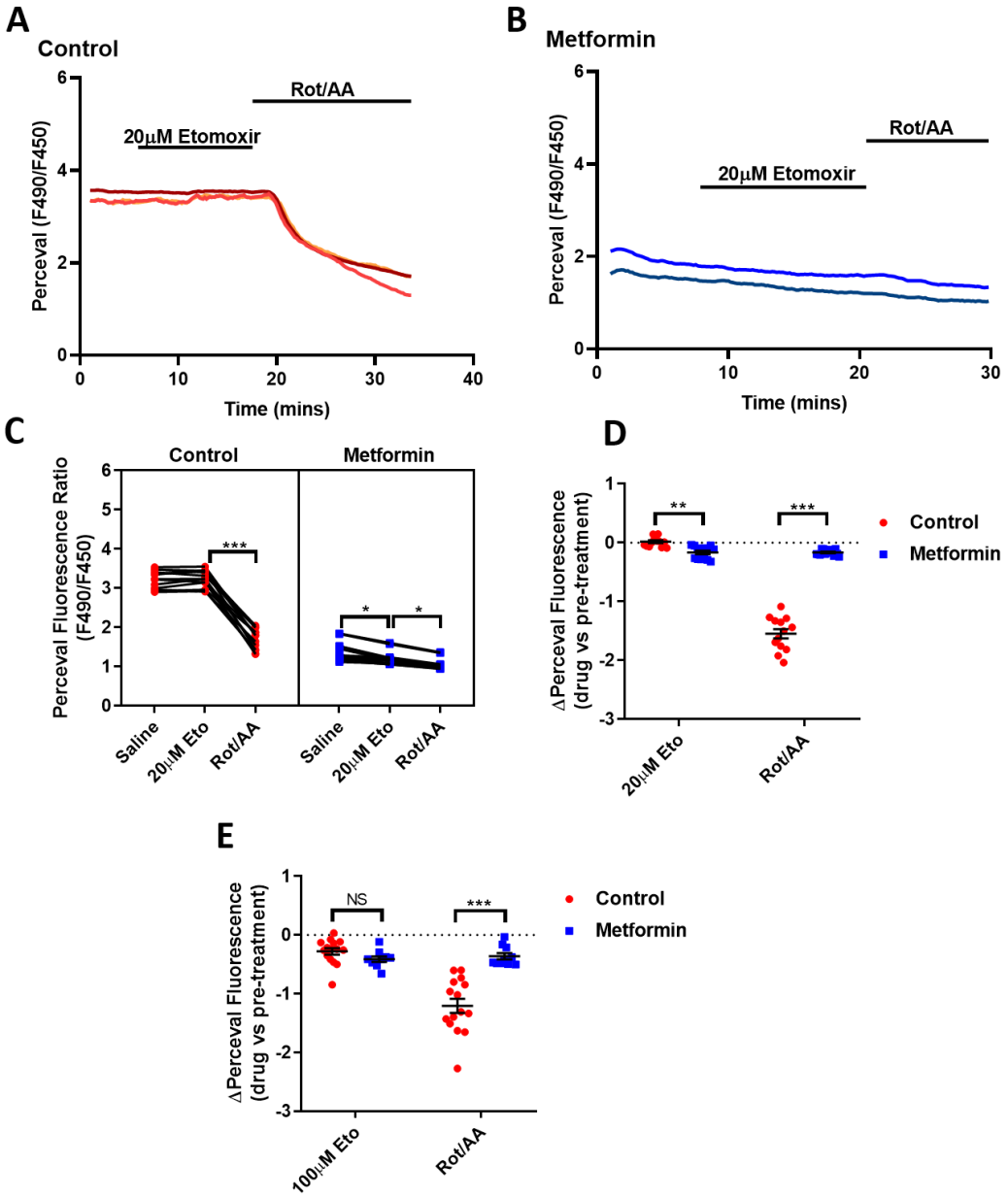

Figure 6.14. Metformin slightly increased fatty acid oxidation in intestinal cells. (A and B) The effects of 20μM etomoxir on Perceval fluorescence in Control (red, A) and Metformin (blue, B) treated cells. Etomoxir (Eto, 20μM) and Rotenone/Antimycin A (Rot/AA, 1μM each) were applied as indicated on the traces. Different coloured lines denote responses from different cells. (C) Measured Perceval fluorescence ratios in control (red) and metformin-treated (blue) cells to 20μM etomoxir and Rot/AA. Control: N=30 cells from 8 dishes, metformin: N=27 cells from 7 dishes. NS; not significant. ***; P<0.001, Friedman test and Dunn's post-hoc test. (D) Changes in Perceval fluorescence in response to 20μM etomoxir and Rot/AA in control and metformin treated cells. Data are mean ± SEM. ***, P<0.001. Two-way ANOVA and Bonferroni post-hoc test. (E) Changes in Perceval fluorescence in response to 100μM etomoxir and Rot/AA in control and metformin treated cells. Data are mean ± SEM. ***, NS; not significant, ***; P<0.001. Two-way ANOVA and Bonferroni post-hoc test.

6.5 Discussion

6.5.1 Metformin and mitochondrial oxidation in intestinal cells

Confirming a vast body of literature that metformin is a complex I inhibitor of mitochondrial respiration *(203, 204, 207, 569, 570)*, the metabolic flux experiments demonstrated that metformin decreased oxygen consumption rate during glucose and glutamine metabolism in intestinal monolayers (Figure 6.1 and Figure 6.12), whilst metformin abolished the effect of rotenone and antimycin A in Perceval fluorescence from glucose oxidation (Figure 6.4). Furthermore, application of the mitochondrial pyruvate carrier UK-5099 to inhibit the uptake of pyruvate (produced from glycolysis) had little to no effect on Pyronic fluorescence or oxygen consumption in metformin treated cells, demonstrating little to no oxidation of pyruvate produced from glycolysis (Figure 6.9 and Figure 6.11). Autofluorescence imaging experiments demonstrated that metformin diminished the magnitude of NAD(P)H autofluorescence increased by glycolysis and lowered by FCCP (Figure 6.2). Metformin treatment also blunted the effect of glucose and FCCP on FAD autofluorescence. These results support existing literature reporting that metformin reduces TCA cycle flux *(205, 206)*, either caused by elevated mitochondrial NADH (which would indirectly inhibit oxidative TCA cycle reactions and thus FAD oxidation) *(396, 569, 571)*, or extraneous effects on mitochondrial bioenergetics such as uncoupled respiration *(205)*.

The mitochondria of intestinal cells seem to exhibit some degree of fuel flexibility. This is supported by multiple observations. First, application of UK-5099 to inhibit mitochondrial pyruvate transporter changes the Pyronic fluorescence and oxygen consumption but has no effect on the Perceval fluorescence in control cells (Figure 6.9 and Figure 6.11). Second, exogenous pyruvate and glutamine treatments (Figure 6.10 and Figure 6.12) showed negligible effects on Perceval fluorescence in intestinal cells, despite evidence for glutamine oxidation and endogenous pyruvate oxidation in control cells in the Seahorse data. Since Rotenone and Antimycin A drastically decreased mitochondrial respiration in control cells in the presence of glucose, glutamine or pyruvate (with limited effect in metformin treated cells), this clearly indicates an important role of the mitochondria in ATP production. Metformin, by inhibiting mitochondrial respiration, could potentially handicap the capability of the mitochondria to metabolise fuels resulting in a lower cellular ATP/AMP ratio *(204)*, which would activate AMPK signalling *(210)* and glycolysis *(207)*.

Although metformin has been demonstrated to deplete TCA cycle intermediates in cancer cells from some studies *(205, 206, 572)*, others argue that inhibition of mitochondrial complex I rewires the TCA cycle towards alternative pathways involving biosynthesis *(394, 396, 397, 571, 573, 574)*. Amongst

these pathways include altering the malate aspartate shuttle towards aspartate synthesis *(396, 397, 573)*, and increased reductive glutamine carboxylation towards lipid and amino acid generation *(394, 571, 574, 575)*. Although it remains to be proven whether these pathways are altered by metformin in intestinal cells, the observations that intestinal cells do not depend on glutamine and pyruvate as fuels for ATP generation may alternatively suggest the roles of these fuels in metabolic biosynthesis. The observations that pyruvate *(187)*, glutamine *(540)* and fatty acid *(188)* metabolism are important in regulating proliferation and/or fate determination of intestinal cells along the crypt/villus axis seems to suggest the importance of mitochondrial metabolism beyond ATP generation.

6.5.2 Metformin and intestinal glucose metabolism

The evidence presented in this study demonstrates that metformin maximises glycolysis, increased glycolytic capacity and glycolytic ATP production in intestinal cells (Figure 6.3 and Figure 6.4). This is supported by the transcriptomic data which highlighted increased expression of key glycolytic enzymes by metformin (see chapter 3). Increased glucose utilisation and lactate production were previously observed as the intestinal mucosa accumulates high levels of metformin *(64, 116, 207, 239–242, 312)*. A recent study by Schommers *et al.,* further elaborated this by demonstrating that metformin increased lactate release from the intestinal wall into the splanchnic bed, and that metformin increased the ratio of *Ldha/Ldhb* expression in the intestine (favouring pyruvate metabolism to lactate) and decreased *Ldha/Ldhb* expression (favouring lactate metabolism to pyruvate) in the liver *(207)*. The authors suggested that metformin causes a futile glucose-lactate cycle involving glycolysis in the intestine and gluconeogenesis in the liver predominantly through altered LDH expression, despite several studies demonstrating that metformin suppresses hepatic gluconeogenesis *(207, 220, 225–227)*. In the RNA-seq data, metformin did not change mRNA expression of either of those LDH isoforms (data not shown), despite increasing the expression of *Ldhd* expression (see chapter 3). However, LDH activity was decreased in metformin treated cells (Figure 6.5C), which challenges the observations in that study in describing the precise molecular mechanisms involved in glucose metabolism to lactate.

Inhibition of LDH by oxamate or inhibiting lactate-transport by MCT inhibitors AR-C155858 and Syrosingopine partially suppressed lactate secretion, elicited increases in Peredox fluorescence (Figure 6.5) and modestly decreased Perceval fluorescence in metformin treated cells (Figure 6.6). This could suggest that pyruvate metabolism to lactate plays only a minor contribution in maintaining glycolysis under metformin treatment, with some flexibility to discard of surplus pyruvate/lactate through other pathways, for example transamination to alanine (see below). The alternative explanation is incomplete pathway inhibition by the drugs. Inhibiting NAD+ regeneration through the LDH pathway

could also lead to compensation by other pathways such as the glycerolphosphate shuttle in sustaining glycolysis. In the case of MCT transport inhibition, changes in intracellular pH mediated by lactate accumulation may decrease Perceval fluorescence due to interference of the fluorescent protein, although lactate accumulation would also inhibit NAD+ regeneration and this could reduce glycolysis flux *(556)*.

Metformin treatment also increased aspartate and alanine transaminase activity in metformin treated cells (confirming increased Gpt1 expression in transcriptomic data), and perceval imaging studies demonstrate some role for alanine aminotransferases in contributing to intestinal glycolysis (Figure 6.7). In the liver, pyruvate-alanine cycling is important in regulating gluconeogenesis from alanine as substrates, particularly under conditions where mitochondrial uptake of pyruvate is blocked *(535, 576–580)*. Gpt1 transcript and protein expression in the mouse and rat intestine is comparable to the liver *(558, 581)*. Several studies have confirmed that pyruvate generated from glycolysis are used for glutamine transamination in intestinal cells, and that alanine is a major fate of glutamine metabolism *(177–179, 535)*. A recent study investigating L-alanine administration in hepatic cell lines reported decreased ATP levels, but increased the NAD+/NADH ratio and intracellular lactate levels *(582)*. If transamination to alanine is an important fate of pyruvate in intestinal cells in the presence of metformin, inhibiting alanine aminotransferases could lead to pyruvate accumulation and redirecting pyruvate towards lactate production, which may decrease Perceval fluorescence via lactate accumulation and alter the intracellular pH or the cytosolic NAD+/NADH ratio.

However, neither LDH nor alanine aminotransferase inhibition alone influenced the effects of 2-DG on the Perceval fluorescence in control and metformin treated cells, suggesting that neither of these pathways are rate-limiting to glycolysis. Future studies should investigate whether combining LDH or alanine aminotransferase inhibitors are sufficient to inhibit glycolysis by measuring Perceval fluorescence in control and metformin treated cells. The limitations of pharmacological compounds used in this study should also be acknowledged, particularly the putative glycerolphosphate shuttle inhibitor iGP1 and the MAS inhibitor phenylsuccinate (Figure 6.8), in which no appropriate controls were available. Even so, the steps that control glycolytic flux are still debateable. Whilst previous literature suggested that NADH regeneration via mitochondrial shuttles and LDH activity involved in maintaining glycolysis flux *(583, 584)*, other studies identified the importance of enzymes such as aldolase A *(585)*, GAPDH *(586)*, pyruvate kinase *(587)* and LDHA *(207, 588)*. A recent study demonstrated that glucose uptake, lactate export, hexokinase and phosphofructokinase activity were essential in determining glycolytic flux when glycolysis enzymes or transporters were individually

overexpressed in two mammalian cell lines*(376)*. The transcriptomic and functional data in this study suggests that glycolysis and glycolytic capacity is determined by the functions of glycolysis enzymes such as hexokinases, as opposed to downstream pyruvate metabolism enzymes such as LDH or alanine transaminases.

What are the signalling mechanisms that explain the effect of metformin on glycolysis? The evidence in this study suggests that attenuating mitochondrial respiration seem sufficient to increase glycolysis as a compensatory mechanism. The observations that (1) oligomycin A further increased glycolytic ECAR (Figure 6.3) and (2) inhibition of pyruvate uptake into the mitochondria abolished the differences of 2-DG in glycolytic ATP production between control and metformin treated cells (Figure 6.9), seem to support this hypothesis. Moreover, hexokinase and phosphofructokinase directly interacts with, and are regulated by ATP/AMP *(219)*. Alternative explanations could be the regulation of phosphofructokinases by AMPK *(379)*, or transcriptomic changes in glycolysis genes (Chapter 3). This would explain metformin causing a Warburg effect in intestinal cells to maximise glycolytic ATP production as a quick ATP source to sustain cellular processes.

6.5.3 Metformin and intestinal energy stores

The existence of intestinal glycogen stores has previously been reported and is particularly elevated in diabetic or suckling rats, which were associated with increased intestinal gluconeogenesis *(386, 390, 589)*. The observations from the Perceval fluorescence imaging seem to suggest a role of glycogen breakdown in sustaining ATP levels in intestinal cells in the absence of glucose. Existing literature reporting the functional significance of intestinal glycogen are limited, with some speculating that it may contribute to intestinal gluconeogenesis *(590, 591)*. Metformin seemed to decrease glycogenolysis in intestinal cells, and it seems that intestinal cells metabolise glycogen for ATP production in the absence of glucose (Figure 6.13). The effects of metformin on intestinal glycogen stores remains to be determined. The role of metformin in hepatic glycogenolysis is controversial, with some studies demonstrating reduced glycogenolysis or a glycogen-sparing effect of metformin in the liver *(389, 543, 544)*, whilst a study in type-2 diabetic patients indicated that metformin does not affect hepatic glycogenolysis *(227)*.

In contrast to the effects of metformin in glucose and glutamine oxidation, metformin paradoxically increases fatty acid oxidation *(210, 211, 229, 230)*. Etomoxir (at 20μM) seemed to mediate a slight reduction in Perceval fluorescence in metformin (but not control) treated cells, which may suggest increased endogenous fatty acid oxidation in metformin treated cells(Figure 6.14). The RNA-seq data does not show substantialchanges in fatty acid metabolism genes either (chapter 3). Although

evidence for intestinal fatty acid metabolism has been reported *(177, 537–539)*, stored lipids does not seem to be the main choice of fuel in intestinal cells.

6.6 Conclusions

In summary, the following working model is proposed (see Figure 6.15). Intestinal cells normally produce ATP from glycolysis and mitochondrial oxidation, whilst maintaining some intestinal glycogen to maintain ATP levels in the absence of glucose. The mitochondria may also have the flexibility to metabolise glutamine or pyruvate. Metformin inhibits mitochondrial respiration, which causes the cells to compensate by increasing glucose uptake and glycolysis to produce lactate and alanine. Metformin could potentially increase the limited metabolism of stored lipids although it is not certain whether the modest effects of etomoxir on ATP levels are genuine, or a false positive effect associated with declining ATP levels in the absence of glucose. Therefore, intestinal cells could metabolise glucose (via glycolysis), pyruvate, glutamine and glycogen, but seem to mostly rely on glycolysis in the presence of metformin.

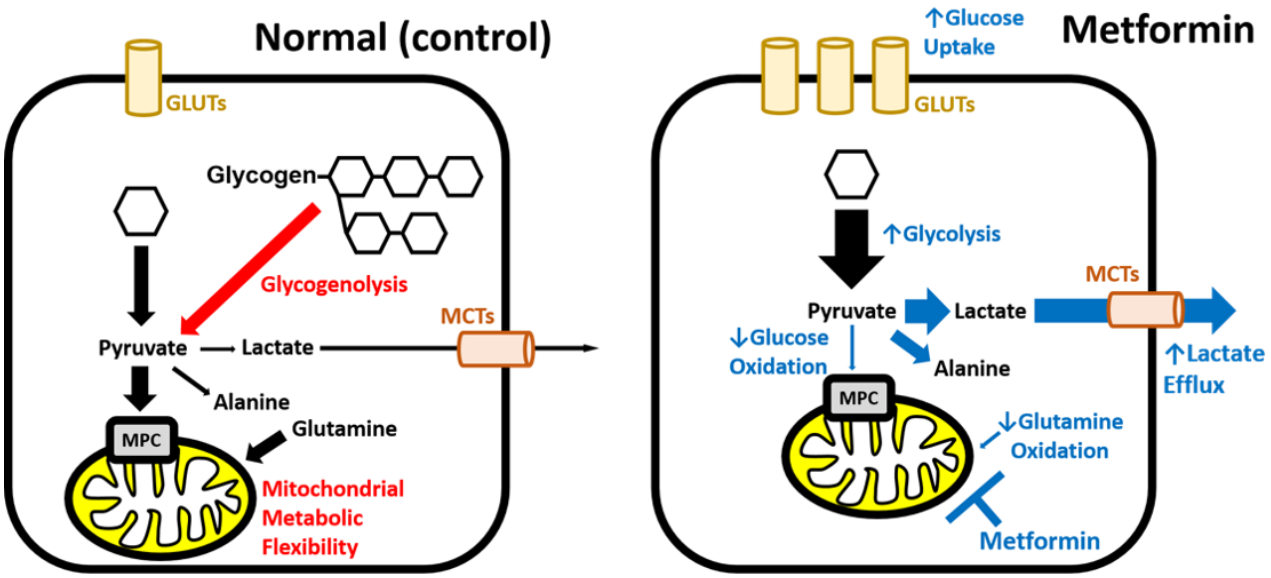

Figure 6.15. Working model describing the effects of metformin on intestinal metabolism. Red indicates hallmarks of cellular metabolism in control cells, whilst blue indicates changes in metabolic pathways by metformin. GLUTs; facilitative glucose transporters, MCTs; monocarboxylate transporters, MPC; mitochondrial pyruvate carrier.

Altogether, this model provides a cellular mechanism supporting the existing literature to demonstrate the importance of metformin in increasing glucose utilisation in the intestine *(116)*. This supports the developing hypothesis that the intestine acts as a "glucose sink" to metabolise glucose from the blood as a potential mechanism to support the effects of metformin in improving glycaemic control in patients with Type 2 Diabetes. Future studies should follow up the data with metabolomic or metabolic flux experiments to confirm the effects of metformin on the metabolic pathways in intestinal cells.

Chapter 7: General Discussion

7.1. Summary of findings

7.1.1. Metformin alters the transcriptome of intestinal cells

Previous transcriptomic profiling to investigate mechanisms of metformin action have been performed on hepatocytes, skeletal muscle and adipose tissue biopsies, but not in intestinal cells *(365, 366)*. In chapter 3, RNA-Sequencing was performed in duodenal 2D monolayer cultures, which identified metformin-responsive genes and pathways. Amongst the prominent findings in the RNA-seq data were the alterations in glucose metabolism pathways. This included upregulation of key genes involved in glycolysis, downregulation of fructose metabolism genes and altered expression of genes involved in the pentose phosphate pathway. Metformin also altered the expression of genes involved in amino acid metabolism, such as serine/threonine and folate metabolism. In mouse hepatocytes, metformin has been reported to alter the expression of genes and result in suppression of gluconeogenesis and lipogenesis, and it was speculated that these changes are part of the mechanism by which metformin lowers blood glucose levels and reduces fatty liver disease development, respectively *(210, 365)*. In human skeletal muscle, metformin increased the expression of genes involved in glycolysis and pyruvate metabolism; supporting other functional studies that metformin may be involved in peripheral glucose uptake *(366)*. The transcriptomic studies suggest that differences in metabolism in different organs could contribute to the beneficial metabolic effects of metformin.

In contrast to hepatocytes, metformin did not cause a consistent alteration of genes involved in the AMPK signalling pathway in intestinal cells *(365)*. However, the potential post-translational effects of metformin on AMPK activity in intestinal cells cannot be ruled out. Changes in other signalling pathways such as the upregulation of HIF1A signalling, Hippo signalling and lysosome pathways were also identified. As discussed in chapter 4 and 5, HIF1A appears to be involved in GDF-15 secretion and glucose uptake in intestinal cells. Furthermore, activation of autophagy is an established downstream mechanism of AMPK activation by metformin and autophagy is essential to preserve intestinal epithelia function *(352–355)*. No previous study has identified transcriptomic changes in the Hippo signalling pathway associated with the metformin response, which warrants further confirmation via functional studies.

7.1.1.1 Future directions

Although transcriptomic changes could suggest potential changes in function in intestinal cells, it is possible that the gene expression findings may not be entirely replicated at the protein level *(450)*. Therefore, assessment of protein changes should also be incorporated in future studies to provide a more substantial picture of metformin action in intestinal cells. The transcriptomic changes in metabolism genes should also be studied further, such as via metabolic tracing of metabolites. This would support the functional effects of the transcriptomic changes in metabolic pathways in the presence of metformin and possibly identify novel metabolic pathways. Metabolic tracing has provided detailed insights into the different metabolic adaptations by metformin in cancer cells *(206, 394, 396)*.

Some of the metabolism/signalling genes (such as key glycolysis and HIF1A signalling genes) identified in the organoid studies should be confirmed in the intestinal tissues of metformin-treated HFD-fed mice. An even more ambitious future direction would be to compare global expression changes in different sections of the mouse intestines, as well as other metabolically important organs such as the liver, adipose tissue and skeletal muscle in HFD-fed mice that had been orally administered metformin. A "temporal" transcriptomic analysis could be performed to compare acute (e.g. 6 hours) or chronic (11 days) effects of metformin in different organs. A similar inter-organ systems transcriptomic approach has been performed to investigate organ-specific changes in metabolism and signalling genes after Roux-en-Y gastric bariatric surgery in mice and humans *(42)*. Investigating the transcriptomic changes in different organs following metformin treatment could validate many of the previous observations regarding metformin in mice and provide a more integrative picture into the metabolic responses of the different organs to metformin.

7.1.2. Metformin stimulates GDF-15 secretion through mitochondrial stress

As mentioned in chapter 4, our collaborators observed that plasma GDF-15 concentrations are associated with the weight-loss effects of metformin and that GDF-15 expression is upregulated in small intestinal and colonic tissues (but not in the other metabolically important organs such as the liver and adipose tissue) after oral metformin gavage. From the RNA-seq data in 2D monolayer intestinal cultures, *Gdf15* was one of the top significantly upregulated genes by metformin, and metformin robustly stimulated GDF-15 secretion from these cultures. The RNA-seq and secretion data also demonstrated that metformin stimulated GDF-15 secretion via mitochondrial stress whilst metformin downregulated the expression of genes involved in mitochondrial translation and mtDNA genome maintenance. Studies involving human primary hepatocytes also identified *Gdf15* as an

upregulated gene not associated with the activation of the AMPK signalling pathway by high concentrations of metformin *(365)*. Similarly, serum levels of GDF-15 are elevated in patients with mitochondrial disease and mouse models of mitochondrial myopathy *(286, 374, 447, 448)*. This study, consistent with studies in other models, suggested that metformin increases GDF-15 expression and secretion via a mitochondria-dependent mechanism. Metformin stimulated GDF-15 secretion via the ISR, since the EIF2A phosphorylation inhibitor ISRIB attenuated metformin-stimulated GDF-15 secretion whilst *Ddit3* mRNA expression was upregulated in intestinal tissues of HFD-fed mice treated with metformin. These studies are consistent with the findings from other collaborators involving metformin in primary hepatocytes and the effects of phenformin on ISR in MEF cells *(321)*. The ISR has previously been reported to be important for the induction of *Gdf15* expression in response to a variety of cellular stressors such as ER stress and hypoxia *(287)*. It is unknown how mitochondrial stress elicited by metformin stimulates GDF-15 secretion; inhibition of GCN2 (reportedly activated by oxidative stress) did not affect GDF-15 secretion and the PERK inhibitor GSK-2606414 modestly reduced metformin-stimulated GDF-15 secretion. Other EIF2A kinases (such as PKR or HRI) might be associated with metformin-stimulated GDF-15 secretion, which could be investigated in future studies.

Interestingly, HIF-1A inhibitors also inhibited metformin stimulated GDF-15 secretion, which to our knowledge have not previously been reported in the literature. The results suggest that the HIF signalling pathway is important in determining metformin stimulated GDF-15 secretion. Currently, studies are underway to investigate metformin and HIF-1A protein levels in intestinal cells. Future studies would investigate the effects prolyl hydroxylase or VHL inhibitors, or using Hif1a or Vhl knockout mouse intestines on GDF-15 secretion.

The results in chapter 4 confirm that intestinal cells are capable of secreting GDF-15 into the media in response to metformin and other mitochondrial stressors. From the in situ hybridisation data, *Gdf15* induction by metformin seems to be localised to the numerous transit-amplifying cells of the epithelia in the distal small intestine and colonocytes in the colonic epithelia, whereas almost all other gut hormones identified to date are released by enteroendocrine cells that encompass 1% of the intestinal epithelial population *(159)*. Therefore, based on this study and supporting in vivo data *(321)*, GDF-15 could be a novel and atypical “gut hormone” released by intestinal epithelial cells that may provide a cellular mechanism that explains the effects of metformin on body weight.

7.1.2.1 Future directions

Although this study suggests that metformin stimulates GDF-15 secretion via mitochondrial stress, there is no direct evidence that metformin causes other aspects of mitochondrial dysfunction other

than inhibiting oxidative phosphorylation (OXPHOS) in intestinal cells. Furthermore, transcriptomic analysis did not reveal changes in mitochondrial OXPHOS or oxidative stress genes. A more comprehensive study into other aspects of mitochondrial stress is warranted, such as superoxide production (such as using the MitoSOX dye) as an indicator of oxidative stress, mitochondrial membrane potential (using Mitotracker Orange), mitochondrial morphology (such as Mitotracker Green or electron microscopy), or mitochondrial calcium signalling (via measurements using the Rhod-2 dye). Downregulation of mitochondrial translation genes and altered expression of mitochondrial folding genes could also be studied via other in vitro studies (e.g. proteomics of mitochondrial translation proteins).

The results in chapter 4 and findings from our collaborators collectively suggest that the weight loss effects of metformin might be mediated by a mechanism involving the gut-brain axis involving GDF-15 released from the gut, which targets the brainstem to cause weight loss (see Figure 7) *(321)*. To provide direct evidence and fully establish the role of GDF-15 as a potential hormone involved in a gut-brain axis that addresses the weight loss effects of metformin, one of the future directions could involve physiological investigations into an intestine specific (e.g. Villin-cre) *Gdf15* knockout mouse model. The effects of metformin on metabolic parameters such as body weight, food intake and energy expenditure could be measured in these mice to investigate the role of this gut-brain cross-talk in metformin suppression of appetite. Alternatively, comparisons in serum levels of GDF-15 and food intake could be made in mice that had been intravenously or orally administered metformin, as differences in glycaemic control have previously been reported to be dependent on different routes of metformin administration *(316)*.

7.1.3. Metformin increases GLUT transporter mediated glucose uptake

In chapter 5, expression data in 2D monolayer cultures and intestinal tissues from HFD-fed mice showed that metformin decreased the expression of numerous hexose transporters, such as *Slc2a2* (GLUT2) and *Slc5a1* (SGLT1), but increased the expression of *Slc2a1* (GLUT1). Metformin also increased glucose uptake in intestinal cells mediated by GLUT (presumably GLUT1) transporters (See Figure 7). To our knowledge, no previous study has investigated the effects of metformin on GLUT1 expression in intestinal cells. The upregulation of GLUT transporters in the small intestine may explain the observed increase in intestinal glucose accumulation as reported in PET-CT imaging studies in mice and humans (Figure 7) *(237, 364, 490, 517–519)*. After RYGB surgery, GLUT1 expression was increased in the alimentary limb, which was directly associated with increased glucose utilisation and glucose-lowering effects *(42, 43)*. Similarly, downregulation of *Slc2a2* (GLUT2) and *Slc5a1* (SGLT1) genes could

potentially suggest a molecular basis by which metformin decreases intestinal absorption of ingested glucose *(234–236, 488, 489, 516, 523)*. Yet, these findings do not support other investigations that report increased GLUT2 abundance in the intestinal epithelium *(523, 592)*.

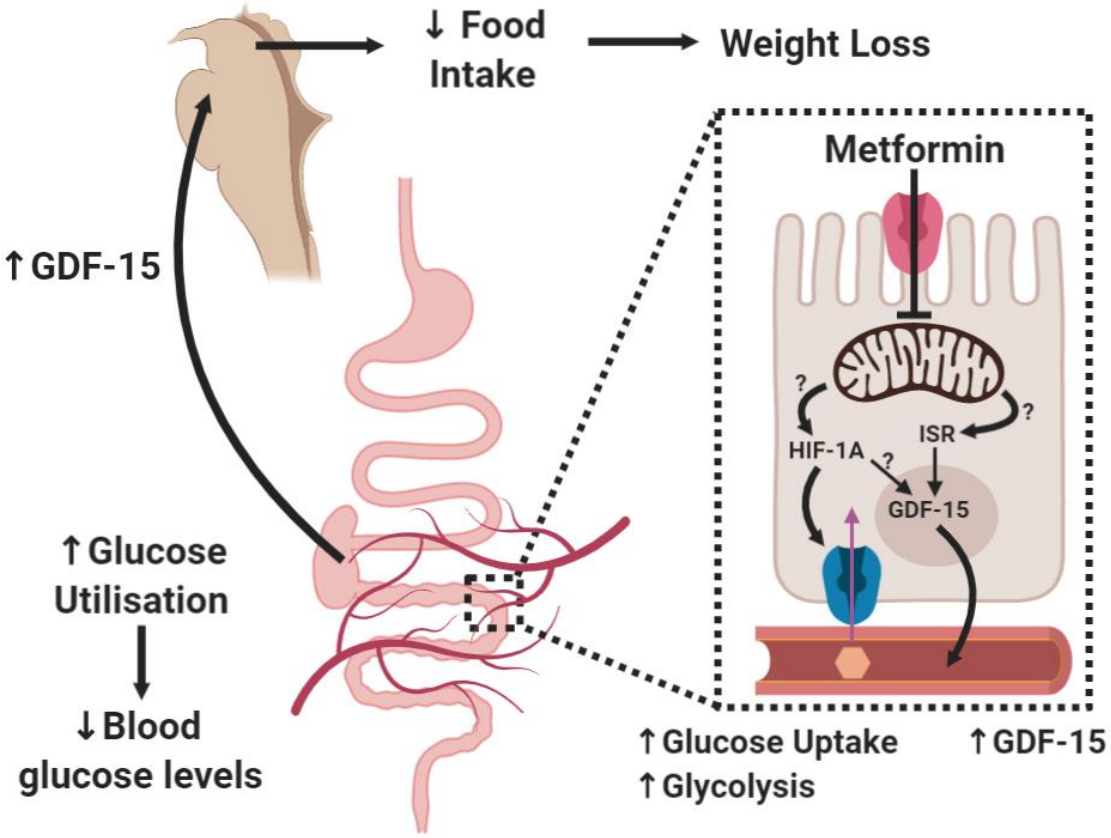

Figure 7. A proposed physiological mechanism of metformin action in increasing GDF-15 secretion and glucose utilisation in intestinal cells to achieve glycaemic control and weight loss.

The roles of the AMPK and HIF1A signalling pathways in metformin altered glucose transporter expression and glucose uptake in intestinal cells were investigated to identify the plausible signalling pathways involved. The results suggest that upregulation of the HIF1A pathway, and to a lesser extent increased post-translational AMPK activation, are involved in metformin stimulated glucose uptake. The role of AMPK activation in glucose uptake in muscle cells has been well established *(210, 336, 338–341)*, so it is not surprising that the AMPK activator stimulates glucose uptake in intestinal cells. HIF1A is important in regulating intestinal function *(593)*, but the apparent role of the HIF-1A signalling pathway in the mechanism of metformin-stimulated glucose transporter expression and glucose uptake was unexpected. The observations that HIF-1A inhibitors decreased *Slc2a1* (GLUT1) expression and glucose uptake in both control and metformin treated cells suggests that GLUT mediated glucose uptake seems to be dependent on the HIF-1A signalling pathway (chapter 4). The results also

complement the RNA-seq data which identified upregulation of HIF1A signalling/target genes in metformin treated intestinal cultures.

7.1.3.1 Future directions

This results in chapter 5 suggest that metformin increases glucose uptake mediated by GLUT1 transporters, based on the RNA-seq data and examination of pharmacological inhibitors on glucose uptake. Generation of a GLUT1 knockout mouse intestinal organoid line is currently in progress. Studies investigating glucose transporter expression and glucose uptake involving GLUT1 knockout organoids would provide direct evidence of GLUT1 on glucose uptake.

Furthermore, the role of HIF1A on glucose utilisation in intestinal cells could be investigated using HIF1A inhibitors, HIF1A knockout mice, or mouse models of increased HIF1A stability (such as VHL knockout mice). This could strengthen the evidence in support of a role for HIF1A downstream of metformin action in intestinal cells.

Since the distal small intestine is predominantly associated with changes in glucose transporter expression in metformin treated HFD fed mice, it would also be important to replicate the experiments of glucose uptake in mouse ileal organoids.

7.1.4. Metformin limits the metabolic plasticity of intestinal cells

Although the evidence for metformin action on intestinal glucose uptake is well established based on PET-CT scan observations, the effects on glucose handling in the small intestine are not fully understood since there is evidence supporting both altered intestinal glucose metabolism as well as basal-to-apical export of glucose into the lumen via GLUT2 expression on the brush-border membrane *(207, 488, 523)*. The results from chapter 6 in this study support the RNA-seq data, showing that metformin increases glucose metabolism through glycolysis and lactate production/secretion as an indirect consequence of inhibiting OXPHOS. Indeed, the results from Perceval imaging measurements suggest that intestinal cells exhibit metabolic flexibility of glutamine, pyruvate (generated from glycolysis) and glycogen metabolism, which is lost in metformin treated cells as they rely almost solely on glycolysis (and very limited oxidation of fatty acids) for ATP synthesis.

Recent studies involving metabolomics measurements of arterial-venous differences in pigs revealed that visceral organs (including the GI tract) are the biggest consumers of glucose (60%) and amino acids *(186)*. Furthermore, orally administered metformin also accumulates at the highest concentrations in the GI tract; these concentrations are high enough to inhibit mitochondrial respiration *(204, 312)*. Furthermore, Schommers *et al.,* used metabolic tracing in HFD-fed mice to

demonstrate that metformin increases glucose metabolism to lactate in the intestine as a result of mitochondrial dysfunction *(207)*. These studies provide in vivo evidence in support of our observations in intestinal 2D cultures in suggesting the importance of intestinal glucose metabolism in metformin action.

The effects of metformin in increasing fasting plasma lactate levels are well established, and lactic acidosis is a side effect in a small number of patients associated with metformin use *(45, 594)*. However, the underlying physiological mechanisms are not clear. The kidney was thought to be involved due to the clinical observations that the risk of lactic acidosis was more closely associated with metformin use in patients with acute kidney injury *(312, 595)*. The liver was another candidate since inhibition of the glycerolphosphate shuttle by metformin has been associated with reduced metabolism of lactate to glucose via gluconeogenesis, which would instead lead to the release of lactate by the liver *(226)*. The exact mechanisms that explain the effects of metformin on lactic acidosis are therefore not completely understood. In pigs, the spleen and the colon made the largest contributions to net lactate release into the circulation whereas the liver and kidneys were associated with net lactate uptake under physiological conditions *(186)*. Oral metformin administration has been associated with increased lactate generation in the walls of the small intestine in mice and human intestinal tissues *(64, 207, 370)*. It remains to be demonstrated how much the GI tract contributes to lactate generation during metformin administration, and studies into the contributions of different organs in lactate generation in metformin treatment are warranted.

7.1.4.1 Future directions

This study provides evidence to support the observations from the KEGG pathway analysis through live cell imaging of metabolites and Seahorse bioanalyser assays in 2D monolayer cultures. As mentioned in section 7.1.1.1, a metabolomics approach to study the effects of metformin in intestinal cells would provide the most direct evidence to support the observations that metformin alters nutrient metabolism. Another warranted investigation is to examine the contributions of glucose metabolism and lactate production by the small intestine in contributing to the glucose lowering effects of metformin. Currently, collaborations are underway with Professor Jens Holst (University of Coppenhagen, Denmark) to examine mechanisms of metformin treatment on glucose metabolism and lactate release in the perfused intestine model. Validation of this technique to study glucose metabolism could enable more detailed investigations into the signalling mechanisms and metabolic alterations affected by metformin in intestinal tissues in a more physiological setting.

As an extension from chapter 3 and 5, the contributions of the various cellular pathways such as AMPK and HIF1A signalling to the changes of glucose metabolism in metformin treated cells should also be investigated using the Seahorse bioanalyser or Perceval/Peredox imaging of intracellular metabolites.

7.2 Limitations of this study

One of the limitations of this study is the use of the 2D monolayer culture system involving intestinal cells seeded in Matrigel-coated dishes/plates to investigate the transcriptomic and functional changes triggered by metformin in intestinal cells. Although these intestinal cultures do not alter the specifications of cell-types in the intestine (the presence of goblet cells and enteroendocrine cells is maintained, and GLP-1 secretion has been reported using this model), the intestinal cells in this culture system lose apical-basolateral polarity *(324, 596)*. This limits the ability to study the roles of SGLT1 and GLUT2 in transepithelial transport, which could not be investigated using this model. Future studies could incorporate transport studies using monolayers seeded into transwell systems, which maintain this apical-basolateral polarity *(597, 598)*. However, using the transwell system also limits the ability to study other aspects of intestinal function, such as nutrient metabolism via live-cell imaging and Seahorse bioanalyser assays. The effects of metformin on the mRNA expression of glucose transporters and Gdf15 in the intestinal 2D monolayer culture model were also validated in intestinal tissues of HFD-fed mice, which suggests that some of these observations in vitro might not be too different from the intestinal epithelia in vivo.

Another limitation in this study is that the RNA-seq data was generated using murine intestinal cells from organoids. Transcriptomic observations performed in human intestinal cells are likely to be different. This was the case in investigating the effects of metformin in hepatocytes since genes encoding the glucose-6-phosphatase (G6pc) isoforms were amongst the top downregulated genes identified in hepatocytes from db/db mice treated with metformin but were not differentially expressed in human hepatocyte cultures *(365, 599)*. Furthermore, the transcriptomic changes observed in mouse organs and tissues after RYGB surgery in mice were only partially replicated in humans *(42)*. Future experiments should replicate and validate the experiments in human organoids in 2D cultures, which have recently been established in our laboratory.

7.3. Other considerations into metformin action in the GI tract

7.3.1. The physiological effects of metformin: the liver or the gut?

This study suggests that the GI tract is an important site of metformin action in the regulation of glycaemic control and body weight. The results from this study support other findings in suggesting that accumulation of metformin at high concentrations in intestinal cells increased intestinal glucose utilisation and GDF-15 secretion, both of which probably involve the mitochondria. Metformin also inhibits hepatic glucose production in the liver to regulate blood glucose levels *(210, 220, 225–227, 544)*. However, several recent studies reported an opposite effect of increasing hepatic glucose production by metformin *(207, 228)*. Particularly, Schommers *et al.,* demonstrated that lactate generated from intestinal glycolysis is taken up by the liver for gluconeogenesis *(207)*. Clinical trials involving the "delayed-release" formulation of metformin also seem to suggest a more important role of the gut compared to the liver in mediating the glycaemic control effects of metformin *(86, 319, 320)*. Moreover, although the liver is capable of inducing *Gdf15* expression in primary hepatocytes in response to supraphysiological metformin concentrations in culture, *Gdf15* expression was induced in the distal intestine, but not in the liver of HFD-fed mice given metformin for 6 hours or 11 days *(321)*. This observation suggests that the small intestine, rather than the liver, is the primary organ that releases GDF-15 in response to metformin to mediate its weight-loss effects *(321)*.

7.3.2. Metformin stimulated GDF-15 secretion and glucose utilisation- all of the cells?

Two of the key findings presented in this study are the roles of metformin in stimulating GDF-15 secretion and increasing glucose uptake and glycolysis which may explain the roles of metformin in weight loss and glycaemic control, respectively. The imaging experiments and other in vitro assays did not specify whether all, or some of the intestinal cells are involved. It would be interesting to investigate whether the same effects of metformin occur in every cell type in the small intestinal epithelium or in a specialised group of cells. As discussed in chapter 4 and in section 7.1.2, in-situ hybridisation experiments in mouse colonic tissues suggest that cells situated predominantly in the crypts are involved in metformin induced *Gdf15* expression *(321)*. This suggests that some, but not all of the intestinal cells in the small intestine and colon respond with induction of *Gdf15* expression. Although GLUT1 expression is generally low in the small intestine, it is unknown how GLUT1 expression changes in the small intestine in response to metformin and this should be investigated via in-situ hybridisation.

7.3.3 Are the mechanisms of metformin action in the gut the same as those following bariatric surgery?

Bariatric surgery greatly improves glycaemic control and causes profound weight loss. Like metformin, the alimentary limb of the small intestine also exhibits upregulated HIF1A and GLUT1 expression, and increased glucose uptake and glycolysis after RYGB surgery *(42, 43)*. Increased intestinal glucose utilisation after RYGB has also been reported to contribute to its glucose-lowering effects *(43, 600)*. Other gastrointestinal changes during metformin treatment and after gastric bypass exhibit a number of similarities. First, metformin and RYGB cause altered bile acid metabolism, although this is due to reconstruction of the GI tract in bariatric surgery as opposed to reduced intestinal reabsorption of bile acids by metformin *(601)*. Second, like metformin, RYGB surgery decreases glucose absorption and postrandial glucose response in humans, which has been reported to associate with diversion of bile and decreasing the amount of sodium usually brought about with bile transit in the intestines, which decreases sodium dependent glucose cotransport *(602)*. Third, metformin and bariatric surgery increased circulating GLP-1 and PYY levels, likely due to a relative shift of glucose absorption to the distal gut *(41)*. Fourth, both metformin and RYGB cause changes in the gut microbiome *(603)*. Furthermore, serum levels of GDF-15 were significantly elevated after 2 weeks in a cohort of 47 obese patients that had undergone RYGB surgery *(604)*. However, by contrast to the crucial role of the GDF-15/GFRAL axis in mediating the weight loss effects of metformin from food intake studies in knockout mice, GDF-15 does not seem to be necessary for mediating the weight loss effects after bariatric surgery in mice *(321, 605)*. Unlike bariatric surgery, the clinical trials investigating the effects of metformin on body weight did not report consistent weight loss across all of the studies *(32, 81)*. There are no clinical trials to date that compared the effects of metformin and bariatric surgery interventions on glycaemic control. It would be tempting to speculate that some of the effects of metformin in the gut are similar to, but more modest than, those observed after bariatric surgery.

7.4. Concluding remarks

This PhD thesis has provided a comprehensive transcriptomic characterisation of metformin action in small intestinal cells, which was used as a basis to study functional mechanisms of metformin action. Metformin caused transcriptomic changes in metabolism and signalling pathways in intestinal cells. Metformin also robustly stimulated GDF-15 secretion in intestinal cells via a mechanism dependent on mitochondrial stress, the integrated stress response and the HIF-1A signalling pathway. Increased basal intestinal glucose uptake mediated by metformin could be associated with upregulation of GLUT transporters by a mechanism that could involve AMPK and HIF-1A signalling. By inhibiting mitochondrial respiration, metformin limits the metabolic plasticity of intestinal cells, which instead rely predominantly on glycolysis for energy. Together, the results of this thesis argue for the role of

the GI tract in mediating the effects of metformin in the control of blood glucose levels and body weight.

References

1. World Health Organisation (2014).

2. World Health Organisation (2016).

3. J. E. Manson, W. C. Willett, S. Liu, C. G. Solomon, G. Colditz, F. B. Hu, M. J. Stampfer, Diet, Lifestyle, and the Risk of Type 2 Diabetes Mellitus in Women, *Obstet. Gynecol. Surv.* (2003), doi:10.1097/00006254-200203000-00018.

4. S. N. Bhupathiraju, F. B. Hu, Epidemiology of obesity and diabetes and their cardiovascular complications, *Circ. Res.* (2016), doi:10.1161/CIRCRESAHA.115.306825.

5. J. M. Chan, E. B. Rimm, G. A. Colditz, M. J. Stampfer, W. C. Willett, Obesity, fat distribution, and weight gain as risk factors for clinical diabetes in men., *Diabetes Care* **17**, 961–9 (1994).

6. G. A. Colditz, W. C. Willett, A. Rotnitzky, J. E. Manson, Weight gain as a risk factor for clinical diabetes mellitus in women, *Ann. Intern. Med.* (1995), doi:10.7326/0003-4819-122-7-199504010-00001.

7. K. G. M. M. Alberti, R. H. Eckel, S. M. Grundy, P. Z. Zimmet, J. I. Cleeman, K. A. Donato, J. C. Fruchart, W. P. T. James, C. M. Loria, S. C. Smith, Harmonizing the metabolic syndrome: A joint interim statement of the international diabetes federation task force on epidemiology and prevention; National heart, lung, and blood institute; American heart association; World heart federation; International atherosclerosis society; And international association for the study of obesity*Circulation* (2009), doi:10.1161/CIRCULATIONAHA.109.192644.

8. P. A. Dyson, The therapeutics of lifestyle management on obesity*Diabetes, Obes. Metab.* (2010), doi:10.1111/j.1463-1326.2010.01256.x.

9. A. Liebl, K. Khunti, D. Orozco-Beltran, J. F. Yale, Health economic evaluation of type 2 diabetes mellitus: A clinical practice focused review*Clin. Med. Insights Endocrinol. Diabetes* (2015), doi:10.4137/CMED.S20906.

10. R. A. Defronzo, in *Diabetes*, (2009), vol. 58, pp. 773–795.

11. 2. Classification and diagnosis of diabetes, *Diabetes Care* (2015), doi:10.2337/dc15-S005.

12. P. González-Muniesa, M.-A. Mártinez-González, F. B. Hu, J.-P. Després, Y. Matsuzawa, R. J. F Loos, L. A. Moreno, G. A. Bray, J. Alfredo Martinez, Obesity, *Nat. Rev. Dis. Prim.* **3** (2017), doi:10.1038/nrdp.2017.34.

13. G. I. Shulman, Ectopic fat in insulin resistance, dyslipidemia, and cardiometabolic disease., *N. Engl. J. Med.* **371**, 2237–8 (2014).

14. A. A. Tahrani, A. H. Barnett, C. J. Bailey, Pharmacology and therapeutic implications of current drugs for type 2 diabetes mellitus., *Nat. Rev. Endocrinol.* **12**, 566–92 (2016).

15. K. Maedler, R. D. Carr, D. Bosco, R. A. Zuellig, T. Berney, M. Y. Donath, Sulfonylurea induced beta-cell apoptosis in cultured human islets., *J. Clin. Endocrinol. Metab.* **90**, 501–6 (2005).

16. S. E. Kahn, S. M. Haffner, M. A. Heise, W. H. Herman, R. R. Holman, N. P. Jones, B. G. Kravitz, J. M. Lachin, M. C. O'Neill, B. Zinman, G. Viberti, Glycemic Durability of Rosiglitazone, Metformin, or Glyburide Monotherapy, *N. Engl. J. Med.* **355**, 2427–2443 (2006).

17. R. C. Turner, C. A. Cull, V. Frighi, R. R. Holman, Glycemic control with diet, sulfonylurea, metformin, or insulin in patients with type 2 diabetes mellitus: progressive requirement for multiple therapies (UKPDS 49). UK Prospective Diabetes Study (UKPDS) Group., *JAMA* **281**, 2005–12 (1999).

18. D. E. DeWitt, I. B. Hirsch, Outpatient Insulin Therapy in Type 1 and Type 2 Diabetes Mellitus: Scientific Review*J. Am. Med. Assoc.* (2003), doi:10.1001/jama.289.17.2254.

19. C. K. Boughton, R. Hovorka, Advances in artificial pancreas systems, *Sci. Transl. Med.* (2019), doi:10.1126/scitranslmed.aaw4949.

20. C. Mathieu, P. Gillard, K. Benhalima, Insulin analogues in type 1 diabetes mellitus: Getting better all the time*Nat. Rev. Endocrinol.* (2017), doi:10.1038/nrendo.2017.39.

21. M. A. Nauck, E. Homberger, E. G. Siegel, R. C. Allen, R. P. Eaton, R. Ebert, W. Creutzfeldt, Incretin effects of increasing glucose loads in man calculated from venous insulin and C-peptide responses., *J. Clin. Endocrinol. Metab.* **63**, 492–8 (1986).

22. H. Elrick, L. Stimmler, C. J. Hlad, Y. Arai, PLASMA INSULIN RESPONSE TO ORAL AND INTRAVENOUS GLUCOSE, *J Clin Endocrinol Metab* (1964), doi:http://dx.doi.org/10.1210/jcem-24-10-1076.

23. L. Van Gaal, E. Dirinck, Pharmacological Approaches in the Treatment and Maintenance of Weight Loss., *Diabetes Care* **39 Suppl 2**, S260-7 (2016).

24. P. M. O'Neil, S. R. Smith, N. J. Weissman, M. C. Fidler, M. Sanchez, J. Zhang, B. Raether, C. M. Anderson, W. R. Shanahan, Randomized placebo-controlled clinical trial of lorcaserin for weight loss in type 2 diabetes mellitus: the BLOOM-DM study., *Obesity (Silver Spring).* **20**, 1426–36 (2012).

25. S. R. Smith, M. Sanchez, E. Chuang, W. R. Shanahan, C. M. Anderson, H. Bays, N. J. Weissman, S.

Stubbe, Multicenter, Placebo-Controlled Trial of Lorcaserin for Weight Management, *N. Engl. J. Med.* (2010), doi:10.1056/nejmoa0909809.

26. N. T. Nguyen, J. E. Varela, Bariatric surgery for obesity and metabolic disorders: State of the art*Nat. Rev. Gastroenterol. Hepatol.* (2017), doi:10.1038/nrgastro.2016.170.

27. L. Sjöström, A.-K. Lindroos, M. Peltonen, J. Torgerson, C. Bouchard, B. Carlsson, S. Dahlgren, B. Larsson, K. Narbro, C. D. Sjöström, M. Sullivan, H. Wedel, Swedish Obese Subjects Study Scientific Group, Lifestyle, diabetes, and cardiovascular risk factors 10 years after bariatric surgery., *N. Engl. J. Med.* **351**, 2683–93 (2004).

28. C. L.M.S., P. M., A. S., A. Å., B. C., C. B., J. P., L. H., M. C., N. I., P. C., R. S., S. K., S. E., W. H., S. P.-A., S. L., L. M. S. Carlsson, M. Peltonen, S. Ahlin, A. Anveden, C. Bouchard, B. Carlsson, P. Jacobson, H. Lonroth, C. Maglio, I. Naslund, C. Pirazzi, S. Romeo, K. Sjoholm, E. Sjostrom, H. Wedel, P.-A. Svensson, L. Sjostrom, Bariatric surgery and prevention of type 2 diabetes in Swedish obese subjects, *N. Engl. J. Med.* (2012), doi:10.1056/NEJMoa1112082.

29. L. Sjostrom, Review of the key results from the Swedish Obese Subjects (SOS) trial - a prospective controlled intervention study of bariatric surgery, *J. Intern. Med.* (2013), doi:10.1111/joim.12012.

30. L. Sjöström, K. Narbro, C. D. Sjöström, K. Karason, B. Larsson, H. Wedel, T. Lystig, M. Sullivan, C. Bouchard, B. Carlsson, C. Bengtsson, S. Dahlgren, A. Gummesson, P. Jacobson, J. Karlsson, A.-K. Lindroos, H. Lönroth, I. Näslund, T. Olbers, K. Stenlöf, J. Torgerson, G. Ågren, L. M. S. Carlsson, Effects of Bariatric Surgery on Mortality in Swedish Obese Subjects, *N. Engl. J. Med.* (2007), doi:10.1056/nejmoa066254.

31. A. P. Courcoulas, N. J. Christian, S. H. Belle, P. D. Berk, D. R. Flum, L. Garcia, M. Horlick, M. A. Kalarchian, W. C. King, J. E. Mitchell, E. J. Patterson, J. R. Pender, A. Pomp, W. J. Pories, R. C. Thirlby, S. Z. Yanovski, B. M. Wolfe, Weight change and health outcomes at 3 years after bariatric surgery among individuals with severe obesity, *JAMA - J. Am. Med. Assoc.* (2013), doi:10.1001/jama.2013.280928.

32. A. D. Miras, C. W. Le Roux, Mechanisms underlying weight loss after bariatric surgery*Nat. Rev. Gastroenterol. Hepatol.* (2013), doi:10.1038/nrgastro.2013.119.

33. S. N. Karamanakos, K. Vagenas, F. Kalfarentzos, T. K. Alexandrides, Weight loss, appetite suppression, and changes in fasting and postprandial ghrelin and peptide-yy levels after roux-en-y gastric bypass and sleeve gastrectomy a prospective, double blind study, *Ann. Surg.* (2008), doi:10.1097/SLA.0b013e318156f012.

34. K. Chandarana, C. Gelegen, E. Karra, A. I. Choudhury, M. E. Drew, V. Fauveau, B. Viollet, F. Andreelli, D. J. Withers, R. L. Batterham, Diet and gastrointestinal bypass-induced weight loss: the roles of ghrelin and peptide YY., *Diabetes* **60**, 810–8 (2011).

35. R. L. Batterham, D. E. Cummings, Mechanisms of diabetes improvement following bariatric/metabolic surgery, *Diabetes Care* (2016), doi:10.2337/dc16-0145.

36. F. Rubino, A. Forgione, D. E. Cummings, M. Vix, D. Gnuli, G. Mingrone, M. Castagneto, J. Marescaux, The mechanism of diabetes control after gastrointestinal bypass surgery reveals a role of the proximal small intestine in the pathophysiology of type 2 diabetes., *Ann. Surg.* **244**, 741–9 (2006).

37. F. Rubino, P. Zizzari, C. Tomasetto, M.-T. Bluet-Pajot, A. Forgione, M. Vix, D. Grouselle, J. Marescaux, The role of the small bowel in the regulation of circulating ghrelin levels and food intake in the obese Zucker rat., *Endocrinology* **146**, 1745–51 (2005).

38. M. Salehi, R. L. Prigeon, D. A. D'Alessio, Gastric bypass surgery enhances glucagon-like peptide 1-stimulated postprandial insulin secretion in humans, *Diabetes* (2011), doi:10.2337/db11-0203.

39. C. Dirksen, D. L. Hansen, S. Madsbad, L. E. Hvolris, L. S. Naver, J. J. Holst, D. Worm, Postprandial diabetic glucose tolerance is normalized by gastric bypass feeding as opposed to gastric feeding and is associated with exaggerated GLP-1 secretion: A case report, *Diabetes Care* (2010), doi:10.2337/dc09-1374.

40. A. P. Chambers, L. Jessen, K. K. Ryan, S. Sisley, H. E. Wilson-Pérez, M. A. Stefater, S. G. Gaitonde, J. E. Sorrell, M. Toure, J. Berger, D. A. D'Alessio, S. C. Woods, R. J. Seeley, D. A. Sandoval, Weight-independent changes in blood glucose homeostasis after gastric bypass or vertical sleeve gastrectomy in rats., *Gastroenterology* **141**, 950–8 (2011).

41. P. Larraufie, G. P. Roberts, A. K. McGavigan, R. G. Kay, J. Li, A. Leiter, A. Melvin, E. K. Biggs, P. Ravn, K. Davy, D. C. Hornigold, G. S. H. Yeo, R. H. Hardwick, F. Reimann, F. M. Gribble, Important Role of the GLP-1 Axis for Glucose Homeostasis after Bariatric Surgery, *Cell Rep.* (2019), doi:10.1016/j.celrep.2019.01.047.

42. D. Ben-Zvi, L. Meoli, W. M. Abidi, R. C. Anafi, A. P. Courcoulas, N. Stylopoulos Correspondence, E. Nestoridi, C. Panciotti, E. Castillo, P. Pizarro, E. Shirley, W. F. Gourash, C. C. Thompson, R. Munoz, C. B. Clish, N. Stylopoulos, Time-Dependent Molecular Responses Differ between Gastric Bypass and Dieting but Are Conserved Across Species Cell Metabolism Resource Time-Dependent Molecular Responses Differ between Gastric Bypass and Dieting but Are Conserved Across Species, *Cell Metab.*

28, 310-323.e6 (2018).

43. J.-B. Cavin, A. Couvelard, R. Lebtahi, R. Ducroc, K. Arapis, E. Voitellier, F. Cluzeaud, L. Gillard, M. Hourseau, N. Mikail, L. Ribeiro-Parenti, N. Kapel, J.-P. Marmuse, A. Bado, M. Le Gall, Differences in Alimentary Glucose Absorption and Intestinal Disposal of Blood Glucose After Roux-en-Y Gastric Bypass vs Sleeve Gastrectomy, *Gastroenterology* **150**, 454-464.e9 (2016).

44. UK Prospective Diabetes Study (UKPDS) Group, Effect of intensive blood-glucose control with metformin on complications in overweight patients with type 2 diabetes (UKPDS 34), *Lancet* (2002), doi:10.1016/s0140-6736(98)07037-8.

45. E. Sanchez-Rangel, S. E. Inzucchi, Metformin: clinical use in type 2 diabetes*Diabetologia* (2017), doi:10.1007/s00125-017-4336-x.

46. C. J. Bailey, C. Day, Metformin: Its botanical background, *Pract. Diabetes Int.* (2004), doi:10.1002/pdi.606.

47. C. J. Bailey, Metformin: historical overview*Diabetologia* (2017), doi:10.1007/s00125-017-4318-z.

48. C. K. WATANABE, STUDIES IN THE METABOLIC CHANGES INDUCED BY THE ADMINISTRATION OF GUANIDINE BASES, *J. Biol. Chem.* , 253–265 (1917).

49. E. A. Werner, J. Bell, CCXIV. - The preparation of methylguanidine, and of ββ- dimethylguanidine by the interaction of dicyanodiamide, and methylammonium and dimethylammonium chlorides respectively, *J. Chem. Soc. Trans.* (1922), doi:10.1039/CT9222101790.

50. K. H. Slotta, R. Tschesche, Über Biguanide, II.: Die blutzucker-senkende Wirkung der Biguanide, *Berichte der Dtsch. Chem. Gesellschaft (A B Ser.* (1929), doi:10.1002/cber.19290620605.

51. E. Hesse, G. Taubmann, Die Wirkung des Biguanids und seiner Derivate auf den Zuckerstoffwechsel, *Arch. für Exp. Pathol. und Pharmakologie* (1929), doi:10.1007/BF02000097.

52. J. STERNE, [Blood sugar-lowering effect of 1,1-dimethylbiguanide]., *Therapie* **13**, 650–9 (1958).

53. G. UNGAR, L. FREEDMAN, S. L. SHAPIRO, Pharmacological studies of a new oral hypoglycemic drug., *Proc. Soc. Exp. Biol. Med.* **95**, 190–2 (1957).

54. A. BERINGER, [Treatment of diabetes mellitus with biguanides]., *Wien. Med. Wochenschr.* **108**, 880–2 (1958).

55. J. B. McKendry, K. Kuwayti, P. P. Rado, Clinical experience with DBI (phenformin) in the management of diabetes., *Can. Med. Assoc. J.* (1959).

56. D. Luft, R. M. Schmülling, M. Eggstein, Lactic acidosis in biguanide-treated diabetics - A review of 330 cases, *Diabetologia* (1978), doi:10.1007/BF01263444.

57. R. S. WALKER, A. L. LINTON, Phenethyldiguanide: a dangerous side-effect., *Br. Med. J.* **2**, 1005–6 (1959).

58. The University Group Diabetes Program. A study of the effects of hypoglycemic agents on vascular complications in patients with adult-onset diabetes. V. Evaluation of pheniformin therapy., *Diabetes* **24 Suppl 1**, 65–184 (1975).

59. O. Jalling, C. Olsen, The effects of metformin compared to the effects of phenformin on the lactate production and the metabolism of isolated parenchymal rat liver cell., *Acta Pharmacol. Toxicol. (Copenh).* **54**, 327–32 (1984).

60. N. Wollen, C. J. Bailey, Inhibition of hepatic gluconeogenesis by metformin. Synergism with insulin., *Biochem. Pharmacol.* **37**, 4353–8 (1988).

61. C. J. Bailey, J. A. Puah, Effect of metformin on glucose metabolism in mouse soleus muscle., *Diabete Metab.* (1986).

62. L. S. Hermann, Metformin: a review of its pharmacological properties and therapeutic use., *Diabete Metab.* **5**, 233–45 (1979).

63. I. W. Campbell, H. C. S. Howlett, Worldwide Experience of Metformin as an Effective Glucose-lowering Agent: A Meta-analysis, *Diabetes. Metab. Rev.* (1995), doi:10.1002/dmr.5610110509.

64. C. J. Bailey, C. Wilcock, C. Day, Effect of metformin on glucose metabolism in the splanchnic bed., *Br. J. Pharmacol.* **105**, 1009–13 (1992).

65. R. A. DeFronzo, A. M. Goodman, Efficacy of metformin in patients with non-insulin-dependent diabetes mellitus. The Multicenter Metformin Study Group., *N. Engl. J. Med.* (1995), doi:10.1056/NEJM199508313330902.

66. A. J. Garber, T. G. Duncan, A. M. Goodman, D. J. Mills, J. L. Rohlf, Efficacy of metformin in type II diabetes: Results of a double-blind, placebo-controlled, dose-response trial, *Am. J. Med.* **103**, 491–497 (1997).

67. M. G. Wulffelé, A. Kooy, P. Lehert, D. Bets, J. C. Ogterop, B. Borger van der Burg, A. J. M. Donker, C. D. A. Stehouwer, Combination of insulin and metformin in the treatment of type 2 diabetes., *Diabetes Care* **25**, 2133–40 (2002).

68. H. Yki-Järvinen, L. Ryysy, K. Nikkilä, T. Tulokas, R. Vanamo, M. Heikkilä, Comparison of bedtime

insulin regimens in patients with type 2 diabetes mellitus. A randomized, controlled trial., *Ann. Intern. Med.* **130**, 389–96 (1999).

69. S. E. Inzucchi, D. G. Maggs, G. R. Spollett, S. L. Page, F. S. Rife, V. Walton, G. I. Shulman, Efficacy and Metabolic Effects of Metformin and Troglitazone in Type II Diabetes Mellitus, *N. Engl. J. Med.* **338**, 867–873 (1998).

70. J. Rosenstock, L. Chuck, M. González-Ortiz, K. Merton, J. Craig, G. Capuano, R. Qiu, Initial Combination Therapy With Canagliflozin Plus Metformin Versus Each Component as Monotherapy for Drug-Naïve Type 2 Diabetes., *Diabetes Care* **39**, 353–62 (2016).

71. C. J. Bailey, J. L. Gross, A. Pieters, A. Bastien, J. F. List, Effect of dapagliflozin in patients with type 2 diabetes who have inadequate glycaemic control with metformin: a randomised, double-blind, placebo-controlled trial., *Lancet (London, England)* **375**, 2223–33 (2010).

72. E. Søfteland, J. J. Meier, B. Vangen, R. Toorawa, M. Maldonado-Lutomirsky, U. C. Broedl, Empagliflozin as Add-on Therapy in Patients With Type 2 Diabetes Inadequately Controlled With Linagliptin and Metformin: A 24-Week Randomized, Double-Blind, Parallel-Group Trial., *Diabetes Care* **40**, 201–209 (2017).

73. I. Vardarli, E. Arndt, C. F. Deacon, J. J. Holst, M. A. Nauck, Effects of Sitagliptin and Metformin Treatment on Incretin Hormone and Insulin Secretory Responses to Oral and “Isoglycemic” Intravenous Glucose, *Diabetes* **63**, 663–674 (2014).

74. R. Scott, T. Loeys, M. J. Davies, S. S. Engel, Sitagliptin Study 801 Group, Efficacy and safety of sitagliptin when added to ongoing metformin therapy in patients with type 2 diabetes., *Diabetes. Obes. Metab.* **10**, 959–69 (2008).

75. C. F. Deacon, E. Mannucci, B. Ahrén, Glycaemic efficacy of glucagon-like peptide-1 receptor agonists and dipeptidyl peptidase-4 inhibitors as add-on therapy to metformin in subjects with type 2 diabetes-a review and meta analysis., *Diabetes. Obes. Metab.* **14**, 762–7 (2012).

76. Diabetes Prevention Program Research Group, T. D. P. P. R. Diabetes Prevention Program Research Group, Long-term safety, tolerability, and weight loss associated with metformin in the Diabetes Prevention Program Outcomes Study., *Diabetes Care* **35**, 731–7 (2012).

77. Diabetes Prevention Program Research Group, 10-year follow-up of diabetes incidence and weight loss in the Diabetes Prevention Program Outcomes Study, *Lancet* (2009), doi:10.1016/S0140-6736(09)61457-4.

78. G. A. Bray, K. S. Polonsky, P. G. Watson, R. B. Goldberg, S. M. Haffner, R. F. Hamman, E. S. Horton,

S. F. Kahn, A. E. Kitabchi, B. E. Metzger, D. M. Nathan, J. M. Olefsky, F. X. Pi-Sunyer, M. J. Prince, R. E. Ratner, M. F. Saad, S. Dagogo Jack, C. D. Saudek, D. S. Schade, H. Shamoon, R. R. Wing, R. F. Arakaki, W. C. Krowler, R. Bain, S. M. Marcovina, P. M. Rautaharju, E. J. Mayer-Davis, D. H. O'Leary, E. R. Stamm, The Diabetes Prevention Program: Design and methods for a clinical trial in the prevention of type 2 diabetes*Diabetes Care* (1999), doi:10.2337/diacare.22.4.623.

79. N. D. D. P. P. R. G. Knowler WC, Barrett-Connor E, Fowler SE, Hamman RF, Lachin JM, Walker EA, Reduction in the incidence of type 2 diabetes with lifestyle intervention or metformin., *N. Engl. J. Med.* **346(6)**, 393–403 (2002).

80. V. R. Aroda, W. C. Knowler, J. P. Crandall, L. Perreault, S. L. Edelstein, S. L. Jeffries, M. E. Molitch, X. Pi-Sunyer, C. Darwin, B. M. Heckman-Stoddard, M. Temprosa, S. E. Kahn, D. M. Nathan, Metformin for diabetes prevention: insights gained from the Diabetes Prevention Program/Diabetes Prevention Program Outcomes Study*Diabetologia* (2017), doi:10.1007/s00125-017-4361-9.

81. A. Golay, Metformin and body weight*Int. J. Obes.* (2008), doi:10.1038/sj.ijo.0803695.

82. G. Viberti, S. E. Kahn, D. A. Greene, W. H. Herman, B. Zinman, R. R. Holman, S. M. Haffner, D. Levy, J. M. Lachin, R. A. Berry, M. A. Heise, N. P. Jones, M. I. Freed, A Diabetes Outcome Progression Trial (ADOPT): An international multicenter study of the comparative efficacy of rosiglitazone, glyburide, and metformin in recently diagnosed type 2 diabetes, *Diabetes Care* (2002), doi:10.2337/diacare.25.10.1737.

83. E. J. Bastyr, C. A. Stuart, R. G. Brodows, S. Schwartz, C. J. Graf, A. Zagar, K. E. Robertson, Therapy focused on lowering postprandial glucose, not fasting glucose, may be superior for lowering HbA1c. IOEZ Study Group., *Diabetes Care* **23(9)**, 1236–41 (2000).

84. M. Hanefeld, P. Brunetti, G. H. Schernthaner, D. R. Matthews, B. H. Charbonnel, QUARTET Study Group, One-year glycemic control with a sulfonylurea plus pioglitazone versus a sulfonylurea plus metformin in patients with type 2 diabetes., *Diabetes Care* **27**, 141–7 (2004).

85. J. Gerich, P. Raskin, L. Jean-Louis, D. Purkayastha, M. A. Baron, PRESERVE-beta: two-year efficacy and safety of initial combination therapy with nateglinide or glyburide plus metformin., *Diabetes Care* **28**, 2093–9 (2005).

86. R. A. DeFronzo, J. B. Buse, T. Kim, C. Burns, S. Skare, A. Baron, M. Fineman, Once-daily delayed-release metformin lowers plasma glucose and enhances fasting and postprandial GLP-1 and PYY: results from two randomised trials, *Diabetologia* **59**, 1645–1654 (2016).

87. K. A. Virtanen, K. Hällsten, R. Parkkola, T. Janatuinen, F. Lönnqvist, T. Viljanen, T. Rönnemaa, J.

Knuuti, R. Huupponen, P. Lönnroth, P. Nuutila, Differential effects of rosiglitazone and metformin on adipose tissue distribution and glucose uptake in type 2 diabetic subjects., *Diabetes* **52**, 283–90 (2003).

88. A. Fontbonne, M. A. Charles, I. Juhan-Vague, J. M. Bard, P. André, F. Isnard, J. M. Cohen, P. Grandmottet, P. Vague, M. E. Safar, E. Eschwège, The effect of metformin on the metabolic abnormalities associated with upper-body fat distribution. BIGPRO Study Group., *Diabetes Care* **19**, 920–6 (1996).

89. A. Gokcel, Y. Gumurdulu, H. Karakose, E. Melek Ertorer, N. Tanaci, N. BascilTutuncu, N. Guvener, Evaluation of the safety and efficacy of sibutramine, orlistat and metformin in the treatment of obesity., *Diabetes. Obes. Metab.* **4**, 49–55 (2002).

90. A. Saenz, A. Mataix, A. S. M, R. F. M, D. Moher, Metformin monotherapy for type 2 diabetes mellitus (Review), *Cochrane Database Syst Rev* (2013), doi:10.1002/14651858.CD002966.pub3.

91. K. Johansen, Efficacy of metformin in the treatment of NIDDM: Meta-analysis, *Diabetes Care* (1999), doi:10.2337/diacare.22.1.33.

92. S. J. Griffin, J. K. Leaver, G. J. Irving, Impact of metformin on cardiovascular disease: a meta-analysis of randomised trials among people with type 2 diabetes, *Diabetologia* **60**, 1620–1629 (2017).

93. J. E. Nestler, D. J. Jakubowicz, Decreases in ovarian cytochrome P450c17 alpha activity and serum free testosterone after reduction of insulin secretion in polycystic ovary syndrome., *N. Engl. J. Med.* **335**, 617–23 (1996).

94. J. E. Nestler, D. J. Jakubowicz, Lean women with polycystic ovary syndrome respond to insulin reduction with decreases in ovarian P450c17 alpha activity and serum androgens., *J. Clin. Endocrinol. Metab.* **82**, 4075–9 (1997).

95. R. S. Lindsay, M. R. Loeken, Metformin use in pregnancy: promises and uncertainties*Diabetologia* (2017), doi:10.1007/s00125-017-4351-y.

96. J. A. Rowan, W. M. Hague, W. Gao, M. R. Battin, M. P. Moore, Metformin versus Insulin for the Treatment of Gestational Diabetes, *N. Engl. J. Med.* **358**, 2003–2015 (2008).

97. B. M. Heckman-Stoddard, A. DeCensi, V. V. Sahasrabuddhe, L. G. Ford, Repurposing metformin for the prevention of cancer and cancer recurrence*Diabetologia* (2017), doi:10.1007/s00125-017-4372-6.

98. I. C. Lega, P. S. Shah, D. Margel, J. Beyene, P. A. Rochon, L. L. Lipscombe, The effect of metformin on mortality following canceramong patients with diabetes*Cancer Epidemiol. Biomarkers Prev.* (2014), doi:10.1158/1055-9965.EPI-14-0327.

99. A. DeCensi, M. Puntoni, P. Goodwin, M. Cazzaniga, A. Gennari, B. Bonanni, S. Gandini, Metformin and Cancer Risk in Diabetic Patients: A Systematic Review and Meta-analysis, *Cancer Prev. Res.* **3**, 1451–1461 (2010).

100. M. Franciosi, G. Lucisano, E. Lapice, G. F. M. Strippoli, F. Pellegrini, A. Nicolucci, Metformin therapy and risk of cancer in patients with type 2 diabetes: systematic review., *PLoS One* **8**, e71583 (2013).

101. R. J. Stevens, R. Ali, C. R. Bankhead, M. A. Bethel, B. J. Cairns, R. P. Camisasca, F. L. Crowe, A. J. Farmer, S. Harrison, J. A. Hirst, P. Home, S. E. Kahn, J. H. McLellan, R. Perera, A. Plüddemann, A. Ramachandran, N. W. Roberts, P. W. Rose, A. Schweizer, G. Viberti, R. R. Holman, Cancer outcomes and all-cause mortality in adults allocated to metformin: systematic review and collaborative meta-analysis of randomised clinical trials., *Diabetologia* **55**, 2593–2603 (2012).

102. Z. J. Zhang, S. Li, The prognostic value of metformin for cancer patients with concurrent diabetes: A systematic review and meta-analysis, *Diabetes, Obes. Metab.* (2014), doi:10.1111/dom.12267.

103. P. Zhang, H. Li, X. Tan, L. Chen, S. Wang, Association of metformin use with cancer incidence and mortality: a meta-analysis., *Cancer Epidemiol.* **37**, 207–18 (2013).

104. B. M. Heckman-Stoddard, S. Gandini, B. K. Dunn, E. Szabo, A. DeCensi, M. Puntoni, L. Ford, Metformin and Cancer Risk and Mortality: A Systematic Review and Meta-analysis Taking into Account Biases and Confounders, *Cancer Prev. Res.* (2014), doi:10.1158/1940-6207.capr-13-0424.

105. L. Wu, J. Zhu, L. J. Prokop, M. Hassan Murad, Pharmacologic Therapy of Diabetes and Overall Cancer Risk and Mortality: A Meta-Analysis of 265 Studies, *Sci. Rep.* (2015), doi:10.1038/srep10147.

106. B. Thakkar, K. N. Aronis, M. T. Vamvini, K. Shields, C. S. Mantzoros, Metformin and sulfonylureas in relation to cancer risk in type II diabetes patients: a meta-analysis using primary data of published studies., *Metabolism.* **62**, 922–34 (2013).

107. D. Soranna, L. Scotti, A. Zambon, C. Bosetti, G. Grassi, A. Catapano, C. La Vecchia, G. Mancia, G. Corrao, Cancer risk associated with use of metformin and sulfonylurea in type 2 diabetes: a meta-analysis., *Oncologist* **17**, 813–22 (2012).

108. H. Noto, A. Goto, T. Tsujimoto, M. Noda, Cancer risk in diabetic patients treated with

metformin: A systematic review and meta-analysis, *PLoS One* (2012), doi:10.1371/journal.pone.0033411.

109. A. M. Joshua, V. E. Zannella, M. R. Downes, B. Bowes, K. Hersey, M. Koritzinsky, M. Schwab, U. Hofmann, A. Evans, T. van der Kwast, J. Trachtenberg, A. Finelli, N. Fleshner, J. Sweet, M. Pollak, A pilot "window of opportunity" neoadjuvant study of metformin in localised prostate cancer., *Prostate Cancer Prostatic Dis.* **17**, 252–8 (2014).

110. S. Hadad, T. Iwamoto, L. Jordan, C. Purdie, S. Bray, L. Baker, G. Jellema, S. Deharo, D. G. Hardie, L. Pusztai, S. Moulder-Thompson, J. A. Dewar, A. M. Thompson, Evidence for biological effects of metformin in operable breast cancer: a pre-operative, window-of-opportunity, randomized trial., *Breast Cancer Res. Treat.* **128**, 783–94 (2011).

111. A. Mitsuhashi, T. Kiyokawa, Y. Sato, M. Shozu, Effects of metformin on endometrial cancer cell growth in vivo: a preoperative prospective trial., *Cancer* **120**, 2986–95 (2014).

112. V. N. Sivalingam, S. Kitson, R. McVey, C. Roberts, P. Pemberton, K. Gilmour, S. Ali, A. G. Renehan, H. C. Kitchener, E. J. Crosbie, Measuring the biological effect of presurgical metformin treatment in endometrial cancer., *Br. J. Cancer* **114**, 281–9 (2016).

113. K. M. Schuler, B. S. Rambally, M. J. DiFurio, B. P. Sampey, P. A. Gehrig, L. Makowski, V. L. Bae-Jump, Antiproliferative and metabolic effects of metformin in a preoperative window clinical trial for endometrial cancer., *Cancer Med.* **4**, 161–73 (2015).

114. B. Bonanni, M. Puntoni, M. Cazzaniga, G. Pruneri, D. Serrano, A. Guerrieri-Gonzaga, A. Gennari, M. S. Trabacca, V. Galimberti, P. Veronesi, H. Johansson, V. Aristarco, F. Bassi, A. Luini, M. Lazzeroni, C. Varricchio, G. Viale, P. Bruzzi, A. Decensi, Dual effect of metformin on breast cancer proliferation in a randomized presurgical trial., *J. Clin. Oncol.* **30**, 2593–600 (2012).

115. K. Hosono, H. Endo, H. Takahashi, M. Sugiyama, E. Sakai, T. Uchiyama, K. Suzuki, H. Iida, Y. Sakamoto, K. Yoneda, T. Koide, C. Tokoro, Y. Abe, M. Inamori, H. Nakagama, A. Nakajima, Metformin suppresses colorectal aberrant crypt foci in a short-term clinical trial, *Cancer Prev. Res.* (2010), doi:10.1158/1940-6207.CAPR-10-0186.

116. L. J. McCreight, C. J. Bailey, E. R. Pearson, Metformin and the gastrointestinal tract, *Diabetologia* **59**, 426–435 (2016).

117. T. Dujic, K. Zhou, L. A. Donnelly, R. Tavendale, C. N. A. Palmer, E. R. Pearson, Association of Organic Cation Transporter 1 With Intolerance to Metformin in Type 2 Diabetes: A GoDARTS Study, *Diabetes* **64**, 1786–1793 (2015).

118. A. Y. Dawed, K. Zhou, N. van Leeuwen, A. Mahajan, N. Robertson, R. Koivula, P. J. M. Elders, S. P. Rauh, A. G. Jones, R. W. Holl, J. C. Stingl, P. W. Franks, M. I. McCarthy, L. M. 't Hart, E. R. Pearson, IMI DIRECT Consortium, Variation in the Plasma Membrane Monoamine Transporter (PMAT) (Encoded by SLC29A4) and Organic Cation Transporter 1 (OCT1) (Encoded by SLC22A1) and Gastrointestinal Intolerance to Metformin in Type 2 Diabetes: An IMI DIRECT Study., *Diabetes Care* **42**, 1027–1033 (2019).

119. F. F. Richy, M. Sabidó-Espin, S. Guedes, F. A. Corvino, U. Gottwald-Hostalek, Incidence of lactic acidosis in patients with type 2 diabetes with and without renal impairment treated with metformin: a retrospective cohort study., *Diabetes Care* **37**, 2291–5 (2014).

120. J. de Jager, A. Kooy, P. Lehert, M. G. Wulffelé, J. van der Kolk, D. Bets, J. Verburg, A. J. M. Donker, C. D. A. Stehouwer, Long term treatment with metformin in patients with type 2 diabetes and risk of vitamin B-12 deficiency: randomised placebo controlled trial., *BMJ* **340**, c2181 (2010).

121. V. R. Aroda, S. L. Edelstein, R. B. Goldberg, W. C. Knowler, S. M. Marcovina, T. J. Orchard, G. A. Bray, D. S. Schade, M. G. Temprosa, N. H. White, J. P. Crandall, Diabetes Prevention Program Research Group, Long-term Metformin Use and Vitamin B12 Deficiency in the Diabetes Prevention Program Outcomes Study., *J. Clin. Endocrinol. Metab.* **101**, 1754–61 (2016).

122. K. Zhou, L. Donnelly, J. Yang, M. Li, H. Deshmukh, N. Van Zuydam, E. Ahlqvist, C. C. Spencer, L. Groop, A. D. Morris, H. M. Colhoun, P. C. Sham, M. I. McCarthy, C. N. A. Palmer, E. R. Pearson, Heritability of variation in glycaemic response to metformin: a genome-wide complex trait analysis, *Lancet Diabetes Endocrinol.* **2**, 481–487 (2014).

123. J. C. Florez, The pharmacogenetics of metformin*Diabetologia* (2017), doi:10.1007/s00125-017-4335-y.

124. K. A. Jablonski, J. B. McAteer, P. I. W. de Bakker, P. W. Franks, T. I. Pollin, R. L. Hanson, R. Saxena, S. Fowler, A. R. Shuldiner, W. C. Knowler, D. Altshuler, J. C. Florez, for the D. P. P. R. Diabetes Prevention Program Research Group, Common variants in 40 genes assessed for diabetes incidence and response to metformin and lifestyle intervention in the diabetes prevention program., *Diabetes* **59**, 2672–81 (2010).

125. K. GoDARTS and UKPDS Diabetes Pharmacogenetics Study Group, C. Wellcome Trust Case Control Consortium 2, K. Zhou, C. Bellenguez, C. C. A. Spencer, A. J. Bennett, R. L. Coleman, R. Tavendale, S. A. Hawley, L. A. Donnelly, C. Schofield, C. J. Groves, L. Burch, F. Carr, A. Strange, C. Freeman, J. M. Blackwell, E. Bramon, M. A. Brown, J. P. Casas, A. Corvin, N. Craddock, P. Deloukas, S. Dronov, A. Duncanson, S. Edkins, E. Gray, S. Hunt, J. Jankowski, C. Langford, H. S. Markus, C. G.

Mathew, R. Plomin, A. Rautanen, S. J. Sawcer, N. J. Samani, R. Trembath, A. C. Viswanathan, N. W. Wood, A. T. MAGIC investigators, L. W. Harries, A. T. Hattersley, A. S. F. Doney, H. Colhoun, A. D. Morris, C. Sutherland, D. G. Hardie, L. Peltonen, M. I. McCarthy, R. R. Holman, C. N. A. Palmer, P. Donnelly, E. R. Pearson, Common variants near ATM are associated with glycemic response to metformin in type 2 diabetes., *Nat. Genet.* **43**, 117–20 (2011).

126. S. W. Yee, L. Chen, K. M. Giacomini, The role of ATM in response to metformin treatment and activation of AMPK*Nat. Genet.* (2012), doi:10.1038/ng.2236.

127. J. C. Florez, K. A. Jablonski, A. Taylor, K. Mather, E. Horton, N. H. White, E. Barrett-Connor, W. C. Knowler, A. R. Shuldiner, T. I. Pollin, for the D. P. P. R. Diabetes Prevention Program Research Group, The C allele of ATM rs11212617 does not associate with metformin response in the Diabetes Prevention Program., *Diabetes Care* **35**, 1864–7 (2012).

128. N. van Leeuwen, G. Nijpels, M. L. Becker, H. Deshmukh, K. Zhou, B. H. C. Stricker, A. G. Uitterlinden, A. Hofman, E. van ’t Riet, C. N. A. Palmer, B. Guigas, P. E. Slagboom, P. Durrington, R. A. Calle, A. Neil, G. Hitman, S. J. Livingstone, H. Colhoun, R. R. Holman, M. I. McCarthy, J. M. Dekker, L. M. ’t Hart, E. R. Pearson, A gene variant near ATM is significantly associated with metformin treatment response in type 2 diabetes: a replication and meta-analysis of five cohorts., *Diabetologia* **55**, 1971–7 (2012).

129. K. Zhou, S. W. Yee, E. L. Seiser, N. van Leeuwen, R. Tavendale, A. J. Bennett, C. J. Groves, R. L. Coleman, A. A. van der Heijden, J. W. Beulens, C. E. de Keyser, L. Zaharenko, D. M. Rotroff, M. Out, K. A. Jablonski, L. Chen, M. Javorský, J. Židzik, A. M. Levin, L. K. Williams, T. Dujic, S. Semiz, M. Kubo, H.-C. Chien, S. Maeda, J. S. Witte, L. Wu, I. Tkáč, A. Kooy, R. H. N. van Schaik, C. D. A. Stehouwer, L. Logie, C. Sutherland, J. Klovins, V. Pirags, A. Hofman, B. H. Stricker, A. A. Motsinger-Reif, M. J. Wagner, F. Innocenti, L. M. ’t Hart, R. R. Holman, M. I. McCarthy, M. M. Hedderson, C. N. A. Palmer, J. C. Florez, K. M. Giacomini, E. R. Pearson, J. C. Florez, K. M. Giacomini, E. R. Pearson, Variation in the glucose transporter gene SLC2A2 is associated with glycemic response to metformin, *Nat. Genet.* **48**, 1055–1059 (2016).

130. W. Rathmann, K. Strassburger, B. Bongaerts, O. Kuss, K. Müssig, V. Burkart, J. Szendroedi, J. Kotzka, B. Knebel, H. Al-Hasani, M. Roden, for the G. Group, A variant of the glucose transporter gene SLC2A2 modifies the glycaemic response to metformin therapy in recently diagnosed type 2 diabetes, *Diabetologia* **62**, 286–291 (2019).

131. Y. Shu, S. A. Sheardown, C. Brown, R. P. Owen, S. Zhang, R. A. Castro, A. G. Ianculescu, L. Yue, J. C. Lo, E. G. Burchard, C. M. Brett, K. M. Giacomini, Effect of genetic variation in the organic cation

transporter 1 (OCT1) on metformin action, *J. Clin. Invest.* **117**, 1422–1431 (2007).

132. Y. Shu, M. K. Leabman, B. Feng, L. M. Mangravite, C. C. Huang, D. Stryke, M. Kawamoto, S. J. Johns, J. DeYoung, E. Carlson, T. E. Ferrin, I. Herskowitz, K. M. Giacomini, Pharmacogenetics Of Membrane Transporters Investigators, Evolutionary conservation predicts function of variants of the human organic cation transporter, OCT1., *Proc. Natl. Acad. Sci. U. S. A.* **100**, 5902–7 (2003).

133. R. Kerb, U. Brinkmann, N. Chatskaia, D. Gorbunov, V. Gorboulev, E. Mornhinweg, A. Keil, M. Eichelbaum, H. Koepsell, Identification of genetic variations of the human organic cation transporter hOCT1 and their functional consequences., *Pharmacogenetics* **12**, 591–5 (2002).

134. J. Gram, J. E. Henriksen, E. Grodum, H. Juhl, T. B. Hansen, C. Christiansen, K. Yderstræde, H. Gjessing, H. M. Hansen, V. Vestergaard, J. Hangaard, H. Beck-Nielsen, Pharmacological treatment of the pathogenetic defects in type 2 diabetes: the randomized multicenter South Danish Diabetes Study., *Diabetes Care* **34**, 27–33 (2011).

135. E. I. O. Sundelin, L. C. Gormsen, J. B. Jensen, M. H. Vendelbo, S. Jakobsen, O. L. Munk, M. M. H. Christensen, K. Brøsen, J. Frøkiær, N. Jessen, Genetic Polymorphisms in Organic Cation Transporter 1 Attenuates Hepatic Metformin Exposure in Humans, *Clin. Pharmacol. Ther.* (2017), doi:10.1002/cpt.701.

136. M. L. Becker, L. E. Visser, R. H. N. N. van Schaik, A. Hofman, A. G. Uitterlinden, B. H. C. C. Stricker, Genetic variation in the organic cation transporter 1 is associated with metformin response in patients with diabetes mellitus, **9**, 242–247 (2009).

137. K. Zhou, L. A. Donnelly, C. H. Kimber, P. T. Donnan, A. S. F. Doney, G. Leese, A. T. Hattersley, M. I. Mccarthy, A. D. Morris, C. N. a Palmer, E. R. Pearson, Organic Cation Transporter 1 and Glycemic Response to Metformin : A GoDARTS Study, *Diabetes* (2009), doi:10.2337/db08-0896.

138. M. L. Becker, L. E. Visser, R. H. N. Van Schaik, A. Hofman, A. G. Uitterlinden, B. H. C. Stricker, Genetic variation in the multidrug and toxin extrusion 1 transporter protein influences the glucose-lowering effect of metformin in patients with diabetes: A preliminary study, *Diabetes* (2009), doi:10.2337/db08-1028.

139. M. L. Becker, L. E. Visser, R. H. N. van Schaik, A. Hofman, A. G. Uitterlinden, B. H. C. Stricker, Interaction between polymorphisms in the OCT1 and MATE1 transporter and metformin response., *Pharmacogenet. Genomics* **20**, 38–44 (2010).

140. I. Tkáč, L. Klimčáková, M. Javorský, M. Fabianová, Z. Schroner, H. Hermanová, E. Babjaková, R. Tkáčová, Pharmacogenomic association between a variant in SLC47A1 gene and therapeutic

response to metformin in type 2 diabetes., *Diabetes. Obes. Metab.* **15**, 189–91 (2013).

141. D. M. Rotroff, S. W. Yee, K. Zhou, S. W. Marvel, H. S. Shah, J. R. Jack, T. M. Havener, M. M. Hedderson, M. Kubo, M. A. Herman, H. Gao, J. C. Mychaleckyi, H. L. McLeod, A. Doria, K. M. Giacomini, E. R. Pearson, M. J. Wagner, J. B. Buse, A. A. Motsinger-Reif, M. MetGen Investigators, A. ACCORD/ACCORDion Investigators, Genetic Variants in CPA6 and PRPF31 Are Associated With Variation in Response to Metformin in Individuals With Type 2 Diabetes., *Diabetes* **67**, 1428–1440 (2018).

142. H. Gehart, H. Clevers, Tales from the crypt: new insights into intestinal stem cells*Nat. Rev. Gastroenterol. Hepatol.* (2019), doi:10.1038/s41575-018-0081-y.

143. J. B. Furness, The enteric nervous system and neurogastroenterology*Nat. Rev. Gastroenterol. Hepatol.* (2012), doi:10.1038/nrgastro.2012.32.

144. A. L. Haber, M. Biton, N. Rogel, R. H. Herbst, K. Shekhar, C. Smillie, G. Burgin, T. M. Delorey, M. R. Howitt, Y. Katz, I. Tirosh, S. Beyaz, D. Dionne, M. Zhang, R. Raychowdhury, W. S. Garrett, O. Rozenblatt-Rosen, H. N. Shi, O. Yilmaz, R. J. Xavier, A. Regev, A single-cell survey of the small intestinal epithelium, *Nature* **551**, 333–339 (2017).

145. H. Cheng, C. P. Leblond, Origin, differentiation and renewal of the four main epithelial cell types in the mouse small intestine. V. Unitarian Theory of the origin of the four epithelial cell types., *Am. J. Anat.* **141**, 537–61 (1974).

146. S. J. A. Buczacki, H. I. Zecchini, A. M. Nicholson, R. Russell, L. Vermeulen, R. Kemp, D. J. Winton, Intestinal label-retaining cells are secretory precursors expressing lgr5, *Nature* (2013), doi:10.1038/nature11965.

147. N. Barker, J. H. Van Es, J. Kuipers, P. Kujala, M. Van Den Born, M. Cozijnsen, A. Haegebarth, J. Korving, H. Begthel, P. J. Peters, H. Clevers, Identification of stem cells in small intestine and colon by marker gene Lgr5, *Nature* (2007), doi:10.1038/nature06196.

148. T. Sato, R. G. Vries, H. J. Snippert, M. van de Wetering, N. Barker, D. E. Stange, J. H. van Es, A. Abo, P. Kujala, P. J. Peters, H. Clevers, Single Lgr5 stem cells build crypt-villus structures in vitro without a mesenchymal niche., *Nature* **459**, 262–5 (2009).

149. T. Sato, J. H. van Es, H. J. Snippert, D. E. Stange, R. G. Vries, M. van den Born, N. Barker, N. F. Shroyer, M. van de Wetering, H. Clevers, Paneth cells constitute the niche for Lgr5 stem cells in intestinal crypts. Supplementary information, *Nature* (2011), doi:10.1038/nature09637.

150. M. J. Rodríguez-Colman, M. Schewe, M. Meerlo, E. Stigter, J. Gerrits, M. Pras-Raves, A.

Sacchetti, M. Hornsveld, K. C. Oost, H. J. Snippert, N. Verhoeven-Duif, R. Fodde, B. M. T. Burgering, Interplay between metabolic identities in the intestinal crypt supports stem cell function, *Nature* **543**, 424–427 (2017).

151. J. H. van Es, T. Sato, M. van de Wetering, A. Lyubimova, A. N. Yee Nee, A. Gregorieff, N. Sasaki, L. Zeinstra, M. van den Born, J. Korving, A. C. M. Martens, N. Barker, A. van Oudenaarden, H. Clevers, Dll1+ secretory progenitor cells revert to stem cells upon crypt damage., *Nat. Cell Biol.* **14**, 1099–1104 (2012).

152. P. W. Tetteh, O. Basak, H. F. Farin, K. Wiebrands, K. Kretzschmar, H. Begthel, M. van den Born, J. Korving, F. de Sauvage, J. H. van Es, A. van Oudenaarden, H. Clevers, Replacement of Lost Lgr5-Positive Stem Cells through Plasticity of Their Enterocyte-Lineage Daughters., *Cell Stem Cell* **18**, 203–13 (2016).

153. M. Bjerknes, C. Khandanpour, T. Möröy, T. Fujiyama, M. Hoshino, T. J. Klisch, Q. Ding, L. Gan, J. Wang, M. G. Martín, H. Cheng, Origin of the brush cell lineage in the mouse intestinal epithelium., *Dev. Biol.* **362**, 194–218 (2012).

154. N. F. Shroyer, M. A. Helmrath, V. Y.-C. Wang, B. Antalffy, S. J. Henning, H. Y. Zoghbi, Intestine-specific ablation of mouse atonal homolog 1 (Math1) reveals a role in cellular homeostasis., *Gastroenterology* **132**, 2478–88 (2007).

155. K. A. Knoop, N. Kumar, B. R. Butler, S. K. Sakthivel, R. T. Taylor, T. Nochi, H. Akiba, H. Yagita, H. Kiyono, I. R. Williams, RANKL is necessary and sufficient to initiate development of antigen-sampling M cells in the intestinal epithelium., *J. Immunol.* **183**, 5738–47 (2009).

156. N. A. Mabbott, D. S. Donaldson, H. Ohno, I. R. Williams, A. Mahajan, Microfold (M) cells: Important immunosurveillance posts in the intestinal epithelium*Mucosal Immunol.* (2013), doi:10.1038/mi.2013.30.

157. J. H. Van Es, M. E. Van Gijn, O. Riccio, M. Van Den Born, M. Vooijs, H. Begthel, M. Cozijnsen, S. Robine, D. J. Winton, F. Radtke, H. Clevers, Notch/γ-secretase inhibition turns proliferative cells in intestinal crypts and adenomas into goblet cells, *Nature* (2005), doi:10.1038/nature03659.

158. F. Reimann, A. M. Habib, G. Tolhurst, H. E. Parker, G. J. Rogers, F. M. Gribble, Glucose sensing in L cells: a primary cell study., *Cell Metab.* **8**, 532–9 (2008).

159. F. M. Gribble, F. Reimann, Enteroendocrine Cells: Chemosensors in the Intestinal Epithelium, *Annu. Rev. Physiol.* **78**, annurev-physiol-021115-105439 (2015).

160. N. Petersen, F. Reimann, J. H. van Es, B. M. van den Berg, C. Kroone, R. Pais, E. Jansen, H.

Clevers, F. M. Gribble, E. J. P. de Koning, Targeting development of incretin-producing cells increases insulin secretion., *J. Clin. Invest.* **125**, 379–85 (2015).

161. F. Gerbe, E. Sidot, D. J. Smyth, M. Ohmoto, I. Matsumoto, V. Dardalhon, P. Cesses, L. Garnier, M. Pouzolles, B. Brulin, M. Bruschi, Y. Harcus, V. S. Zimmermann, N. Taylor, R. M. Maizels, P. Jay, Intestinal epithelial tuft cells initiate type 2 mucosal immunity to helminth parasites., *Nature* **529**, 226–30 (2016).

162. J. Von Moltke, M. Ji, H. E. Liang, R. M. Locksley, Tuft-cell-derived IL-25 regulates an intestinal ILC2-epithelial response circuit, *Nature* (2016), doi:10.1038/nature16161.

163. N. Barker, R. A. Ridgway, J. H. van Es, M. van de Wetering, H. Begthel, M. van den Born, E. Danenberg, A. R. Clarke, O. J. Sansom, H. Clevers, Crypt stem cells as the cells-of-origin of intestinal cancer., *Nature* **457**, 608–11 (2009).

164. M. van den Born, B.-K. Koo, S. F. Boj, H. Clevers, J. Korving, P. Kujala, A. Haegebarth, A. van Oudenaarden, S. Itzkovitz, J. H. van Es, S. Robine, A Critical Role for the Wnt Effector Tcf4 in Adult Intestinal Homeostatic Self-Renewal, *Mol. Cell. Biol.* (2012), doi:10.1128/mcb.06288-11.

165. A. Ootani, X. Li, E. Sangiorgi, Q. T. Ho, H. Ueno, S. Toda, H. Sugihara, K. Fujimoto, I. L. Weissman, M. R. Capecchi, C. J. Kuo, Sustained in vitro intestinal epithelial culture within a Wnt-dependent stem cell niche., *Nat. Med.* **15**, 701–6 (2009).

166. C. J. Kuo, F. Kuhnert, J. Yuan, C. R. Davis, P. Chu, H.-T. Wang, M. Lee, R. Nusse, Essential requirement for Wnt signaling in proliferation of adult small intestine and colon revealed by adenoviral expression of Dickkopf-1, *Proc. Natl. Acad. Sci.* (2004), doi:10.1073/pnas.2536800100.

167. V. Korinek, N. Barker, P. Moerer, E. van Donselaar, G. Huls, P. J. Peters, H. Clevers, Depletion of epithelial stem-cell compartments in the small intestine of mice lacking Tcf-4., *Nat. Genet.* **19**, 379–83 (1998).

168. M. Shoshkes-Carmel, Y. J. Wang, K. J. Wangensteen, B. Tóth, A. Kondo, E. E. Massassa, S. Itzkovitz, K. H. Kaestner, Subepithelial telocytes are an important source of Wnts that supports intestinal crypts, *Nature* (2018), doi:10.1038/s41586-018-0084-4.

169. W. De Lau, N. Barker, T. Y. Low, B. K. Koo, V. S. W. Li, H. Teunissen, P. Kujala, A. Haegebarth, P. J. Peters, M. Van De Wetering, D. E. Stange, J. Van Es, D. Guardavaccaro, R. B. M. Schasfoort, Y. Mohri, K. Nishimori, S. Mohammed, A. J. R. Heck, H. Clevers, Lgr5 homologues associate with Wnt receptors and mediate R-spondin signalling, *Nature* (2011), doi:10.1038/nature10337.

170. J. C. H. Hardwick, G. R. Van Den Brink, S. A. Bleuming, I. Ballester, J. M. H. Van Den Brande, J. J.

Keller, G. J. A. Offerhaus, S. J. H. Van Deventer, M. P. Peppelenbosch, Bone Morphogenetic Protein 2 Is Expressed by, and Acts Upon, Mature Epithelial Cells in the Colon, *Gastroenterology* (2004), doi:10.1053/j.gastro.2003.10.067.

171. C. Kosinski, V. S. W. Li, A. S. Y. Chan, J. Zhang, C. Ho, W. Y. Tsui, T. L. Chan, R. C. Mifflin, D. W. Powell, S. T. Yuen, S. Y. Leung, X. Chen, Gene expression patterns of human colon tops and basal crypts and BMP antagonists as intestinal stem cell niche factors, *Proc. Natl. Acad. Sci.* (2007), doi:10.1073/pnas.0707210104.

172. X. C. He, J. Zhang, W.-G. Tong, O. Tawfik, J. Ross, D. H. Scoville, Q. Tian, X. Zeng, X. He, L. M. Wiedemann, Y. Mishina, L. Li, BMP signaling inhibits intestinal stem cell self-renewal through suppression of Wnt-beta-catenin signaling., *Nat. Genet.* **36**, 1117–21 (2004).

173. A.-P. G. Haramis, H. Begthel, M. van den Born, J. van Es, S. Jonkheer, G. J. A. Offerhaus, H. Clevers, De novo crypt formation and juvenile polyposis on BMP inhibition in mouse intestine., *Science* **303**, 1684–6 (2004).

174. S. Steensels, I. Depoortere, Chemoreceptors in the Gut., *Annu. Rev. Physiol.* **80**, 117–141 (2018).

175. S. R. D. van der Schoor, P. J. Reeds, B. Stoll, J. F. Henry, J. R. Rosenberger, D. G. Burrin, J. B. van Goudoever, The high metabolic cost of a functional gut, *Gastroenterology* **123**, 1931–1940 (2002).

176. M. A. Mcnurlan, P. J. Garlick, *Contribution of Rat Liver and Gastrointestinal Tract to Whole-Body Protein Synthesis in the Rat* (1980; http://www.biochemj.org/content/186/1/381.full-text.pdf).

177. E. A. Newsholme, A. L. Carrié, Quantitative aspects of glucose and glutamine metabolism by intestinal cells., *Gut* **35**, S13-7 (1994).

178. M. Watford, P. Lund, H. A. Krebs, Isolation and metabolic characteristics of rat and chicken enterocytes., *Biochem. J.* **178**, 589–96 (1979).

179. G. Mithieux, New data and concepts on glutamine and glucose metabolism in the gut*Curr. Opin. Clin. Nutr. Metab. Care* (2001), doi:10.1097/00075197-200107000-00004.

180. B. Stoll, D. G. Burrin, J. Henry, H. Yu, F. Jahoor, P. J. Reeds, Substrate oxidation by the portal drained viscera of fed piglets, *Am. J. Physiol. Metab.* **277**, E168–E175 (1999).

181. M. S. Ardawi, Glutamine and ketone-body metabolism in the gut of streptozotocin-diabetic rats., *Biochem. J.* **249**, 565–72 (1988).

182. H. G. Windmueller, A. E. Spaeth, Identification of ketone bodies and glutamine as the major respiratory fuels in vivo for postabsorptive rat small intestine., *J. Biol. Chem.* **253**, 69–76 (1978).

183. H. G. Windmueller, A. E. Spaeth, *Respiratory Fuels and Nitrogen Metabolism in Vivo in Small Intestine of Fed Rats QUANTITATIVE IMPORTANCE OF GLUTAMINE, GLUTAMATE, AND ASPARTATE** (1980; http://www.jbc.org/).

184. C. Rich-Denson, R. E. Kimura, Evidence in vivo that most of the intraluminally absorbed glucose is absorbed intact into the portal vein and not metabolized to lactate., *Biochem. J.* **254**, 931–4 (1988).

185. L. M. Srivastava, G. Hübscher, Glucose metabolism in the mucosa of the small intestine. Glycolysis in subcellular preparations from the cat and rat., *Biochem. J.* **100**, 458–66 (1966).

186. C. Jang, S. Hui, X. Zeng, A. J. Cowan, L. Wang, L. Chen, R. J. Morscher, J. Reyes, C. Frezza, H. Y. Hwang, A. Imai, Y. Saito, K. Okamoto, C. Vaspoli, L. Kasprenski, G. A. Zsido, J. H. Gorman, R. C. Gorman, J. D. Rabinowitz, Metabolite Exchange between Mammalian Organs Quantified in Pigs, *Cell Metab.* (2019), doi:10.1016/j.cmet.2019.06.002.

187. J. C. Schell, D. R. Wisidagama, C. Bensard, H. Zhao, P. Wei, J. Tanner, A. Flores, J. Mohlman, L. K. Sorensen, C. S. Earl, K. A. Olson, R. Miao, T. C. Waller, D. Delker, P. Kanth, L. Jiang, R. J. DeBerardinis, M. P. Bronner, D. Y. Li, J. E. Cox, H. R. Christofk, W. E. Lowry, C. S. Thummel, J. Rutter, Control of intestinal stem cell function and proliferation by mitochondrial pyruvate metabolism, *Nat. Cell Biol.* (2017), doi:10.1038/ncb3593.

188. M. M. Mihaylova, C. W. Cheng, A. Q. Cao, S. Tripathi, M. D. Mana, K. E. Bauer-Rowe, M. Abu-Remaileh, L. Clavain, A. Erdemir, C. A. Lewis, E. Freinkman, A. S. Dickey, A. R. La Spada, Y. Huang, G. W. Bell, V. Deshpande, P. Carmeliet, P. Katajisto, D. M. Sabatini, Ö. H. Yilmaz, Fasting Activates Fatty Acid Oxidation to Enhance Intestinal Stem Cell Function during Homeostasis and Aging, *Cell Stem Cell* (2018), doi:10.1016/j.stem.2018.04.001.

189. C. Stringari, R. A. Edwards, K. T. Pate, M. L. Waterman, P. J. Donovan, E. Gratton, Metabolic trajectory of cellular differentiation in small intestine by Phasor Fluorescence Lifetime Microscopy of NADH, *Sci. Rep.* **2**, 568 (2012).

190. F. M. Gribble, F. Reimann, Function and mechanisms of enteroendocrine cells and gut hormones in metabolism*Nat. Rev. Endocrinol.* (2019), doi:10.1038/s41574-019-0168-8.

191. J. R. Spence, C. N. Mayhew, S. A. Rankin, M. F. Kuhar, J. E. Vallance, K. Tolle, E. E. Hoskins, V. V. Kalinichenko, S. I. Wells, A. M. Zorn, N. F. Shroyer, J. M. Wells, Directed differentiation of human pluripotent stem cells into intestinal tissue in vitro, *Nature* **470**, 105–109 (2010).

192. B.-K. Koo, D. E. Stange, T. Sato, W. Karthaus, H. F. Farin, M. Huch, J. H. van Es, H. Clevers,

Controlled gene expression in primary Lgr5 organoid cultures, *Nat. Methods* **9**, 81–83 (2011).

193. G. Schwank, A. Andersson-Rolf, B.-K. Koo, N. Sasaki, H. Clevers, D. Unutmaz, Ed. Generation of BAC Transgenic Epithelial Organoids, *PLoS One* **8**, e76871 (2013).

194. G. Schwank, B.-K. Koo, V. Sasselli, J. F. Dekkers, I. Heo, T. Demircan, N. Sasaki, S. Boymans, E. Cuppen, C. K. van der Ent, E. E. S. Nieuwenhuis, J. M. Beekman, H. Clevers, Functional Repair of CFTR by CRISPR/Cas9 in Intestinal Stem Cell Organoids of Cystic Fibrosis Patients, *Cell Stem Cell* **13**, 653–658 (2013).

195. N. Petersen, F. Reimann, S. Bartfeld, H. F. Farin, F. C. Ringnalda, R. G. J. Vries, S. van den Brink, H. Clevers, F. M. Gribble, E. J. P. de Koning, Generation of L cells in mouse and human small intestine organoids., *Diabetes* **63**, 410–20 (2014).

196. J. F. Dekkers, G. Berkers, E. Kruisselbrink, A. Vonk, H. R. De Jonge, H. M. Janssens, I. Bronsveld, E. A. Van De Graaf, E. E. S. Nieuwenhuis, R. H. J. Houwen, F. P. Vleggaar, J. C. Escher, Y. B. De Rijke, C. J. Majoor, H. G. M. Heijerman, K. M. De Winter-De Groot, H. Clevers, C. K. Van Der Ent, J. M. Beekman, Characterizing responses to CFTR-modulating drugs using rectal organoids derived from subjects with cystic fibrosis, *Sci. Transl. Med.* (2016), doi:10.1126/scitranslmed.aad8278.

197. M. Van De Wetering, H. E. Francies, J. M. Francis, G. Bounova, F. Iorio, A. Pronk, W. Van Houdt, J. Van Gorp, A. Taylor-Weiner, L. Kester, A. McLaren-Douglas, J. Blokker, S. Jaksani, S. Bartfeld, R. Volckman, P. Van Sluis, V. S. W. Li, S. Seepo, C. Sekhar Pedamallu, K. Cibulskis, S. L. Carter, A. McKenna, M. S. Lawrence, L. Lichtenstein, C. Stewart, J. Koster, R. Versteeg, A. Van Oudenaarden, J. Saez-Rodriguez, R. G. J. Vries, G. Getz, L. Wessels, M. R. Stratton, U. McDermott, M. Meyerson, M. J. Garnett, H. Clevers, Prospective derivation of a living organoid biobank of colorectal cancer patients, *Cell* (2015), doi:10.1016/j.cell.2015.03.053.

198. P. H. Dedhia, N. Bertaux-Skeirik, Y. Zavros, J. R. Spence, Organoid Models of Human Gastrointestinal Development and Disease*Gastroenterology* (2016), doi:10.1053/j.gastro.2015.12.042.

199. P. Schlaermann, B. Toelle, H. Berger, S. C. Schmidt, M. Glanemann, J. Ordemann, S. Bartfeld, H. J. Mollenkopf, T. F. Meyer, A novel human gastric primary cell culture system for modelling Helicobacter pylori infection in vitro., *Gut* **65**, 202–13 (2016).

200. J. G. In, J. Foulke-Abel, M. K. Estes, N. C. Zachos, O. Kovbasnjuk, M. Donowitz, Human mini-guts: New insights into intestinal physiology and host-pathogen interactions*Nat. Rev. Gastroenterol. Hepatol.* (2016), doi:10.1038/nrgastro.2016.142.

201. H. R. Bridges, A. J. Y. Jones, M. N. Pollak, J. Hirst, Effects of metformin and other biguanides on oxidative phosphorylation in mitochondria., *Biochem. J.* **462**, 475–87 (2014).

202. M. R. OWEN, E. DORAN, A. P. HALESTRAP, Evidence that metformin exerts its anti-diabetic effects through inhibition of complex 1 of the mitochondrial respiratory chain, *Biochem. J.* **348**, 607 (2000).

203. W. W. Wheaton, S. E. Weinberg, R. B. Hamanaka, S. Soberanes, L. B. Sullivan, E. Anso, A. Glasauer, E. Dufour, G. M. Mutlu, G. S. Budigner, N. S. Chandel, Metformin inhibits mitochondrial complex I of cancer cells to reduce tumorigenesis., *Elife* **3**, e02242 (2014).

204. M. R. Owen, E. Doran, A. P. Halestrap, Evidence that metformin exerts its anti-diabetic effects through inhibition of complex 1 of the mitochondrial respiratory chain., *Biochem. J.* **348 Pt 3**, 607–14 (2000).

205. S. Andrzejewski, S.-P. Gravel, M. Pollak, J. St-Pierre, Metformin directly acts on mitochondria to alter cellular bioenergetics., *Cancer Metab.* **2**, 12 (2014).

206. T. Griss, E. E. Vincent, R. Egnatchik, J. Chen, E. H. Ma, B. Faubert, B. Viollet, R. J. DeBerardinis, R. G. Jones, D. R. Green, Ed. Metformin Antagonizes Cancer Cell Proliferation by Suppressing Mitochondrial-Dependent Biosynthesis, *PLOS Biol.* **13**, e1002309 (2015).

207. P. Schommers, A. Thurau, I. Bultmann-Mellin, M. Guschlbauer, A. R. Klatt, J. Rozman, M. Klingenspor, M. H. de Angelis, J. Alber, D. Gründemann, A. Sterner-Kock, R. J. Wiesner, Metformin causes a futile intestinal-hepatic cycle which increases energy expenditure and slows down development of a type 2 diabetes-like state., *Mol. Metab.* **6**, 737–747 (2017).

208. E.-M. Blumrich, R. Dringen, Metformin Accelerates Glycolytic Lactate Production in Cultured Primary Cerebellar Granule Neurons, *Neurochem. Res.* **44**, 188–199 (2019).

209. S. A. Hawley, F. A. Ross, C. Chevtzoff, K. A. Green, A. M. Evans, S. Fogarty, M. C. Towler, L. J. Brown, O. A. Ogunbayo, A. M. Evans, D. G. Hardie, Use of Cells Expressing γ Subunit Variants to Identify Diverse Mechanisms of AMPK Activation, *Cell Metab.* **11**, 554–565 (2010).

210. G. Zhou, R. Myers, Y. Li, Y. Chen, X. Shen, J. Fenyk-Melody, M. Wu, J. Ventre, T. Doebber, N. Fujii, N. Musi, M. F. Hirshman, L. J. Goodyear, D. E. Moller, Role of AMP-activated protein kinase in mechanism of metformin action., *J. Clin. Invest.* **108**, 1167–74 (2001).

211. M. Zang, A. Zuccollo, X. Hou, D. Nagata, K. Walsh, H. Herscovitz, P. Brecher, N. B. Ruderman, R. A. Cohen, AMP-activated Protein Kinase Is Required for the Lipid-lowering Effect of Metformin in Insulin-resistant Human HepG2 Cells, *J. Biol. Chem.* **279**, 47898–47905 (2004).

212. F. A. Duca, C. D. Côté, B. A. Rasmussen, M. Zadeh-Tahmasebi, G. A. Rutter, B. M. Filippi, T. K. T. Lam, Metformin activates a duodenal Ampk–dependent pathway to lower hepatic glucose production in rats, *Nat. Med.* **21**, 506–511 (2015).

213. G. Rena, E. R. Pearson, K. Sakamoto, Molecular mechanism of action of metformin: old or new insights?, *Diabetologia* **56**, 1898–1906 (2013).

214. M. Foretz, B. Guigas, L. Bertrand, M. Pollak, B. Viollet, Metformin: From Mechanisms of Action to Therapies, *Cell Metab.* **20**, 953–966 (2014).

215. Y. D. Kim, K.-G. Park, Y.-S. Lee, Y.-Y. Park, D.-K. Kim, B. Nedumaran, W. G. Jang, W.-J. Cho, J. Ha, I.-K. Lee, C.-H. Lee, H.-S. Choi, Metformin Inhibits Hepatic Gluconeogenesis Through AMP-Activated Protein Kinase–Dependent Regulation of the Orphan Nuclear Receptor SHP, *Diabetes* **57**, 306–314 (2008).

216. L. He, A. Sabet, S. Djedjos, R. Miller, X. Sun, M. A. Hussain, S. Radovick, F. E. Wondisford, Metformin and Insulin Suppress Hepatic Gluconeogenesis through Phosphorylation of CREB Binding Protein, *Cell* **137**, 635–646 (2009).

217. J.-M. Lee, W.-Y. Seo, K.-H. Song, D. Chanda, Y. D. Kim, D.-K. Kim, M.-W. Lee, D. Ryu, Y.-H. Kim, J.-R. Noh, C.-H. Lee, J. Y. L. Chiang, S.-H. Koo, H.-S. Choi, AMPK-dependent repression of hepatic gluconeogenesis via disruption of CREB.CRTC2 complex by orphan nuclear receptor small heterodimer partner., *J. Biol. Chem.* **285**, 32182–91 (2010).

218. R. J. Shaw, K. A. Lamia, D. Vasquez, S.-H. Koo, N. Bardeesy, R. A. Depinho, M. Montminy, L. C. Cantley, The Kinase LKB1 Mediates Glucose Homeostasis in Liver and Therapeutic Effects of Metformin, *Science (80-.).* **310**, 1642–1646 (2005).

219. I. Pernicova, M. Korbonits, Metformin—mode of action and clinical implications for diabetes and cancer, *Nat. Rev. Endocrinol.* **10**, 143–156 (2014).

220. M. Foretz, S. Hébrard, J. Leclerc, E. Zarrinpashneh, M. Soty, G. Mithieux, K. Sakamoto, F. Andreelli, B. Viollet, Metformin inhibits hepatic gluconeogenesis in mice independently of the LKB1/AMPK pathway via a decrease in hepatic energy state, *J. Clin. Invest.* **120**, 2355–2369 (2010).

221. A. Kalender, A. Selvaraj, S. Y. Kim, P. Gulati, S. Brûlé, B. Viollet, B. E. Kemp, N. Bardeesy, P. Dennis, J. J. Schlager, A. Marette, S. C. Kozma, G. Thomas, Metformin, Independent of AMPK, Inhibits mTORC1 in a Rag GTPase-Dependent Manner, *Cell Metab.* **11**, 390–401 (2010).

222. J. J. Howell, K. Hellberg, M. Turner, A. Saghatelian, R. J. Shaw, B. D. Manning, Metformin Inhibits Hepatic mTORC1 Signaling via Dose-Dependent Mechanisms Involving AMPK and the TSC Complex In

Brief, *Cell Metab.* **25**, 463–471 (2017).

223. A. Maida, B. J. Lamont, X. Cao, D. J. Drucker, Metformin regulates the incretin receptor axis via a pathway dependent on peroxisome proliferator-activated receptor-α in mice, *Diabetologia* **54**, 339–349 (2011).

224. R. A. Miller, Q. Chu, J. Xie, M. Foretz, B. Viollet, M. J. Birnbaum, Biguanides suppress hepatic glucagon signalling by decreasing production of cyclic AMP, *Nature* **494**, 256–260 (2013).

225. A. K. Madiraju, Y. Qiu, R. J. Perry, Y. Rahimi, X.-M. Zhang, D. Zhang, J.-P. G. Camporez, G. W. Cline, G. M. Butrico, B. E. Kemp, G. Casals, G. R. Steinberg, D. F. Vatner, K. F. Petersen, G. I. Shulman, Metformin inhibits gluconeogenesis via a redox-dependent mechanism in vivo, *Nat. Med.* **24**, 1384–1394 (2018).

226. A. K. Madiraju, D. M. Erion, Y. Rahimi, X.-M. Zhang, D. T. Braddock, R. A. Albright, B. J. Prigaro, J. L. Wood, S. Bhanot, M. J. MacDonald, M. J. Jurczak, J.-P. Camporez, H.-Y. Lee, G. W. Cline, V. T. Samuel, R. G. Kibbey, G. I. Shulman, Metformin suppresses gluconeogenesis by inhibiting mitochondrial glycerophosphate dehydrogenase., *Nature* **510**, 542–6 (2014).

227. R. S. Hundal, M. Krssak, S. Dufour, D. Laurent, V. Lebon, V. Chandramouli, S. E. Inzucchi, W. C. Schumann, K. F. Petersen, B. R. Landau, G. I. Shulman, Mechanism by which metformin reduces glucose production in type 2 diabetes., *Diabetes* **49**, 2063–9 (2000).

228. L. C. Gormsen, E. Søndergaard, N. L. Christensen, K. Brøsen, N. Jessen, S. Nielsen, Metformin increases endogenous glucose production in non-diabetic individuals and individuals with recent-onset type 2 diabetes., *Diabetologia* **62**, 1251–1256 (2019).

229. B. Cool, B. Zinker, W. Chiou, L. Kifle, N. Cao, M. Perham, R. Dickinson, A. Adler, G. Gagne, R. Iyengar, G. Zhao, K. Marsh, P. Kym, P. Jung, H. S. Camp, E. Frevert, Identification and characterization of a small molecule AMPK activator that treats key components of type 2 diabetes and the metabolic syndrome, *Cell Metab.* **3**, 403–416 (2006).

230. A. Herms, M. Bosch, B. J. N. Reddy, N. L. Schieber, A. Fajardo, C. Rupérez, A. Fernández-Vidal, C. Ferguson, C. Rentero, F. Tebar, C. Enrich, R. G. Parton, S. P. Gross, A. Pol, AMPK activation promotes lipid droplet dispersion on detyrosinated microtubules to increase mitochondrial fatty acid oxidation, *Nat. Commun.* **6**, 7176 (2015).

231. N. Boudaba, A. Marion, C. Huet, R. Pierre, B. Viollet, M. Foretz, AMPK Re-Activation Suppresses Hepatic Steatosis but its Downregulation Does Not Promote Fatty Liver Development, *EBioMedicine* **28**, 194–209 (2018).

232. D. Garcia, K. Hellberg, A. Chaix, M. Wallace, S. Herzig, M. G. Badur, T. Lin, M. N. Shokhirev, A. F. M. Pinto, D. S. Ross, A. Saghatelian, S. Panda, L. E. Dow, C. M. Metallo, R. J. Shaw, Genetic Liver-Specific AMPK Activation Protects against Diet-Induced Obesity and NAFLD, *Cell Rep.* **26**, 192-208.e6 (2019).

233. M. D. Fullerton, S. Galic, K. Marcinko, S. Sikkema, T. Pulinilkunnil, Z.-P. Chen, H. M. O'Neill, R. J. Ford, R. Palanivel, M. O'Brien, D. G. Hardie, S. L. Macaulay, J. D. Schertzer, J. R. B. Dyck, B. J. van Denderen, B. E. Kemp, G. R. Steinberg, Single phosphorylation sites in Acc1 and Acc2 regulate lipid homeostasis and the insulin-sensitizing effects of metformin, *Nat. Med.* **19**, 1649–1654 (2013).

234. W. F. Caspary, W. Creutzfeldt, Analysis of the inhibitory effect of biguanides on glucose absorption: Inhibition of active sugar transport, *Diabetologia* **7**, 379–385 (1971).

235. E. Lorch, *Inhibition of Intestinal Absorption and Improvement of 0ral Glucose Tolerance by Biguanldes in the Normal and in the Streptozotocin-Diabetic Rat* (Springer-Verlag, 1971; https://link.springer.com/content/pdf/10.1007/BF01212553.pdf).

236. O. Horakova, P. Kroupova, K. Bardova, J. Buresova, P. Janovska, J. Kopecky, M. Rossmeisl, Metformin acutely lowers blood glucose levels by inhibition of intestinal glucose transport, *Sci. Rep.* **9**, 6156 (2019).

237. J. P. Koffert, K. Mikkola, K. A. Virtanen, A.-M. D. Andersson, L. Faxius, K. Hällsten, M. Heglind, L. Guiducci, T. Pham, J. M. U. Silvola, J. Virta, O. Eriksson, S. P. Kauhanen, A. Saraste, S. Enerbäck, P. Iozzo, R. Parkkola, M. F. Gomez, P. Nuutila, Metformin treatment significantly enhances intestinal glucose uptake in patients with type 2 diabetes: Results from a randomized clinical trial, *Diabetes Res. Clin. Pract.* **131**, 208–216 (2017).

238. J.-R. Oh, H.-C. Song, A. Chong, J.-M. Ha, S.-Y. Jeong, J.-J. Min, H.-S. Bom, Impact of Medication Discontinuation on Increased Intestinal FDG Accumulation in Diabetic Patients Treated With Metformin, *Am. J. Roentgenol.* **195**, 1404–1410 (2010).

239. C. J. Bailey, K. J. Mynett, T. Page, Importance of the intestine as a site of metformin-stimulated glucose utilization., *Br. J. Pharmacol.* **112**, 671–5 (1994).

240. C. J. Bailey, C. Wilcock, J. H. B. Scarpello, Metformin and the intestine, *Diabetologia* **51**, 1552–1553 (2008).

241. J. D. Lalau, C. Lacroix, P. Compagnon, B. de Cagny, J. P. Rigaud, G. Bleichner, P. Chauveau, P. Dulbecco, C. Guérin, J. M. Haegy, Role of metformin accumulation in metformin-associated lactic acidosis., *Diabetes Care* **18**, 779–84 (1995).

242. T. M. Davis, D. Jackson, W. A. Davis, D. G. Bruce, P. Chubb, The relationship between metformin therapy and the fasting plasma lactate in type 2 diabetes: The Fremantle Diabetes Study., *Br. J. Clin. Pharmacol.* **52**, 137–44 (2001).

243. Y. Li, Z. Cai, S. S. Li, J. Zhu, F. Zhang, S. Liang, W. Zhang, Y. Guan, D. Shen, Y. Peng, D. Zhang, Z. Jie, W. Wu, Y. Qin, W. Xue, J. Li, L. Han, D. Lu, P. Wu, Y. Dai, X. Sun, Z. Li, A. Tang, S. Zhong, X. Li, W. Chen, R. Xu, M. Wang, Q. Feng, M. Gong, J. Yu, Y. Zhang, M. Zhang, T. Hansen, G. Sanchez, J. Raes, G. Falony, S. Okuda, M. Almeida, E. LeChatelier, P. Renault, N. Pons, J.-M. Batto, Z. Zhang, H. Chen, R. Yang, W. Zheng, S. S. Li, H. Yang, J. J. Wang, S. D. Ehrlich, R. Nielsen, O. Pedersen, K. Kristiansen, J. J. Wang, J. Qin, Y. Li, Z. Cai, S. S. Li, J. Zhu, F. Zhang, S. Liang, W. Zhang, Y. Guan, D. Shen, Y. Peng, D. Zhang, Z. Jie, W. Wu, Y. Qin, W. Xue, J. Li, L. Han, D. Lu, P. Wu, Y. Dai, X. Sun, Z. Li, A. Tang, S. Zhong, X. Li, W. Chen, R. Xu, M. Wang, Q. Feng, M. Gong, J. Yu, Y. Zhang, M. Zhang, T. Hansen, G. Sanchez, J. Raes, G. Falony, S. Okuda, M. Almeida, E. LeChatelier, P. Renault, N. Pons, J.-M. Batto, Z. Zhang, H. Chen, R. Yang, W. Zheng, S. S. Li, H. Yang, J. J. Wang, S. D. Ehrlich, R. Nielsen, O. Pedersen, K. Kristiansen, J. J. Wang, A metagenome-wide association study of gut microbiota in type 2 diabetes, *Nature* (2012), doi:http://dx.doi.org/10.1038/nature11450.

244. P. J. Turnbaugh, R. E. Ley, M. A. Mahowald, V. Magrini, E. R. Mardis, J. I. Gordon, An obesity-associated gut microbiome with increased capacity for energy harvest, *Nature* (2006), doi:10.1038/nature05414.

245. F. H. Karlsson, V. Tremaroli, I. Nookaew, G. Bergström, C. J. Behre, B. Fagerberg, J. Nielsen, F. Bäckhed, Gut metagenome in European women with normal, impaired and diabetic glucose control, *Nature* (2013), doi:10.1038/nature12198.

246. H. Wu, E. Esteve, V. Tremaroli, M. T. Khan, R. Caesar, L. Mannerås-Holm, M. Ståhlman, L. M. Olsson, M. Serino, M. Planas-Fèlix, G. Xifra, J. M. Mercader, D. Torrents, R. Burcelin, W. Ricart, R. Perkins, J. M. Fernàndez-Real, F. Bäckhed, Metformin alters the gut microbiome of individuals with treatment-naive type 2 diabetes, contributing to the therapeutic effects of the drug, *Nat. Med.* (2017), doi:10.1038/nm.4345.

247. K. Forslund, F. Hildebrand, T. Nielsen, G. Falony, E. Le Chatelier, S. Sunagawa, E. Prifti, S. Vieira-Silva, V. Gudmundsdottir, H. Krogh Pedersen, M. Arumugam, K. Kristiansen, A. Yvonne Voigt, H. Vestergaard, R. Hercog, P. Igor Costea, J. Roat Kultima, J. Li, T. Jørgensen, F. Levenez, J. Dore, H. Bjørn Nielsen, S. Brunak, J. Raes, T. Hansen, J. Wang, S. Dusko Ehrlich, P. Bork, O. Pedersen, O. Pedersen, Disentangling type 2 diabetes and metformin treatment signatures in the human gut microbiota, *Nature* **528**, 262–266 (2015).

248. E. P. Velásquez-Mejía, J. M. Abad, V. Corrales-Agudelo, N. T. Mueller, J. S. Escobar, J. de la Cuesta-Zuluaga, J. A. Carmona, Metformin Is Associated With Higher Relative Abundance of Mucin-Degrading Akkermansia muciniphila and Several Short-Chain Fatty Acid–Producing Microbiota in the Gut , *Diabetes Care* (2016), doi:10.2337/dc16-1324.

249. A. Everard, C. Belzer, L. Geurts, J. P. Ouwerkerk, C. Druart, L. B. Bindels, Y. Guiot, M. Derrien, G. G. Muccioli, N. M. Delzenne, W. M. de Vos, P. D. Cani, Cross-talk between Akkermansia muciniphila and intestinal epithelium controls diet-induced obesity, *Proc. Natl. Acad. Sci.* (2013), doi:10.1073/pnas.1219451110.

250. C. Depommier, A. Everard, C. Druart, H. Plovier, M. Van Hul, S. Vieira-Silva, G. Falony, J. Raes, D. Maiter, N. M. Delzenne, M. de Barsy, A. Loumaye, M. P. Hermans, J.-P. Thissen, W. M. de Vos, P. D. Cani, Supplementation with Akkermansia muciniphila in overweight and obese human volunteers: a proof-of-concept exploratory study, *Nat. Med.* (2019), doi:10.1038/s41591-019-0495-2.

251. P. V. Bauer, F. A. Duca, T. M. Z. Waise, B. A. Rasmussen, M. A. Abraham, H. J. Dranse, A. Puri, C. A. O'Brien, T. K. T. Lam, Metformin Alters Upper Small Intestinal Microbiota that Impact a Glucose-SGLT1-Sensing Glucoregulatory Pathway, *Cell Metab.* (2018), doi:10.1016/j.cmet.2017.09.019.

252. F. G. Schaap, M. Trauner, P. L. M. Jansen, Bile acid receptors as targets for drug development*Nat. Rev. Gastroenterol. Hepatol.* (2014), doi:10.1038/nrgastro.2013.151.

253. D. Carter, H. C. S. Howlett, N. F. Wiernsperger, C. Bailey, Effects of metformin on bile salt transport by monolayers of human intestinal Caco-2 cells, *Diabetes, Obes. Metab.* **4**, 424–427 (2002).

254. D. Carter, H. C. S. Howlett, N. F. Wiernsperger, C. J. Bailey, Differential effects of metformin on bile salt absorption from the jejunum and ileum., *Diabetes. Obes. Metab.* **5**, 120–5 (2003).

255. W. F. Caspary, I. Zavada, W. Reimold, U. Deuticke, D. Emrich, B. Willms, Alteration of bile acid metabolism and vitamin-B12-absorption in diabetics on biguanides., *Diabetologia* **13**, 187–93 (1977).

256. J. H. B. Scarpello, E. Hodgson, H. C. S. Howlett, Effect of metformin on bile salt circulation and intestinal motility in Type 2 diabetes mellitus, *Diabet. Med.* **15**, 651–656 (1998).

257. F. Lien, A. Berthier, E. Bouchaert, C. Gheeraert, J. Alexandre, G. Porez, J. Prawitt, H. Dehondt, M. Ploton, S. Colin, A. Lucas, A. Patrice, F. Pattou, H. Diemer, A. Van Dorsselaer, C. Rachez, J. Kamilic, A. K. Groen, B. Staels, P. Lefebvre, Metformin interferes with bile acid homeostasis through AMPK-FXR crosstalk, *J. Clin. Invest.* **124**, 1037–1051 (2014).

258. T. Inagaki, M. Choi, A. Moschetta, L. Peng, C. L. Cummins, J. G. McDonald, G. Luo, S. A. Jones, B. Goodwin, J. A. Richardson, R. D. Gerard, J. J. Repa, D. J. Mangelsdorf, S. A. Kliewer, Fibroblast growth

factor 15 functions as an enterohepatic signal to regulate bile acid homeostasis, *Cell Metab.* **2**, 217–225 (2005).

259. M. Choi, A. Moschetta, A. L. Bookout, L. Peng, M. Umetani, S. R. Holmstrom, K. Suino-Powell, H. E. Xu, J. A. Richardson, R. D. Gerard, D. J. Mangelsdorf, S. A. Kliewer, Identification of a hormonal basis for gallbladder filling, *Nat. Med.* **12**, 1253–1255 (2006).

260. L. Sun, C. Xie, G. Wang, Y. Wu, Q. Wu, X. Wang, J. Liu, Y. Deng, J. Xia, B. Chen, S. Zhang, C. Yun, G. Lian, X. Zhang, H. Zhang, W. H. Bisson, J. Shi, X. Gao, P. Ge, C. Liu, K. W. Krausz, R. G. Nichols, J. Cai, B. Rimal, A. D. Patterson, X. Wang, F. J. Gonzalez, C. Jiang, Gut microbiota and intestinal FXR mediate the clinical benefits of metformin, *Nat. Med.* **24**, 1919–1929 (2018).

261. L. L. Baggio, D. J. Drucker, Biology of incretins: GLP-1 and GIP., *Gastroenterology* **132**, 2131–57 (2007).

262. E. Mannucci, A. Ognibene, F. Cremasco, G. Bardini, A. Mencucci, E. Pierazzuoli, S. Ciani, G. Messeri, C. M. Rotella, Effect of metformin on glucagon-like peptide 1 (GLP-1) and leptin levels in obese nondiabetic subjects., *Diabetes Care* **24**, 489–94 (2001).

263. E. Bahne, E. W. L. Sun, R. L. Young, M. Hansen, D. P. Sonne, J. S. Hansen, U. Rohde, A. P. Liou, M. L. Jackson, D. de Fontgalland, P. Rabbitt, P. Hollington, L. Sposato, S. Due, D. A. Wattchow, J. F. Rehfeld, J. J. Holst, D. J. Keating, T. Vilsbøll, F. K. Knop, D. de Fontgalland, P. Rabbitt, P. Hollington, L. Sposato, S. Due, D. A. Wattchow, J. F. Rehfeld, J. J. Holst, D. J. Keating, T. Vilsbøll, F. K. Knop, Metformin-induced glucagon-like peptide-1 secretion contributes to the actions of metformin in type 2 diabetes, *JCI Insight* **3** (2018) (available at https://insight.jci.org/articles/view/93936).

264. A. Napolitano, S. Miller, A. W. Nicholls, D. Baker, S. Van Horn, E. Thomas, D. Rajpal, A. Spivak, J. R. Brown, D. J. Nunez, Novel gut-based pharmacology of metformin in patients with type 2 diabetes mellitus., *PLoS One* **9**, e100778 (2014).

265. T. Wu, S. S. Thazhath, M. J. Bound, K. L. Jones, M. Horowitz, C. K. Rayner, Mechanism of increase in plasma intact GLP-1 by metformin in type 2 diabetes: Stimulation of GLP-1 secretion or reduction in plasma DPP-4 activity?, *Diabetes Res. Clin. Pract.* **106**, e3–e6 (2014).

266. J. R. Lindsay, N. A. Duffy, A. M. McKillop, J. Ardill, F. P. M. O'Harte, P. R. Flatt, P. M. Bell, Inhibition of dipeptidyl peptidase IV activity by oral metformin in Type 2 diabetes, *Diabet. Med.* **22**, 654–657 (2005).

267. A. Brønden, A. Albér, U. Rohde, J. F. Rehfeld, J. J. Holst, T. Vilsbøll, F. K. Knop, Single-Dose Metformin Enhances Bile Acid–Induced Glucagon-Like Peptide-1 Secretion in Patients With Type 2

Diabetes, *J. Clin. Endocrinol. Metab.* **102**, 4153–4162 (2017).

268. S. A. Hinke, K. Kühn-Wache, T. Hoffmann, R. A. Pederson, C. H. S. McIntosh, H.-U. Demuth, Metformin Effects on Dipeptidylpeptidase IV Degradation of Glucagon-like Peptide-1, *Biochem. Biophys. Res. Commun.* **291**, 1302–1308 (2002).

269. B. D. Green, N. Irwin, N. A. Duffy, V. A. Gault, F. P. M. O'Harte, P. R. Flatt, Inhibition of dipeptidyl peptidase-IV activity by metformin enhances the antidiabetic effects of glucagon-like peptide-1, *Eur. J. Pharmacol.* **547**, 192–199 (2006).

270. J. Cuthbertson, S. Patterson, F. P. M. O'Harte, P. M. Bell, Investigation of the effect of oral metformin on dipeptidylpeptidase-4 (DPP-4) activity in Type 2 diabetes, *Diabet. Med.* **26**, 649–654 (2009).

271. S. K. Thondam, A. Cross, D. J. Cuthbertson, J. P. Wilding, C. Daousi, Effects of chronic treatment with metformin on dipeptidyl peptidase-4 activity, glucagon-like peptide 1 and ghrelin in obese patients with Type 2 diabetes mellitus, *Diabet. Med.* **29**, e205–e210 (2012).

272. E. M. Migoya, R. Bergeron, J. L. Miller, R. N. K. Snyder, M. Tanen, D. Hilliard, B. Weiss, P. Larson, M. Gutierrez, G. Jiang, F. Liu, K. A. Pryor, J. Yao, L. Zhu, J. J. Holst, C. Deacon, G. Herman, N. Thornberry, J. Amatruda, D. Williams-Herman, J. A. Wagner, R. SinhaRoy, Dipeptidyl Peptidase-4 Inhibitors Administered in Combination With Metformin Result in an Additive Increase in the Plasma Concentration of Active GLP-1, *Clin. Pharmacol. Ther.* **88**, 801–808 (2010).

273. M.-H. Kim, J.-H. Jee, S. Park, M.-S. Lee, K.-W. Kim, M.-K. Lee, Metformin enhances glucagon-like peptide 1 via cooperation between insulin and Wnt signaling, *J. Endocrinol.* **220**, 117–128 (2014).

274. A. J. Mulherin, A. H. Oh, H. Kim, A. Grieco, L. M. Lauffer, P. L. Brubaker, Mechanisms Underlying Metformin-Induced Secretion of Glucagon-Like Peptide-1 from the Intestinal L Cell, *Endocrinology* **152**, 4610–4619 (2011).

275. C. Thomas, A. Gioiello, L. Noriega, A. Strehle, J. Oury, G. Rizzo, A. Macchiarulo, H. Yamamoto, C. Mataki, M. Pruzanski, R. Pellicciari, J. Auwerx, K. Schoonjans, TGR5-mediated bile acid sensing controls glucose homeostasis., *Cell Metab.* **10**, 167–77 (2009).

276. H. C. Gerstein, G. Pare, S. Hess, R. J. Ford, J. Sjaarda, K. Raman, M. McQueen, S. Lee, H. Haenel, G. R. Steinberg, ORIGIN Investigators, Growth Differentiation Factor 15 as a Novel Biomarker for Metformin., *Diabetes Care* **40**, 280–283 (2017).

277. A. Natali, L. Nesti, E. Venturi, A. C. Shore, F. Khan, K. Gooding, P. E. Gates, H. C. Looker, F. Dove, I. Goncalves, M. Persson, J. Nilsson, Metformin is the key factor in elevated plasma growth

differentiation factor-15 levels in type 2 diabetes: A nested, case-control study, *Diabetes, Obes. Metab.* **21**, 412–416 (2019).

278. M. R. Bootcov, A. R. Bauskin, S. M. Valenzuela, A. G. Moore, M. Bansal, X. Y. He, H. P. Zhang, M. Donnellan, S. Mahler, K. Pryor, B. J. Walsh, R. C. Nicholson, W. D. Fairlie, S. B. Por, J. M. Robbins, S. N. Breit, MIC-1, a novel macrophage inhibitory cytokine, is a divergent member of the TGF- superfamily, *Proc. Natl. Acad. Sci.* **94**, 11514–11519 (1997).

279. Q. Ding, T. Mracek, P. Gonzalez-Muniesa, K. Kos, J. Wilding, P. Trayhurn, C. Bing, Identification of Macrophage Inhibitory Cytokine-1 in Adipose Tissue and Its Secretion as an Adipokine by Human Adipocytes, *Endocrinology* **150**, 1688–1696 (2009).

280. W. D. Fairlie, A. G. Moore, A. R. Bauskin, P. K. Russell, H.-P. Zhang, S. N. Breit, MIC-1 is a novel TGF-β superfamily cytokine associated with macrophage activation, *J. Leukoc. Biol.* **65**, 2–5 (1999).

281. M. Böttner, C. Suter-Crazzolara, A. Schober, K. Unsicker, Expression of a novel member of the TGF-beta superfamily, growth/differentiation factor-15/macrophage-inhibiting cytokine-1 (GDF-15/MIC-1) in adult rat tissues., *Cell Tissue Res.* **297**, 103–10 (1999).

282. M. Yokoyama-Kobayashi, M. Saeki, S. Sekine, S. Kato, Human cDNA encoding a novel TGF-beta superfamily protein highly expressed in placenta., *J. Biochem.* **122**, 622–6 (1997).

283. L. N. Lawton, M. F. Bonaldo, P. C. Jelenc, L. Qiu, S. A. Baumes, R. A. Marcelino, G. M. de Jesus, S. Wellington, J. A. Knowles, D. Warburton, S. Brown, M. B. Soares, Identification of a novel member of the TGF-beta superfamily highly expressed in human placenta., *Gene* **203**, 17–26 (1997).

284. T. A. Zimmers, X. Jin, E. C. Hsiao, S. A. McGrath, A. F. Esquela, L. G. Koniaris, Growth differentiation factor-15/macrophage inhibitory cytokine-1 induction after kidney and lung injury., *Shock* **23**, 543–8 (2005).

285. E. C. Hsiao, L. G. Koniaris, T. Zimmers-Koniaris, S. M. Sebald, T. V Huynh, S. J. Lee, Characterization of growth-differentiation factor 15, a transforming growth factor beta superfamily member induced following liver injury., *Mol. Cell. Biol.* **20**, 3742–51 (2000).

286. H. K. Chung, D. Ryu, K. S. Kim, J. Y. Chang, Y. K. Kim, H.-S. Yi, S. G. Kang, M. J. Choi, S. E. Lee, S.-B. Jung, M. J. Ryu, S. J. Kim, G. R. Kweon, H. Kim, J. H. Hwang, C.-H. Lee, S.-J. Lee, C. E. Wall, M. Downes, R. M. Evans, J. Auwerx, M. Shong, Growth differentiation factor 15 is a myomitokine governing systemic energy homeostasis., *J. Cell Biol.* **216**, 149–165 (2017).

287. S. Patel, A. Alvarez-Guaita, A. Melvin, D. Rimmington, A. Dattilo, E. L. Miedzybrodzka, I. Cimino, A.-C. Maurin, G. P. Roberts, C. L. Meek, S. Virtue, L. M. Sparks, S. A. Parsons, L. M. Redman, G. A.

Bray, A. P. Liou, R. M. Woods, S. A. Parry, P. B. Jeppesen, A. J. Kolnes, H. P. Harding, D. Ron, A. Vidal-Puig, F. Reimann, F. M. Gribble, C. J. Hulston, I. S. Farooqi, P. Fafournoux, S. R. Smith, J. Jensen, D. Breen, Z. Wu, B. B. Zhang, A. P. Coll, D. B. Savage, S. O'Rahilly, GDF15 Provides an Endocrine Signal of Nutritional Stress in Mice and Humans, *Cell Metab.* **29**, 707-718.e8 (2019).

288. D. A. Brown, A. R. Bauskin, W. D. Fairlie, M. D. Smith, T. Liu, N. Xu, S. N. Breit, Antibody-based approach to high-volume genotyping for MIC-1 polymorphism., *Biotechniques* **33**, 118–20, 122, 124 passim (2002).

289. V. W. W. Tsai, Y. Husaini, A. Sainsbury, D. A. Brown, S. N. Breit, Cell Metabolism The MIC-1/GDF15-GFRAL Pathway in Energy Homeostasis: Implications for Obesity, Cachexia, and Other Associated Diseases, (2018), doi:10.1016/j.cmet.2018.07.018.

290. S. E. Mullican, S. M. Rangwala, Uniting GDF15 and GFRAL: Therapeutic Opportunities in Obesity and Beyond., *Trends Endocrinol. Metab.* **29**, 560–570 (2018).

291. H. Johnen, S. Lin, T. Kuffner, D. A. Brown, V. W.-W. Tsai, A. R. Bauskin, L. Wu, G. Pankhurst, L. Jiang, S. Junankar, M. Hunter, W. D. Fairlie, N. J. Lee, R. F. Enriquez, P. A. Baldock, E. Corey, F. S. Apple, M. M. Murakami, E.-J. Lin, C. Wang, M. J. During, A. Sainsbury, H. Herzog, S. N. Breit, Tumor-induced anorexia and weight loss are mediated by the TGF-β superfamily cytokine MIC-1, *Nat. Med.* **13**, 1333–1340 (2007).

292. V. W.-W. Tsai, L. Macia, H. Johnen, T. Kuffner, R. Manadhar, S. B. Jørgensen, K. K. M. Lee-Ng, H. P. Zhang, L. Wu, C. P. Marquis, L. Jiang, Y. Husaini, S. Lin, H. Herzog, D. A. Brown, A. Sainsbury, S. N. Breit, C. Morrison, Ed. TGF-b Superfamily Cytokine MIC-1/GDF15 Is a Physiological Appetite and Body Weight Regulator, *PLoS One* **8**, e55174 (2013).

293. V. W.-W. Tsai, R. Manandhar, S. B. Jørgensen, K. K. M. Lee-Ng, H. P. Zhang, C. P. Marquis, L. Jiang, Y. Husaini, S. Lin, A. Sainsbury, P. E. Sawchenko, D. A. Brown, S. N. Breit, M. Covasa, Ed. The Anorectic Actions of the TGFβ Cytokine MIC-1/GDF15 Require an Intact Brainstem Area Postrema and Nucleus of the Solitary Tract, *PLoS One* **9**, e100370 (2014).

294. T. Tran, J. Yang, J. Gardner, Y. Xiong, J. M. Peterson, Ed. GDF15 deficiency promotes high fat diet-induced obesity in mice, *PLoS One* **13**, e0201584 (2018).

295. L. Yang, C.-C. Chang, Z. Sun, D. Madsen, H. Zhu, S. B. Padkjær, X. Wu, T. Huang, K. Hultman, S. J. Paulsen, J. Wang, A. Bugge, J. B. Frantzen, P. Nørgaard, J. F. Jeppesen, Z. Yang, A. Secher, H. Chen, X. Li, L. M. John, B. Shan, Z. He, X. Gao, J. Su, K. T. Hansen, W. Yang, S. B. Jørgensen, GFRAL is the receptor for GDF15 and is required for the anti-obesity effects of the ligand, *Nat. Med.* **23**, 1158–

1166 (2017).

296. J.-Y. Hsu, S. Crawley, M. Chen, D. A. Ayupova, D. A. Lindhout, J. Higbee, A. Kutach, W. Joo, Z. Gao, D. Fu, C. To, K. Mondal, B. Li, A. Kekatpure, M. Wang, T. Laird, G. Horner, J. Chan, M. McEntee, M. Lopez, D. Lakshminarasimhan, A. White, S.-P. Wang, J. Yao, J. Yie, H. Matern, M. Solloway, R. Haldankar, T. Parsons, J. Tang, W. D. Shen, Y. Alice Chen, H. Tian, B. B. Allan, Non-homeostatic body weight regulation through a brainstem-restricted receptor for GDF15, *Nature* **550**, 255–259 (2017).

297. K. H. Kim, Y. T. Jeong, S. H. Kim, H. S. Jung, K. S. Park, H.-Y. Lee, M.-S. Lee, Metformin-induced inhibition of the mitochondrial respiratory chain increases FGF21 expression via ATF4 activation, *Biochem. Biophys. Res. Commun.* **440**, 76–81 (2013).

298. Y. Wang, N. Dang, P. Sun, J. Xia, C. Zhang, S. Pang, The effects of metformin on fibroblast growth factor 19, 21 and fibroblast growth factor receptor 1 in high-fat diet and streptozotocin induced diabetic rats, *Endocr. J.* **64**, 543–552 (2017).

299. S. M. Solon-Biet, V. C. Cogger, T. Pulpitel, M. Heblinski, D. Wahl, A. C. McMahon, A. Warren, J. Durrant-Whyte, K. A. Walters, J. R. Krycer, F. Ponton, R. Gokarn, J. A. Wali, K. Ruohonen, A. D. Conigrave, D. E. James, D. Raubenheimer, C. D. Morrison, D. G. Le Couteur, S. J. Simpson, Defining the Nutritional and Metabolic Context of FGF21 Using the Geometric Framework, *Cell Metab.* (2016), doi:10.1016/j.cmet.2016.09.001.

300. T. Laeger, T. M. Henagan, D. C. Albarado, L. M. Redman, G. A. Bray, R. C. Noland, H. Münzberg, S. M. Hutson, T. W. Gettys, M. W. Schwartz, C. D. Morrison, FGF21 is an endocrine signal of protein restriction, *J. Clin. Invest.* (2014), doi:10.1172/JCI74915.

301. S. Talukdar, B. M. Owen, P. Song, G. Hernandez, Y. Zhang, Y. Zhou, W. T. Scott, B. Paratala, T. Turner, A. Smith, B. Bernardo, C. P. Müller, H. Tang, D. J. Mangelsdorf, B. Goodwin, S. A. Kliewer, FGF21 regulates sweet and alcohol preference, *Cell Metab.* (2016), doi:10.1016/j.cmet.2015.12.008.

302. L. D. BonDurant, M. Ameka, M. C. Naber, K. R. Markan, S. O. Idiga, M. R. Acevedo, S. A. Walsh, D. M. Ornitz, M. J. Potthoff, FGF21 Regulates Metabolism Through Adipose-Dependent and -Independent Mechanisms, *Cell Metab.* (2017), doi:10.1016/j.cmet.2017.03.005.

303. A. Kharitonenkov, T. L. Shiyanova, A. Koester, A. M. Ford, R. Micanovic, E. J. Galbreath, G. E. Sandusky, L. J. Hammond, J. S. Moyers, R. A. Owens, J. Gromada, J. T. Brozinick, E. D. Hawkins, V. J. Wroblewski, D. S. Li, F. Mehrbod, S. R. Jaskunas, A. B. Shanafelt, FGF-21 as a novel metabolic regulator, *J. Clin. Invest.* (2005), doi:10.1172/JCI23606.

304. S. von Holstein-Rathlou, L. D. BonDurant, L. Peltekian, M. C. Naber, T. C. Yin, K. E. Claflin, A. I.

Urizar, A. N. Madsen, C. Ratner, B. Holst, K. Karstoft, A. Vandenbeuch, C. B. Anderson, M. D. Cassell, A. P. Thompson, T. P. Solomon, K. Rahmouni, S. C. Kinnamon, A. A. Pieper, M. P. Gillum, M. J. Potthoff, FGF21 Mediates Endocrine Control of Simple Sugar Intake and Sweet Taste Preference by the Liver, *Cell Metab.* **23**, 335–343 (2016).

305. S. Søberg, C. H. Sandholt, N. Z. Jespersen, U. Toft, A. L. Madsen, S. von Holstein-Rathlou, T. J. Grevengoed, K. B. Christensen, W. L. P. Bredie, M. J. Potthoff, T. P. J. Solomon, C. Scheele, A. Linneberg, T. Jørgensen, O. Pedersen, T. Hansen, M. P. Gillum, N. Grarup, FGF21 Is a Sugar-Induced Hormone Associated with Sweet Intake and Preference in Humans, *Cell Metab.* (2017), doi:10.1016/j.cmet.2017.04.009.

306. B. M. Owen, X. Ding, D. A. Morgan, K. C. Coate, A. L. Bookout, K. Rahmouni, S. A. Kliewer, D. J. Mangelsdorf, FGF21 Acts Centrally to Induce Sympathetic Nerve Activity, Energy Expenditure, and Weight Loss, *Cell Metab.* **20**, 670–677 (2014).

307. K. R. Markan, M. C. Naber, M. K. Ameka, M. D. Anderegg, D. J. Mangelsdorf, S. A. Kliewer, M. Mohammadi, M. J. Potthoff, Circulating FGF21 is liver derived and enhances glucose uptake during refeeding and overfeeding., *Diabetes* **63**, 4057–63 (2014).

308. B. Emanuelli, S. G. Vienberg, G. Smyth, C. Cheng, K. I. Stanford, M. Arumugam, M. D. Michael, A. C. Adams, A. Kharitonenkov, C. R. Kahn, Interplay between FGF21 and insulin action in the liver regulates metabolism, *J. Clin. Invest.* **124**, 515–527 (2014).

309. L. X. Cubeddu, H. Bönisch, M. Göthert, G. Molderings, K. Racké, G. Ramadori, K. J. Miller, H. Schwörer, Effects of metformin on intestinal 5-hydroxytryptamine (5-HT) release and on 5-HT3 receptors., *Naunyn. Schmiedebergs. Arch. Pharmacol.* **361**, 85–91 (2000).

310. G. M. Mawe, J. M. Hoffman, Serotonin signalling in the gut-functions, dysfunctions and therapeutic targets*Nat. Rev. Gastroenterol. Hepatol.* (2013), doi:10.1038/nrgastro.2013.105.

311. G. G. Graham, J. Punt, M. Arora, R. O. Day, M. P. Doogue, J. K. Duong, T. J. Furlong, J. R. Greenfield, L. C. Greenup, C. M. Kirkpatrick, J. E. Ray, P. Timmins, K. M. Williams, Clinical Pharmacokinetics of Metformin, *Clin. Pharmacokinet.* **50**, 81–98 (2011).

312. C. Wilcock, C. J. Bailey, Accumulation of metformin by tissues of the normal and diabetic mouse, *Xenobiotica* **24**, 49–57 (1994).

313. L. C. Gormsen, E. I. Sundelin, J. B. Jensen, M. H. Vendelbo, S. Jakobsen, O. L. Munk, M. M. Hougaard Christensen, K. Brøsen, J. Frøkiær, N. Jessen, In Vivo Imaging of Human 11C-Metformin in Peripheral Organs: Dosimetry, Biodistribution, and Kinetic Analyses., *J. Nucl. Med.* **57**, 1920–1926

(2016).

314. T. Han, W. R. Proctor, C. L. Costales, H. Cai, R. S. Everett, D. R. Thakker, Four Cation-Selective Transporters Contribute to Apical Uptake and Accumulation of Metformin in Caco-2 Cell Monolayers, *J. Pharmacol. Exp. Ther.* (2015), doi:10.1124/jpet.114.220350.

315. W. R. Proctor, D. L. Bourdet, D. R. Thakker, Mechanisms Underlying Saturable Intestinal Absorption of Metformin, *Drug Metab. Dispos.* **36**, 1650–1658 (2008).

316. D. Stepensky, M. Friedman, I. Raz, A. Hoffman, Pharmacokinetic-pharmacodynamic analysis of the glucose-lowering effect of metformin in diabetic rats reveals first-pass pharmacodynamic effect., *Drug Metab. Dispos.* **30**, 861–8 (2002).

317. E. Bonora, M. Cigolini, O. Bosello, C. Zancanaro, L. Capretti, I. Zavaroni, C. Coscelli, U. Butturini, Lack of effect of intravenous metformin on plasma concentrations of glucose, insulin, C-peptide, glucagon and growth hormone in non-diabetic subjects, *Curr. Med. Res. Opin.* **9**, 47–51 (1984).

318. C.-F. Sum, J. M. Webster, A. B. Johnson, C. Catalano, B. G. Cooper, R. Taylor, The Effect of Intravenous Metformin on Glucose Metabolism During Hyperglycaemia in Type 2 Diabetes, *Diabet. Med.* **9**, 61–65 (1992).

319. J. B. Buse, R. A. DeFronzo, J. Rosenstock, T. Kim, C. Burns, S. Skare, A. Baron, M. Fineman, The Primary Glucose-Lowering Effect of Metformin Resides in the Gut, Not the Circulation. Results From Short-term Pharmacokinetic and 12-Week Dose-Ranging Studies, *Diabetes Care* **39**, dc150488 (2015).

320. R. R. Henry, J. P. Frias, B. Walsh, S. Skare, J. Hemming, C. Burns, T. A. Bicsak, A. Baron, M. Fineman, D. Samocha-Bonet, Ed. Improved glycemic control with minimal systemic metformin exposure: Effects of Metformin Delayed-Release (Metformin DR) targeting the lower bowel over 16 weeks in a randomized trial in subjects with type 2 diabetes, *PLoS One* **13**, e0203946 (2018).

321. A. P. Coll, M. Chen, P. Taskar, D. Rimmington, S. Patel, J. Tadross, I. Cimino, M. Yang, P. Welsh, S. Virtue, D. A. Goldspink, E. Miedzybrodzka, Y. C. L. Tung, S. Rodriguez-Cuenca, R. A. Tomaz, H. P. Harding, A. Melvin, G. S. H. Yeo, D. Preiss, A. Vidal-Puig, L. Vallier, D. Ron, F. M. Gribble, F. Reimann, N. Sattar, D. B. Savage, B. B. Allan, S. O'Rahilly, GDF15 and the beneficial actions of metformin in pre-diabetes, *bioRxiv* , 677831 (2019).

322. B. Svendsen, R. Pais, M. S. Engelstoft, N. B. Milev, P. Richards, C. B. Christiansen, A. Habib, K. L. Egerod, S. M. Jensen, F. Gribble, T. W. Schwartz, F. Reimann, J. J. Holst, GLP1 and GIP cells rarely overlap and differ by bombesin receptor-2 expression and responsiveness, *J. Endocrinol.* **228**, JOE-

15-0247 (2015).

323. A. Adriaenssens, B. Y. H. Lam, L. Billing, K. Skeffington, S. Sewing, F. Reimann, F. Gribble, A Transcriptome-Led Exploration of Molecular Mechanisms Regulating Somatostatin-Producing D-Cells in the Gastric Epithelium., *Endocrinology* **156**, 3924–36 (2015).

324. D. A. Goldspink, V. B. Lu, L. J. Billing, P. Larraufie, G. Tolhurst, F. M. Gribble, F. Reimann, Mechanistic insights into the detection of free fatty and bile acids by ileal glucagon-like peptide-1 secreting cells, *Mol. Metab.* **7**, 90–101 (2018).

325. M. Tantama, J. R. Martínez-François, R. Mongeon, G. Yellen, Imaging energy status in live cells with a fluorescent biosensor of the intracellular ATP-to-ADP ratio., *Nat. Commun.* **4**, 2550 (2013).

326. Y. P. Hung, J. G. Albeck, M. Tantama, G. Yellen, Imaging Cytosolic NADH-NAD+ Redox State with a Genetically Encoded Fluorescent Biosensor, *Cell Metab.* **14**, 545–554 (2011).

327. F. Bartolomé, A. Y. Abramov, in *Methods in molecular biology (Clifton, N.J.)*, (2015), vol. 1264, pp. 263–270.

328. H. Takanaga, B. Chaudhuri, W. B. Frommer, GLUT1 and GLUT9 as major contributors to glucose influx in HepG2 cells identified by a high sensitivity intramolecular FRET glucose sensor, *Biochim. Biophys. Acta - Biomembr.* **1778**, 1091–1099 (2008).

329. K. Gruenwald, J. T. Holland, V. Stromberg, A. Ahmad, D. Watcharakichkorn, S. Okumoto, S. Strack, Ed. Visualization of Glutamine Transporter Activities in Living Cells Using Genetically Encoded Glutamine Sensors, *PLoS One* **7**, e38591 (2012).

330. A. San Martín, S. Ceballo, F. Baeza-Lehnert, R. Lerchundi, R. Valdebenito, Y. Contreras-Baeza, K. Alegría, L. F. Barros, K.-W. Koch, Ed. Imaging Mitochondrial Flux in Single Cells with a FRET Sensor for Pyruvate, *PLoS One* **9**, e85780 (2014).

331. A. S. Divakaruni, A. Paradyse, D. A. Ferrick, A. N. Murphy, M. Jastroch, in *Methods in enzymology*, (2014), vol. 547, pp. 309–354.

332. G. Schumann, R. Bonora, F. Ceriotti, G. Férard, C. A. Ferrero, P. F. H. Franck, F.-J. Gella, W. Hoelzel, P. J. Jørgensen, T. Kanno, A. Kessner, R. Klauke, N. Kristiansen, J.-M. Lessinger, T. P. J. Linsinger, H. Misaki, M. Panteghini, J. Pauwels, F. Schiele, H. G. Schimmel, IFCC Primary Reference Procedures for the Measurement of Catalytic Activity Concentrations of Enzymes at 37°C. Part 4. Reference Procedure for the Measurement of Catalytic Concentration of Alanine Aminotransferase, *Clin. Chem. Lab. Med.* **40** (2002), doi:10.1515/CCLM.2002.124.

333. G. Schumann, R. Aoki, C. a Ferrero, G. Ehlers, G. Férard, F.-J. Gella, P. J. Jørgensen, T. Kanno, A. Kessner, R. Klauke, H.-J. Kytzia, J.-M. Lessinger, W. G. Miller, R. Nagel, J. Pauwels, H. Schimmel, L. Siekmann, G. Weidemann, K. Yoshida, F. Ceriotti, IFCC primary reference procedures for the measurement of catalytic activity concentrations of enzymes at 37 degrees C., *Clin. Chem. Lab. Med.* (2006), doi:10.1515/CCLM.2006.212.

334. L. Siekmann, R. Bonora, C. A. Burtis, F. Ceriotti, P. Clerc-Renaud, G. Férard, C. A. Ferrero, J.-C. Forest, P. F. H. Franck, F.-J. Gella, W. Hoelzel, P. J. Jørgensen, T. Kanno, A. Kessner, R. Klauke, N. Kristiansen, J.-M. Lessinger, T. P. J. Linsinger, H. Misaki, M. M. Mueller, M. Panteghini, J. Pauwels, F. Schiele, H. G. Schimmel, A. Vialle, G. Weidemann, G. Schumann, IFCC primary reference procedures for the measurement of catalytic activity concentrations of enzymes at 37 degrees C. International Federation of Clinical Chemistry and Laboratory Medicine. Part 7. Certification of four reference materials for the determination of enzymatic activity of gamma-glutamyltransferase, lactate dehydrogenase, alanine aminotransferase and creatine kinase accord., *Clin. Chem. Lab. Med.* (2002), doi:10.1515/CCLM.2002.127.

335. G. Schumann, R. Bonora, F. Ceriotti, G. Férard, C. A. Ferrero, P. F. H. Franck, F.-J. Gella, W. Hoelzel, P. J. Jørgensen, T. Kanno, A. Kessner, R. Klauke, N. Kristiansen, J.-M. Lessinger, T. P. J. Linsinger, H. Misaki, M. Panteghini, J. Pauwels, F. Schiele, H. G. Schimmel, G. Weidemann, L. Siekmann, International Federation of Clinical Chemistry and Laboratory Medicine, IFCC Primary Reference Procedures for the Measurement of Catalytic Activity Concentrations of Enzymes at 37°C. Part 5. Reference Procedure for the Measurement of Catalytic Concentration of Aspartate Aminotransferase, *Clin. Chem. Lab. Med.* (2002), doi:10.1515/CCLM.2002.125.

336. G. F. Merrill, E. J. Kurth, D. G. Hardie, W. W. Winder, AICA riboside increases AMP-activated protein kinase, fatty acid oxidation, and glucose uptake in rat muscle, *Am. J. Physiol. Metab.* **273**, E1107–E1112 (1997).

337. S. C. Chen, R. Brooks, J. Houskeeper, S. K. Bremner, J. Dunlop, B. Viollet, P. J. Logan, I. P. Salt, S. F. Ahmed, S. J. Yarwood, Metformin suppresses adipogenesis through both AMP-activated protein kinase (AMPK)-dependent and AMPK-independent mechanisms., *Mol. Cell. Endocrinol.* **440**, 57–68 (2017).

338. N. Musi, M. F. Hirshman, J. Nygren, M. Svanfeldt, P. Bavenholm, O. Rooyackers, G. Zhou, J. M. Williamson, O. Ljunqvist, S. Efendic, D. E. Moller, A. Thorell, L. J. Goodyear, Metformin Increases AMP-Activated Protein Kinase Activity in Skeletal Muscle of Subjects With Type 2 Diabetes, *Diabetes* **51**, 2074–2081 (2002).

339. E. C. Cokorinos, J. Delmore, A. R. Reyes, B. Albuquerque, R. Kjøbsted, N. O. Jørgensen, J.-L. Tran, A. Jatkar, K. Cialdea, R. M. Esquejo, J. Meissen, M. F. Calabrese, J. Cordes, R. Moccia, D. Tess, C. T. Salatto, T. M. Coskran, A. C. Opsahl, D. Flynn, M. Blatnik, W. Li, E. Kindt, M. Foretz, B. Viollet, J. Ward, R. G. Kurumbail, A. S. Kalgutkar, J. F. P. Wojtaszewski, K. O. Cameron, R. A. Miller, Activation of Skeletal Muscle AMPK Promotes Glucose Disposal and Glucose Lowering in Non-human Primates and Mice, *Cell Metab.* **25**, 1147-1159.e10 (2017).

340. J. O. Lee, S. K. Lee, J. H. Jung, J. H. Kim, G. Y. You, S. J. Kim, S. H. Park, K.-O. Uhm, H. S. Kim, Metformin induces Rab4 through AMPK and modulates GLUT4 translocation in skeletal muscle cells, *J. Cell. Physiol.* **226**, 974–981 (2011).

341. H. C. Chen, G. Bandyopadhyay, M. P. Sajan, Y. Kanoh, M. Standaert, R. V Farese, R. V Farese, Activation of the ERK pathway and atypical protein kinase C isoforms in exercise- and aminoimidazole-4-carboxamide-1-beta-D-riboside (AICAR)-stimulated glucose transport., *J. Biol. Chem.* **277**, 23554–62 (2002).

342. P. A. Lochhead, I. P. Salt, K. S. Walker, D. G. Hardie, C. Sutherland, 5-aminoimidazole-4-carboxamide riboside mimics the effects of insulin on the expression of the 2 key gluconeogenic genes PEPCK and glucose-6-phosphatase, *Diabetes* **49**, 896–903 (2000).

343. S. Meng, J. Cao, Q. He, L. Xiong, E. Chang, S. Radovick, F. E. Wondisford, L. He, Metformin activates AMP-activated protein kinase by promoting formation of the αβγ heterotrimeric complex., *J. Biol. Chem.* **290**, 3793–802 (2015).

344. I. Ben Sahra, C. Regazzetti, G. Robert, K. Laurent, Y. Le Marchand-Brustel, P. Auberger, J.-F. Tanti, S. Giorgetti-Peraldi, F. Bost, Metformin, Independent of AMPK, Induces mTOR Inhibition and Cell-Cycle Arrest through REDD1, *Cancer Res.* **71**, 4366–4372 (2011).

345. T. A. Guimarães, L. C. Farias, E. S. Santos, C. A. de C. Fraga, L. A. Orsini, L. de F. Teles, J. D. Feltenberger, S. F. de Jesus, M. G. de Souza, S. H. S. Santos, A. M. B. de Paula, R. S. Gomez, A. L. S. Guimarães, Metformin increases PDH and suppresses HIF-1α under hypoxic conditions and induces cell death in oral squamous cell carcinoma, *Oncotarget* **7**, 55057 (2016).

346. X. Zhou, J. Chen, G. Yi, M. Deng, H. Liu, M. Liang, B. Shi, X. Fu, Y. Chen, L. Chen, Z. He, J. Wang, J. Liu, Metformin suppresses hypoxia-induced stabilization of HIF-1α through reprogramming of oxygen metabolism in hepatocellular carcinoma., *Oncotarget* **7**, 873–84 (2016).

347. S. Narravula, S. P. Colgan, Hypoxia-Inducible Factor 1-Mediated Inhibition of Peroxisome Proliferator-Activated Receptor α Expression During Hypoxia, *J. Immunol.* **166**, 7543–7548 (2001).

348. X. Cai, X. Hu, X. Tan, W. Cheng, Q. Wang, X. Chen, Y. Guan, C. Chen, X. Jing, Metformin Induced AMPK Activation, G0/G1 Phase Cell Cycle Arrest and the Inhibition of Growth of Esophageal Squamous Cell Carcinomas In Vitro and In Vivo., *PLoS One* **10**, e0133349 (2015).

349. Y. Zhuang, W. K. Miskimins, Cell cycle arrest in Metformin treated breast cancer cells involves activation of AMPK, downregulation of cyclin D1, and requires p27^{Kip1} or p21^{Cip1}, *J. Mol. Signal.* **3**, 18 (2008).

350. O. Moiseeva, X. Deschênes-Simard, E. St-Germain, S. Igelmann, G. Huot, A. E. Cadar, V. Bourdeau, M. N. Pollak, G. Ferbeyre, Metformin inhibits the senescence-associated secretory phenotype by interfering with IKK/NF-κB activation, *Aging Cell* **12**, 489–498 (2013).

351. D. Chen, D. Xia, Z. Pan, D. Xu, Y. Zhou, Y. Wu, N. Cai, Q. Tang, C. Wang, M. Yan, J. J. Zhang, K. Zhou, Q. Wang, Y. Feng, X. Wang, H. Xu, X. Zhang, N. Tian, Metformin protects against apoptosis and senescence in nucleus pulposus cells and ameliorates disc degeneration in vivo, *Cell Death Dis.* **7**, e2441–e2441 (2016).

352. T. Tomic, T. Botton, M. Cerezo, G. Robert, F. Luciano, A. Puissant, P. Gounon, M. Allegra, C. Bertolotto, J.-M. Bereder, S. Tartare-Deckert, P. Bahadoran, P. Auberger, R. Ballotti, S. Rocchi, Metformin inhibits melanoma development through autophagy and apoptosis mechanisms, *Cell Death Dis.* **2**, e199–e199 (2011).

353. W.-Y. Shi, D. Xiao, L. Wang, L.-H. Dong, Z.-X. Yan, Z.-X. Shen, S.-J. Chen, Y. Chen, W.-L. Zhao, Therapeutic metformin/AMPK activation blocked lymphoma cell growth via inhibition of mTOR pathway and induction of autophagy, *Cell Death Dis.* **3**, e275–e275 (2012).

354. Z. Xie, K. Lau, B. Eby, P. Lozano, C. He, B. Pennington, H. Li, S. Rathi, Y. Dong, R. Tian, D. Kem, M.-H. Zou, Improvement of cardiac functions by chronic metformin treatment is associated with enhanced cardiac autophagy in diabetic OVE26 mice., *Diabetes* **60**, 1770–8 (2011).

355. Y. M. Song, Y. Lee, J.-W. Kim, D.-S. Ham, E.-S. Kang, B. S. Cha, H. C. Lee, B.-W. Lee, Metformin alleviates hepatosteatosis by restoring SIRT1-mediated autophagy induction via an AMP-activated protein kinase-independent pathway, *Autophagy* **11**, 46–59 (2015).

356. K. Isoda, J. L. Young, A. Zirlik, L. A. MacFarlane, N. Tsuboi, N. Gerdes, U. Schönbeck, P. Libby, Metformin Inhibits Proinflammatory Responses and Nuclear Factor-κB in Human Vascular Wall Cells, *Arterioscler. Thromb. Vasc. Biol.* **26**, 611–617 (2006).

357. H.-M. Lee, J.-J. Kim, H. J. Kim, M. Shong, B. J. Ku, E.-K. Jo, Upregulated NLRP3 Inflammasome Activation in Patients With Type 2 Diabetes, *Diabetes* **62**, 194–204 (2013).

358. T. Quentin, M. Steinmetz, A. Poppe, S. Thoms, Metformin differentially activates ER stress signaling pathways without inducing apoptosis, *Dis. Model. Mech.* **5**, 259–269 (2012).

359. Q. Chen, J. Thompson, Y. Hu, A. Das, E. J. Lesnefsky, Metformin attenuates ER stress–induced mitochondrial dysfunction, *Transl. Res.* **190**, 40–50 (2017).

360. Y. Xue, H. Zhang, X. Sun, M.-J. Zhu, X. Han, Ed. Metformin Improves Ileal Epithelial Barrier Function in Interleukin-10 Deficient Mice, *PLoS One* **11**, e0168670 (2016).

361. J. Deng, L. Zeng, X. Lai, J. Li, L. Liu, Q. Lin, Y. Chen, Metformin protects against intestinal barrier dysfunction via AMPKα1-dependent inhibition of JNK signalling activation., *J. Cell. Mol. Med.* **22**, 546–557 (2018).

362. A. Spruss, G. Kanuri, C. Stahl, S. C. Bischoff, I. Bergheim, Metformin protects against the development of fructose-induced steatosis in mice: role of the intestinal barrier function, *Lab. Investig.* **92**, 1020–1032 (2012).

363. T. M. Z. Waise, M. Rasti, F. A. Duca, S.-Y. Zhang, P. V. Bauer, C. J. Rhodes, T. K. T. Lam, Inhibition of upper small intestinal mTOR lowers plasma glucose levels by inhibiting glucose production, *Nat. Commun.* **10**, 714 (2019).

364. M. Massollo, C. Marini, M. Brignone, L. Emionite, B. Salani, M. Riondato, S. Capitanio, F. Fiz, A. Democrito, A. Amaro, S. Morbelli, M. Piana, D. Maggi, M. Cilli, U. Pfeffer, G. Sambuceti, Metformin temporal and localized effects on gut glucose metabolism assessed using 18F-FDG PET in mice., *J. Nucl. Med.* **54**, 259–66 (2013).

365. M. R. Open Access Citation: Luizon, W. L. Eckalbar, Y. Wang, S. L. Jones, R. P. Smith, M. Laurance, Genomic Characterization of Metformin Hepatic Response, *PLoS Genet* **12**, 1006449 (2016).

366. A. S. Kulkarni, E. F. Brutsaert, V. Anghel, K. Zhang, N. Bloomgarden, M. Pollak, J. C. Mar, M. Hawkins, J. P. Crandall, N. Barzilai, Metformin regulates metabolic and nonmetabolic pathways in skeletal muscle and subcutaneous adipose tissues of older adults, *Aging Cell* **17**, e12723 (2018).

367. W. Yue, T. Wang, E. Zachariah, Y. Lin, C. S. Yang, Q. Xu, R. S. DiPaola, X.-L. Tan, Transcriptomic analysis of pancreatic cancer cells in response to metformin and aspirin: an implication of synergy, *Sci. Rep.* **5**, 13390 (2015).

368. Z. E. Gillespie, C. Wang, F. Vadan, T. Y. Yu, J. Ausió, A. Kusalik, C. H. Eskiw, Metformin induces the AP-1 transcription factor network in normal dermal fibroblasts, *Sci. Rep.* **9**, 5369 (2019).

369. D. Grün, A. Lyubimova, L. Kester, K. Wiebrands, O. Basak, N. Sasaki, H. Clevers, A. van Oudenaarden, Single-cell messenger RNA sequencing reveals rare intestinal cell types, *Nature* **525**, 251–255 (2015).

370. K. Cusi, A. Consoli, R. A. DeFronzo, Metabolic effects of metformin on glucose and lactate metabolism in noninsulin-dependent diabetes mellitus., *J. Clin. Endocrinol. Metab.* **81**, 4059–4067 (1996).

371. G. Wu, Intestinal Mucosal Amino Acid Catabolism, *J. Nutr.* **128**, 1249–1252 (1998).

372. Y. Pan, H. Chen, F. Siu, M. S. Kilberg, Amino acid deprivation and endoplasmic reticulum stress induce expression of multiple activating transcription factor-3 mRNA species that, when overexpressed in HepG2 cells, modulate transcription by the human asparagine synthetase promoter., *J. Biol. Chem.* **278**, 38402–12 (2003).

373. J. Nikkanen, S. Forsström, L. Euro, I. Paetau, R. A. Kohnz, L. Wang, D. Chilov, J. Viinamäki, A. Roivainen, P. Marjamäki, H. Liljenbäck, S. Ahola, J. Buzkova, M. Terzioglu, N. A. Khan, S. Pirnes-Karhu, A. Paetau, T. Lönnqvist, A. Sajantila, P. Isohanni, H. Tyynismaa, D. K. Nomura, B. J. Battersby, V. Velagapudi, C. J. Carroll, A. Suomalainen, Mitochondrial DNA Replication Defects Disturb Cellular dNTP Pools and Remodel One-Carbon Metabolism, *Cell Metab.* **23**, 635–648 (2016).

374. N. A. Khan, J. Nikkanen, S. Yatsuga, C. Jackson, L. Wang, S. Pradhan, R. Kivelä, A. Pessia, V. Velagapudi, A. Suomalainen, mTORC1 Regulates Mitochondrial Integrated Stress Response and Mitochondrial Myopathy Progression., *Cell Metab.* **26**, 419-428.e5 (2017).

375. Y. Benita, H. Kikuchi, A. D. Smith, M. Q. Zhang, D. C. Chung, R. J. Xavier, An integrative genomics approach identifies Hypoxia Inducible Factor-1 (HIF-1)-target genes that form the core response to hypoxia, *Nucleic Acids Res.* **37**, 4587–4602 (2009).

376. L. B. Tanner, A. G. Goglia, M. H. Wei, T. Sehgal, L. R. Parsons, J. O. Park, E. White, J. E. Toettcher, J. D. Rabinowitz, Four Key Steps Control Glycolytic Flux in Mammalian Cells, *Cell Syst.* **7**, 49-62.e8 (2018).

377. D. Da Silva, P. Ausina, E. M. Alencar, W. S. Coelho, P. Zancan, M. Sola-Penna, Metformin reverses hexokinase and phosphofructokinase downregulation and intracellular distribution in the heart of diabetic mice, *IUBMB Life* **64**, 766–774 (2012).

378. D. Di Fusco, V. Dinallo, I. Monteleone, F. Laudisi, I. Marafini, E. Franzè, A. Di Grazia, R. Dwairi, A. Colantoni, A. Ortenzi, C. Stolfi, G. Monteleone, Metformin inhibits inflammatory signals in the gut by controlling AMPK and p38 MAP kinase activation, *Clin. Sci.* **132**, 1155–1168 (2018).

379. A. S. Marsin, L. Bertrand, M. H. Rider, J. Deprez, C. Beauloye, M. F. Vincent, G. Van den Berghe, D. Carling, L. Hue, Phosphorylation and activation of heart PFK-2 by AMPK has a role in the stimulation of glycolysis during ischaemia., *Curr. Biol.* **10**, 1247–55 (2000).

380. N. S. Chandel, E. Maltepe, E. Goldwasser, C. E. Mathieu, M. C. Simon, P. T. Schumacker, Mitochondrial reactive oxygen species trigger hypoxia-induced transcription., *Proc. Natl. Acad. Sci. U. S. A.* **95**, 11715–20 (1998).

381. A. Mogavero, M. V. Maiorana, S. Zanutto, L. Varinelli, F. Bozzi, A. Belfiore, C. C. Volpi, A. Gloghini, M. A. Pierotti, M. Gariboldi, Metformin transiently inhibits colorectal cancer cell proliferation as a result of either AMPK activation or increased ROS production, *Sci. Rep.* **7**, 15992 (2017).

382. Y. Pan, K. D. Mansfield, C. C. Bertozzi, V. Rudenko, D. A. Chan, A. J. Giaccia, M. C. Simon, Multiple Factors Affecting Cellular Redox Status and Energy Metabolism Modulate Hypoxia-Inducible Factor Prolyl Hydroxylase Activity In Vivo and In Vitro, *Mol. Cell. Biol.* **27**, 912–925 (2007).

383. H. Lu, R. A. Forbes, A. Verma, Hypoxia-inducible factor 1 activation by aerobic glycolysis implicates the Warburg effect in carcinogenesis, *J. Biol. Chem.* **277**, 23111–23115 (2002).

384. D. Zhang, Z. Tang, H. Huang, G. Zhou, C. Cui, Y. Weng, W. Liu, S. Kim, S. Lee, M. Perez-Neut, J. Ding, D. Czyz, R. Hu, Z. Ye, M. He, Y. G. Zheng, H. A. Shuman, L. Dai, B. Ren, R. G. Roeder, L. Becker, Y. Zhao, Metabolic regulation of gene expression by histone lactylation, *Nature* **574**, 575–580 (2019).

385. M. Heishi, J. Ichihara, R. Teramoto, Y. Itakura, K. Hayashi, H. Ishikawa, H. Gomi, J. Sakai, M. Kanaoka, M. Taiji, T. Kimura, Global gene expression analysis in liver of obese diabetic db/db mice treated with metformin, *Diabetologia* **49**, 1647–1655 (2006).

386. M. Croset, F. Rajas, C. Zitoun, J. M. Hurot, S. Montano, G. Mithieux, Rat small intestine is an insulin-sensitive gluconeogenic organ, *Diabetes* (2001), doi:10.2337/diabetes.50.4.740.

387. K. C. Patra, N. Hay, The pentose phosphate pathway and cancer, *Trends Biochem. Sci.* **39**, 347–354 (2014).

388. R. Hanczko, D. R. Fernandez, E. Doherty, Y. Qian, G. Vas, B. Niland, T. Telarico, A. Garba, S. Banerjee, F. A. Middleton, D. Barrett, M. Barcza, K. Banki, S. K. Landas, A. Perl, Prevention of hepatocarcinogenesis and increased susceptibility to acetaminophen-induced liver failure in transaldolase-deficient mice by N-acetylcysteine., *J. Clin. Invest.* **119**, 1546–57 (2009).

389. G. Mithieux, L. Guignot, J.-C. Bordet, N. Wiernsperger, Intrahepatic mechanisms underlying the effect of metformin in decreasing basal glucose production in rats fed a high-fat diet., *Diabetes* **51**,

139–43 (2002).

390. E. A. Horne, H. E. Magee, Glycogen synthesis in the small intestine., *J. Physiol.* **78**, 288–94 (1933).

391. C. Jang, S. Hui, W. Lu, A. J. Cowan, R. J. Morscher, G. Lee, W. Liu, G. J. Tesz, M. J. Birnbaum, J. D. Rabinowitz, The Small Intestine Converts Dietary Fructose into Glucose and Organic Acids., *Cell Metab.* **27**, 351-361.e3 (2018).

392. X. Zhang, A. Grosfeld, E. Williams, D. Vasiliauskas, S. Barretto, L. Smith, M. Mariadassou, C. Philippe, F. Devime, C. Melchior, G. Gourcerol, N. Dourmap, N. Lapaque, P. Larraufie, H. M. Blottière, C. Herberden, P. Gerard, J. F. Rehfeld, R. P. Ferraris, J. C. Fritton, S. Ellero-Simatos, V. Douard, Fructose malabsorption induces cholecystokinin expression in the ileum and cecum by changing microbiota composition and metabolism, *FASEB J.* **33**, 7126–7142 (2019).

393. J. B. Spinelli, M. C. Haigis, The multifaceted contributions of mitochondria to cellular metabolism, *Nat. Cell Biol.* **20**, 745–754 (2018).

394. X. Liu, I. L. Romero, L. M. Litchfield, E. Lengyel, J. W. Locasale, Metformin Targets Central Carbon Metabolism and Reveals Mitochondrial Requirements in Human Cancers., *Cell Metab.* **24**, 728–739 (2016).

395. S. Saladini, M. Aventaggiato, F. Barreca, E. Morgante, L. Sansone, M. A. Russo, M. Tafani, Metformin Impairs Glutamine Metabolism and Autophagy in Tumour Cells, *Cells* **8**, 49 (2019).

396. D. Y. Gui, L. B. Sullivan, A. Luengo, A. M. Hosios, L. N. Bush, N. Gitego, S. M. Davidson, E. Freinkman, C. J. Thomas, M. G. Vander Heiden, Environment Dictates Dependence on Mitochondrial Complex I for NAD+ and Aspartate Production and Determines Cancer Cell Sensitivity to Metformin, *Cell Metab.* (2016), doi:10.1016/j.cmet.2016.09.006.

397. K. K. Birsoy, T. Wang, W. W. W. Chen, E. Freinkman, M. Abu-Remaileh, D. M. M. Sabatini, An Essential Role of the Mitochondrial Electron Transport Chain in Cell Proliferation Is to Enable Aspartate Synthesis, *Cell* **162**, 540–551 (2015).

398. M. C. G. Van De Poll, G. C. Ligthart-Melis, P. G. Boelens, N. E. P. Deutz, P. A. M. Van Leeuwen, C. H. C. Dejong, Intestinal and hepatic metabolism of glutamine and citrulline in humans, *J. Physiol.* **581**, 819–827 (2007).

399. S. Osowska, C. Moinard, N. Neveux, C. Loï, L. Cynober, Citrulline increases arginine pools and restores nitrogen balance after massive intestinal resection., *Gut* **53**, 1781–6 (2004).

400. D. G. Burrin, P. J. Reeds, Alternative fuels in the gastrointestinal tract, *Curr. Opin. Gastroenterol.* **13**, 165–170 (1997).

401. P. Crenn, B. Messing, L. Cynober, Citrulline as a biomarker of intestinal failure due to enterocyte mass reduction, *Clin. Nutr.* **27**, 328–339 (2008).

402. L. Lutgens, P. Lambin, Biomarkers for radiation-induced small bowel epithelial damage: an emerging role for plasma Citrulline., *World J. Gastroenterol.* **13**, 3033–42 (2007).

403. G. S. Ducker, J. D. Rabinowitz, One-Carbon Metabolism in Health and Disease, *Cell Metab.* **25**, 27–42 (2017).

404. C. F. Labuschagne, N. J. F. van den Broek, G. M. Mackay, K. H. Vousden, O. D. K. Maddocks, Serine, but Not Glycine, Supports One-Carbon Metabolism and Proliferation of Cancer Cells, *Cell Rep.* **7**, 1248–1258 (2014).

405. S. J. Mentch, M. Mehrmohamadi, L. Huang, X. Liu, D. Gupta, D. Mattocks, P. Gómez Padilla, G. Ables, M. M. Bamman, A. E. Thalacker-Mercer, S. N. Nichenametla, J. W. Locasale, Histone Methylation Dynamics and Gene Regulation Occur through the Sensing of One-Carbon Metabolism, *Cell Metab.* **22**, 861–873 (2015).

406. G. Kikuchi, K. Hiraga, T. Yoshida, Role of the glycine-cleavage system in glycine and serine metabolism in various organs., *Biochem. Soc. Trans.* **8**, 504–6 (1980).

407. X. R. Bao, S.-E. Ong, O. Goldberger, J. Peng, R. Sharma, D. A. Thompson, S. B. Vafai, A. G. Cox, E. Marutani, F. Ichinose, W. Goessling, A. Regev, S. A. Carr, C. B. Clish, V. K. Mootha, Mitochondrial dysfunction remodels one-carbon metabolism in human cells, *Elife* **5** (2016), doi:10.7554/eLife.10575.

408. L. L. Sampson, A. K. Davis, M. W. Grogg, Y. Zheng, mTOR disruption causes intestinal epithelial cell defects and intestinal atrophy postinjury in mice, *FASEB J.* **30**, 1263–1275 (2016).

409. J. J. Geerling, M. R. Boon, G. C. van der Zon, S. A. A. van den Berg, A. M. van den Hoek, M. Lombès, H. M. G. Princen, L. M. Havekes, P. C. N. Rensen, B. Guigas, Metformin lowers plasma triglycerides by promoting VLDL-triglyceride clearance by brown adipose tissue in mice., *Diabetes* **63**, 880–91 (2014).

410. M. Ahmadian, J. M. Suh, N. Hah, C. Liddle, A. R. Atkins, M. Downes, R. M. Evans, PPARγ signaling and metabolism: the good, the bad and the future, *Nat. Med.* **19**, 557–566 (2013).

411. D. F. Egan, D. B. Shackelford, M. M. Mihaylova, S. Gelino, R. A. Kohnz, W. Mair, D. S. Vasquez, A.

Joshi, D. M. Gwinn, R. Taylor, J. M. Asara, J. Fitzpatrick, A. Dillin, B. Viollet, M. Kundu, M. Hansen, R. J. Shaw, Phosphorylation of ULK1 (hATG1) by AMP-Activated Protein Kinase Connects Energy Sensing to Mitophagy, *Science (80-.).* **331**, 456–461 (2011).

412. D. Zhang, W. Wang, X. Sun, D. Xu, C. Wang, Q. Zhang, H. Wang, W. Luo, Y. Chen, H. Chen, Z. Liu, AMPK regulates autophagy by phosphorylating BECN1 at threonine 388, *Autophagy* **12**, 1447–1459 (2016).

413. C. He, H. Zhu, H. Li, M.-H. Zou, Z. Xie, Dissociation of Bcl-2-Beclin1 Complex by Activated AMPK Enhances Cardiac Autophagy and Protects Against Cardiomyocyte Apoptosis in Diabetes, *Diabetes* **62**, 1270–1281 (2013).

414. J. Kim, M. Kundu, B. Viollet, K.-L. Guan, AMPK and mTOR regulate autophagy through direct phosphorylation of Ulk1, *Nat. Cell Biol.* **13**, 132–141 (2011).

415. J. L. Benjamin, R. Sumpter, B. Levine, L. V. Hooper, Intestinal Epithelial Autophagy Is Essential for Host Defense against Invasive Bacteria, *Cell Host Microbe* **13**, 723–734 (2013).

416. L. A. Baxt, R. J. Xavier, Role of Autophagy in the Maintenance of Intestinal Homeostasis., *Gastroenterology* **149**, 553–62 (2015).

417. K. Cadwell, J. Y. Liu, S. L. Brown, H. Miyoshi, J. Loh, J. K. Lennerz, C. Kishi, W. Kc, J. A. Carrero, S. Hunt, C. D. Stone, E. M. Brunt, R. J. Xavier, B. P. Sleckman, E. Li, N. Mizushima, T. S. Stappenbeck, H. W. Virgin, IV, A key role for autophagy and the autophagy gene Atg16l1 in mouse and human intestinal Paneth cells., *Nature* **456**, 259–63 (2008).

418. K. G. Lassen, P. Kuballa, K. L. Conway, K. K. Patel, C. E. Becker, J. M. Peloquin, E. J. Villablanca, J. M. Norman, T.-C. Liu, R. J. Heath, M. L. Becker, L. Fagbami, H. Horn, J. Mercer, O. H. Yilmaz, J. D. Jaffe, A. F. Shamji, A. K. Bhan, S. A. Carr, M. J. Daly, H. W. Virgin, S. L. Schreiber, T. S. Stappenbeck, R. J. Xavier, Atg16L1 T300A variant decreases selective autophagy resulting in altered cytokine signaling and decreased antibacterial defense, *Proc. Natl. Acad. Sci.* **111**, 7741–7746 (2014).

419. P. Brest, P. Lapaquette, M. Souidi, K. Lebrigand, A. Cesaro, V. Vouret-Craviari, B. Mari, P. Barbry, J.-F. Mosnier, X. Hébuterne, A. Harel-Bellan, B. Mograbi, A. Darfeuille-Michaud, P. Hofman, A synonymous variant in IRGM alters a binding site for miR-196 and causes deregulation of IRGM-dependent xenophagy in Crohn's disease, *Nat. Genet.* **43**, 242–245 (2011).

420. K. L. Conway, P. Kuballa, J. Song, K. K. Patel, A. B. Castoreno, O. H. Yilmaz, H. B. Jijon, M. Zhang, L. N. Aldrich, E. J. Villablanca, J. M. Peloquin, G. Goel, I. Lee, E. Mizoguchi, H. N. Shi, A. K. Bhan, S. Y. Shaw, S. L. Schreiber, H. W. Virgin, A. F. Shamji, T. S. Stappenbeck, H. Reinecker, R. J. Xavier, Atg16l1

is Required for Autophagy in Intestinal Epithelial Cells and Protection of Mice From Salmonella Infection, *Gastroenterology* **145**, 1347–1357 (2013).

421. K. Y. Hur, M.-S. Lee, New mechanisms of metformin action: Focusing on mitochondria and the gut, *J. Diabetes Investig.* **6**, 600–609 (2015).

422. L. Azzolin, T. Panciera, S. Soligo, E. Enzo, S. Bicciato, S. Dupont, S. Bresolin, C. Frasson, G. Basso, V. Guzzardo, A. Fassina, M. Cordenonsi, S. Piccolo, YAP/TAZ Incorporation in the β-Catenin Destruction Complex Orchestrates the Wnt Response, *Cell* **158**, 157–170 (2014).

423. J. Cai, N. Zhang, Y. Zheng, R. F. de Wilde, A. Maitra, D. Pan, The Hippo signaling pathway restricts the oncogenic potential of an intestinal regeneration program, *Genes Dev.* **24**, 2383–2388 (2010).

424. F. D. Camargo, S. Gokhale, J. B. Johnnidis, D. Fu, G. W. Bell, R. Jaenisch, T. R. Brummelkamp, YAP1 Increases Organ Size and Expands Undifferentiated Progenitor Cells, *Curr. Biol.* **17**, 2054–2060 (2007).

425. M. DeRan, J. Yang, C.-H. Shen, E. C. Peters, J. Fitamant, P. Chan, M. Hsieh, S. Zhu, J. M. Asara, B. Zheng, N. Bardeesy, J. Liu, X. Wu, Energy Stress Regulates Hippo-YAP Signaling Involving AMPK-Mediated Regulation of Angiomotin-like 1 Protein, *Cell Rep.* **9**, 495–503 (2014).

426. J.-S. Mo, Z. Meng, Y. C. Kim, H. W. Park, C. G. Hansen, S. Kim, D.-S. Lim, K.-L. Guan, Cellular energy stress induces AMPK-mediated regulation of YAP and the Hippo pathway, *Nat. Cell Biol.* **17**, 500–510 (2015).

427. M. Mohseni, J. Sun, A. Lau, S. Curtis, J. Goldsmith, V. L. Fox, C. Wei, M. Frazier, O. Samson, K.-K. Wong, C. Kim, F. D. Camargo, A genetic screen identifies an LKB1–MARK signalling axis controlling the Hippo–YAP pathway, *Nat. Cell Biol.* **16**, 108–117 (2014).

428. W. Wang, Z.-D. Xiao, X. Li, K. E. Aziz, B. Gan, R. L. Johnson, J. Chen, AMPK modulates Hippo pathway activity to regulate energy homeostasis, *Nat. Cell Biol.* **17**, 490–499 (2015).

429. H. Jiang, M. O. Grenley, M.-J. Bravo, R. Z. Blumhagen, B. A. Edgar, EGFR/Ras/MAPK Signaling Mediates Adult Midgut Epithelial Homeostasis and Regeneration in Drosophila, *Cell Stem Cell* **8**, 84–95 (2011).

430. V. W. Y. Wong, D. E. Stange, M. E. Page, S. Buczacki, A. Wabik, S. Itami, M. van de Wetering, R. Poulsom, N. A. Wright, M. W. B. Trotter, F. M. Watt, D. J. Winton, H. Clevers, K. B. Jensen, Lrig1 controls intestinal stem-cell homeostasis by negative regulation of ErbB signalling, *Nat. Cell Biol.* **14**, 401–408 (2012).

431. J. Holmberg, M. Genander, M. M. Halford, C. Annerén, M. Sondell, M. J. Chumley, R. E. Silvany, M. Henkemeyer, J. Frisén, EphB Receptors Coordinate Migration and Proliferation in the Intestinal Stem Cell Niche, *Cell* **125**, 1151–1163 (2006).

432. I. N. Alimova, B. Liu, Z. Fan, S. M. Edgerton, T. Dillon, S. E. Lind, A. D. Thor, Metformin inhibits breast cancer cell growth, colony formation and induces cell cycle arrest in vitro, *Cell Cycle* **8**, 909–915 (2009).

433. X. Sun, Q. Yang, C. J. Rogers, M. Du, M.-J. Zhu, AMPK improves gut epithelial differentiation and barrier function via regulating Cdx2 expression, *Cell Death Differ.* **24**, 819–831 (2017).

434. M. Lynch, G. K. Marinov, The bioenergetic costs of a gene., *Proc. Natl. Acad. Sci. U. S. A.* **112**, 15690–5 (2015).

435. T. Kempf, A. Guba-Quint, J. Torgerson, M. C. Magnone, C. Haefliger, M. Bobadilla, K. C. Wollert, Growth differentiation factor 15 predicts future insulin resistance and impaired glucose control in obese nondiabetic individuals: results from the XENDOS trial, *Eur. J. Endocrinol.* **167**, 671–678 (2012).

436. G. Vila, M. Riedl, C. Anderwald, M. Resl, A. Handisurya, M. Clodi, G. Prager, B. Ludvik, M. Krebs, A. Luger, The Relationship between Insulin Resistance and the Cardiovascular Biomarker Growth Differentiation Factor-15 in Obese Patients, *Clin. Chem.* **57**, 309–316 (2011).

437. M. Karczewska-Kupczewska, I. Kowalska, A. Nikolajuk, A. Adamska, E. Otziomek, M. Gorska, M. Straczkowski, Hyperinsulinemia acutely increases serum macrophage inhibitory cytokine-1 concentration in anorexia nervosa and obesity, *Clin. Endocrinol. (Oxf).* **76**, 46–50 (2012).

438. M. H. Schernthaner-Reiter, D. Kasses, C. Tugendsam, M. Riedl, S. Peric, G. Prager, M. Krebs, M. Promintzer-Schifferl, M. Clodi, A. Luger, G. Vila, Growth differentiation factor 15 increases following oral glucose ingestion: effect of meal composition and obesity, *Eur. J. Endocrinol.* **175**, 623–631 (2016).

439. I. Dostálová, T. Roubíček, M. Bártlová, M. Mráz, Z. Lacinová, D. Haluzíková, P. Kaválková, M. Matoulek, M. Kasalický, M. Haluzík, Increased serum concentrations of macrophage inhibitory cytokine-1 in patients with obesity and type 2 diabetes mellitus: the influence of very low calorie diet, *Eur. J. Endocrinol.* **161**, 397–404 (2009).

440. N. Nair, E. Gongora, GDF-15 Correlates Positively with Matrix Metalloproteinases in Idiopathic Dilated Cardiomyopathy, *J. Hear. Lung Transplant.* **35**, S274 (2016).

441. T. Kempf, M. Eden, J. Strelau, M. Naguib, C. Willenbockel, J. Tongers, J. Heineke, D. Kotlarz, J. Xu, J. D. Molkentin, H. W. Niessen, H. Drexler, K. C. Wollert, The Transforming Growth Factor-β

Superfamily Member Growth-Differentiation Factor-15 Protects the Heart From Ischemia/Reperfusion Injury, *Circ. Res.* **98**, 351–360 (2006).

442. D. A. Brown, J. Moore, H. Johnen, T. J. Smeets, A. R. Bauskin, T. Kuffner, H. Weedon, S. T. Milliken, P. P. Tak, M. D. Smith, S. N. Breit, Serum macrophage inhibitory cytokine 1 in rheumatoid arthritis: A potential marker of erosive joint destruction, *Arthritis Rheum.* **56**, 753–764 (2007).

443. K. H. Kim, S. H. Kim, D. H. Han, Y. S. Jo, Y. Lee, M.-S. Lee, Growth differentiation factor 15 ameliorates nonalcoholic steatohepatitis and related metabolic disorders in mice, *Sci. Rep.* **8**, 6789 (2018).

444. Y. Kim, N. Noren Hooten, M. K. Evans, CRP Stimulates GDF15 Expression in Endothelial Cells through p53, *Mediators Inflamm.* **2018**, 1–9 (2018).

445. M. Tan, Y. Wang, K. Guan, Y. Sun, PTGF-beta, a type beta transforming growth factor (TGF-beta) superfamily member, is a p53 target gene that inhibits tumor cell growth via TGF-beta signaling pathway., *Proc. Natl. Acad. Sci. U. S. A.* **97**, 109–14 (2000).

446. N. M. Ratnam, J. M. Peterson, E. E. Talbert, K. J. Ladner, P. V. Rajasekera, C. R. Schmidt, M. E. Dillhoff, B. J. Swanson, E. Haverick, R. D. Kladney, T. M. Williams, G. W. Leone, D. J. Wang, D. C. Guttridge, NF-κB regulates GDF-15 to suppress macrophage surveillance during early tumor development, *J. Clin. Invest.* **127**, 3796–3809 (2017).

447. Y. Fujita, M. Ito, T. Kojima, S. Yatsuga, Y. Koga, M. Tanaka, GDF15 is a novel biomarker to evaluate efficacy of pyruvate therapy for mitochondrial diseases, *Mitochondrion* **20**, 34–42 (2015).

448. R. Montero, D. Yubero, J. Villarroya, D. Henares, C. Jou, M. A. Rodríguez, F. Ramos, A. Nascimento, C. I. Ortez, J. Campistol, B. Perez-Dueñas, M. O'Callaghan, M. Pineda, A. Garcia-Cazorla, J. C. Oferil, J. Montoya, E. Ruiz-Pesini, S. Emperador, M. Meznaric, L. Campderros, S. G. Kalko, F. Villarroya, R. Artuch, C. Jimenez-Mallebrera, G. Nogales-Gadea, Ed. GDF-15 Is Elevated in Children with Mitochondrial Diseases and Is Induced by Mitochondrial Dysfunction, *PLoS One* **11**, e0148709 (2016).

449. S. Kalko, S. Paco, C. Jou, M. Rodríguez, M. Meznaric, M. Rogac, M. Jekovec-Vrhovsek, M. Sciacco, M. Moggio, G. Fagiolari, B. De Paepe, L. De Meirleir, I. Ferrer, M. Roig-Quilis, F. Munell, J. Montoya, E. López-Gallardo, E. Ruiz-Pesini, R. Artuch, R. Montero, F. Torner, A. Nascimento, C. Ortez, J. Colomer, C. Jimenez-Mallebrera, Transcriptomic profiling of TK2 deficient human skeletal muscle suggests a role for the p53 signalling pathway and identifies growth and differentiation factor-15 as a potential novel biomarker for mitochondrial myopathies, *BMC Genomics* **15**, 91 (2014).

450. P. M. Quirós, M. A. Prado, N. Zamboni, D. D'Amico, R. W. Williams, D. Finley, S. P. Gygi, J. Auwerx, Multi-omics analysis identifies ATF4 as a key regulator of the mitochondrial stress response in mammals., *J. Cell Biol.* **216**, 2027–2045 (2017).

451. D. Li, H. Zhang, Y. Zhong, Hepatic GDF15 is regulated by CHOP of the unfolded protein response and alleviates NAFLD progression in obese mice, *Biochem. Biophys. Res. Commun.* **498**, 388–394 (2018).

452. V. Vasiliou, D. Ross, D. W. Nebert, Update of the NAD(P)H:quinone oxidoreductase (NQO) gene family., *Hum. Genomics* **2**, 329–35 (2006).

453. M. A. Bianchet, M. Faig, L. M. Amzel, in *Methods in enzymology*, (2004), vol. 382, pp. 144–174.

454. A. E. Dikalova, A. T. Bikineyeva, K. Budzyn, R. R. Nazarewicz, L. McCann, W. Lewis, D. G. Harrison, S. I. Dikalov, Therapeutic targeting of mitochondrial superoxide in hypertension., *Circ. Res.* **107**, 106–16 (2010).

455. E. L. Robb, J. M. Gawel, D. Aksentijević, H. M. Cochemé, T. S. Stewart, M. M. Shchepinova, H. Qiang, T. A. Prime, T. P. Bright, A. M. James, M. J. Shattock, H. M. Senn, R. C. Hartley, M. P. Murphy, Selective superoxide generation within mitochondria by the targeted redox cycler MitoParaquat, *Free Radic. Biol. Med.* **89**, 883–894 (2015).

456. L. M. Booty, J. M. Gawel, F. Cvetko, S. T. Caldwell, A. R. Hall, J. F. Mulvey, A. M. James, E. C. Hinchy, T. A. Prime, S. Arndt, C. Beninca, T. P. Bright, M. R. Clatworthy, J. R. Ferdinand, H. A. Prag, A. Logan, J. Prudent, T. Krieg, R. C. Hartley, M. P. Murphy, Selective Disruption of Mitochondrial Thiol Redox State in Cells and In Vivo, *Cell Chem. Biol.* **26**, 449-461.e8 (2019).

457. N. Moullan, L. Mouchiroud, X. Wang, D. Ryu, E. G. Williams, A. Mottis, V. Jovaisaite, M. V Frochaux, P. M. Quiros, B. Deplancke, R. H. Houtkooper, J. Auwerx, Tetracyclines Disturb Mitochondrial Function across Eukaryotic Models: A Call for Caution in Biomedical Research., *Cell Rep.* **10**, 1681–1691 (2015).

458. U. Richter, T. Lahtinen, P. Marttinen, F. Suomi, B. J. Battersby, Quality control of mitochondrial protein synthesis is required for membrane integrity and cell fitness., *J. Cell Biol.* **211**, 373–89 (2015).

459. D. V Dabir, S. A. Hasson, K. Setoguchi, M. E. Johnson, P. Wongkongkathep, C. J. Douglas, J. Zimmerman, R. Damoiseaux, M. A. Teitell, C. M. Koehler, A small molecule inhibitor of redox-regulated protein translocation into mitochondria., *Dev. Cell* **25**, 81–92 (2013).

460. S. E. Calvo, K. R. Clauser, V. K. Mootha, MitoCarta2.0: an updated inventory of mammalian mitochondrial proteins, *Nucleic Acids Res.* **44**, D1251–D1257 (2016).

461. J. Deng, H. P. Harding, B. Raught, A.-C. Gingras, J. J. Berlanga, D. Scheuner, R. J. Kaufman, D. Ron, N. Sonenberg, Activation of GCN2 in UV-Irradiated Cells Inhibits Translation, *Curr. Biol.* **12**, 1279–1286 (2002).

462. H. P. Harding, Y. Zhang, A. Bertolotti, H. Zeng, D. Ron, Perk is essential for translational regulation and cell survival during the unfolded protein response., *Mol. Cell* **5**, 897–904 (2000).

463. S. K. Young, R. C. Wek, Upstream Open Reading Frames Differentially Regulate Gene-specific Translation in the Integrated Stress Response., *J. Biol. Chem.* **291**, 16927–35 (2016).

464. T. Narita, S. Yin, C. F. Gelin, C. S. Moreno, M. Yepes, K. C. Nicolaou, E. G. Van Meir, Identification of a novel small molecule HIF-1alpha translation inhibitor., *Clin. Cancer Res.* **15**, 6128–36 (2009).

465. N. M. Chau, P. Rogers, W. Aherne, V. Carroll, I. Collins, E. McDonald, P. Workman, M. Ashcroft, Identification of novel small molecule inhibitors of hypoxia-inducible factor-1 that differentially block hypoxia-inducible factor-1 activity and hypoxia-inducible factor-1α induction in response to hypoxic stress and growth factors, *Cancer Res.* **65**, 4918–4928 (2005).

466. S. Song, L. J. Wheeler, C. K. Mathews, Deoxyribonucleotide pool imbalance stimulates deletions in HeLa cell mitochondrial DNA., *J. Biol. Chem.* **278**, 43893–6 (2003).

467. S. Song, Z. F. Pursell, W. C. Copeland, M. J. Longley, T. A. Kunkel, C. K. Mathews, DNA precursor asymmetries in mammalian tissue mitochondria and possible contribution to mutagenesis through reduced replication fidelity., *Proc. Natl. Acad. Sci. U. S. A.* **102**, 4990–5 (2005).

468. J. A. Stuart, M. F. Brown, Mitochondrial DNA maintenance and bioenergetics, *Biochim. Biophys. Acta - Bioenerg.* **1757**, 79–89 (2006).

469. N. Gattermann, M. Dadak, G. Hofhaus, M. Wulfert, M. Berneburg, M. L. Loeffler, H. A. Simmonds, Severe Impairment of Nucleotide Synthesis Through Inhibition of Mitochondrial Respiration, *Nucleosides, Nucleotides and Nucleic Acids* **23**, 1275–1279 (2004).

470. M. Löffler, J. Jöckel, G. Schuster, C. Becker, Dihydroorotat-ubiquinone oxidoreductase links mitochondria in the biosynthesis of pyrimidine nucleotides., *Mol. Cell. Biochem.* **174**, 125–9 (1997).

471. E. B. Nygaard, S. G. Vienberg, C. Ørskov, H. S. Hansen, B. Andersen, Metformin Stimulates FGF21 Expression in Primary Hepatocytes, *Exp. Diabetes Res.* **2012**, 1–8 (2012).

472. N. Li, K. Ragheb, G. Lawler, J. Sturgis, B. Rajwa, J. A. Melendez, J. P. Robinson, Mitochondrial Complex I Inhibitor Rotenone Induces Apoptosis through Enhancing Mitochondrial Reactive Oxygen Species Production, *J. Biol. Chem.* **278**, 8516–8525 (2003).

473. W. H. Park, Y. W. Han, S. H. Kim, S. Z. Kim, An ROS generator, antimycin A, inhibits the growth of HeLa cells via apoptosis, *J. Cell. Biochem.* **102**, 98–109 (2007).

474. C. M. Haynes, D. Ron, The mitochondrial UPR - protecting organelle protein homeostasis., *J. Cell Sci.* **123**, 3849–55 (2010).

475. A. M. Nargund, M. W. Pellegrino, C. J. Fiorese, B. M. Baker, C. M. Haynes, Mitochondrial import efficiency of ATFS-1 regulates mitochondrial UPR activation., *Science* **337**, 587–90 (2012).

476. Q. Zhao, J. Wang, I. V. Levichkin, S. Stasinopoulos, M. T. Ryan, N. J. Hoogenraad, A mitochondrial specific stress response in mammalian cells, *EMBO J.* **21**, 4411–4419 (2002).

477. B. M. Baker, A. M. Nargund, T. Sun, C. M. Haynes, N.-G. Larsson, Ed. Protective Coupling of Mitochondrial Function and Protein Synthesis via the eIF2α Kinase GCN-2, *PLoS Genet.* **8**, e1002760 (2012).

478. E. Rath, E. Berger, A. Messlik, T. Nunes, B. Liu, S. C. Kim, N. Hoogenraad, M. Sans, R. B. Sartor, D. Haller, Induction of dsRNA-activated protein kinase links mitochondrial unfolded protein response to the pathogenesis of intestinal inflammation, *Gut* **61**, 1269–1278 (2012).

479. T. Quentin, M. Steinmetz, A. Poppe, S. Thoms, Metformin differentially activates ER stress signaling pathways without inducing apoptosis., *Dis. Model. Mech.* **5**, 259–69 (2012).

480. A. Tsuru, Y. Imai, M. Saito, K. Kohno, Novel mechanism of enhancing IRE1α-XBP1 signalling via the PERK-ATF4 pathway, *Sci. Rep.* **6**, 24217 (2016).

481. M. Zhang, W. Sun, J. Qian, Y. Tang, Fasting exacerbates hepatic growth differentiation factor 15 to promote fatty acid β-oxidation and ketogenesis via activating XBP1 signaling in liver, *Redox Biol.* **16**, 87–96 (2018).

482. C. Loubiere, S. Clavel, J. Gilleron, R. Harisseh, J. Fauconnier, I. Ben-Sahra, L. Kaminski, K. Laurent, S. Herkenne, S. Lacas-Gervais, D. Ambrosetti, D. Alcor, S. Rocchi, M. Cormont, J.-F. Michiels, B. Mari, N. M. Mazure, L. Scorrano, A. Lacampagne, A. Gharib, J.-F. Tanti, F. Bost, The energy disruptor metformin targets mitochondrial integrity via modification of calcium flux in cancer cells, *Sci. Rep.* **7**, 5040 (2017).

483. S. Lakhal, N. P. Talbot, A. Crosby, C. Stoepker, A. R. M. Townsend, P. A. Robbins, C. W. Pugh, P. J. Ratcliffe, D. R. Mole, Regulation of growth differentiation factor 15 expression by intracellular iron., *Blood* **113**, 1555–63 (2009).

484. A. J. Majmundar, W. J. Wong, M. C. Simon, Hypoxia-Inducible Factors and the Response to

Hypoxic Stress*Mol. Cell* **40**, 294–309 (2010).

485. E. Berger, E. Rath, D. Yuan, N. Waldschmitt, S. Khaloian, M. Allgäuer, O. Staszewski, E. M. Lobner, T. Schöttl, P. Giesbertz, O. I. Coleman, M. Prinz, A. Weber, M. Gerhard, M. Klingenspor, K.-P. Janssen, M. Heikenwalder, D. Haller, Mitochondrial function controls intestinal epithelial stemness and proliferation, *Nat. Commun.* **7**, 13171 (2016).

486. K. B. Hahm, Y. H. Im, T. W. Parks, S. H. Park, S. Markowitz, H. Y. Jung, J. Green, S. J. Kim, Loss of transforming growth factor beta signalling in the intestine contributes to tissue injury in inflammatory bowel disease., *Gut* **49**, 190–8 (2001).

487. H. Xiao, J. Zhang, Z. Xu, Y. Feng, M. Zhang, J. Liu, R. Chen, J. Shen, J. Wu, Z. Lu, X. Fang, J. Li, Y. Zhang, Metformin is a novel suppressor for transforming growth factor (TGF)-β1., *Sci. Rep.* **6**, 28597 (2016).

488. T. Ikeda, K. Iwata, H. Murakami, Inhibitory effect of metformin on intestinal glucose absorption in the perfused rat intestine, *Biochem. Pharmacol.* **59**, 887–890 (2000).

489. C. WILCOCK, C. J. BAILEY, Reconsideration of inhibitory effect of metformin on intestinal glucose absorption, *J. Pharm. Pharmacol.* **43**, 120–121 (1991).

490. T. Özülker, F. Özülker, M. Mert, T. Özpaçacı, Clearance of the high intestinal 18 F-FDG uptake associated with metformin after stopping the drug, *Eur. J. Nucl. Med. Mol. Imaging* **37**, 1011–1017 (2010).

491. V. Gorboulev, A. Schürmann, V. Vallon, H. Kipp, A. Jaschke, D. Klessen, A. Friedrich, S. Scherneck, T. Rieg, R. Cunard, M. Veyhl-Wichmann, A. Srinivasan, D. Balen, D. Breljak, R. Rexhepaj, H. E. Parker, F. M. Gribble, F. Reimann, F. Lang, S. Wiese, I. Sabolic, M. Sendtner, H. Koepsell, Na(+)-D-glucose cotransporter SGLT1 is pivotal for intestinal glucose absorption and glucose-dependent incretin secretion., *Diabetes* **61**, 187–96 (2012).

492. P. V. Röder, K. E. Geillinger, T. S. Zietek, B. Thorens, H. Koepsell, H. Daniel, The role of SGLT1 and GLUT2 in intestinal glucose transport and sensing, *PLoS One* **9** (2014), doi:10.1371/journal.pone.0089977.

493. E. M. Wright, *THE INTESTINAL Na + IGLUCOSE COTRANSPORTER* (1993; www.annualreviews.org).

494. M. G. Martín, E. Turk, M. P. Lostao, C. Kerner, E. M. Wright, Defects in Na+/glucose cotransporter (SGLT1) trafficking and function cause glucose-galactose malabsorption, *Nat. Genet.* **12**, 216–220 (1996).

495. M. Kasahara, M. Maeda, S. Hayashi, Y. Mori, T. Abe, A missense mutation in the Na + /glucose cotransporter gene SGLT1 in a patient with congenital glucose-galactose malabsorption: Normal trafficking but inactivation of the mutant protein, *Biochim. Biophys. Acta - Mol. Basis Dis.* **1536**, 141–147 (2001).

496. J. T. Lam, M. G. Martín, E. Turk, B. A. Hirayama, N. U. Bosshard, B. Steinmann, E. M. Wright, Missense mutations in SGLT1 cause glucose-galactose malabsorption by trafficking defects, *Biochim. Biophys. Acta - Mol. Basis Dis.* **1453**, 297–303 (1999).

497. M. Uldry, M. Ibberson, M. Hosokawa, B. Thorens, GLUT2 is a high affinity glucosamine transporter., *FEBS Lett.* **524**, 199–203 (2002).

498. C. I. Cheeseman, GLUT2 is the transporter for fructose across the rat intestinal basolateral membrane., *Gastroenterology* **105**, 1050–6 (1993).

499. B. Thorens, Z. Q. Cheng, D. Brown, H. F. Lodish, Liver glucose transporter: a basolateral protein in hepatocytes and intestine and kidney cells., *Am. J. Physiol.* **259**, C279-85 (1990).

500. G. L. Kellett, E. Brot-Laroche, Apical GLUT2: A major pathway of intestinal sugar absorption*Diabetes* **54**, 3056–3062 (2005).

501. F. Gouyon, L. Caillaud, V. Carriere, C. Klein, V. Dalet, D. Citadelle, G. L. Kellett, B. Thorens, A. Leturque, E. Brot-Laroche, Simple-sugar meals target GLUT2 at enterocyte apical membranes to improve sugar absorption: a study in GLUT2-null mice., *J. Physiol.* **552**, 823–32 (2003).

502. J. A. Affleck, P. A. Helliwell, G. L. Kellett, Immunocytochemical detection of GLUT2 at the rat intestinal brush-border membrane., *J. Histochem. Cytochem.* **51**, 1567–74 (2003).

503. O. J. Mace, J. Affleck, N. Patel, G. L. Kellett, Sweet taste receptors in rat small intestine stimulate glucose absorption through apical GLUT2., *J. Physiol.* **582**, 379–92 (2007).

504. A. Au, A. Gupta, P. Schembri, C. I. Cheeseman, Rapid insertion of GLUT2 into the rat jejunal brush-border membrane promoted by glucagon-like peptide 2, *Biochem. J.* **367**, 247–254 (2002).

505. A. Ait-Omar, M. Monteiro-Sepulveda, C. Poitou, M. Le Gall, A. Cotillard, J. Gilet, K. Garbin, A. Houllier, D. Château, A. Lacombe, N. Veyrie, D. Hugol, J. Tordjman, C. Magnan, P. Serradas, K. Clément, A. Leturque, E. Brot-Laroche, GLUT2 accumulation in enterocyte apical and intracellular membranes: a study in morbidly obese human subjects and ob/ob and high fat-fed mice., *Diabetes* **60**, 2598–607 (2011).

506. M. T. Guillam, R. Burcelin, B. Thorens, B. Thorens, Normal hepatic glucose production in the

absence of GLUT2 reveals an alternative pathway for glucose release from hepatocytes., *Proc. Natl. Acad. Sci. U. S. A.* **95**, 12317–21 (1998).

507. F. Manz, H. Bickel, J. Brodehl, D. Feist, K. Gellissen, B. Geschöll-Bauer, G. Gilli, E. Harms, H. Helwig, W. Nützenadel, Fanconi-Bickel syndrome., *Pediatr. Nephrol.* **1**, 509–18 (1987).

508. M. Brivet, N. Moatti, A. Corriat, A. Lemonnier, M. Odievre, Defective galactose oxidation in a patient with glycogen storage disease and Fanconi syndrome., *Pediatr. Res.* **17**, 157–61 (1983).

509. T. Yoshikawa, R. Inoue, M. Matsumoto, T. Yajima, K. Ushida, T. Iwanaga, Comparative expression of hexose transporters (SGLT1, GLUT1, GLUT2 and GLUT5) throughout the mouse gastrointestinal tract, *Histochem. Cell Biol.* **135**, 183–194 (2011).

510. S. Boyer, P. A. Sharp, E. S. Debnam, S. A. Baldwin, S. K. S. Srai, Streptozotocin diabetes and the expression of GLUT1 at the brush border and basolateral membranes of intestinal enterocytes, *FEBS Lett.* **396**, 218–222 (1996).

511. H. Takayama, M. Ohta, K. Tada, K. Watanabe, T. Kawasaki, Y. Endo, Y. Iwashita, M. Inomata, Additional effects of duodenojejunal bypass on glucose metabolism in a rat model of sleeve gastrectomy., *Surg. Today* **49**, 637–644 (2019).

512. N. O. Davidson, A. M. Hausman, C. A. Ifkovits, J. B. Buse, G. W. Gould, C. F. Burant, G. I. Bell, Human intestinal glucose transporter expression and localization of GLUT5, *Am. J. Physiol. Physiol.* **262**, C795–C800 (1992).

513. C. F. Burant, J. Takeda, E. Brot-Laroche, G. I. Bell, N. O. Davidson, Fructose transporter in human spermatozoa and small intestine is GLUT5., *J. Biol. Chem.* **267**, 14523–6 (1992).

514. S. Barone, S. L. Fussell, A. K. Singh, F. Lucas, J. Xu, C. Kim, X. Wu, Y. Yu, H. Amlal, U. Seidler, J. Zuo, M. Soleimani, Slc2a5 (Glut5) Is Essential for the Absorption of Fructose in the Intestine and Generation of Fructose-induced Hypertension, *J. Biol. Chem.* **284**, 5056–5066 (2009).

515. C. Cheeseman, GLUT7: a new intestinal facilitated hexose transporter, *Am. J. Physiol. Metab.* **295**, E238–E241 (2008).

516. T. Wu, C. Xie, H. Wu, K. L. Jones, M. Horowitz, C. K. Rayner, Metformin reduces the rate of small intestinal glucose absorption in type 2 diabetes, *Diabetes, Obes. Metab.* **19**, 290–293 (2017).

517. B. Bybel, I. D. Greenberg, J. Paterson, J. Ducharme, W. D. Leslie, Increased F-18 FDG intestinal uptake in diabetic patients on metformin: A matched case-control analysis, *Clin. Nucl. Med.* **36**, 452–456 (2011).

518. E. Gontier, E. Fourme, M. Wartski, C. Blondet, G. Bonardel, E. Le Stanc, M. Mantzarides, H. Foehrenbach, A. P. Pecking, J. L. Alberini, High and typical 18F-FDG bowel uptake in patients treated with metformin, *Eur. J. Nucl. Med. Mol. Imaging* **35**, 95–99 (2008).

519. L. Bahler, K. Stroek, J. B. Hoekstra, H. J. Verberne, F. Holleman, Metformin-related colonic glucose uptake; potential role for increasing glucose disposal?-A retrospective analysis of 18F-FDG uptake in the colon on PET-CT, *Diabetes Res. Clin. Pract.* **114**, 55–63 (2016).

520. S. H. Lee, S. Jin, H. S. Lee, J. S. Ryu, J. J. Lee, Metformin discontinuation less than 72 h is suboptimal for F-18 FDG PET/CT interpretation of the bowel, *Ann. Nucl. Med.* **30**, 629–636 (2016).

521. R. Hamidizadeh, A. Eftekhari, E. A. Wiley, D. Wilson, T. Alden, F. Bénard, Metformin discontinuation prior to FDG PET/CT: A randomized controlled study to compare 24- and 48-hour bowel activity, *Radiology* **289**, 418–425 (2018).

522. D. W. Steenkamp, M. E. Mcdonnell, S. Meibom, Metformin may be associated with false-negative cancer detection in the gastrointestinal tract on PET/CT*Endocr. Pract.* **20**, 1079–1083 (2014).

523. Y. Sakar, B. Meddah, M. A. Faouzi, Y. Cherrah, A. Bado, R. Ducroc, Metformin-induced regulation of the intestinal D-glucose transporters., *J. Physiol. Pharmacol.* **61**, 301–7 (2010).

524. J. Walker, H. B. Jijon, H. Diaz, P. Salehi, T. Churchill, K. L. Madsen, 5-Aminoimidazole-4-carboxamide riboside (AICAR) enhances GLUT2-dependent jejunal glucose transport: A possible role for AMPK, *Biochem. J.* **385**, 485–491 (2005).

525. M. Panayotova-Heiermann, D. D. F. Loo, E. M. Wright, Kinetics of steady-state currents and charge movements associated with the rat Na+/glucose cotransporter, *J. Biol. Chem.* **270**, 27099–27105 (1995).

526. K. Kapoor, J. S. Finer-Moore, B. P. Pedersen, L. Caboni, A. Waight, R. C. Hillig, P. Bringmann, I. Heisler, T. Müller, H. Siebeneicher, R. M. Stroud, Mechanism of inhibition of human glucose transporter GLUT1 is conserved between cytochalasin B and phenylalanine amides, *Proc. Natl. Acad. Sci. U. S. A.* **113**, 4711–4716 (2016).

527. S. Wandel, A. Buchs, A. Schürmann, S. A. Summers, A. C. Powers, M. F. Shanahan, H. G. Joost, Glucose transport activity and ligand binding (cytochalasin B, IAPS-forskolin) of chimeric constructs of GLUT2 and GLUT4 expressed in COS-7-cells, *Biochim. Biophys. Acta - Biomembr.* **1284**, 56–62 (1996).

528. B. Hellwig, H. G. Joost, Differentiation of erythrocyte-(GLUT1), liver-(GLUT2), and adipocyte-

type (GLUT4) glucose transporters by binding of the inhibitory ligands cytochalasin B, forskolin, dipyridamole, and isobutylmethylxanthine., *Mol. Pharmacol.* **40** (1991).

529. L. Bultot, T. E. Jensen, Y. C. Lai, A. L. B. Madsen, C. Collodet, S. Kviklyte, M. Deak, A. Yavari, M. Foretz, S. Ghaffari, M. Bellahcene, H. Ashrafian, M. H. Rider, E. A. Richter, K. Sakamoto, Benzimidazole derivative small-molecule 991 enhances AMPK activity and glucose uptake induced by AICAR or contraction in skeletal muscle, *Am. J. Physiol. - Endocrinol. Metab.* **311**, E706–E719 (2016).

530. B. Xiao, M. J. Sanders, D. Carmena, N. J. Bright, L. F. Haire, E. Underwood, B. R. Patel, R. B. Heath, P. A. Walker, S. Hallen, F. Giordanetto, S. R. Martin, D. Carling, S. J. Gamblin, Structural basis of AMPK regulation by small molecule activators., *Nat. Commun.* **4**, 3017 (2013).

531. S. Lenzen, S. Lortz, M. Tiedge, Effects of metformin on SGLT1, GLUT2, and GLUT5 hexose transporter gene expression in small intestine from rats, *Biochem. Pharmacol.* **51**, 893–896 (1996).

532. C. Chen, N. Pore, A. Behrooz, F. Ismail-Beigi, A. Maity, Regulation of glut1 mRNA by hypoxia-inducible factor-1. Interaction between H-ras and hypoxia., *J. Biol. Chem.* **276**, 9519–25 (2001).

533. Y. Wang, Y. Liu, S. N. Malek, P. Zheng, Y. Liu, Targeting HIF1α eliminates cancer stem cells in hematological malignancies, *Cell Stem Cell* **8**, 399–411 (2011).

534. J. Karhausen, G. T. Furuta, J. E. Tomaszewski, R. S. Johnson, S. P. Colgan, V. H. Haase, Epithelial hypoxia-inducible factor-1 is protective in murine experimental colitis., *J. Clin. Invest.* **114**, 1098–106 (2004).

535. J. D. Cremin, S. E. Fleming, Glycolysis is a source of pyruvate for transamination of glutamine amino nitrogen in jejunal epithelial cells, *Am. J. Physiol. Liver Physiol.* **272**, G575–G588 (1997).

536. P. J. Hanson, D. S. Parsons, Factors affecting the utilization of ketone bodies and other substrates by rat jejunum: effects of fasting and of diabetes., **278**, 55–67 (1978).

537. J. Storch, Y. X. Zhou, W. S. Lagakos, Metabolism of apical versus basolateral *sn* -2-monoacylglycerol and fatty acids in rodent small intestine, *J. Lipid Res.* **49**, 1762–1769 (2008).

538. S. E. Fleming, M. D. Fitch, S. DeVries, M. L. Liu, C. Kight, Nutrient Utilization by Cells Isolated from Rat Jejunum, Cecum and Colon, *J. Nutr.* **121**, 869–878 (1991).

539. M. D. Robertson, M. Parkes, B. F. Warren, D. J. P. Ferguson, K. G. Jackson, D. P. Jewell, K. N. Frayn, Mobilisation of enterocyte fat stores by oral glucose in humans., *Gut* **52**, 834–9 (2003).

540. S. R. Moore, M. M. Guedes, T. B. Costa, J. Vallance, E. A. Maier, K. J. Betz, E. Aihara, M. M. Mahe, A. A. M. Lima, R. B. Oriá, N. F. Shroyer, Glutamine and alanyl-glutamine promote crypt

expansion and mTOR signaling in murine enteroids., *Am. J. Physiol. Gastrointest. Liver Physiol.* **308**, G831-9 (2015).

541. H. Yang, X. Wang, X. Xiong, Y. Yin, Energy metabolism in intestinal epithelial cells during maturation along the crypt-villus axis, *Sci. Rep.* (2016), doi:10.1038/srep31917.

542. R. W. Hunter, C. C. Hughey, L. Lantier, E. I. Sundelin, M. Peggie, E. Zeqiraj, F. Sicheri, N. Jessen, D. H. Wasserman, K. Sakamoto, Metformin reduces liver glucose production by inhibition of fructose-1-6-bisphosphatase., *Nat. Med.* **24**, 1395–1406 (2018).

543. C. A. Chu, N. Wiernsperger, N. Muscato, M. Knauf, D. W. Neal, A. D. Cherrington, The acute effect of metformin on glucose production in the conscious dog is primarily attributable to inhibition of glycogenolysis, *Metabolism* **49**, 1619–1626 (2000).

544. M. Otto, J. Breinholt, N. Westergaard, Metformin inhibits glycogen synthesis and gluconeogenesis in cultured rat hepatocytes., *Diabetes. Obes. Metab.* **5**, 189–94 (2003).

545. M. M. González-Barroso, A. Anedda, E. Gallardo-Vara, M. Redondo-Horcajo, L. Rodríguez-Sánchez, E. Rial, Fatty acids revert the inhibition of respiration caused by the antidiabetic drug metformin to facilitate their mitochondrial β-oxidation, *Biochim. Biophys. Acta - Bioenerg.* **1817**, 1768–1775 (2012).

546. I. A. Okkelman, T. Foley, D. B. Papkovsky, R. I. Dmitriev, Live cell imaging of mouse intestinal organoids reveals heterogeneity in their oxygenation, *Biomaterials* **146**, 86–96 (2017).

547. N. Berndt, O. Kann, H.-G. Holzhütter, Physiology-Based Kinetic Modeling of Neuronal Energy Metabolism Unravels the Molecular Basis of NAD(P)H Fluorescence Transients, *J. Cereb. Blood Flow Metab.* **35**, 1494–1506 (2015).

548. A. M. Brennan, J. A. Connor, C. W. Shuttleworth, NAD(P)H Fluorescence Transients after Synaptic Activity in Brain Slices: Predominant Role of Mitochondrial Function, *J. Cereb. Blood Flow Metab.* **26**, 1389–1406 (2006).

549. C. Manlio Díaz-García, R. Mongeon, C. Lahmann, D. Koveal, H. Zucker, G. Y. Correspondence, G. Yellen, Neuronal Stimulation Triggers Neuronal Glycolysis and Not Lactate Uptake Cell Metabolism Article Neuronal Stimulation Triggers Neuronal Glycolysis and Not Lactate Uptake, *Cell Metab.* **26**, 361-374.e4 (2017).

550. C. W. Shuttleworth, Use of NAD(P)H and flavoprotein autofluorescence transients to probe neuron and astrocyte responses to synaptic activation, *Neurochem. Int.* **56**, 379–386 (2010).

551. T. Schulze, M. Morsi, K. Reckers, D. Brüning, N. Seemann, U. Panten, I. Rustenbeck, Metabolic amplification of insulin secretion is differentially desensitized by depolarization in the absence of exogenous fuels, *Metabolism* **67**, 1–13 (2017).

552. K. Eto, Y. Tsubamoto, Y. Terauchi, T. Sugiyama, T. Kishimoto, N. Takahashi, N. Yamauchi, N. Kubota, S. Murayama, T. Aizawa, Y. Akanuma, S. Aizawa, H. Kasai, Y. Yazaki, T. Kadowaki, Role of NADH Shuttle System in Glucose-Induced Activation of Mitochondrial Metabolism and Insulin Secretion, *Science (80-.).* **283**, 981–985 (1999).

553. R. Dumollard, Z. Ward, J. Carroll, M. R. Duchen, Regulation of redox metabolism in the mouse oocyte and embryo., *Development* **134**, 455–65 (2007).

554. S. A. Mookerjee, D. G. Nicholls, M. D. Brand, J. Zhang, Ed. Determining Maximum Glycolytic Capacity Using Extracellular Flux Measurements, *PLoS One* **11**, e0152016 (2016).

555. B. Trivedi, W. H. Danforth, Effect of pH on the kinetics of frog muscle phosphofructokinase., *J. Biol. Chem.* **241**, 4110–2 (1966).

556. D. Benjamin, D. Robay, S. K. Hindupur, J. Pohlmann, M. Colombi, M. Y. El-Shemerly, S.-M. Maira, C. Moroni, H. A. Lane, M. N. Hall, Dual Inhibition of the Lactate Transporters MCT1 and MCT4 Is Synthetic Lethal with Metformin due to NAD+ Depletion in Cancer Cells, *Cell Rep.* **25**, 3047-3058.e4 (2018).

557. M. J. Ovens, A. J. Davies, M. C. Wilson, C. M. Murray, A. P. Halestrap, AR-C155858 is a potent inhibitor of monocarboxylate transporters MCT1 and MCT2 that binds to an intracellular site involving transmembrane helices 7–10, *Biochem. J.* **425**, 523–530 (2010).

558. S. B. Jadaho, R.-Z. Yang, Q. Lin, H. Hu, F. A. Anania, A. R. Shuldiner, D.-W. Gong, Murine alanine aminotransferase: cDNA cloning, functional expression, and differential gene regulation in mouse fatty liver, *Hepatology* **39**, 1297–1302 (2004).

559. E. L. Mills, K. A. Pierce, M. P. Jedrychowski, R. Garrity, S. Winther, S. Vidoni, T. Yoneshiro, J. B. Spinelli, G. Z. Lu, L. Kazak, A. S. Banks, M. C. Haigis, S. Kajimura, M. P. Murphy, S. P. Gygi, C. B. Clish, E. T. Chouchani, Accumulation of succinate controls activation of adipose tissue thermogenesis, *Nature* **560**, 102–106 (2018).

560. R. Hussain, Z. Shaukat, M. Khan, R. Saint, S. L. Gregory, Phosphoenolpyruvate Carboxykinase Maintains Glycolysis-driven Growth in Drosophila Tumors, *Sci. Rep.* **7**, 11531 (2017).

561. A. L. Orr, D. Ashok, M. R. Sarantos, R. Ng, T. Shi, A. A. Gerencser, R. E. Hughes, M. D. Brand, V. D. Appanna, Ed. Novel Inhibitors of Mitochondrial sn-Glycerol 3-phosphate Dehydrogenase, *PLoS One*

9, e89938 (2014).

562. S. Köhler, U. Winkler, M. Sicker, J. Hirrlinger, NBCe1 mediates the regulation of the NADH/NAD $^+$ redox state in cortical astrocytes by neuronal signals, *Glia* **66**, 2233–2245 (2018).

563. A. Pecinova, Z. Drahota, J. Kovalcikova, N. Kovarova, P. Pecina, L. Alan, M. Zima, J. Houstek, T. Mracek, Pleiotropic Effects of Biguanides on Mitochondrial Reactive Oxygen Species Production, *Oxid. Med. Cell. Longev.* **2017**, 1–11 (2017).

564. J. Pfleger, M. He, M. Abdellatif, Mitochondrial complex II is a source of the reserve respiratory capacity that is regulated by metabolic sensors and promotes cell survival, *Cell Death Dis.* **6**, e1835–e1835 (2015).

565. N. D. Amoedo, G. Punzi, E. Obre, D. Lacombe, A. De Grassi, C. L. Pierri, R. Rossignol, AGC1/2, the mitochondrial aspartate-glutamate carriers, *Biochim. Biophys. Acta - Mol. Cell Res.* **1863**, 2394–2412 (2016).

566. B. Raud, D. G. Roy, A. S. Divakaruni, T. N. Tarasenko, R. Franke, E. H. Ma, B. Samborska, W. Y. Hsieh, A. H. Wong, P. Stüve, C. Arnold-Schrauf, M. Guderian, M. Lochner, S. Rampertaap, K. Romito, J. Monsale, M. Brönstrup, S. J. Bensinger, A. N. Murphy, P. J. McGuire, R. G. Jones, T. Sparwasser, L. Berod, Etomoxir Actions on Regulatory and Memory T Cells Are Independent of Cpt1a-Mediated Fatty Acid Oxidation, *Cell Metab.* **28**, 504-515.e7 (2018).

567. A. S. Divakaruni, W. Y. Hsieh, L. Minarrieta, T. N. Duong, K. K. O. Kim, B. R. Desousa, A. Y. Andreyev, C. E. Bowman, K. Caradonna, B. P. Dranka, D. A. Ferrick, M. Liesa, L. Stiles, G. W. Rogers, D. Braas, T. P. Ciaraldi, M. J. Wolfgang, T. Sparwasser, L. Berod, S. J. Bensinger, A. N. Murphy, Etomoxir Inhibits Macrophage Polarization by Disrupting CoA Homeostasis, *Cell Metab.* **28**, 490-503.e7 (2018).

568. C.-H. Yao, G.-Y. Liu, R. Wang, S. H. Moon, R. W. Gross, G. J. Patti, J. Locasale, Ed. Identifying off-target effects of etomoxir reveals that carnitine palmitoyltransferase I is essential for cancer cell proliferation independent of β-oxidation, *PLOS Biol.* **16**, e2003782 (2018).

569. A. R. Cameron, L. Logie, K. Patel, S. Erhardt, S. Bacon, P. Middleton, J. Harthill, C. Forteath, J. T. Coats, C. Kerr, H. Curry, D. Stewart, K. Sakamoto, P. Repiščák, M. J. Paterson, I. Hassinen, G. McDougall, G. Rena, Metformin selectively targets redox control of complex I energy transduction., *Redox Biol.* **14**, 187–197 (2018).

570. M.-Y. El-Mir, V. Nogueira, E. Fontaine, N. Avéret, M. Rigoulet, X. Leverve, Dimethylbiguanide Inhibits Cell Respiration via an Indirect Effect Targeted on the Respiratory Chain Complex I, *J. Biol. Chem.* **275**, 223–228 (2000).

571. E. Gaude, C. Schmidt, P. A. Gammage, A. Dugourd, T. Blacker, S. P. Chew, J. Saez-Rodriguez, J. S. O'Neill, G. Szabadkai, M. Minczuk, C. Frezza, NADH Shuttling Couples Cytosolic Reductive Carboxylation of Glutamine with Glycolysis in Cells with Mitochondrial Dysfunction, *Mol. Cell* (2018), doi:10.1016/j.molcel.2018.01.034.

572. A. Janzer, N. J. German, K. N. Gonzalez-Herrera, J. M. Asara, M. C. Haigis, K. Struhl, Metformin and phenformin deplete tricarboxylic acid cycle and glycolytic intermediates during cell transformation and NTPs in cancer stem cells., *Proc. Natl. Acad. Sci. U. S. A.* **111**, 10574–9 (2014).

573. L. B. Sullivan, D. Y. Gui, A. M. Hosios, L. N. Bush, E. Freinkman, M. G. Vander Heiden, Supporting Aspartate Biosynthesis Is an Essential Function of Respiration in Proliferating Cells, *Cell* (2015), doi:10.1016/j.cell.2015.07.017.

574. S.-M. Fendt, E. L. Bell, M. A. Keibler, S. M. Davidson, G. J. Wirth, B. Fiske, J. R. Mayers, M. Schwab, G. Bellinger, A. Csibi, A. Patnaik, M. J. Blouin, L. C. Cantley, L. Guarente, J. Blenis, M. N. Pollak, A. F. Olumi, M. G. Vander Heiden, G. Stephanopoulos, Metformin decreases glucose oxidation and increases the dependency of prostate cancer cells on reductive glutamine metabolism., *Cancer Res.* **73**, 4429–38 (2013).

575. A. R. Mullen, W. W. Wheaton, E. S. Jin, P.-H. Chen, L. B. Sullivan, T. Cheng, Y. Yang, W. M. Linehan, N. S. Chandel, R. J. DeBerardinis, Reductive carboxylation supports growth in tumour cells with defective mitochondria, *Nature* **481**, 385–388 (2012).

576. K. S. McCommis, Z. Chen, X. Fu, W. G. McDonald, J. R. Colca, R. F. Kletzien, S. C. Burgess, B. N. Finck, Loss of mitochondrial pyruvate carrier 2 in the liver leads to defects in gluconeogenesis and compensation via pyruvate-alanine cycling, *Cell Metab.* (2015), doi:10.1016/j.cmet.2015.07.028.

577. L. R. Gray, M. R. Sultana, A. J. Rauckhorst, L. Oonthonpan, S. C. Tompkins, A. Sharma, X. Fu, R. Miao, A. D. Pewa, K. S. Brown, E. E. Lane, A. Dohlman, D. Zepeda-Orozco, J. Xie, J. Rutter, A. W. Norris, J. E. Cox, S. C. Burgess, M. J. Potthoff, E. B. Taylor, Hepatic mitochondrial pyruvate carrier 1 is required for efficient regulation of gluconeogenesis and whole-body glucose homeostasis, *Cell Metab.* (2015), doi:10.1016/j.cmet.2015.07.027.

578. M. MacDonald, N. Neufeldt, B. Park, M. Berger, N. Ruderman, Alanine metabolism and gluconeogenesis in the rat, *Am. J. Physiol. Content* **231**, 619–626 (1976).

579. J. Mendes-Mourão, A. Halestrap, D. M. Crisp, C. I. Pogson, The involvement of mitochondrial pyruvate transport in the pathways of gluconeogenesis from serine and alanine in isolated rat and mouse liver cells, *FEBS Lett.* **53**, 29–32 (1975).

580. P. Felig, T. Pozefsky, E. Marliss, G. F. Cahill, Alanine: key role in gluconeogenesis., *Science* **167**, 1003–4 (1970).

581. R.-Z. Yang, S. Park, W. J. Reagan, R. Goldstein, S. Zhong, M. Lawton, F. Rajamohan, K. Qian, L. Liu, D.-W. Gong, Alanine aminotransferase isoenzymes: Molecular cloning and quantitative analysis of tissue expression in rats and serum elevation in liver toxicity, *Hepatology* **49**, 598–607 (2009).

582. Y. Adachi, A. L. De Sousa-Coelho, I. Harata, C. Aoun, S. Weimer, X. Shi, K. N. Gonzalez Herrera, H. Takahashi, C. Doherty, Y. Noguchi, L. J. Goodyear, M. C. Haigis, R. E. Gerszten, M.-E. Patti, l-Alanine activates hepatic AMP-activated protein kinase and modulates systemic glucose metabolism, *Mol. Metab.* **17**, 61–70 (2018).

583. J. W. Locasale, L. C. Cantley, Metabolic Flux and the Regulation of Mammalian Cell Growth, *Cell Metab.* **14**, 443–451 (2011).

584. R. J. DeBerardinis, J. J. Lum, G. Hatzivassiliou, C. B. Thompson, The Biology of Cancer: Metabolic Reprogramming Fuels Cell Growth and Proliferation, *Cell Metab.* **7**, 11–20 (2008).

585. H. Hu, A. Juvekar, C. A. Lyssiotis, E. C. Lien, J. G. Albeck, D. Oh, G. Varma, Y. P. Hung, S. Ullas, J. Lauring, P. Seth, M. R. Lundquist, D. R. Tolan, A. K. Grant, D. J. Needleman, J. M. Asara, L. C. Cantley, G. M. Wulf, Phosphoinositide 3-Kinase Regulates Glycolysis through Mobilization of Aldolase from the Actin Cytoskeleton, *Cell* **164**, 433–446 (2016).

586. A. A. Shestov, X. Liu, Z. Ser, A. A. Cluntun, Y. P. Hung, L. Huang, D. Kim, A. Le, G. Yellen, J. G. Albeck, J. W. Locasale, Quantitative determinants of aerobic glycolysis identify flux through the enzyme GAPDH as a limiting step., *Elife* **3** (2014), doi:10.7554/eLife.03342.

587. H. R. Christofk, M. G. Vander Heiden, M. H. Harris, A. Ramanathan, R. E. Gerszten, R. Wei, M. D. Fleming, S. L. Schreiber, L. C. Cantley, The M2 splice isoform of pyruvate kinase is important for cancer metabolism and tumour growth, *Nature* **452**, 230–233 (2008).

588. O. Alcazar, M. Tiedge, S. Lenzen, Importance of lactate dehydrogenase for the regulation of glycolytic flux and insulin secretion in insulin-producing cells., *Biochem. J.* **352 Pt 2**, 373–80 (2000).

589. P. Hahn, H. Wei-Ning, Gluconeogenesis from Lactate in the Small Intestinal Mucosa of Suckling Rats, *Pediatr. Res.* **20**, 1321–1323 (1986).

590. P. Hahn, H. Wei-Ning, Gluconeogenesis from lactate in the small intestinal mucosa of suckling rats, *Pediatr. Res.* (1986), doi:10.1203/00006450-198612000-00027.

591. M. Watford, Is the small intestine a gluconeogenic organ?*Nutr. Rev.* (2005),

doi:10.1301/nr.2005.oct.356-360.

592. T. Ikeda, K. Iwata, H. Murakami, Inhibitory effect of metformin on intestinal glucose absorption in the perfused rat intestine, *Biochem. Pharmacol.* **59**, 887–890 (2000).

593. S. Van Welden, A. C. Selfridge, P. Hindryckx, Intestinal hypoxia and hypoxia-induced signalling as therapeutic targets for IBD, *Nat. Rev. Gastroenterol. Hepatol.* **14**, 596–611 (2017).

594. R. I. Misbin, L. Green, B. V. Stadel, J. L. Gueriguian, A. Gubbi, G. A. Fleming, Lactic Acidosis in Patients with Diabetes Treated with Metformin, *N. Engl. J. Med.* **338**, 265–266 (1998).

595. P. J. Connelly, M. Lonergan, E. Soto-Pedre, L. Donnelly, K. Zhou, E. R. Pearson, Acute kidney injury, plasma lactate concentrations and lactic acidosis in metformin users: A GoDarts study, *Diabetes, Obes. Metab.* **19**, 1579–1586 (2017).

596. D. A. Goldspink, F. Reimann, F. M. Gribble, Models and Tools for Studying Enteroendocrine Cells*Endocrinology* **159**, 3874–3884 (2018).

597. X. Wang, Y. Yamamoto, L. H. Wilson, T. Zhang, B. E. Howitt, M. A. Farrow, F. Kern, G. Ning, Y. Hong, C. C. Khor, B. Chevalier, D. Bertrand, L. Wu, N. Nagarajan, F. A. Sylvester, J. S. Hyams, T. Devers, R. Bronson, D. B. Lacy, K. Y. Ho, C. P. Crum, F. McKeon, W. Xian, Cloning and variation of ground state intestinal stem cells, *Nature* **522**, 173–178 (2015).

598. M. Schweinlin, S. Wilhelm, I. Schwedhelm, J. Hansmann, R. Rietscher, C. Jurowich, H. Walles, M. Metzger, Development of an Advanced Primary Human In Vitro Model of the Small Intestine., *Tissue Eng. Part C. Methods* **22**, 873–83 (2016).

599. M. Heishi, J. Ichihara, R. Teramoto, Y. Itakura, K. Hayashi, H. Ishikawa, H. Gomi, J. Sakai, M. Kanaoka, M. Taiji, T. Kimura, M. J. Heishi Ichihara R Teramoto Y Itakura K Hayashi H Ishikawa H Gomi J Sakai M Kanaoka M Taiji T Kimura, M. Heishi, J. Ichihara, R. Teramoto, Y. Itakura, K. Hayashi, H. Ishikawa, H. Gomi, J. Sakai, M. Kanaoka, M. Taiji, T. Kimura, Global gene expression analysis in liver of obese diabetic db/db mice treated with metformin, *Diabetologia* **49**, 1647–1655 (2006).

600. N. Saeidi, L. Meoli, E. Nestoridi, N. K. Gupta, S. Kvas, J. Kucharczyk, A. A. Bonab, A. J. Fischman, M. L. Yarmush, N. Stylopoulos, Reprogramming of intestinal glucose metabolism and glycemic control in rats after gastric bypass, *Science (80-.).* **341**, 406–410 (2013).

601. C. R. Flynn, V. L. Albaugh, S. Cai, J. Cheung-Flynn, P. E. Williams, R. M. Brucker, S. R. Bordenstein, Y. Guo, D. H. Wasserman, N. N. Abumrad, Bile diversion to the distal small intestine has comparable metabolic benefits to bariatric surgery, *Nat. Commun.* **6** (2015), doi:10.1038/ncomms8715.

602. G. Baud, M. Daoudi, T. Hubert, V. Raverdy, M. Pigeyre, E. Hervieux, M. Devienne, M. Ghunaim, C. Bonner, A. Quenon, P. Pigny, A. Klein, J. Kerr-Conte, V. Gmyr, R. Caiazzo, F. Pattou, Bile diversion in roux-en-y gastric bypass modulates sodium-dependent glucose intestinal uptake, *Cell Metab.* **23**, 547–553 (2016).

603. V. Tremaroli, F. Karlsson, M. Werling, M. Ståhlman, P. Kovatcheva-Datchary, T. Olbers, L. Fändriks, C. W. Le Roux, J. Nielsen, F. Bäckhed, Roux-en-Y Gastric Bypass and Vertical Banded Gastroplasty Induce Long-Term Changes on the Human Gut Microbiome Contributing to Fat Mass Regulation, *Cell Metab.* **22**, 228–238 (2015).

604. M. Kleinert, K. N. Bojsen-Møller, N. B. Jørgensen, M. S. Svane, X. C. Martinussen, B. Kiens, J. F. P. Wojtaszewski, S. Madsbad, E. A. Richter, X. C. Clemmensen, Effect of bariatric surgery on plasma gdf15 in humans, *Am. J. Physiol. - Endocrinol. Metab.* **316**, E615–E621 (2019).

605. H. Frikke-Schmidt, K. Hultman, J. W. Galaske, S. B. Jørgensen, M. G. Myers, R. J. Seeley, GDF15 acts synergistically with liraglutide but is not necessary for the weight loss induced by bariatric surgery in mice, *Mol. Metab.* **21**, 13–21 (2019).

Appendix

Drug/Reagent	Mechanism of Action and Target
Chapter 4	
Antimycin A	Inhibitor of mitochondrial respiration and oxygen consumption by targeting Complex III of electron transport chain
Rotenone	Inhibitor of mitochondrial respiration and oxygen consumption by targeting Complex I of electron transport chain
FCCP	Mitochondrial proton uncoupler that maximises oxygen consumption
Az-991	AMPK activator
UK-5099	Inhibitor of mitochondrial pyruvate carrier (MPC)
NMN (Nicotinamide Mononucleotide)	Increases cellular NAD+ via the salvage pathway
Duroquinone	Substrate for NAD(P)H dehydrogenase (NQOs) involved in redox balance predominantly in the cytosol.
MitoTEMPO	MnSOD mimetic superoxide scavenger (Mitochondrial targeted antioxidant)
MitoPQ	Redox cycler that stimulates mitochondrial superoxide production
MitocDNB1	Depletes glutathione by acting as a substrate for glutathione S-transferase
Doxycycline	Inhibitor of mitochondrial translation
Actinonin	Inhibitor of de novo turnover of mitochondrial proteins
MitoBloCK6	Inhibitor of mitochondrial protein import through TIM22 and Mia40/Erv1 pathways
Ciprofloxacin	Inhibitor of mtDNA replication by inhibiting mitochondrial topoisomerases from relaxing its supercoil structure
ISRIB	Inhibitor of eIF2A phosphorylation and activation of the integrated stress response
GSK-2606414	Inhibits PERK activation
A-92	Inhibitor of GCN2
Histidinol	Inhibitor of histidyl-tRNA syntethetase to mimic amino acid deprivation
KC7F2	Inhibitor of HIF-1A translation by targeting Rps6 pathway
NSC-134754	Inhibitor of HIF-1A transcription, translation and stability
Chapter 5	
Phloridzin	Non-specific blocker of SGLTs
Phloretin	Non-specific blocker of GLUTs
Cytochalasin B	Non-specific blocker of GLUTs
Forskolin	Non-specific blocker of GLUTs, with a higher affinity for GLUT1/3/4 compared to GLUT2
Glucosamine	High affinity substrate for GLUT2
Fructose	Substrate for GLUT2 with similar affinity compared to glucose
Chapter 6	
2-Deoxyglucose	Inhibitor of hexokinase and therefore glycolysis
Oxamate	Inhibitor of LDH
AR-C155858	Inhibitor of MCT2 and MCT4
Syrosingopine	Inhibitor of MCT1 and MCT4

AOA (Aminooxyacetate)	Broad-spectrum inhibitor of transaminase enzymes, including aspartate transaminases involved in the malate-aspartate shuttle and alanine transaminases
βCLA (β-chloro-alanine)	Selective inhibitor of alanine transaminases
Phenylsuccinate	Inhibitor of oxoglutarate-glutamate transporters involved in the malate-aspartate shuttle
iGP-1	Inhibitor of mGPDH involved in the glycerolphosphate shuttle
GPi-688	Inhibitor of glycogen phosphorylase, therefore glycogenolysis
Etomoxir	Inhibitor of CPT-1 shuttle involved in fatty acid oxidation in the mitochondria

Appendix 1: Mechanisms of drugs and reagents used in this study.